IMPACT RESISTANCE OF SINGLE-LAYER AND MULTI-LAYERED MATERIALS

By

Karrar Alquraishi

Undergraduate Degree

A THESIS

Submitted in Partial Fulfillment of the

Requirements for the Degree of

Master of Science

(in Mechanical Engineering)

The Graduate School

The University of Maine

August, 2017

Advisory Committee:

Vincent Caccese, Professor of Mechanical Engineering, Advisor

Senthil S. Vel, Ph.D. Arthur O. Willey Professor of Mechanical Engineering

Caitlin Howell, Assistant Professor in Biological Engineering

IMPACT RESISTANCE OF SINGLE-LAYER AND MULTI-LAYERED MATERIALS

By

Karrar Al-Quraishi

Thesis Advisor: Dr. Vincent Caccese

An Abstract of the Thesis Presented

in Partial Fulfillment of the Requirements for the

Degree of Master of Science

(in Mechanical Engineering)

August, 2017

Use of impact resisting materials to prevent head injury and concussion is the subject of much study in protective equipment for sports and other activities. Understanding the mechanical response of impact resistant materials and how this response changes with geometric and material parameters is important when designing and optimizing new materials. This thesis summarizes the impact resistance of various material combinations using a twin wire drop tower. A database of the response of numerous samples subject to a step impact drop test was created. The maximum acceleration versus drop height, impact force versus displacement and time history of the impact impulse are presented for each sample tested. At a given impact height, the most optimal material response should have a stiffness allowing for maximum energy absorption which will decrease the forces due to the impact. The variation in material properties and geometry can be used to create a design criterion that can achieve a certain performance requirement.

In this study, there were two types of impact resistant materials, urethane honeycomb and polymeric foam materials that were tested in various combinations including layer height, cell structure and material properties. The foam material which is classified mathematically as a hyperfoam material is categorized according to the material stiffness as P09, P15 and P25, based upon density parameters provided by the manufacturer. The honeycomb material is classified mathematically as hyperelastic and has a varying cellular structure where the cell wall shape and dimensions can be modified. The honeycomb material is classified according to material durometer (hardness) as H561, H781, H1036 and H1056 and according to cell geometric structure. Regular hexagonal shapes and irregular shapes were tested.

One layer results of the foam material showed that a stiffer material is generally more optimal when the impact height increases. Stiffness in the materials tested is directly related to the density. Increasing the thickness and accordingly the deformation of the energy absorbing material allows the use of softer materials resulting in lesser impact forces and acceleration. Regarding the results of one layer of urethane honeycomb, increasing of the material thickness has the same net effect as in the foam. Overall stiffness of the honeycomb material is controlled by the material durometer and the solids ratio. In addition, the response is influenced by buckling of the cell walls which tend to limit forces imparted until the material is consolidated. Modification of the cell wall thickness or the cell size leads to changes in response that can be used to optimize the structure under impact. In addition, multilayered structures may be used to mitigate impact over a wider range of input energy than could a single layer material. Accordingly, the impact attenuation of several multi-layer samples was explored. Those samples consist of combinations from soft, moderate and stiff material to get reasonable values of the acceleration and displacement at every impact height.

DEDICATION

To my loving family.

ACKNOWLEDGMENTS

* I would like to thank Dr. Vincent Caccese for giving me the opportunity for working with him for two years and for advising me throughout my project.

* Many thanks to my advisory committee, Professor Senthil S, Vel and Caitlin Howell, for their invaluable participation on my thesis.

* I would like to thank the HCED in Iraq for their financial support.

*I would also like to thank the staff of the Advanced Manufacturing Center for all of their help in all phases of the project.

*I am grateful to my family and friends who provided invaluable support whenever I needed it.

TABLE OF CONTENTS

LIST OF TABLES

LIST OF FIGURES

CHAPTER ONE

INTRODUCTION

One of the most important concerns to individuals, families and healthcare organizations is injury due to impact from falls, vehicular accidents and sports related events. Prevention of impact related injury is important to the majority of people and especially athletes and the elderly. [According to the National Electronic Injury Surveillance System (NEISS)], Table 1-1 shows a survey of the number of injures for some sports activities in the year 2015 [1]. According to the Centers for Disease Control and Prevention (CDC), 20% of falls cause a head injury or broken bones. Because of the fall injury, over 800,000 patients are hospitalized each year and most of these injuries occur to the hip or the head. Furthermore, most traumatic brain injuries (TBI) happen because of falls. Falls contribute to 95.0 % of hip fractures. The cost of taking care of and treating the patients who suffer from fall injuries are estimated to be $31 billion annually [2]. It is estimated that about 20,000 people died in 2009 due to falls and the number is increasing.

Various systems have been used for reducing fall related injuries in the elderly. For instance, in elder care facilities alarms can be installed on the bed to alert the medical staff when older adults leave their beds. Also, bedside mats can be provided to protect the person when they fall, [3]. These types of procedures are not enough because there are hundreds of other causes that lead to falls. Also, the elderly population desires to lead independent lives, [3].

Table 1-1 - Survey for the number of injures in the years of 2015 for different activities, [1].

Product Groupings	Estimated Number of Injuries*	CV*	Number of Injuries*	Estimated Number of Injuries and *Estimated Rate of Product-Related Injuries per 100,000 Population in the United States and Territories (listed in italic)* that Were Treated in Hospital Emergency Departments*									
				Age						Sex		Disposition	
				All Ages	0-4	5-14	15-24	25-64	65+	Male	Female	Treated & Rel.	Hosp. & DOA
Child Nursery Equipment													
All Nursery Equipment	94,524	.12	3,132	94,524	69,226	3,097	3,738	16,394	2,069	44,276	50,247	89,993	4,530
				29.2	*347.4*	*7.5*	*8.6*	*9.6*	*4.2*	*27.8*	*30.6*	*27.8*	*1.4*
Toys													
All Toys	244,181	.09	7,245	244,181	88,155	93,149	20,392	36,711	5,774	141,545	102,636	237,748	6,433
				75.4	*442.3*	*226.8*	*46.8*	*21.6*	*11.7*	*88.8*	*62.4*	*73.4*	*2.0*
Sports & Recreational Equipment													
ATV's, Mopeds, Minibikes, etc.	212,030	.09	4,452	212,030	4,178	42,064	61,748	88,885	15,064	153,085	58,944	185,042	26,987
				65.5	*21.0*	*102.4*	*141.7*	*52.3*	*30.5*	*96.0*	*35.8*	*57.1*	*8.3*
Amusement Attractions (incl. Rides)	46,189	.15	1,244	46,189	5,436	22,855	6,363	11,104	431	20,639	25,550	45,592	597
				14.3	*27.3*	*55.6*	*14.6*	*6.5*	*0.9*	*12.9*	*15.5*	*14.1*	*0.2*
Barbecue Grills, Stoves, Equipment	18,941	.11	472	18,941	2,439	1,932	1,799	11,490	1,280	13,045	5,896	17,335	1,606
				5.8	*12.2*	*4.7*	*4.1*	*6.8*	*2.6*	*8.2*	*3.6*	*5.4*	*0.5*
Baseball, Softball	215,248	.09	5,212	215,248	3,451	92,353	63,979	52,612	2,853	134,230	81,018	209,192	6,056
				66.5	*17.3*	*224.8*	*146.8*	*31.0*	*5.8*	*84.2*	*49.3*	*64.6*	*1.9*
Basketball	493,011	.09	14,345	493,011	1,736	172,998	225,560	91,529	1,158	398,723	94,288	486,164	6,847
				152.2	*8.7*	*421.2*	*517.4*	*53.9*	*2.3*	*250.0*	*57.3*	*150.1*	*2.1*
Beach, Picnic, Camping Equipment	22,153	.11	508	22,153	2,670	3,098	2,284	10,221	3,880	10,944	11,209	21,128	1,026
				6.8	*13.4*	*7.5*	*5.2*	*6.0*	*7.9*	*6.9*	*6.8*	*6.5*	*0.3*
Bicycles & Accessories	497,134	.13	13,157	497,134	20,101	148,370	89,450	202,229	36,952	355,311	141,822	454,361	42,772
				153.5	*100.9*	*361.2*	*205.2*	*119.0*	*74.9*	*222.8*	*86.3*	*140.3*	*13.2*
Boxing	16,897	.11	422	16,897	49	2,259	7,483	7,075	30	14,509	2,389	16,855	43
				5.2	*0.2*	*5.5*	*17.2*	*4.2*	*0.1*	*9.1*	*1.5*	*5.2*	*0.0*
Exercise, Exercise Equipment	464,363	.11	11,572	464,363	8,855	45,732	108,421	250,256	51,082	259,607	204,756	431,354	32,930
				143.4	*44.4*	*111.3*	*248.7*	*147.3*	*103.5*	*162.8*	*124.5*	*133.2*	*10.2*
Football	399,873	.08	11,806	399,873	990	204,795	158,315	35,294	479	375,237	24,636	392,416	7,456
				123.5	*5.0*	*498.6*	*363.2*	*20.8*	*1.0*	*235.3*	*15.0*	*121.2*	*2.3*
Hockey	46,523	.30	1,322	46,523	194	15,162	17,921	12,847	398	39,827	6,696	45,539	984
				14.4	*1.0*	*36.9*	*41.1*	*7.6*	*0.8*	*25.0*	*4.1*	*14.1*	*0.3*
Horseback Riding	56,727	.16	1,278	56,727	754	9,268	14,402	28,055	4,248	16,371	40,356	48,835	7,892
				17.5	*3.8*	*22.6*	*33.0*	*16.5*	*8.6*	*10.3*	*24.5*	*15.1*	*2.4*
In-line Skating	10,723	.20	261	10,723	16	5,680	2,356	2,556	114	4,762	5,961	10,400	323
				3.3	*0.1*	*13.8*	*5.4*	*1.5*	*0.2*	*3.0*	*3.6*	*3.2*	*0.1*
Lacrosse, Rugby, Misc. Ball Games	84,617	.10	2,339	84,617	643	36,229	30,128	13,683	3,935	55,487	29,130	82,364	2,254
				26.1	*3.2*	*88.2*	*69.1*	*8.1*	*8.0*	*34.8*	*17.7*	*25.4*	*0.7*
Nonpowder Guns, BB'S, Pellets	17,594	.08	442	17,594	1,475	7,278	5,261	3,094	486	14,413	3,181	16,354	1,240
				5.4	*7.4*	*17.7*	*12.1*	*1.8*	*1.0*	*9.0*	*1.9*	*5.0*	*0.4*
Playground Equipment	242,844	.11	8,002	242,844	58,354	163,114	10,368	9,524	1,478	129,031	113,813	231,404	11,361
				75.0	*292.8*	*397.1*	*23.8*	*5.6*	*3.0*	*80.9*	*69.2*	*71.4*	*3.5*

*** Estimated Number of Injuries:** Because NEISS is a probability sample, each injury case has a statistical weight. These are national estimates of the number of persons treated in U.S. hospital emergency departments with consumer product-related injuries and are derived by summing the statistical weights for the appropriate injury cases. The data system allows for reporting of up to two products for each person's injury, so a person's injury may be counted in two product groups.

*** CV (Coefficient of Variation):** The CV, the standard error of the estimate divided by the estimate, is a measure of sampling variability (errors that occur by chance because observations are made only on a population sample).

*** Number of Injuries:** The actual number of injury cases collected from the hospitals sampled. Since injury cases have different statistical weights, these "raw" numbers should not be used for comparative purposes.

*** Estimated Rate:** Estimated rates are calculated using the Census Bureau's July 1, 2015 U.S. resident population estimates.

Having aesthetically designed devices that limit injury due to falls can be one way of allowing more independent living and higher risk activities. Systems that mitigate the two major causes of morbidities, head and hip injuries are desirable. The most vulnerable part of the human body is the head, where accelerations reaching 300g can cause serious injuries that may lead to death [3]. Head injuries happen for many reasons. Brain skull fracture and brain injuries occur due to head impact where the acceleration of the head increases dramatically which leads to these injuries. As a result, it is important to design protective devices with materials that have the ability to absorb the transferred energy from the body during the impact, [3].

Traditional helmets and other devices were designed to limit the impact acceleration at one particular impact energy level. This led to designs that were highly optimized for that event but did not necessarily work well under other scenarios. Current thought is that prevention should occur over a range of impact levels requiring novel implementation of material solutions. Having highly optimized layered systems is one approach, and the objective of this thesis is a thorough quantification of materials available for such devices.

Many head injury codes have been used to estimate the severity of the injuries. For example abbreviated injury scale (AIS) and the head injury criteria (HIC). The AIS consists of six levels where level one indicates minor injury and level six indicates serious injury as shown in Figure 1-1 and the Table 1-2. HIC is used to predict the mode and severity of the injury while AIS presents a foundation for HIC comparison, [4].

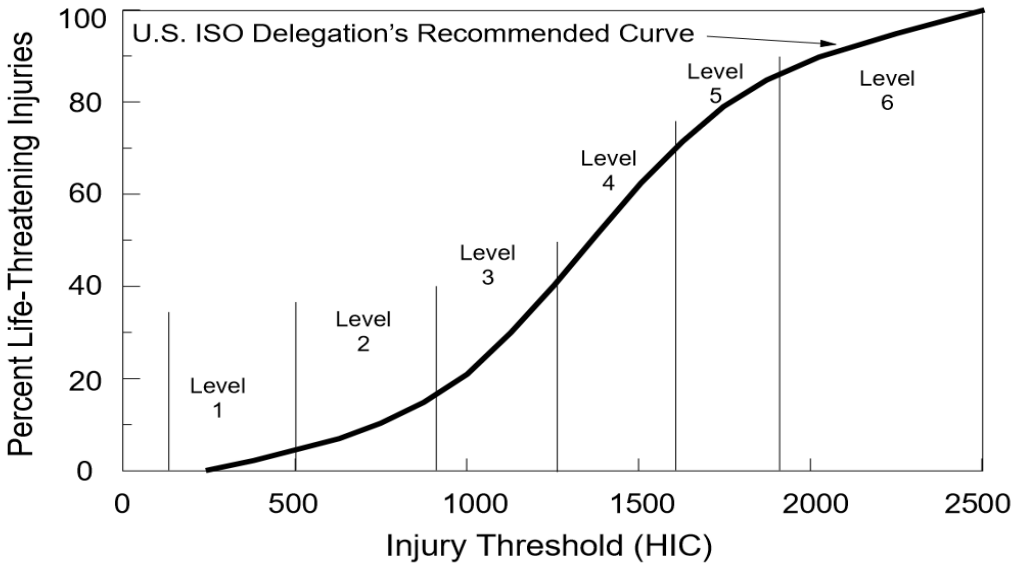

Figure 1-1– AIS and HIC for predicting the level of the injury, [4].

Table 1-2 - The HIC relating to the AIS Code [4].

AIS Code	HIC	Head Injury
1	135-519	Headache or dizziness
2	520-899	Unconscious less than 1 hour; linear fracture
3	900-1254	Unconscious 1 to 6 hours; depressed fracture
4	1255-1574	Unconscious 6 to 24 hours; open fracture
5	1575-1859	Unconscious more than 24 hours; large hematoma
6	>1860	Non-survivable

1.1 Head Injuries

Head injuries can be divided into two group which are skull injury and brain injury. Concussions are an example of mild traumatic brain injury (MTBI). Maxilla fracture is an example of skull injury [3]. Many catastrophic events happen every year due to head injury. For example in city traffic, the head and legs of pedestrians are the most vulnerable to injury where the head injuries represent 31.4 % as shown the Figure 1-2, [5].

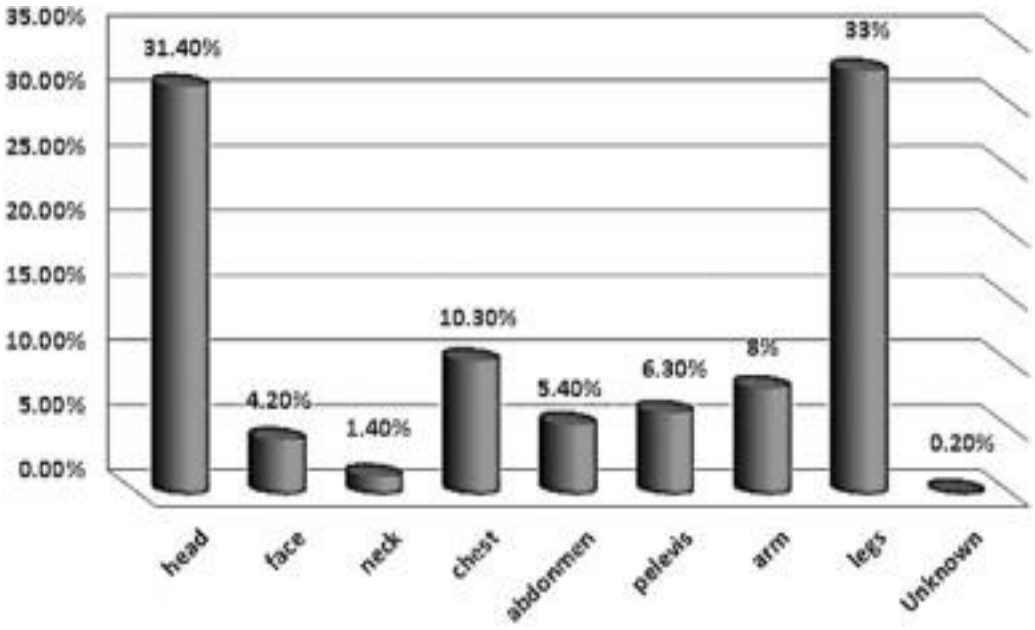

Figure 1-2- Injury distribution in human body due to accidents in city traffic [5].

1.1.1 Head Injury in Football

The Figure 1-3 shows an example of the contact between football players that leads to head injuries while participating in this activity. Football is the most popular sport in the U.S where in high school more than 1.2 million students practiced football in the 2001-2002 academic year. Football has the highest number

of catastrophic injuries reported to the Center for Catastrophic Sports Injury Research among others sports.

During the period 1945-1999, there were 497 fatalities among football players in the U.S., with 69 percent dying due to brain injuries, [6]. Between 1990 and 1999, there were 204,802 football related head injuries that required emergency room treatment. Among that number, 68,861 players were presented to emergency departments due to concussions, [8]. Accordingly, the use of impact resisting materials to prevent head injury and concussion is the subject of much study in protective equipment for football. For example, chronic traumatic encephalopathy (CTE) is a degenerative disease found in people who have been exposed to periodic brain trauma. This disease causes harmful proteins to generate and damages the brain tissue, [19].

A), [9] B), [10]

Figure 1-3 – A and B show how the contact between football players.

1.1.2 Head Injury in Soccer

The Figure 1-4 shows the head to head contact and head to ball contact during a soccer match. The minimum value of the head acceleration that leads to concussion is no less than 80g, ([3], [7] and [20]). The contact between the head and the ball does not normally lead to head injury because the resulted head acceleration is less than 10g (10,000$^{rad}/_{s^2}$). The contact of head to head can produce enough acceleration to cause concussion even without serious head injury [7]. Some other causes of head injury in soccer are goal post strikes, head to ground and head to knee contact. Between 1990 and 1999, there were 86,697 soccer related head injuries that required emergency room treatment. Among that number, 21,715 players were presented to emergency rooms due to concussions, [8].

Figure 1-4 - The head to head contact and Head to ball contact, [7].

1.1.3 Head Injury in Ice Hockey

Repeated concussion and other different traumatic brain injuries (TBI) due to the sport of ice hockey is another concern to individuals, families and healthcare organizations. In North America, concussions and traumatic brain injuries (TBI) occur during ice hockey games no less than 1.7 million times every year. Traumatic brain injuries threaten the public health because these injuries have potential long-term effects [11].

Between 1990 and 1999, there were 17,008 ice hockey related head injuries that required emergency room treatment. Among that number, 4820 players were presented to emergency rooms due to concussions, [8]. Several types of contact that can cause head injury in ice hockey are head to head, head to ice and head to knee contact. Figure 1-5, A and B show how contact between ice hockey players can occur.

A), [12]

B) [13]

Figure 1-5 – A and B show two examples of the contact between Ice hockey players.

1.2 Materials for Impact Injury Prevention

Many tests have been done on different materials by using different mechanisms for obtaining cost effective and highly functional protection materials. Several requirements for choosing the best material are that the material should give minimum value to the acceleration at the required impact energy and be valid for a wide range of designs without reaching the acceleration range of 200-300g to avoid skull fracture and 80–100g to avoid concussion ([3], [7] and [20]). Also, the chosen material should be as thin as possible to make the design more desirable. Furthermore, the material weight is another important factor because a heavy weight makes the user feel uncomfortable and the additional inertia may cause higher forces. People dislike using unaesthetic protective equipment, which adds another challenge. It is important to choose materials that have the ability to absorb the maximum value of the energy at every impact energy level appropriate to its use.

The system studied in this thesis is a honeycomb/dilatant foam system that will be the focus of this discussion. The honeycomb and foam material will be discussed in this literature review because only these two material are used in this research. In addition, the response of multilayered samples will be discussed.

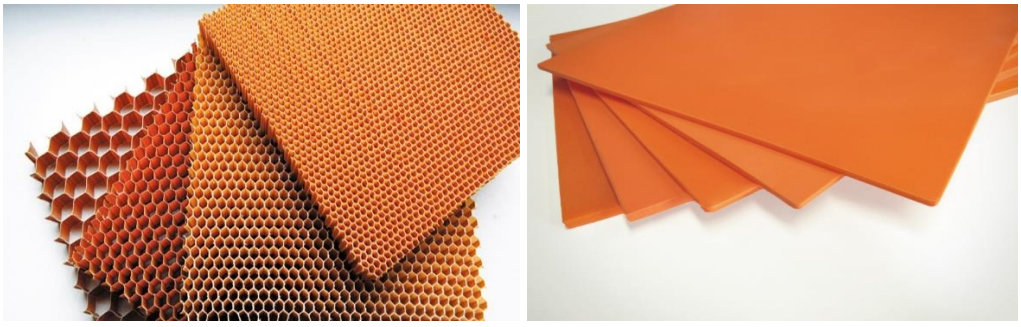

A) [14] B) [15]

Figure 1-6 – Photograph A portrays an example for the cells shape of the honeycomb materials. Photograph B portrays a dilatant foam material.

1.2.1 **Honeycomb Materials**

Urethane honeycomb has a varying cellular structure that can be classified by cell shape, dimensions and material hardness. Figure 1-7 shows the hexagonal honeycomb which represents the regular geometric shape. The geometry of the hexagonal shape of honeycomb material can be defined by the mean side length, (a), the wall thickness (t_w), the mean distance between the two opposite sides (c) and the overall depth (d).

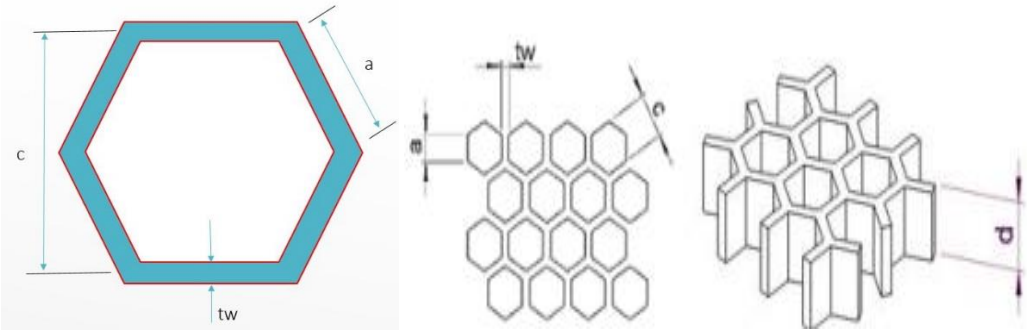

A) B) C)

Figure 1-7 - A) zoomed in view of the hexagonal shape, B) and C) portray the top and side views of the hexagonal shape, respectively.

The Figure 1- 8 shows the honeycomb materials that was tested by Edgecomb [3]. The test procedure is similar to the test procedure used in this work. The tested honeycomb materials were Thermoplastic Green, Thermoplastic White, 40-BK, 20-Y, 35-R and 55-B [3]. He also showed the result for an unprotected base. The numbers refer to nominal durometer (the hardness of the materials) and the letters represent the abbreviated names. The same mass (4.195 kg) and shape (77.4mm radius spherical) of the impactor are used. Also, the cell dimensions for all of the honeycomb materials are 4.7mm cells size and 1.0mm wall thickness of the cells. Furthermore, the anvil that was used was made from stiff concrete covered with a vinyl tile.

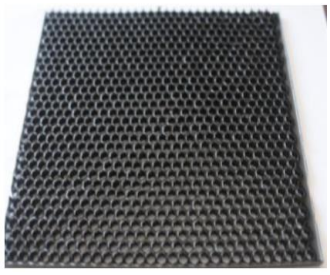

A) cast Honeycomb (40-BK)

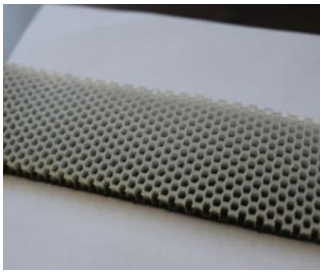

B) Thermoplastic White (TW)

C) Thermoplastic Green (TG)

D) 20-Y

E) 35-R

F) 55-B

Figure 1-8 - A, B, C, D, E and F portray the honeycomb materials that were tested by [3].

The maximum acceleration versus energy curves for Thermoplastic Green, Thermoplastic White, 40-BK, 20-Y, 35-R and 55-B honeycomb materials and unprotected base can be seen in Figure 1-9.

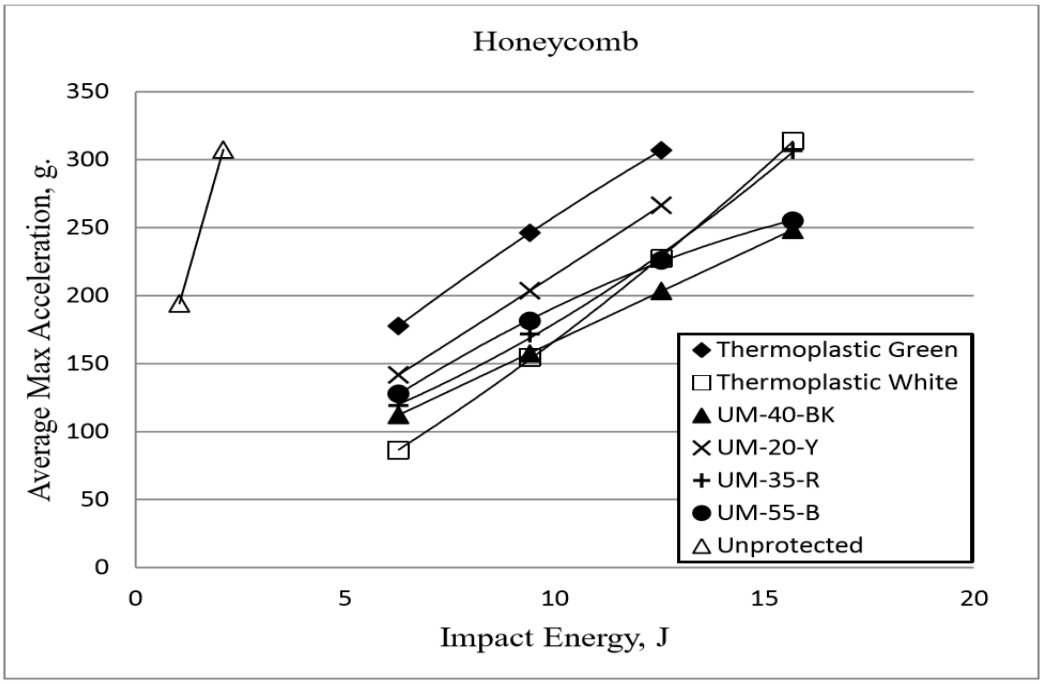

Figure 1-9 - The tests result of the honeycomb materials

In 2013, two types of tests were conducted by Sawal on three different honeycomb materials that were used to study the properties of the honeycomb structure: drop impact test and compression test [21]. The materials are aluminum 6061 (Al 6061), polypropylene (PE), and polystyrene (PS). The dimensions of the three specimens are 200 × 20 × 10 mm for the drop impact tests and 20 × 20 × 10 mm for the compression tests. Also, the length for every side is 4.041mm and the wall thickness is 5 mm. The same mass (2.1kg) and shape (12.5 mm radius hemispherical) of the impactor are used. The results of the drop impact height tests showed the Al 6061 was deformed more than PE and PS materials. The results of the compression tests showed the PE and PS rebounded their shapes again after the test, while Al 6061 showed permanent buckling. Figure 1-10 and Figure 1-11 show the drop impact tests and compression tests, respectively, [21].

Figure 1-10 – Drop impact tests, three different impact heights were used which are 0.2, 0.4 and 0.6 m, [21].

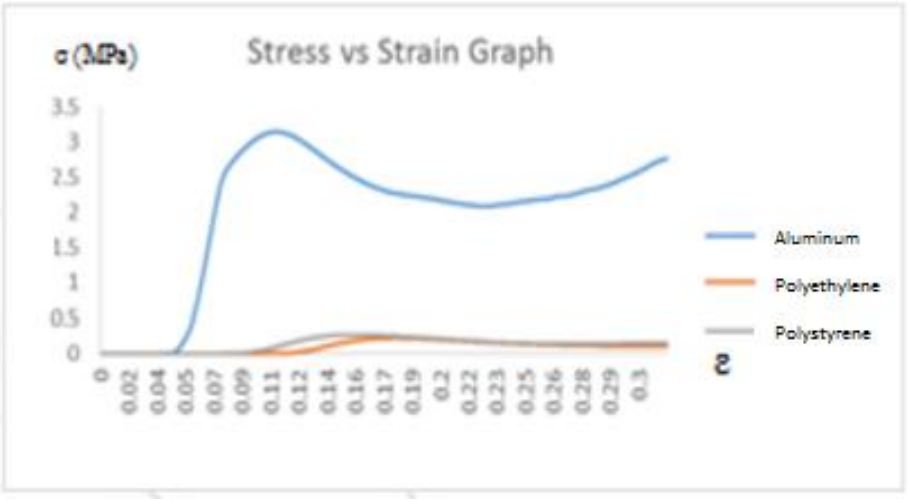

Figure 1-11 – Compression test, [21].

Another study on the two layer honeycomb material has been done to study the effect of the ratio of the wall thickness to the cells sizes on absorbing the energy by using finite element method. In this effort, the sample consists of a solid rubber foam model as the top layer (30mm material thickness) and a honeycomb foam core as a base layer as shown in the Figure 1-12. Four ratio conditions were used which are 1:3, 1:4, 1:5 and 1:6 besides the solid sample. At the impact velocity of 6m/s,

the results of the solid sample, 1:3, 1:4, 1:5 and 1:6 are 239, 204g, 185g, 177g and 166g, respectively. Also, at the impact velocity of 7m/s, the results of the solid sample, 1:3, 1:4, 1:5 and 1:6 ratio are 311g, 269g 235g 222g and 204g, respectively, [23] Lin.

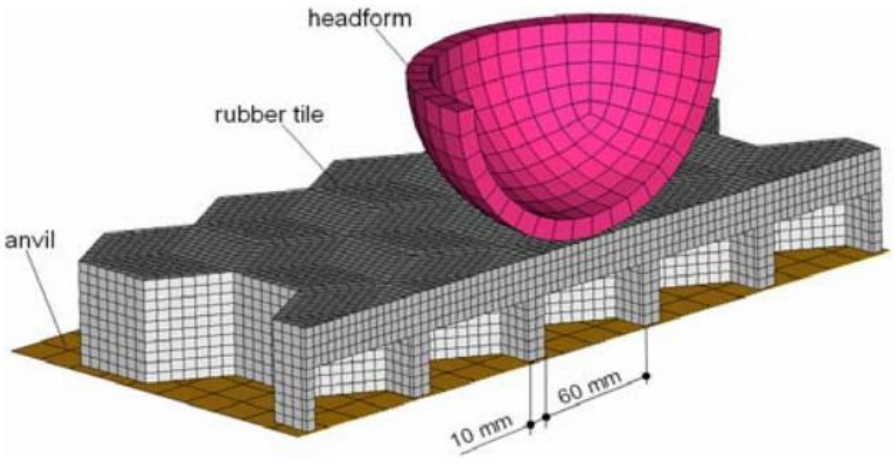

Figure 1-12 - Using the finite element model for studying the effect of the ratio of the wall thickness to cell size of the hexagonal honeycomb material, [23].

Also, when the ratio between the cell sizes and wall thickness increases, the material displacement increases as shown in the Figure 1-13.

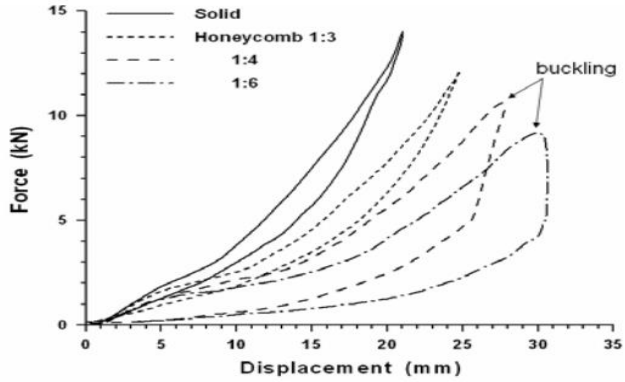

Figure 1-13 - Force-displacement curves of the hexagonal honeycomb materials at the impact height of 2.5 m for different ratios between the wall thickness and cells size, [23].

1.2.1.1 **Honeycomb Solid Ratio**

The solid ratio is the ratio of the area of solid material (As) to the mean enclosed area (Am). The solid ratio is calculated for many reasons. For example, by calculating the solid ratio, we can be sure that the designed honeycomb samples of the same material have different behaviors. Also, when the solid ratio increases, it gives an indication that the displacement of the sample will decrease. Furthermore, by calculating the SR, we can estimate the effective compressive modulus of the honeycomb materials (E_h). If we use the hexagonal honeycomb material (the thicknesses of cell walls are equals) which is shown in the Figure 1-6, we can estimate the area of solid material, the mean area, A_m, solid ratio, SR, and effective compressive modulus, E_h, of the honeycomb materials by using the equations below that were given by [3].

$$A_s = 3 * a * t_w - \frac{\sqrt{3}}{2} * t_w^2 \quad (1\text{-}1)$$

$$A_m = 3 * \frac{\sqrt{3}}{2} * a^2 \quad (1\text{-}2)$$

$$SR = \frac{2}{\sqrt{3}} * \frac{t_w}{a} - \frac{1}{9} * (\frac{t_w}{a})^2 \quad (1\text{-}3)$$

$$E_h = SR * E_s \quad (1\text{-}4)$$

Where E_s is the modulus of elasticity of the solid material.

1.2.1.2 **Honeycomb Buckling.**

Energy absorption and structural response of the honeycomb is influenced by the buckling of the cell walls. The buckling response of the honeycomb materials happens when the cell walls reach the critical response due to the impact load. By using Bleich's plate buckling equation (1-5), we can calculate the elastic buckling of the cell walls.

$$\sigma_{cs} = K * \frac{\pi^2 * E_s}{12*(1-v^2)} * (\frac{t_w}{a})^2 \qquad (1\text{-}5)$$

Where K is the buckling factor

σ_{cs} : The theoretical critical stress at the top of the cell wall.

Also, we can calculate the buckling stress acting over the effective area of the honeycomb materials (σ_{ch}) by multiplying the solid ratio (SR) by the theoretical critical stress(σ_{cs}).

$$\sigma_{ch} = SR * \sigma_{cs} \qquad (1\text{-}6)$$

If the wall thickness of the cells is very thin and these walls are equal in thickness, we can calculate the theoretical critical stress by using the equation (1-7).

$$\sigma_{cs} = 1.044 * K * E_s * \left(\frac{t_w}{a}\right)^3 \qquad (1\text{-}7)$$

1.2.2 **Dilatant Foam Materials**

Dilatant material is classified as a hyper elastic material that is categorized according to the material stiffness. In the work conducted by Edgecomb [3], the tested dilatant materials were XRD-12118, XRD-12236, XRD-15118, XRD-

15158, XRD-25118, XRD-15236 and unprotected materials. The first two digits refer to the density of the materials (the density in $^{lb}/_{ft^3}$ units) and the last three digits refer to the material thickness divided by 1000 (The thicknesses in inches). For example, XRD-15118 refers to the dilatant material at the density $15\frac{lb}{ft^3}$ at the thickness equal to 0.118in. In my research, the XRD-15118 means the P15 material at the thickness 0.118 in (3 mm). The same mass (4.195 kg) and shape (77.4mm radius spherical) of the impactor are used for the testing of the mentioned dilatant materials. Also, the used anvil was made from stiff concrete. The maximum acceleration versus energy curves for the mentioned dilatant materials and unprotected base can be seen in the Figure 1-14.

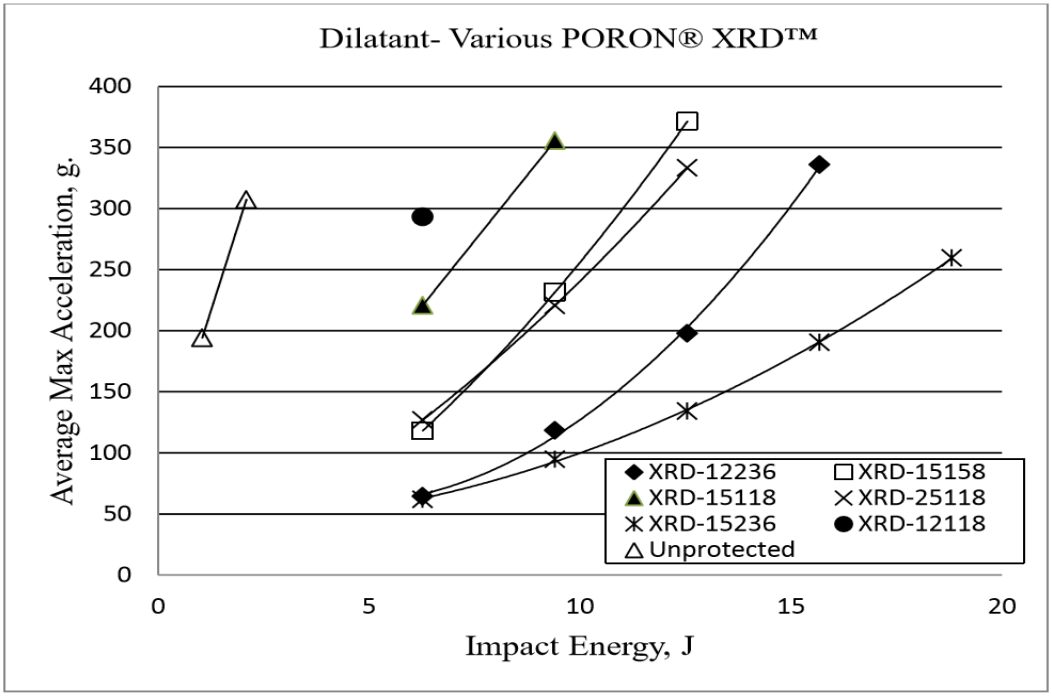

Figure 1-14 - The max acceleration versus energy graph of the dilatant materials and unprotected base, [3].

Using the foam materials as a core of the sandwich panels is one of the most important multi-layered composite materials, because it could be widely used in many applications. For example, it could be used in aircraft structures due to the light weight and stiffness of the sandwich panel. It is important to evaluate the internal and external damage when the sandwich panel is impacted. The apparatus shown in the Figure 1-15 was used for studying the properties of the foam-core sandwich panels, [17].

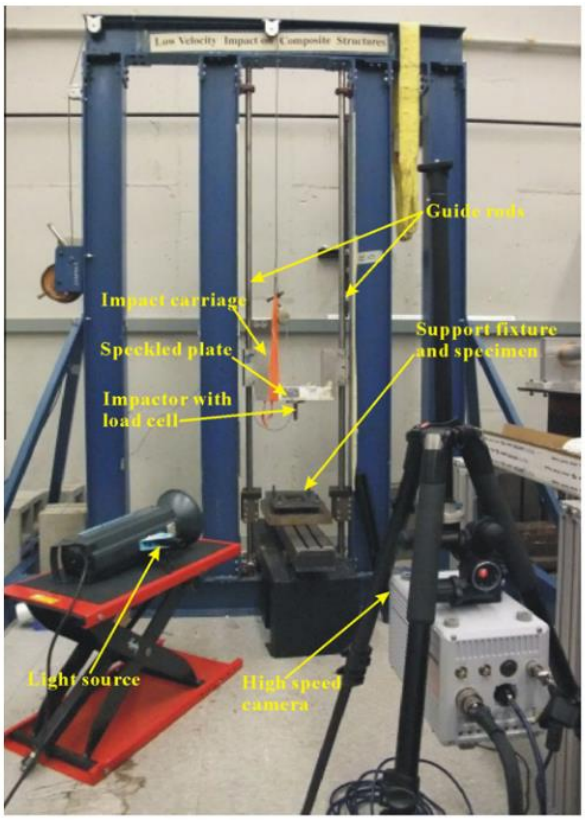

Figure 1-15 - Apparatus used for studying the impact resistance of the foam-core sandwich panels, [17].

In 2012, five different materials were used in drop impact tests to compare their mechanical response by placing them between two high strength skins (Like sandwich plates). The core materials are polypropylene honeycomb, polystyrene foam, cork and two different densities of balsa wood. The dimensions of the specimens are 150 x150 mm. At three different energies, the tests were conducted which are 25 J, 50 J and 75 J. At the energies 50 J and 75 J, Polystyrene material has the highest displacement before yielding and minimum values of stiffness and yield force among others materials. The results showed the cork core absorbs the least value of energy at the higher impact height and the maximum value of energy at the lower impact height, [22].

1.2.3 **Multi-Layered Samples Impact.**

In this section, the literature review of the multi-layered samples will be shown. In the tests done by Edgecomb [3], all the samples consist of dilatant materials in the top and honeycomb materials. The total thicknesses used are 10mm, 12mm and 13mm. The dilatant materials were placed in the top to get the minimum value of the acceleration at the lower impact height (to increase the dispersion in energy). The same mass (4.195 kg) and shape (77.4mm radius spherical) of the impactor were used for the testing of the multi-layered samples. For the thickness of 10mm, the Figure 1-16A show the results of the samples at the thickness 12mm where there are two samples that were tested and both of these two samples consist of two layers only. The first sample consists of XRD-15158 and UM-40-BK, and, the second sample consists of XRD-15158 and UM-55-B.

For the thickness of 12mm, the Figure 1-14B, C and D show the results of the samples at the thickness 12mm. The samples consist of three layers which are XRD-15118, XRD-25118 and one of the three honeycomb materials UM-20-Y,

UM- 40-BK or UM-55-B. The top material of the sample is XRD-15118 or XRD-25118 as shown in the photographs B, C and D of Figure 1-16.

For the thickness of 13mm, Figure 1-16E and F show the results of the samples at the total thickness of 13mm. The samples consist of three layers which are XRD-15158, XRD-25118 and one of the two honeycomb materials UM- 40-BK or UM-55-B. The top material of the sample is either XRD-15158 or XRD-25118 materials as shown in Figure 1-16E and F.

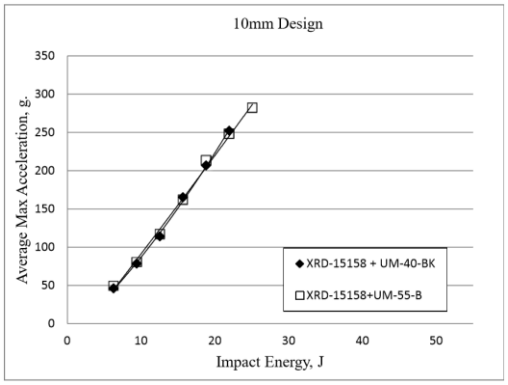

A)

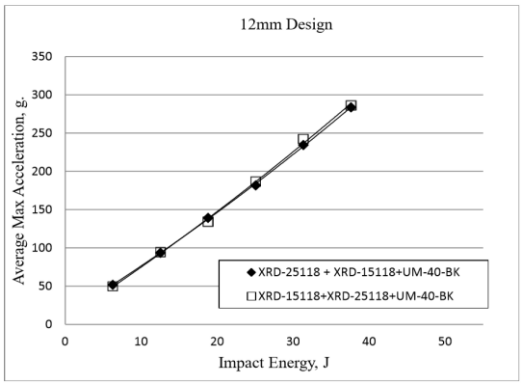

B)

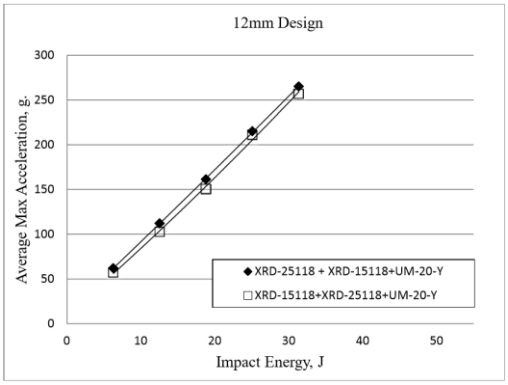

C)

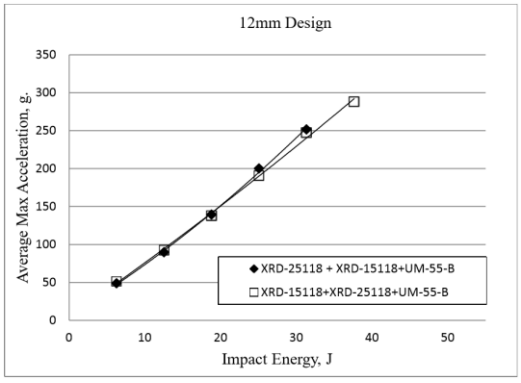

D)

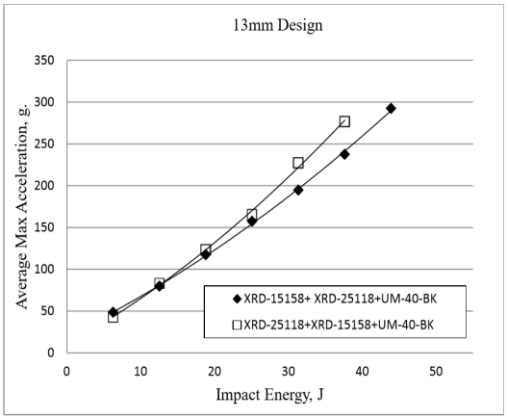

E)

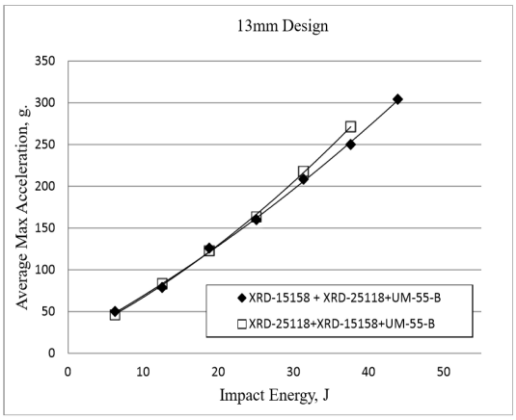

F)

Figure 1-16- The results of multi-layered samples at the total thicknesses of 10mm, 12mm and 13mm, [3].

CHAPTER TWO

TEST APPARATUS AND PROCEDURE

This chapter presents a summary of the test equipment and procedures used in performing the drop impact testing conducted for this effort. Presented will be a brief description of the parts of the apparatus and the purpose for these parts so that one understands the test procedure. The test process will be classified into three main subcomponents, namely, the impact test apparatus, the data acquisition/control system and the sensors.

2.1 Impact Test Apparatus

The test apparatus consists of the drop tower, fly arm, fly arm holder, twin wires, winch, anvil, base, long column and short column. Also of importance are the impactors used in the study that are classified according to their shape and mass.

2.1.1 The Tower

The tower consists of a 6.7 m tall steel column with two twin cables mounted vertically. Figure 2-1, shows most parts of the tower. The cables are used to guide the fly arm so that it drops vertically. A winch is attached near the base and is used to lift and lower the fly arm holder into place.

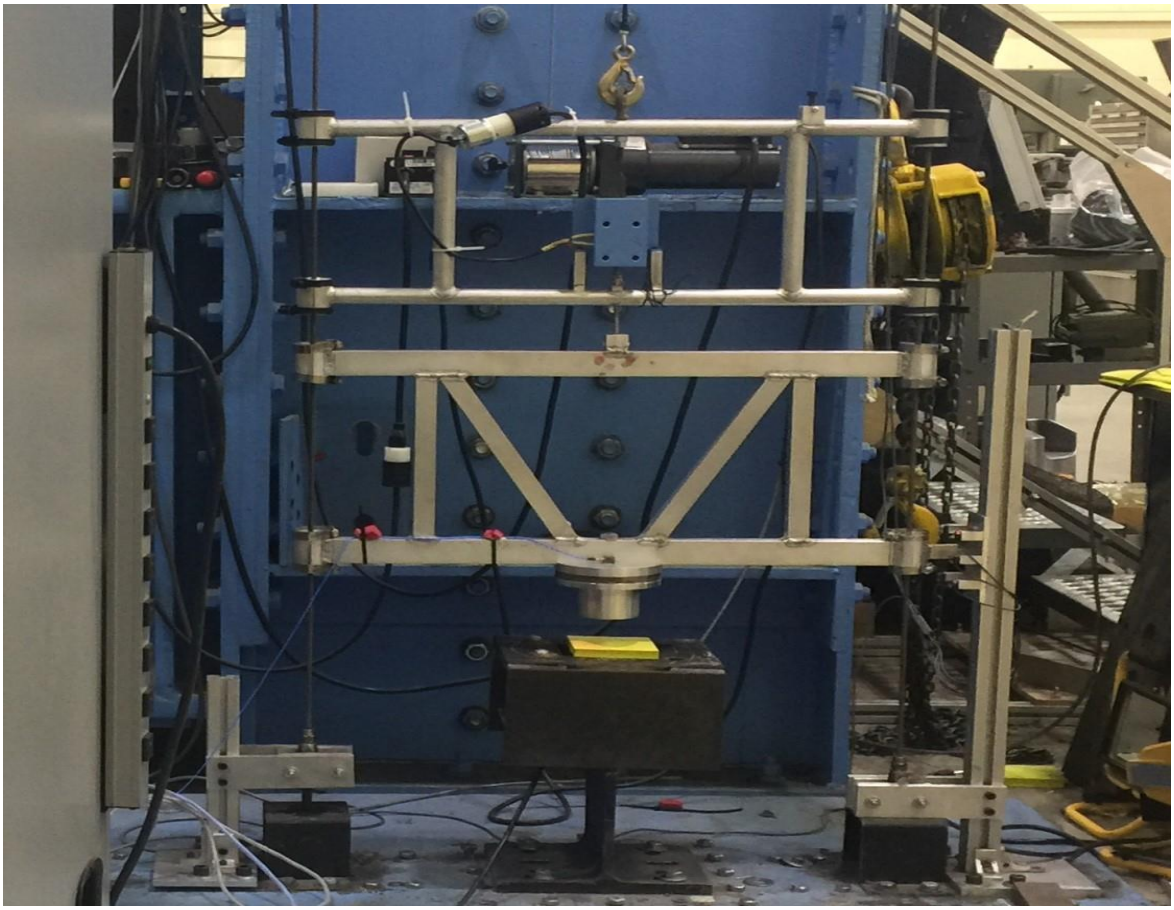

Figure 2-1- The University of Maine twin wire drop tower.

2.1.1.1 The Fly Arm

The fly arm consists of a movable support that is guided vertically along twin wires. Figure 2-2 shows the fly arm that is equipped with a spherical shaped impactor. It is connected to the twin wires using teflon guides held in place by adjustable band clamps in four places (two on each side) to keep the fly arm horizontal when it is released from the fly arm holder. The fly arm is equipped with an impactor that is attached at the bottom by using one bolt. The total weight of

the fly arm and the impactor can be changed according to the requirements of the test by adding the desired weight to the fly arm. The total mass used in the tests described herein is 5.0kg. This mass was measured on a scale LW MEASUREMENTS, LLC with a resolution of 0.01kg

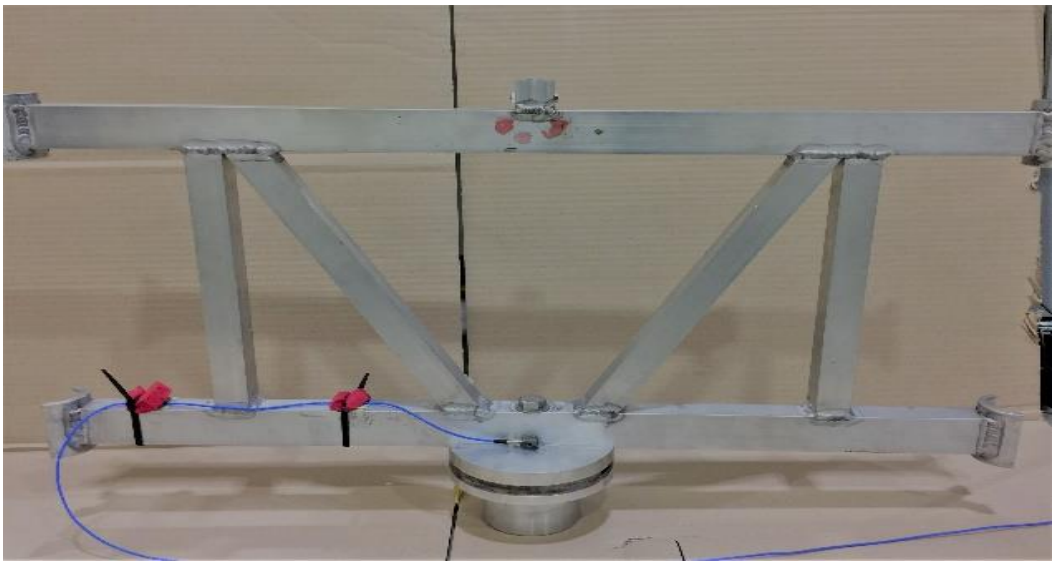

Figure 2-2 - Fly arm with the impactor connected.

2.1.1.2 **The Fly Arm Holder**

The fly arm holder shown in Figure 2-3 is stationed above the fly arm and is connected to the twin wires on both sides by using teflon pads and adjustable band clamps in four places. Also, the fly arm holder is connected to a winch from the top by using a hook and a long wire to lift and lower the fly arm holder to the required impact height. A string potentiometer is connected to the holder for position measurement. There is a quick release pin connected to the bottom of the fly arm holder. The pin is controlled by a digitally actuated solenoid that is activated in the data acquisition software. When the fly arm holder reaches the required

impact height, the quick release pin on the fly arm holder is actuated by the tester releasing the fly arm. The blue box show in Figure 2-3 houses the solenoid and the release pin.

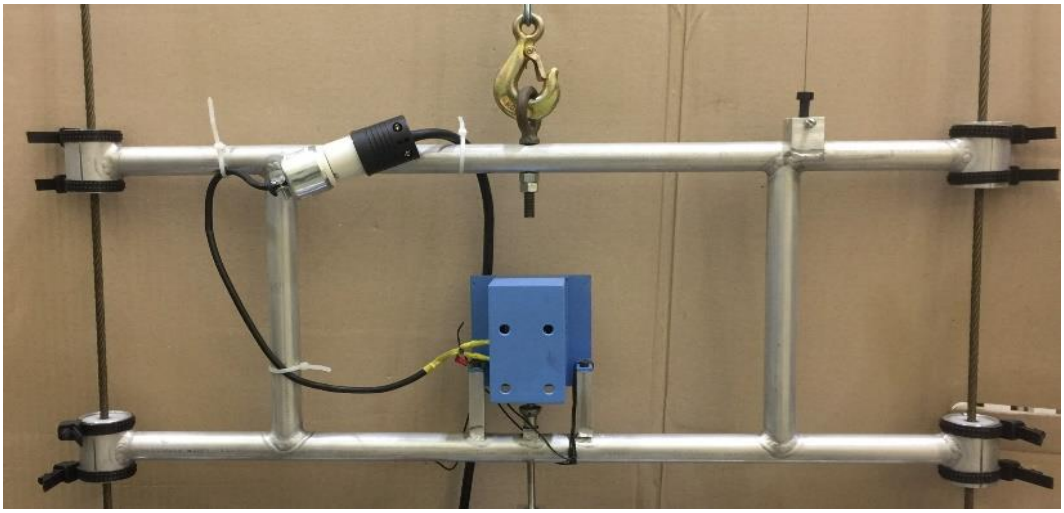

Figure 2-3 - The fly arm holder.

2.1.1.3 **The Anvil**

The anvil used in the drop testing consists of a steel I-shape that is stiffened by vertical plates as shown in Figure 2.4. The bottom flange has a pattern of holes used to bolt the anvil to a steel base pad that is in turn anchored to the concrete floor. Four bolts are used to connect the anvil to the base. The tester needs to insure that the anvil is firmly fixed to the ground to prevent the vibration that may affect the data. The upper flange of the anvil has an 86mm long slot cut near the left side and two holes beside it for passing the beam of a laser displacement sensor. Two long bolts are attached to the top flange to hold the displacement laser that is placed under the slot so that the light beam of the displacement laser strikes the bottom of the impactor plate. The test sample is placed on the top surface of the anvil as shown in the Figure.

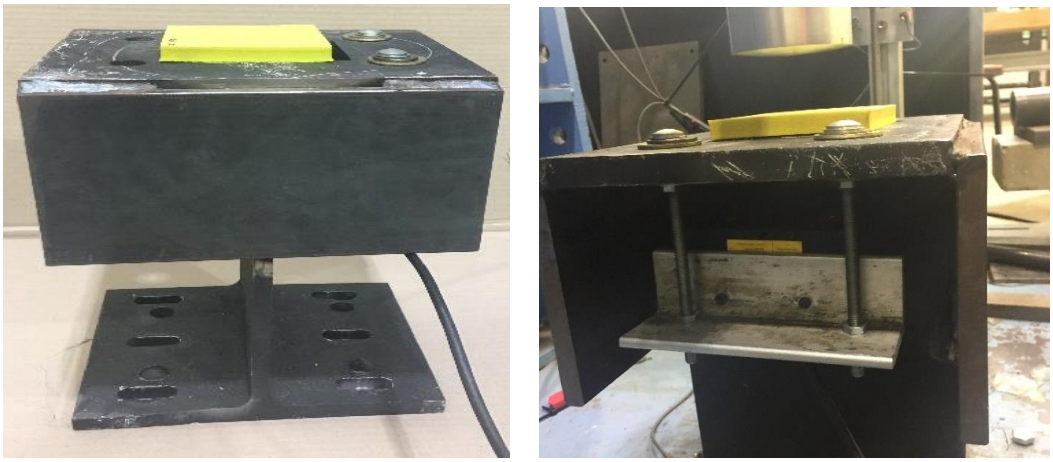

A) B)

Figure 2-4 - Front view (A) and the side view (B) of the anvil.

2.1.1.4 **The Base**

The base is a rectangular steel plate fixed to a concrete floor by an anchor bolt in every corner and two lines of bolts in the middle, which are parallel to the base. As shown in Figure 3-5, the twin wires, column of the velocity gate apparatus and anvil are fixed to the base. The base includes a pattern of threaded holes to accommodate different shapes and styles of anvils.

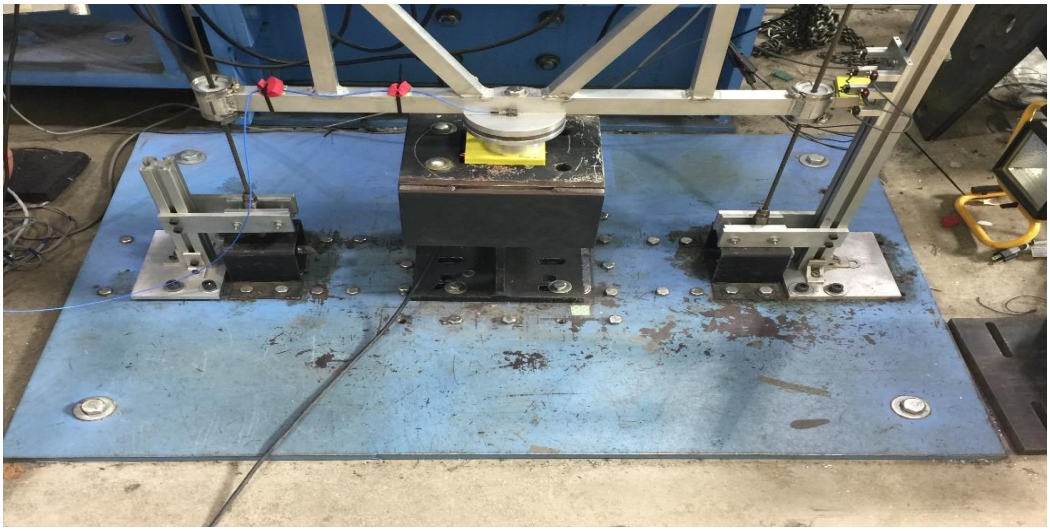

Figure 2-5 - Base of the drop tower.

2.1.1.5 **The Twin Wires and the Column**

The twin wires are two parallel long cables that work as a cable railway. These cables have a 6.35mm diameter bare twisted wire rope to allow the fly arm and fly arm holder to slide easily. The bottom ends of twin wires are fixed to the base as shown in Figure 2-5 using a bolted connector. A clamp was retrofit around the bottom bolt to keep it from loosening and changing the cable tension. The cables are tensioned using a 150 lb*in torque wrench to a value of 60 lb*in +/- 10. It is important that the cable tension is checked periodically. The top ends of the twin wires are connected to a horizontal U-shaped beam.

There is a short aluminum column mounted to the base on the right hand side of the tower used to hold the velocity gate photo sensors. This short column allows the tester to position the laser vertically according to the thickness of the sample. Figures 2-6 A&B shows the twin wires looking toward the top of the tower and the short column, respectively. Finally, the tester can control the lifting and

lowering speed of the fly arm holder by using the manually operated speed controller which is stationed near the winch. A recommended improvement to the test system is to have the speed control adjusted in the computer software.

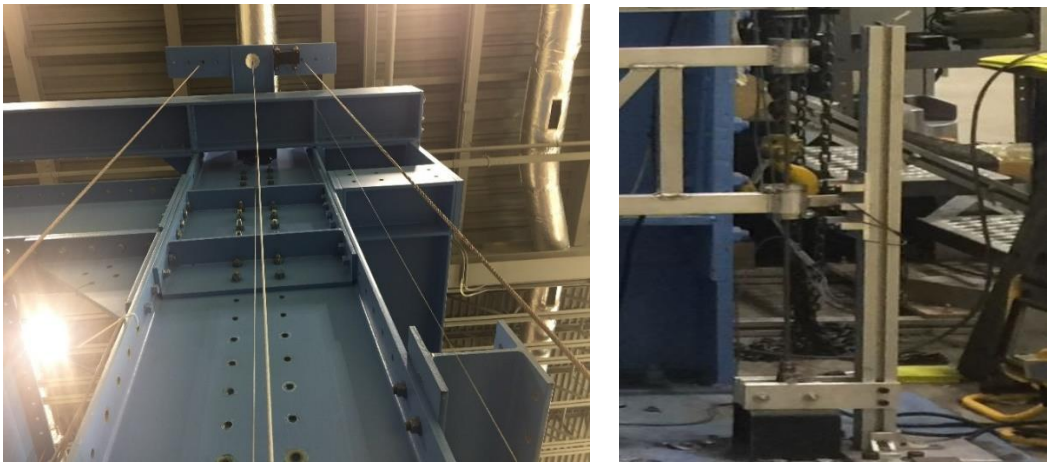

A) B)

Figure 2-6 - Twin wire drop tower guide wires (A) and short column for velocity gate (B).

2.1.2 **Impactors**

The impactor shape and mass has a very important role in the testing. As a result, the test apparatus accommodates several size and shape impactors. Available for this research are two circular impactors and one flat impactor (with a square cross section). In this research, the impactor with a 127mm radius is used. Also there was some data collected using the flat impactor. Because the impactor is tied to the fly arm by using a bolt, the tester has to take into account the weight of the fly arm, impactor, bolt and other attachments when determining the impact mass. Figure 2-7 shows the spherical 127mm and flat impactors, respectively. Drawings of the circular impactors are provided in Appendix A.

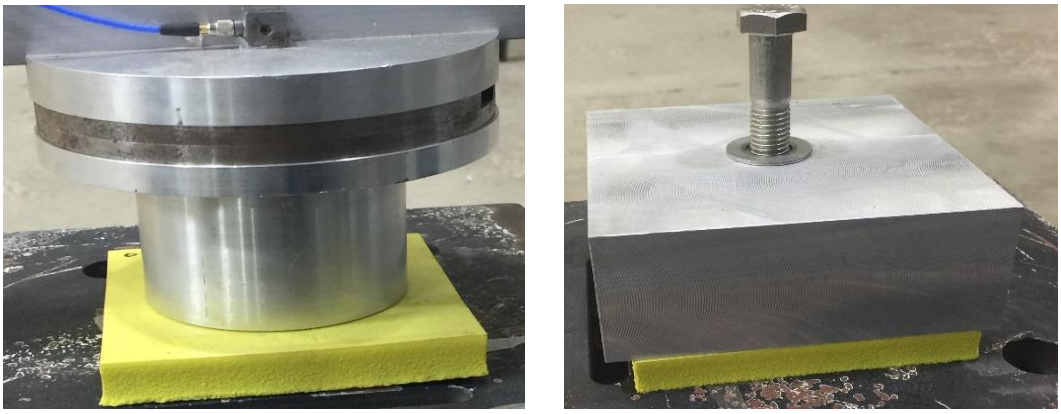

A) B)

Figure 2-7 - Spherical (A) and flat (B) impactors.

It is important to make sure that the center of the impactor strikes the center of the test sample. When the tester adjusts the displacement sensor, the beam light of the displacement laser must hit the bottom left side of the impactor.

2.1.3 **Sensors.**

There are four sensors primarily used in the apparatus for the linear drop testing, which are the displacement laser, the velocity gate photo sensor, the accelerometer and the fly arm position measuring string potentiometer. Figure 2-8 shows the side and top views of the displacement laser. Figure 2-8C shows a side view of the velocity gate and the plate that passes through it.

The serial number and model number of the displacement laser are 1110 1706 and LD1607-50, respectively (the name of manufacturer is PCB PIEZOTRONIC). The laser holder is placed under the long open cut of the upper surface of the anvil to measure the position of the impactor relative to the base. A single sensor was used due to the high cost of this device. It is important to make sure that the light beam of the displacement laser passes through the long slot and reflects from the bottom surface of the impactor to get an accurate result. The

displacement laser has a 50 mm (~2 inch) range, so if the tester has a very thick sample and is expecting the total displacement to be more than 50 mm clipping of the data will result.

The velocity gate is a pair of photo diodes that are attached to the short column. This sensor reads the time of passing between the two sensors that is subsequently converted to the impact velocity. With the current setup the spacing between the sensors is 39.37 mm (1.55 in). The photo diodes are activated by a small plate that is welded with the fly arm. Also, this sensor we can be positioned vertically to reset it according to the sample thickness.

A single axis accelerometer is fixed on the impactor as explained above. This accelerometer is a PCB electronics model no LW135637. The Z-axis only is used with a sensitivity calibrated as 10.27 mV/g

The test apparatus also has a string potentiometer attached to the top of the fly arm holder. The base of the device is attached to the top of the drop tower. The string pot is 7.62 m long (25 ft) with a calibration constant of 0.762 m/V.

A) B) C)

Figure 2-8 - Side (A) and top (B) views of the displacement laser, Side view of the velocity gate (C).

2.1.4 System Data Acquisition and Control

The system data acquisition and control consists of several subcomponents. A computer program called Drop Tower Test was specifically written for this purpose. A screen capture of the main window of the controller is shown in Figure 2-9A. One purpose of the controller is to enable the tester to reset the impactor to the zero position. This is done by allowing the bottom surface of the impactor to touch the upper surface of the sample by using the Up, Down and Stop buttons. When positioned correctly the operator then clicks on the zero button which can be found in the configuration menu. The second function is that the controller is responsible for lifting and lowering the impactor to the required impact drop height by entering the desired height in the edit box then choosing the direction (up or down) and click on the button "Move". Also, the configuration window shown in Figure 2.9B, can be displayed by double clicking on the configuration button. By using this window, the proper calibration factors can be set for the accelerometer, laser and force sensor (if used). In addition the configuration file can be saved and then reloaded at a later time.

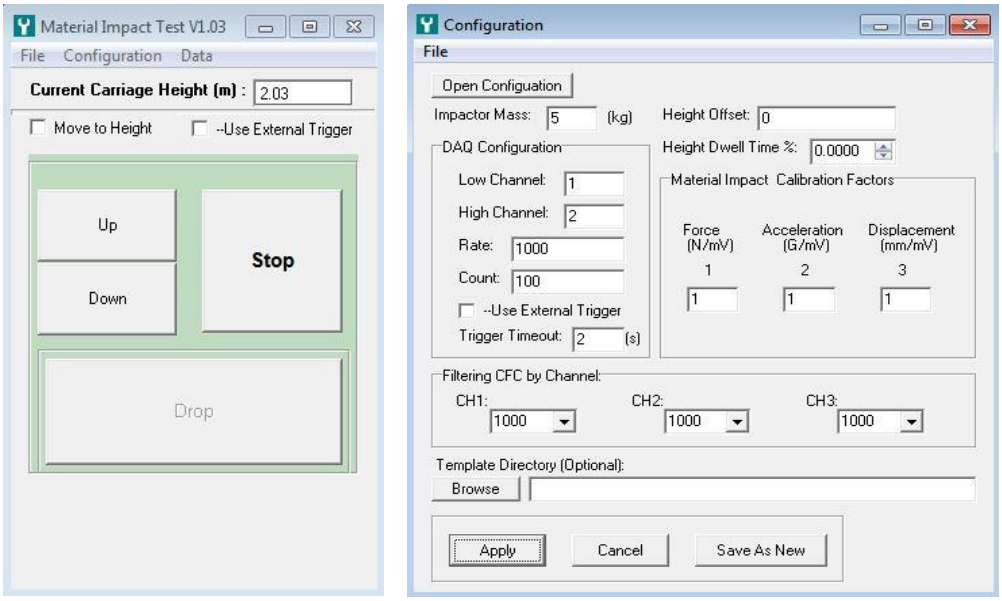

A) B)

Figure 2-9 - Data acquisition program interface.

The system also contains a displacement laser control unit that is responsible to condition the laser signal and to sense the error in the displacement laser. When the tester resets the apparatus according to the thickness of the sample it is necessary that the light beam of the displacement laser reflects from the bottom surface of the impactor. In Figure 2-10A, the error light is not lit which means the displacement laser is correctly reading. On the other hand, the picture B shows there is an error which means we have to change the location of the displacement laser. To make sure that the apparatus will read all the data correctly, the tester has to lift the fly arm to the required impact head and check the device below whether there is an error or not at the estimated maximum and minimum locations.

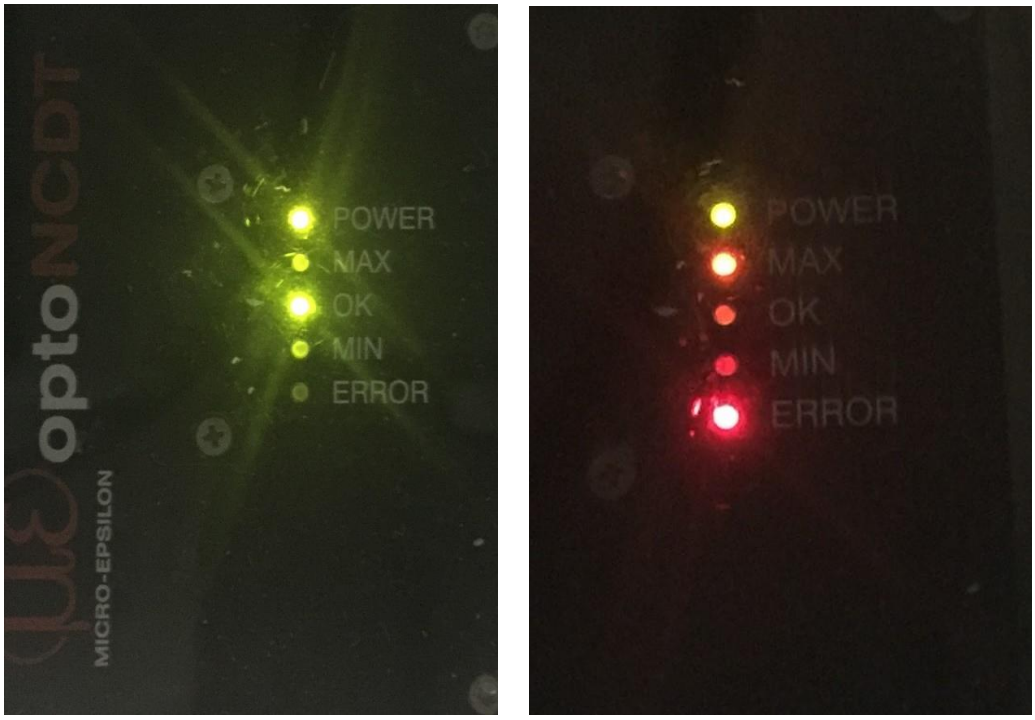

A) B)

Figure 2-10 - No error (A) and Error (B) of the displacement laser reading.

2.2 **Test Procedure**

The step impact tests are conducted where the drop arm is incrementally raised by a set amount. Acceleration is limited to 300g to protect the test equipment. The procedure for testing the impact resisting materials is summarized as follows:

1- Place the sample between the anvil and the fly arm. The sample should be placed beside the open slot of the anvil and the center of the sample should be under the center of the impactor as shown in the Figure 2-11. Also, the sample should be fixed on the anvil by using thin double sided cellophane tape (Distributed by ShurTeck Brand Company).

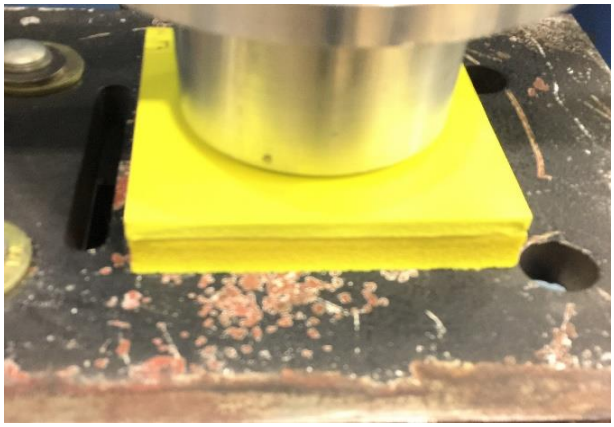

Figure 2-11 - Placement of the samples between the anvil and the impactor.

2- Zero the fly arm position. This is accomplished by reducing the speed of the fly arm positioner using the rate control and then moving the position until the bottom surface of the impactor touches the top surface of the sample without displacing the sample as shown in the Figure 2-12. Click on the zero menu item in the computer software.

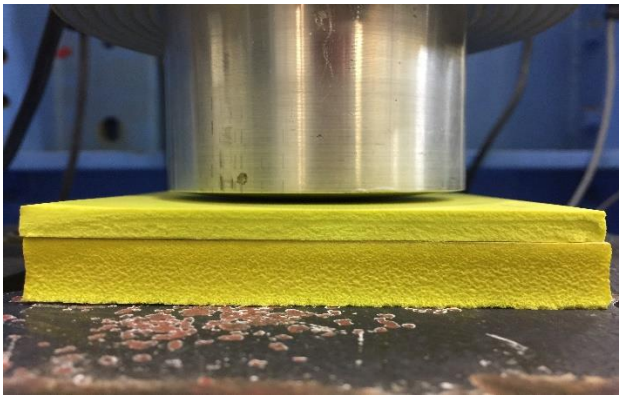

Figure 2-12 - Resetting the distance between the sample and the impactor.

3- Move the velocity gate position until the bottom red light of the laser turns off and the laser beam strikes the center of the tab with the impactor set at the top of the test sample as shown in the Figure (2-13).

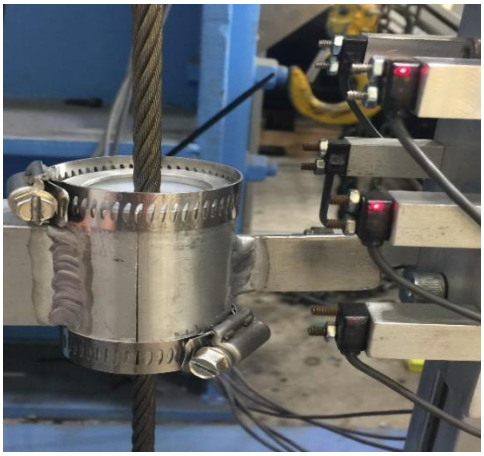

Figure 2-13 - Velocity gate laser after resetting.

4- Reset the apparatus from the controller by double clicking on the configuration and choosing the suitable configuration file for the controller. Figure (2-14) shows the three steps for resetting the apparatus. The Apply button needs to be clicked to activate the drop mechanism. After the configuration is activated, the tester needs to click on the configuration button and choose ‘’Zero Height” to finish the reset. If the configuration is saved after the zero reset, this zero position is stored in the configuration file.

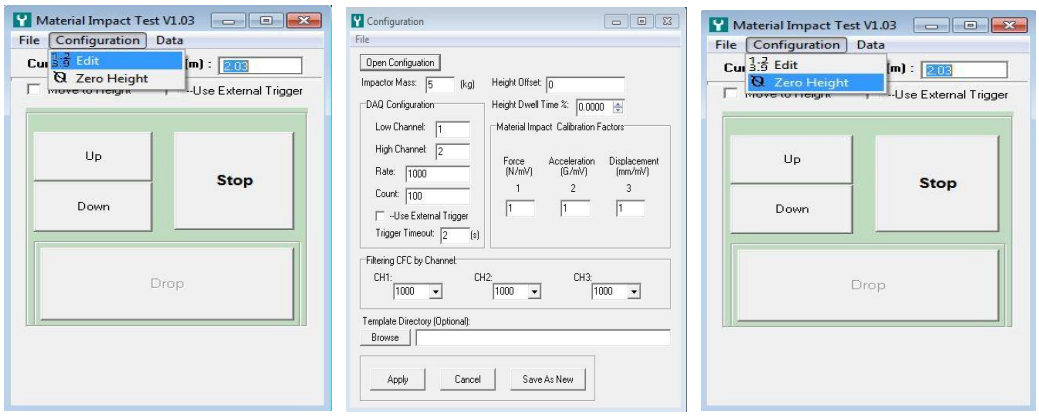

Step A) Step B) Step C)

Figure 2-14 - The three steps for resetting the apparatus.

5- Once the configuration is set correctly, the edit box that can be seen in the controller is used to enter the required impact height, and the tester can use it and then click on the button "Move" to move the drop arm to the entered impact height as shown in Figure 2-9. In general, the tester starts from impact height equal to 0.05m, and then increases the impact height by 0.05 m at every drop. ***It is important that the peak acceleration recorded in the testing is limited to 300g to avoid equipment failures.*** After the impactor is dropped, the window shown in Figure 2-15 will appear. The white boxes shown in the Figure below should be filled. Finally, clicking on "Write Data" to get the required data.

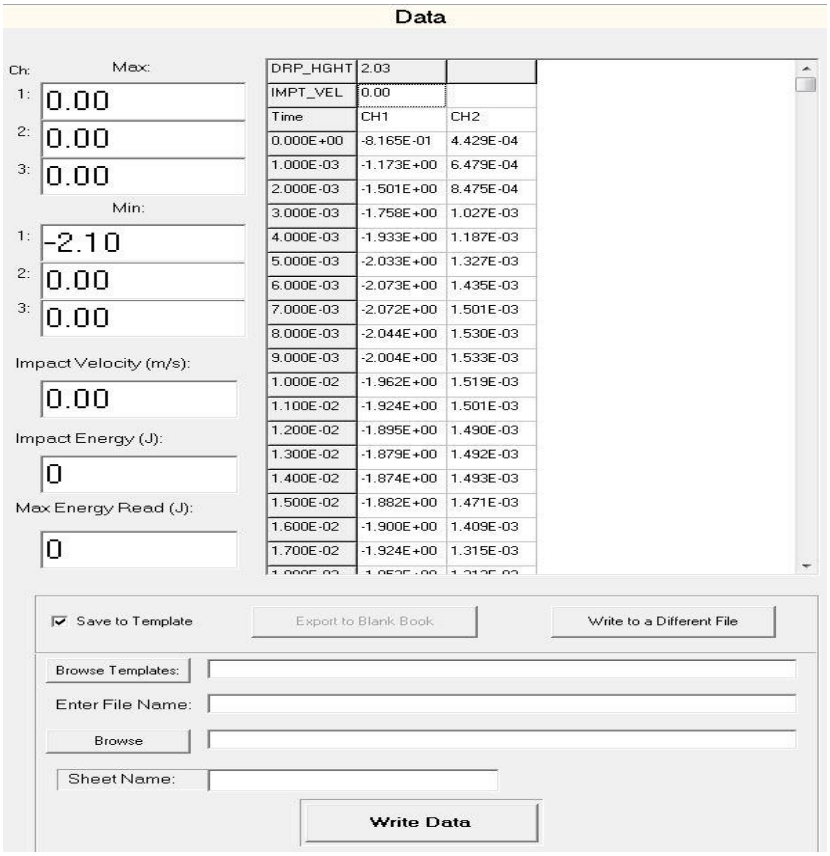

Figure 2-15 - Window that appears after first dropping of the impactor.

2.3 Common Problems

This section will discuss some of the problems regularly occur. The intention is to alert the user to these issues so that the problems can be avoided or easily resolved.

2.3.1 Connection Pin

This pin is responsible for connecting the fly arm holder to the fly arm. The pin is a quick release style with two small ball bearings that are located near the bottom end of the pin. Repeated use causes the ball bearings to wear and the pin becomes unable to connect to the fly arm holder coupling as shown in Figures (2-16A & B). Care should be taken that the fly arm does not accidentally drop as the pin wears. To solve this problem, the tester needs to replace the pin with a new one. To replace the pin, the tester has to remove the blue box shown in Figure (2-16C).

Another issue is that at times the pin does not release the fly arm when the tester clicks on the Drop button. This is typically caused by either the ball bearings sticking or an issue in the control system. An audible sound typically indicates that the control system is functioning and that the ball bearing is stuck.

A) B) C)

Figure 2-16 - A and B show the side and front views for crashed pin, respectively. C shows the blue box and the two black bolt.

2.3.2 **The Impactor Is Unbalanced**

The normal shape of the Force-Displacement graph is shown in Figure (2-17A). Figure 2-17 B shows a case where the force vs. displacement curve loops back on itself. This problem is typically due to the symmetric points of the bottom surface of the impactor not striking the top surface of the sample at the same time which means the fly arm is not horizontal. To solve this problem, the tester can place spacers under the lower side of the anvil. It is easy to check it visually.

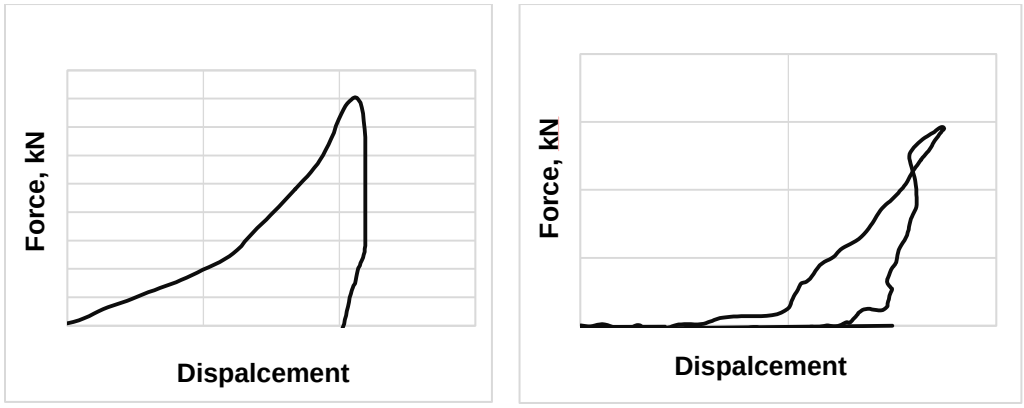

A) B)

Figure 2-17 - A and B show the right and wrong shapes of the Force-Displacement graph, respectively.

2.3.3 **Limitations of the Displacement Laser**

If the displacement of the samples is more than 2 inches, the displacement laser stops reading it as shown in the Figure 2-18. To solve this problem, we should use a laser that has the ability to read a distance greater than 2 inches.

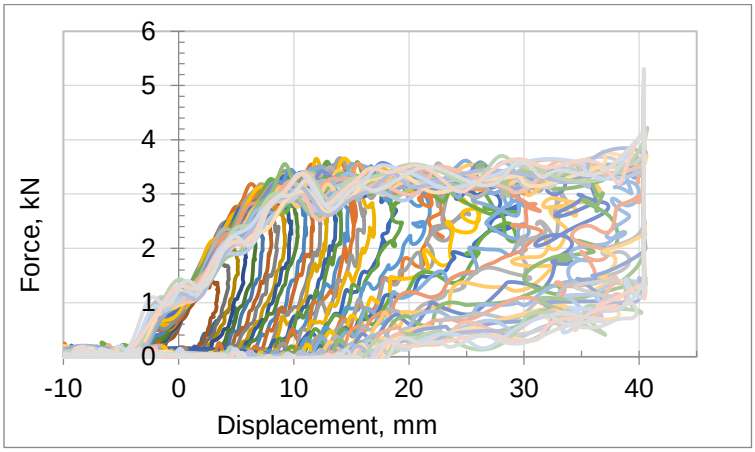

Figure 2-18 - The range reading of the displacement laser.

2.3.4 **Dilatant Material Failure.**

Figure 2-19 shows the shearing in the dilatant materials during the test. For solving this problem reinforcing can be used to protect the dilatant material.

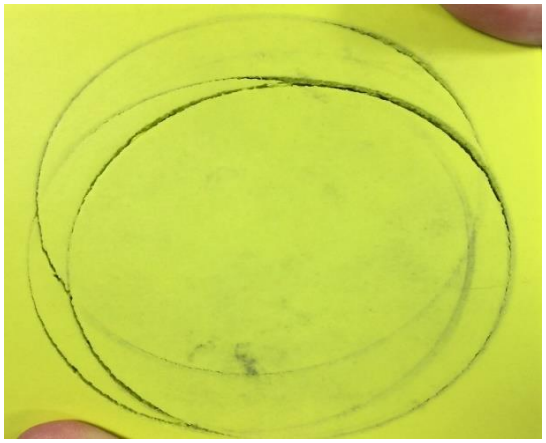

Figure 2-19 - Dilatant material failure during the test.

CHAPTER THREE

TEST RESULTS

As shown in the Figure 3-1, two kinds of protection materials are used in the research, namely a cellular honeycomb structure and dilatant foam. The dilatant materials studied are classified according to the density of material and is designated as P09, P15 and P25. Also, there are several thicknesses for each of these materials. The second one is cast urethane honeycomb material with varying cellular structure. This material can be classified according to cell dimensions, shape and material stiffness. The most common shape is the regular hexagonal honeycomb material. According to the stiffness of the honeycomb material, we can classify the honeycomb materials as H561, H781, H1036 and H1056 material. Also, all of the H561, H781, H1036 and H1056 material have several different cell dimensions, and an additional classification is according to the cell shape. The used impactor for all of the testing presented in this section is the spherical impactor "R-127 mm".

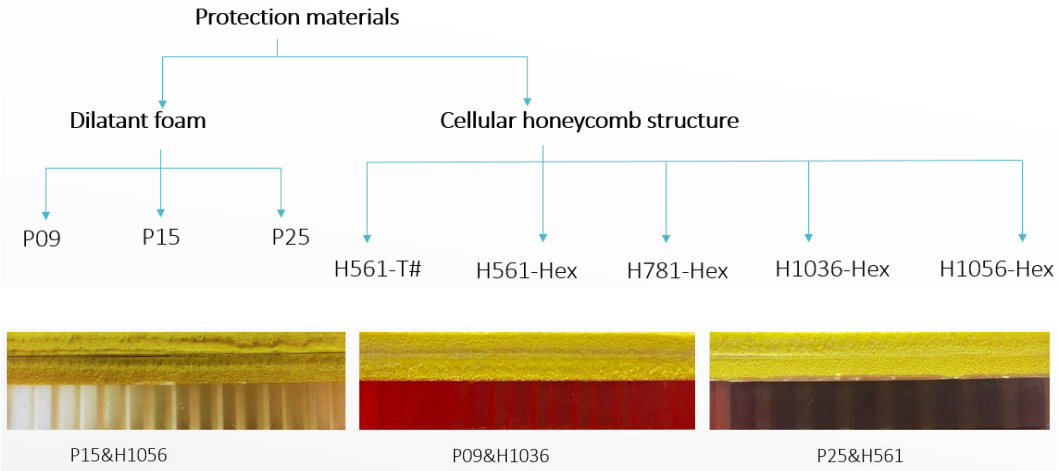

Figure 3-1 - Protection materials diagram.

The first phase of tests were conducted for single layer material of either a honeycomb structure or dilatant foam. The important information collected from these tests is the acceleration, force, impact height, velocity, energy and time history. Graphs of the acceleration-impact height, force-displacement, acceleration-time are provided in this section.

The second testing phase is with multi-layered samples. At first, several layered architectures with two layers were studied. All of the two layers samples consist of the foam dilatant material at the top and honeycomb material at the bottom. These two layers samples can be classified according to the thickness as 12.5 mm and 24.5 mm. The thickness of 12.5 mm consists of a 6 mm thickness dilatant material and 6.5 mm thickness honeycomb materials. The thickness of 24.5 mm consists of 12 mm dilatant materials and 12.5 mm honeycomb material. Samples using a variety of the dilatant materials P09, P15 and P25. Also, regarding to the honeycomb materials, we used the hexagonal shape of the H561, H781, H1036 and H1056 honeycomb materials.

Furthermore, we have tested four and five layers samples. All of the four and five layers consist of individual dilatant and honeycomb layers at different thicknesses.

The testing method employed a step impact type test where the impactor height was incrementally increased until the 300 g test system limit was achieved.

The calculation of the potential energy, J, impact velocity, V, and the acceleration, a, was performed using the basic theoretical equations below.

$$J = m*g*h \quad (3.1)$$

Where: g: gravity acceleration equal to 9.81 $^{m}/_{s^2}$

m: the total mass of the impactor equal to 5 kg.

h: The impact height.

$$V = \sqrt{2 * g * h} \quad (3.2)$$

V: The theoretical velocity when the impactor hits the sample

J: the potential energy,

V_o: The initial velocity of the impactor,

V_f: The final velocity of the impactor.

3.1 **Dilatant Material Test Results**

In this part we will show the tests results of the dilatant materials. This material is considered to be a dilatant hyper-elastic foam. Properties of the dilatant materials are summarized in Table 3-1. Provided is the nominal density (The nominal density is measured by ASTM D3574-95 Test A, xrd.tech [18].), measured density, nominal hardness and measured hardness values for these materials and the thickness that were available for this research where the dilatant material can be classified according to materials density as P09, P15 and P25 material. Also, these materials are categorized according to material thickness to several thickness. For example P15 material has five different thicknesses. The same mass (5kg) and

shape (127 mm radius spherical) of the impactor are used. Furthermore, all samples have a square profile with the length and width, namely "100mm x 100mm".

Table 3-1 - Available dilatant materials.

Material	Nominal Density kg/m^3	Measured Density kg/m^3	Available Thicknesses mm	Nominal Shore 'o' Hardness
P09	144.166	156.3	6 and 12.7	10
P15	240.277	242.5	3, 4, 6, 9.5 and 12.7	32
P25	400.462	398.3	2, 3, and 6	-

3.1.1 **P09 Material**

This section gives the impact test results for the P09 material. The P09 material was available in two thickness of 6 mm and 12.7 mm.

3.1.1.1 **The Maximum Acceleration during Step Impact Height of P09 Material.**

The maximum acceleration due to step impact is shown in the Figure 3-2. According to the tests and the maximum acceleration response P09 material behaves as a relatively soft material at the lower impact height. As bottoming out occurs the behavior of this material changes at the higher impact height and it behaves in a stiff manner. The P09 material at thickness of 6.0 mm behaves in a relatively stiff material almost from the onset and it acceleration response increases dramatically until it reaches the acceleration of 250.0 g at the impact height of 0.3

m. The P09 material at the thickness 12.7 mm changes more gradually and it reaches the acceleration of 250.0 g at impact height equal to 0.78m.

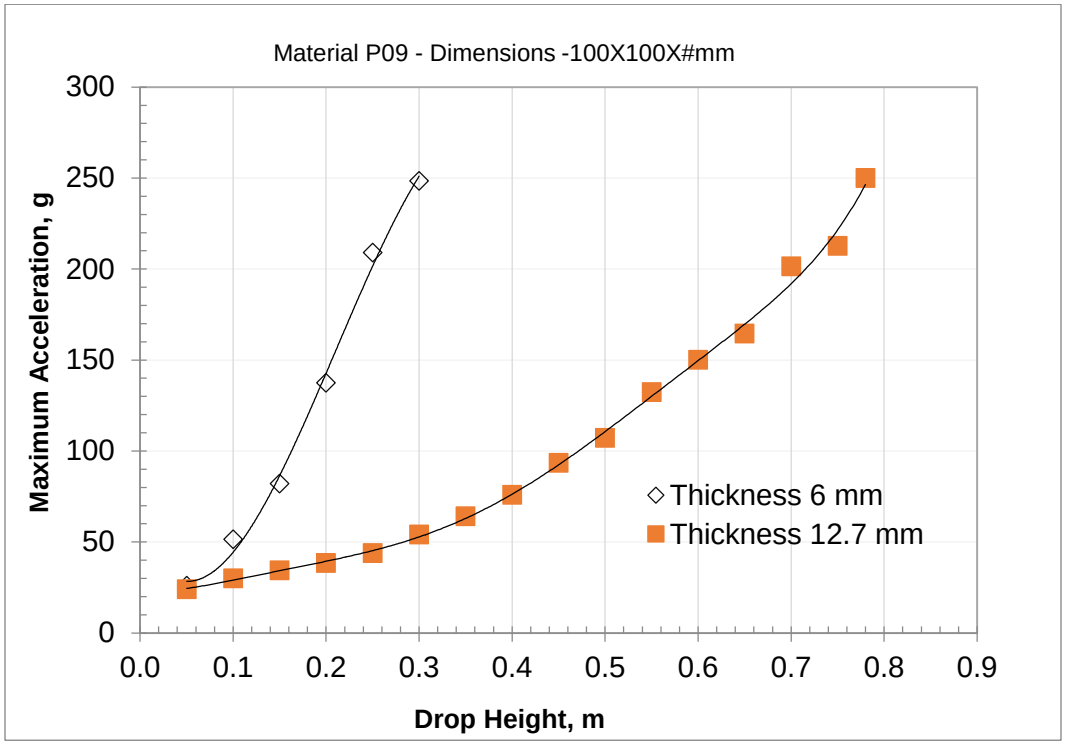

Figure 3-2 - The acceleration behavior of P09 material for various thicknesses.

3.1.1.2 **Force vs Displacement of P09 at Various Thicknesses**

Results of the force versus displacement for the 12.7mm thick P09 material will be presented here as shown in Figure 3-3 and the curves for the 6mm thickness are given in Appendix C. The response is presented at six impact heights ranging from 0.05m to 0.8m. A high percentage of consolidation is expected for the P09 material because it is relatively soft. At a force of 12kN the displacement reaches a value of 11.0mm that is 86.6% of the total thickness of the sample. Also observed

is that the curve at the larger height envelopes the other curves and that the initial slope at the lower impact heights is virtually the same as the higher drop height.

The load versus displacement curves for the thickness 6.0 mm can be seen in the Appendix C and shows at a force of 12kN the displacement reaches a value of 4.9mm that is 82% of the total thickness of the sample.

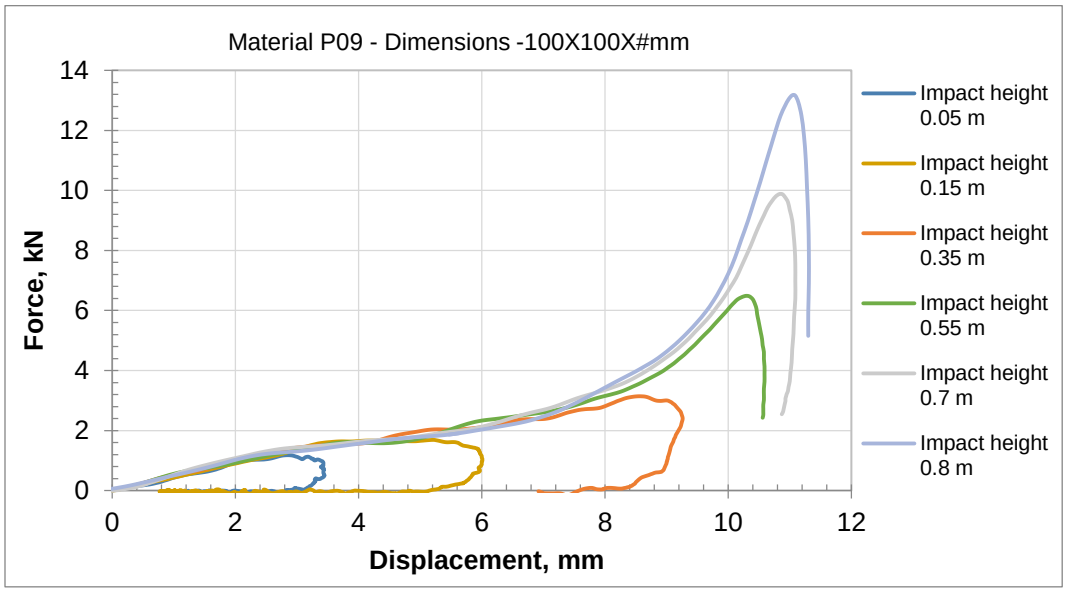

Figure 3-3 - The force versus displacement of the 12.7mm thick P09 material.

3.1.1.3 **Acceleration Time History for P09 Material.**

Figure 3-4 shows the time history at stepped impact heights for the 12.7 mm thick P09 material. It is clear as shown in the figure that the higher impact height gives greater acceleration and shorter time period. At an impact height of 0.8m, the impact period reaches a value of 0.008sec while at an impact height of 0.4m, the impact period reaches a value of 0.0101sec.

The time history at stepped impact height for the 6.0 mm thick P09 material can be seen in Appendix D and shows at the impact height 0.3m, the impact period reaches a value of 0.0063sec while at impact height 0.1m, the impact period reaches a value of 0.0071sec.

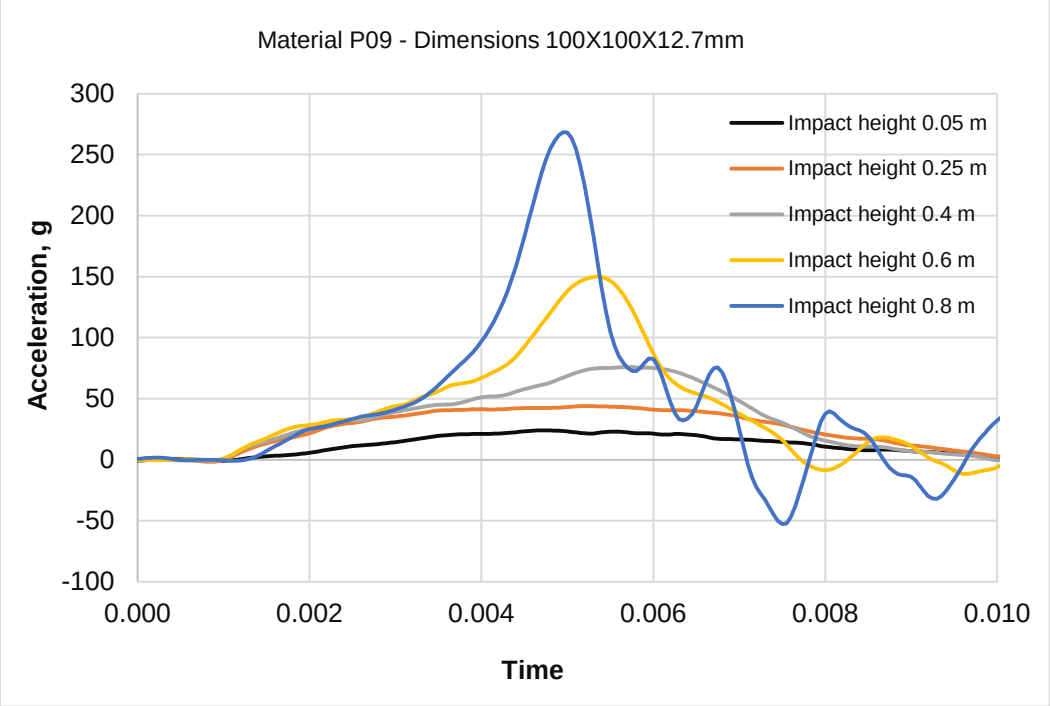

Figure 3-4 – The acceleration time history of the 12.7mm thick P09 material.

3.1.2 **P15 Material.**

The P15 material was available in thickness of 3 mm, 4 mm, 6 mm, 9.5 mm and 12.7 mm. It is stiffer than P09 which is also indicated by its nominal Shore "O" durometer of 32, [18].

3.1.2.1 The Maximum Acceleration during Step Impact Height of P15 Material.

The maximum acceleration during step impact of the five different thicknesses of the P15 material are shown in Figure 3-5. The P15 material at thicknesses of 3.0 mm and 4.0 mm behave in a relatively stiff material almost from the onset and it acceleration response increases dramatically until they reach the acceleration of 250.0 g at the impact heights of 0.23m and 0.32m, respectively. The 15 material at the thicknesses 6.0mm, 9.5mm and 12.7mm changes more gradually and they reach the acceleration of 250.0 g at impact heights equal to 0.59m, 1.0m and 1.5m, respectively.

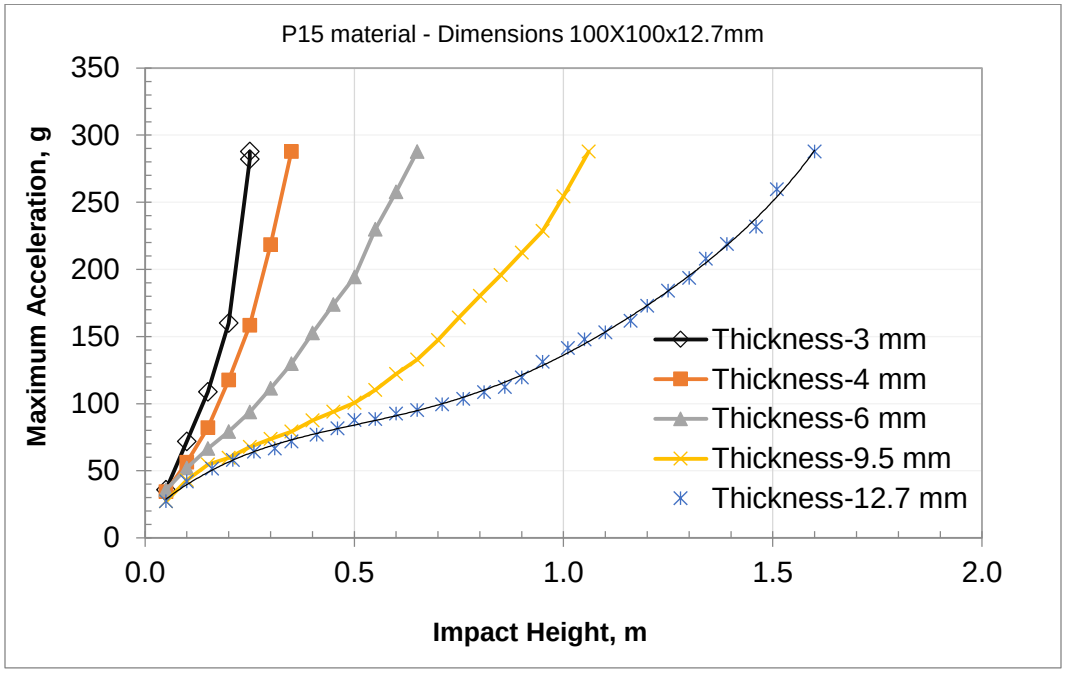

Figure 3-5 - The acceleration behavior of P15 material for various thicknesses.

3.1.2.2 Force vs Displacement of P15 Material for Various Thicknesses

Load versus displacement curves for the 12.7 mm thick P15 material is shown in Figure 3-6 as an example. The load versus displacement curves for the other thicknesses of 3.0 mm, 4.0 mm, 6.0 mm and 9.5 mm are provided in Appendix C. At a force of 12kN the displacement for the 12.7mm thick material is 9.0mm which is 70.9 % of its total thickness. Also, at 12kN the displacements of thicknesses 3.0 mm, 4.0 mm, 6.0 mm and 9.5 mm are 2.25mm, 2.95mm, 4.08mm and 7.1mm, respectively. This corresponds to percentage of total thickness of 75.0%, 73.8%, 68.0% and 74.7%, respectively.

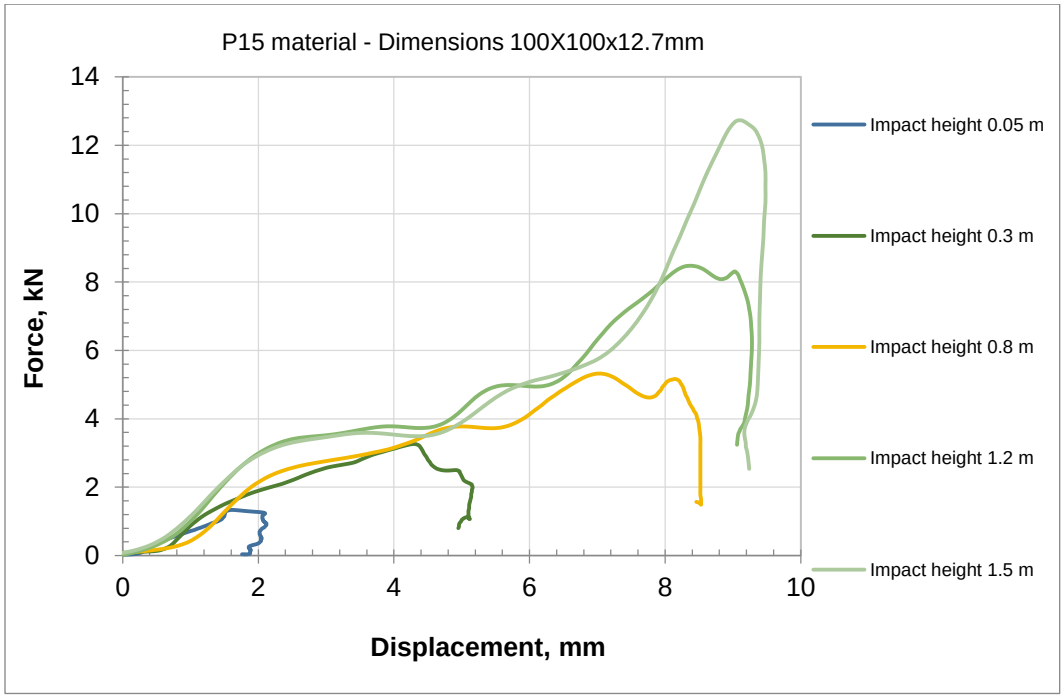

Figure 3-6 – Force versus displacement of the P15 material at thickness of 12.7 mm.

3.1.2.3 **Acceleration Time History for P15 Material.**

Figure 3-7 shows the time history at 5 different impact heights for the 12.7 mm thick P15 material. The higher impact height gives greater acceleration and shorter period time because the P15 material consolidates increasingly more as the impact energy increases. At an impact height of 1.5m, the impact period reaches a value of 0.006sec while at an impact height of 0.4m, the impact period reaches a value of 0.07sec.

The time history at stepped impact height for the thicknesses 3.0 mm, 4.0 mm, 6.0 mm and 9.5 mm of the P15 material can be seen in the appendix D and show the higher impact heights give shorter impact period. For example the thicknesses 9.5 mm, at an impact height of 1.0m, the impact period reaches a value of 0.0074sec while at an impact height of 0.6m, the impact period reaches a value of 0.077sec.

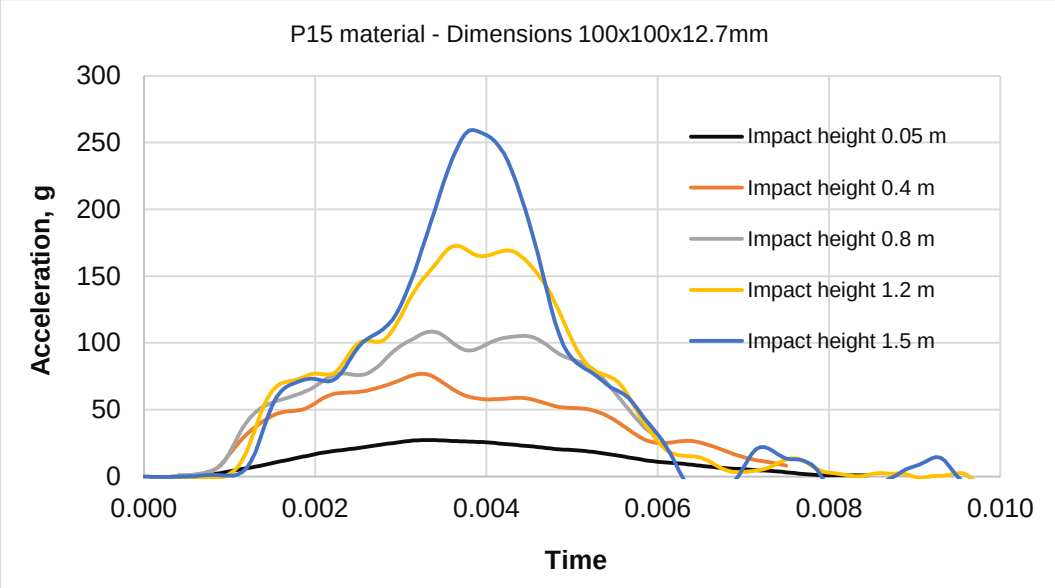

Figure 3-7 – The acceleration time history of the 12.7mm thick P15 material.

3.1.3 P25 Material

The P25 material was available for this study in thicknesses of 2 mm, 3 mm, and 6 mm. According to the information that has been collected during the tests in the lab, P25 material is stiffer than P15 material, which is indicated by its nominal density. The same mass (5kg) and shape (127 mm radius spherical) of the impactor are used. Furthermore, all samples have the same length and width, namely "100mm x 100mm".

3.1.3.1 The Maximum Acceleration during Step Impact Height of P25 Material.

The maximum acceleration due to step impact of the 2.0 mm, 3 mm and 6.0 mm samples is shown in the Figure 3-8. The P25 material at thickness of 2.0 mm behaves as very stiff material and it increases acceleration dramatically at lower drop heights. It reaches the acceleration of 250.0 g at the impact height of 0.19 m. Also, the P25 material at the thicknesses 3 mm changes kind of gradually and it reaches the acceleration of 250.0 g at impact height equal to 0.3 m. Moreover, the 6mm thick P25 material does not reaches the acceleration of 250.0 g until impact height of 0.56 m.

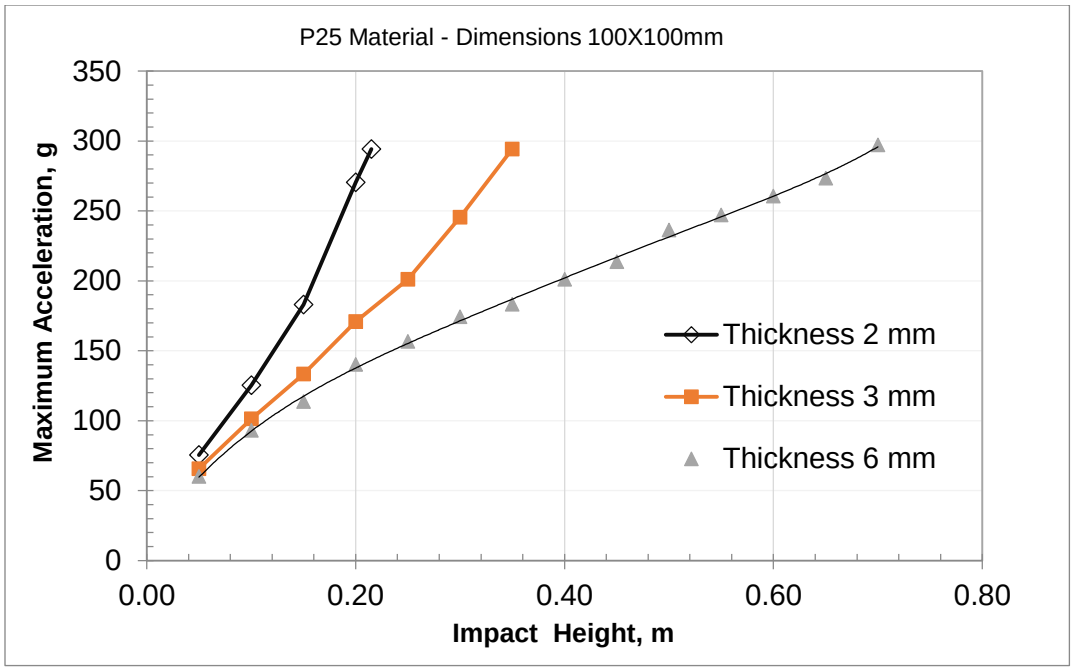

Figure 3-8 - The acceleration behavior of P25 material for various thicknesses

3.1.3.2 **Force vs Displacement of P25 Material.**

Load versus displacement curves for the 6.0 mm thick P25 material is shown in Figure 3-9. At a force of 12kN the displacement for the 6mm thick P25 material is 2.94mm which is 49 % of its total thickness.

The load versus displacement curves for the thicknesses 2.0 mm, and 3.0 mm are presented in Appendix C. Also, at 12kN the displacements of thicknesses 2.0 mm and 3 mm are 1.5mm and 1.95mm, respectively. This corresponds to percentage of total thickness of 75.0% and 65.0%, respectively.

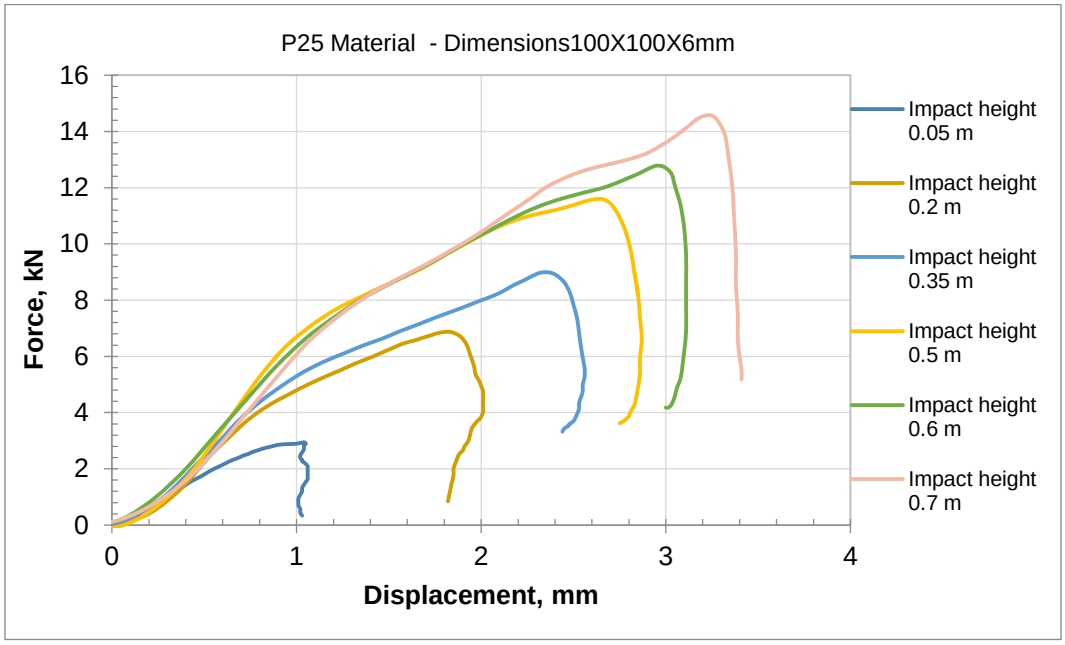

Figure 3-9 - The force versus the displacement of the 6mm thick P25 material.

3.1.3.3 **The Acceleration Time History for P25 Material.**

Figure 3-10 shows the time history at several stepped impact height for 6 mm thick P25 material. It is clear as shown in the figure that, similar to P09 and P15, the higher impact height gives greater acceleration and shorter impact period. Estimates of the impact periods are 0.0028sec and 0.0031sec for drop heights of 0.7m and 0.2m, respectively. The time history at stepped impact height for the thicknesses 2.0 mm and 3.0 mm of the P25 material can be seen in Appendix D. For the thickness 2 mm, estimates of the impact periods are 0.0023sec and 0.0027sec for drop heights of 0.2m and 0.1m, respectively.

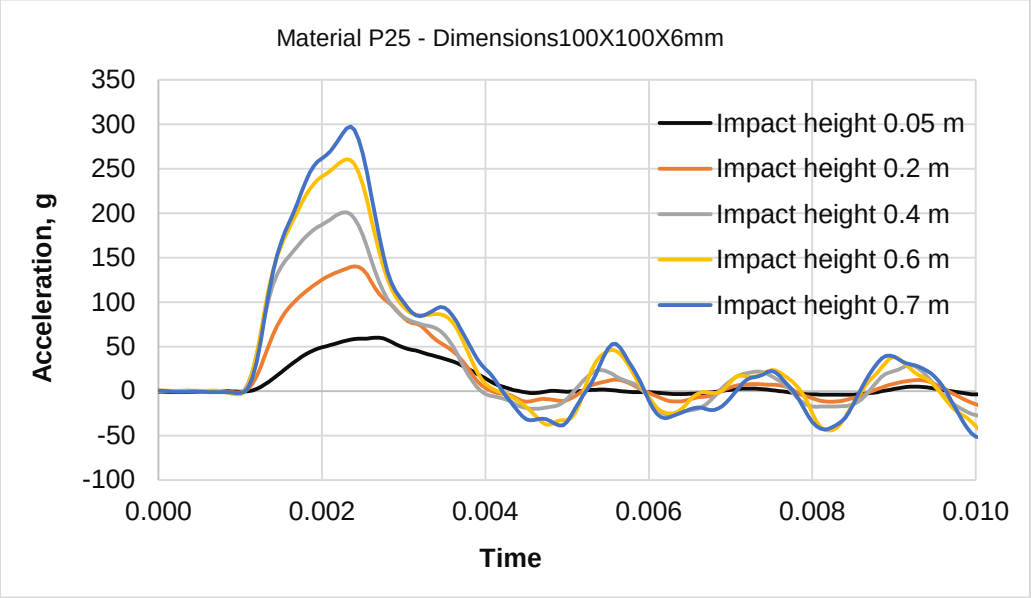

Figure 3-10 - Acceleration time history of the P25 material at the thickness of 6.0mm.

3.2 **Honeycomb Material**

The honeycomb material is another single layer material that was tested. It has a varying cellular structure that can be classified by cell shape, cell size, cell wall thickness, total thickness and material hardness (durometer). Figure 3-11 A shows the most common honeycomb shape which is the regular hexagonal In addition, 3 irregular cell structures named T1, T2 and T3 were tested as shown in the Figure 3-11B, C and D. The hexagonal shape was tested for the material variants H781, H1036 and H1056. The H561 material was tested in the regular hexagonal shape and the 3 irregular shapes. The same mass (5kg) and shape (127 mm radius spherical) of the impactor are used. Furthermore, all square samples have the same length and width, namely "100mm x 100mm". In addition circular shaped samples were studied with the diameter of 100 m.

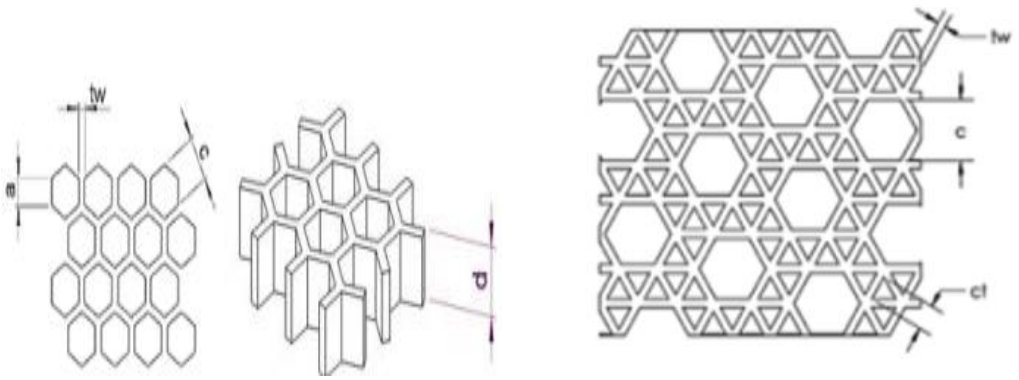

A) **B)**

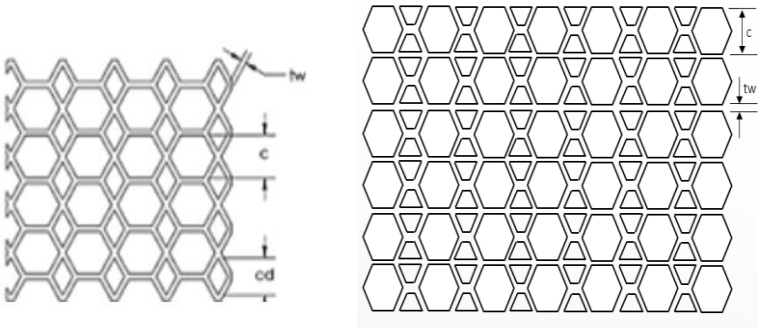

C) **D)**

Figure 3-11 - Side view and top view (A) of the regular shape, (B), (C) and (D) three irregular cell structures named T1, T2 and T3, respectively.

Properties of the honeycomb materials are summarized in Table 3.2. Provided is the nominal density and reported Shore A hardness values for these materials and the geometric parameters that were available for this research.

Table 3-2 - Summary of the honeycomb material properties.

Material	Nominal durometer	Measured durometer	No. of samples	Density g/cm^3
H561	65A	66.0	13	1.06
H781	80A	81.6	2	1.01
H1036	35A	29.4	3	1.16
H1056	55A	47.5	2	1.16

Dimensions are summarized in Table 3.3. Provided Structure cell size (c), cell wall thickness (tw), side length (a) and solid ratio (SR) of the honeycomb materials.

Table 3-3 - Honeycomb cell structure designation.

Designator	Structure	Cell size, c mm	Cell wall thickness, tw, mm	Side length (a) mm	a/tw	Solid ratio SR
H561 - Hex 3 x 0.8	Regular Hex	3	0.8	1.7	2.2	0.51
H561- Hex 3 x 1.0	Regular Hex	3	1	1.7	1.7	0.63
H561- Hex 4.7625 x 1.0	Regular Hex	4.7625	1	2.7	2.7	0.41
H561- Hex 6.0 x 1.0	Regular Hex	6	1	3.5	3.5	0.32
H561- Hex 8.0 x 1.0	Regular Hex	8	1	4.6	4.6	0.24
H781- Hex 4.7625 x 1.0	Regular Hex	4.7625	1	2.7	2.7	0.41
H781- Hex 4.7625 x 1.5	Regular Hex	4.7625	1.5	2.7	1.8	0.60
H1036- Hex 3 x 1.0	Regular Hex	3	1	1.7	1.7	0.63
H1036- Hex 4.7625 x 1.0	Regular Hex	4.7625	1	2.7	2.7	0.41
H1036- Hex 4.7625 x 1.5	Regular Hex	4.7625	1.5	2.7	1.8	0.60
H1056- Hex 4.7625 x 1.0	Regular Hex	4.7625	1	2.7	2.7	0.41
H1056- Hex 4.7625 x 1.5	Regular Hex	4.7625	1.5	2.7	1.8	0.60

3.2.1 **H1056 Material**

In this section, the response of H1056 material will be shown. The H1056 material is shown in the Figure 3-12. Two different wall thicknesses, t_w, of cells are used, namely, 1.0 mm and 1.5 mm. The material thickness, d, is kept constant at 12.5 mm. Also, a square shape sample is used. The cell size, c, is kept constant at 4.7 mm for both wall thickness.

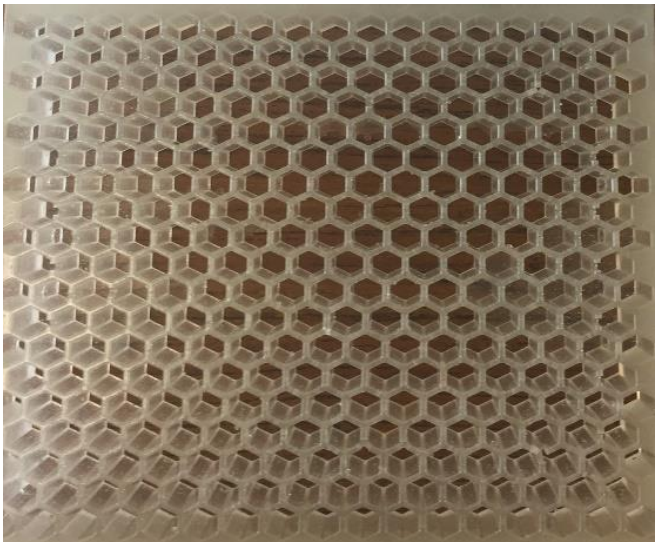

Figure 3-12 - H1056 material

3.2.1.1 **The Maximum Acceleration during Step Impact Height of H1056 Material.**

The maximum acceleration due to step impact of the 1.0 mm and 1.5 mm wall thicknesses are shown in Figure 3-13 for the honeycomb made of the H1056 material. The H1056 material at wall thickness of 1.0 mm behaves as a soft material at the lower impact height and it increases gradually until an impact height of 0.2 m where it behaves as stiffer material during consolidation. It reaches 250.0 g maximum acceleration at the impact height of 0.47 m. The H1056 changes more gradually at a wall thickness of 1.5 mm and it reaches a maximum acceleration of

250.0 g at impact height equal to 0.65 m. Little change in peak acceleration is observed at drop height between 0.1 m to 0.2 m as the peak force response is limited by buckling.

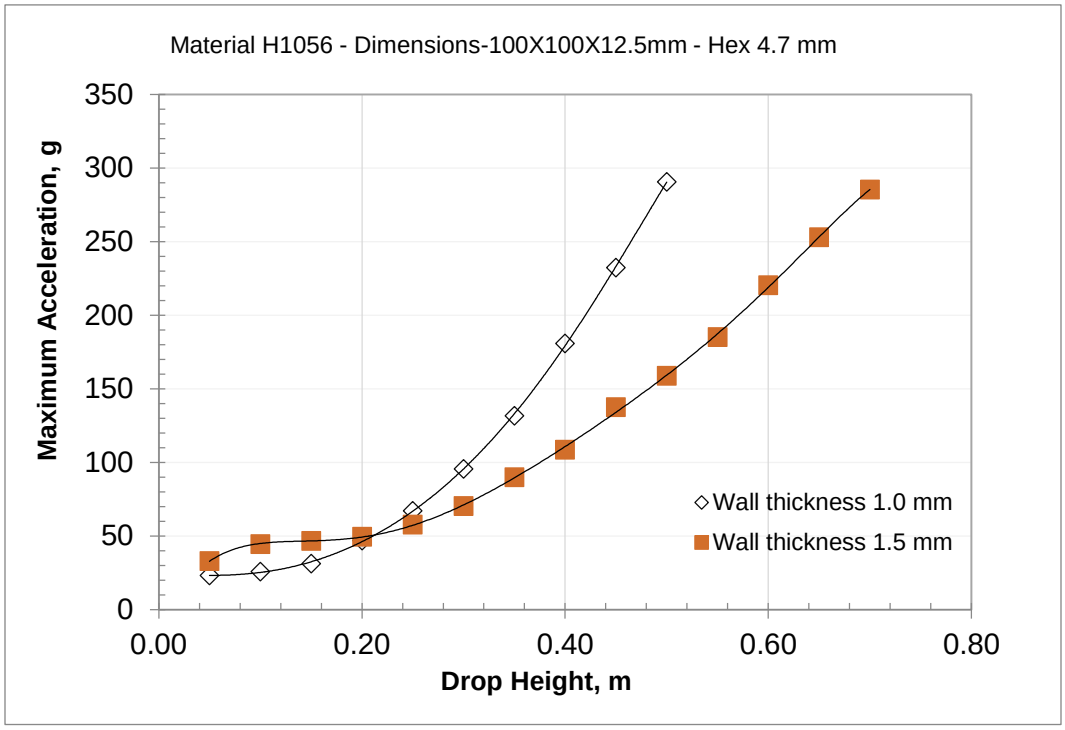

Figure 3-13 - The acceleration behavior of H1056 material for various wall thicknesses.

3.2.1.2 **Force vs Displacement of H1056 Material.**

Load versus displacement curves for the wall thickness 1.0 mm of H1056 material is shown in Figure 3-14 at different drop heights. The load versus displacement curves for the wall thickness of 1.5 mm are provided in Appendix C. It is expected that the displacement percentage for the H1056 material will be

relatively high because it is a soft material. At a force of 12kN the sample with a wall thickness of 1.0 mm results in a peak displacement of 9.2 mm, which is a displacement percentage of 73.6 %. The displacement of the 1.5 mm wall thickness sample is 8.8 mm corresponding to a displacement percentage of 70.4%.

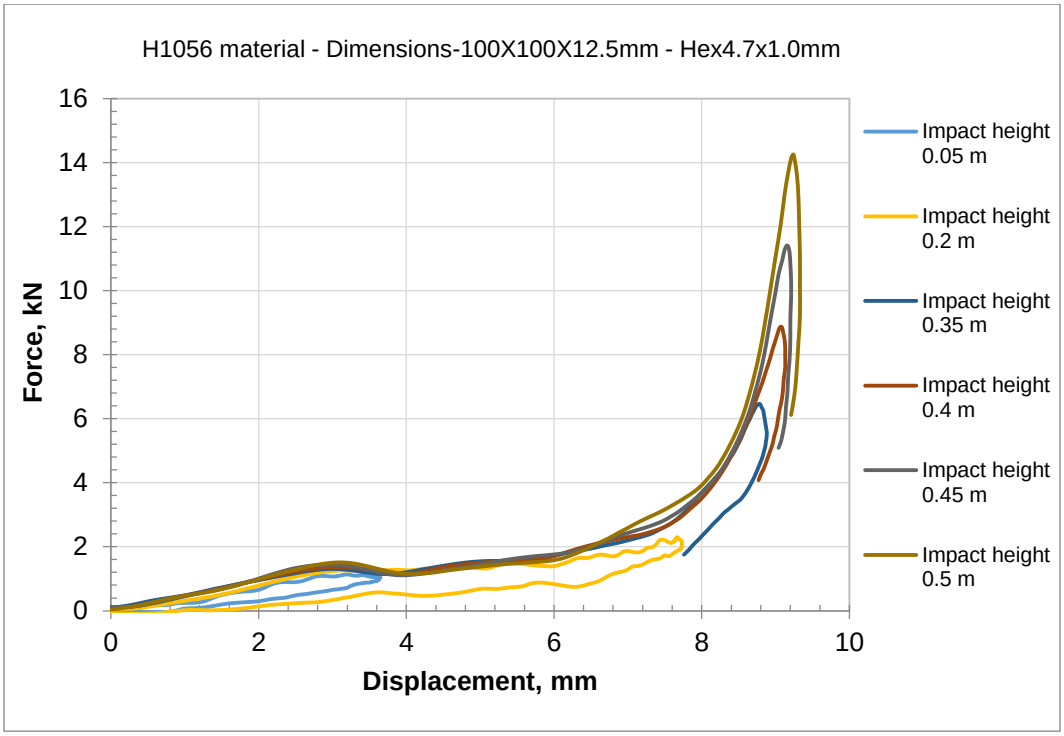

Figure 3-14 - The force versus the displacement of the H1056 material at the wall thickness 1.0 mm.

3.2.1.3 **The Acceleration Time History for H1056 Material.**

Figure 3-15 shows the time history at stepped impact height for the 1.0 mm wall thickness of the H1056 material. It is clear as shown in the figure that the higher impact height gives greater acceleration and shorter period. Estimates of the impact periods are 0.008sec and 0.012sec for drop heights of 0.5m and 0.2m, respectively.

The time history at stepped impact height for the wall thicknesses 1.5 mm of the H1056 material can be seen in the appendix D and shows the impact periods are 0.0066sec and 0.0088sec for drop heights of 0.7m and 0.45m, respectively

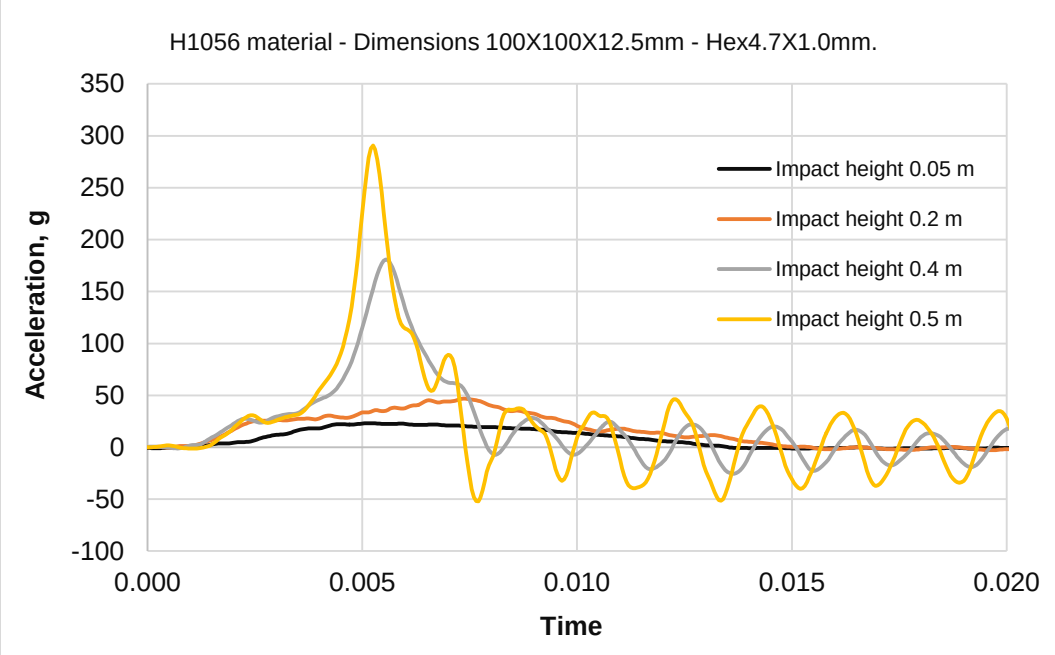

Figure 3-15 - Acceleration time history of the H1056 material at the wall thickness of 1.0mm.

3.2.2 **H1036 Material**

In this section, the response of H1036 material will be shown. The H1036 material is shown in the Figure 3-16. Three different cells dimensions are used, namely, Hex3.0x1.0mm, Hex4.7x1.0mm and Hex4.7x1.5mm. The material thickness, d, is kept constant at 12.5 mm. Also, square shape of the sample is used.

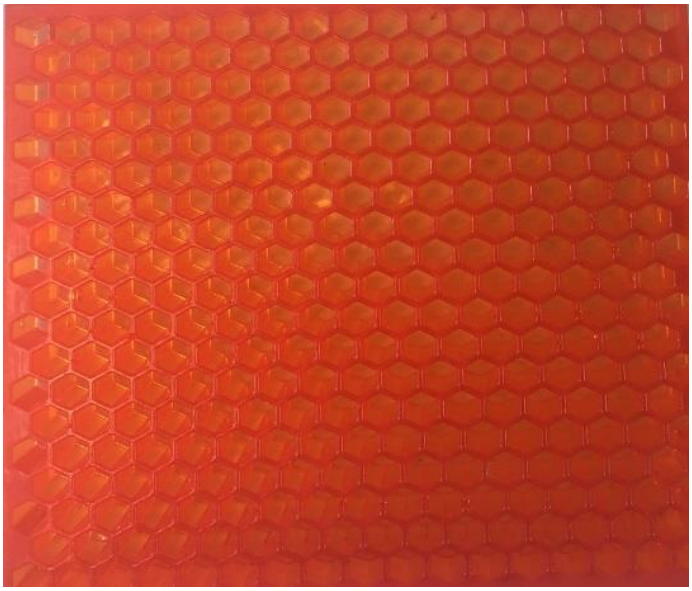

Figure 3-16 - H1036 material.

3.2.2.1 The Maximum Acceleration during Step Impact of the H1036 Material.

The maximum acceleration due to step impact of the Hex3.0x1.0mm, Hex4.7x1.0mm and Hex4.7x1.5mm cell dimensions are shown in the Figure 3-17. The H1036 material at cell dimensions of Hex3.0X1.0mm behaves as a soft material at the lower impact height and its response increases gradually until impact height 0.2 m then it behaves as a stiffer material due to consolidation. It reaches the acceleration of 250.0 g at the impact height of 0.6 m. The H1036 material at the cell dimensions of Hex4.7X1.5, it gave the similar results to the cell dimensions of Hex3.0X1.0mm because the solid ratio SR (See Section 1.2.1.1 Chapter one) is the same for both. Finally, the cells dimensions of Hex4.7X1.0mm behave as a relatively soft material and it reaches the acceleration of 250.0 g at impact height equal to 0.42 m.

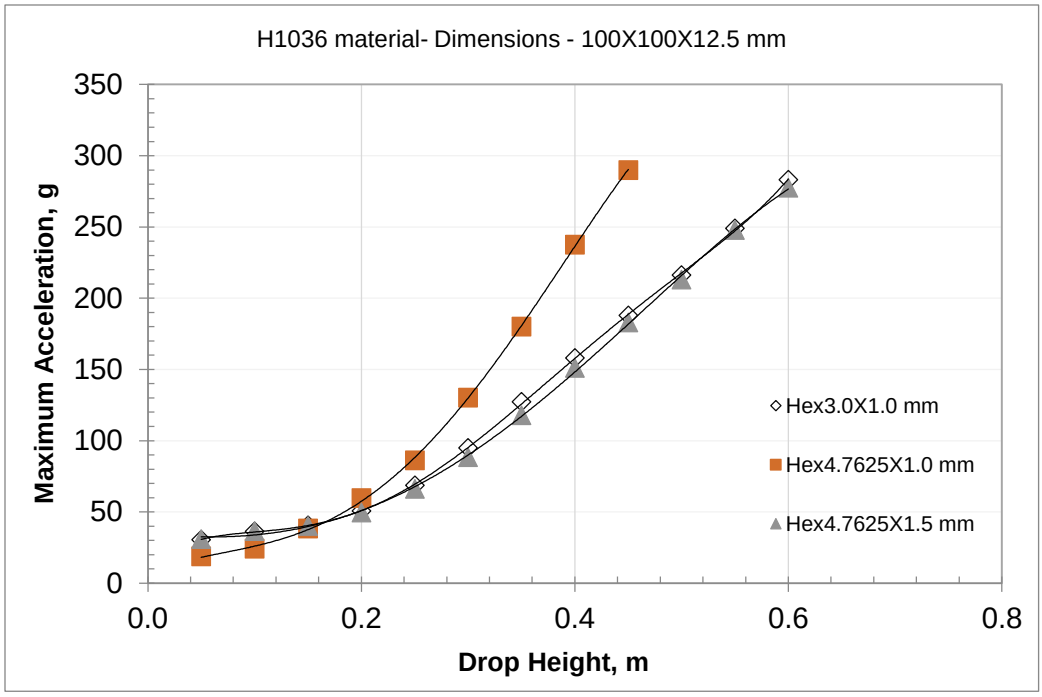

Figure 3-17 -The acceleration behavior of H1036 material for various cells dimensions

3.2.2.2 **Force vs Displacement of H1036 Material for Various Cells Dimensions.**

Load versus displacement curves for the cell dimensions of Hex3.0x1.0mm for the H1036 material is shown in Figure 3-18. At a force of 12kN, the displacement of the cell dimensions of Hex3.0x1.0mm is 8.5 mm which corresponds to the displacement percentage of 68.0 %. The load versus displacement curves for cells dimensions of Hex4.7X1.0mm and Hex4.7X1.5mm can be seen in Appendix C and shows the displacement at a force 12kN are 9.2 mm and 8.5 mm, respectively corresponding to displacement percentage 73.6% and 0.68% respectively.

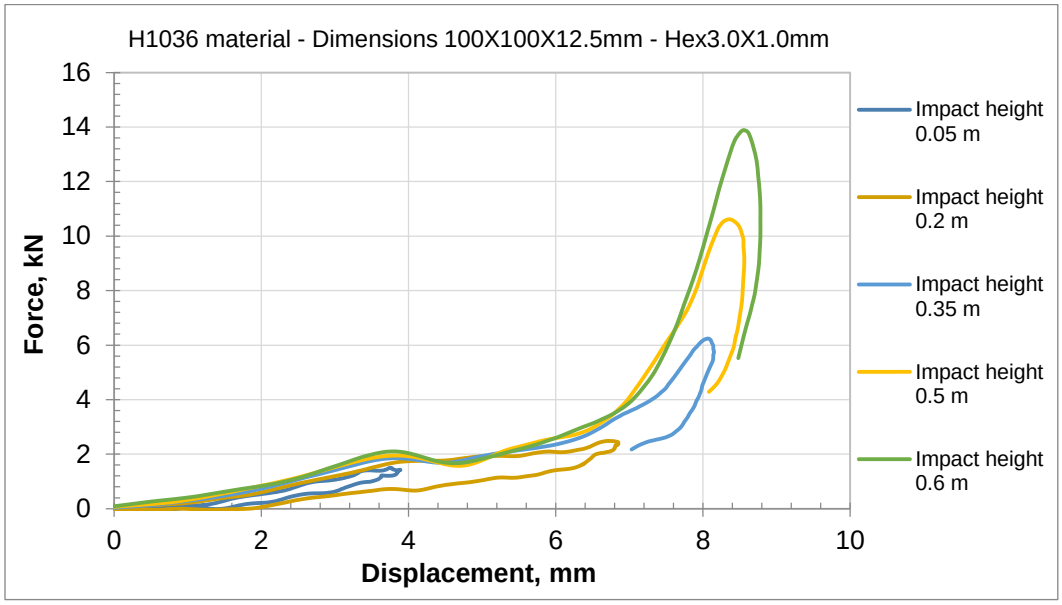

Figure 3-18 - The force versus the displacement of the H1036 material at the cells dimensions Hex3.0X1.0mm.

3.2.2.3 **The Acceleration Time History for H1036 Material.**

Figure 3-19 shows the time history at various step impact heights for the cell dimensions of Hex3.0x1.0mm of the H1036 material. It is clear as shown in the figure that the higher impact height gives greater acceleration and shorter time period time. Estimates of the impact periods are 0.0066sec and 0.01sec for drop heights of 0.6m and 0.3m, respectively.

The time history at stepped impact height for cells dimensions of Hex4.7X1.0mm and Hex4.7X1.5mm of H1036 material are given in Appendix D. For example, cells dimensions of Hex4.7X1.0mm shows the impact periods are 0.0096sec and 0.0111sec for drop heights of 0.45m and 0.35m, respectively

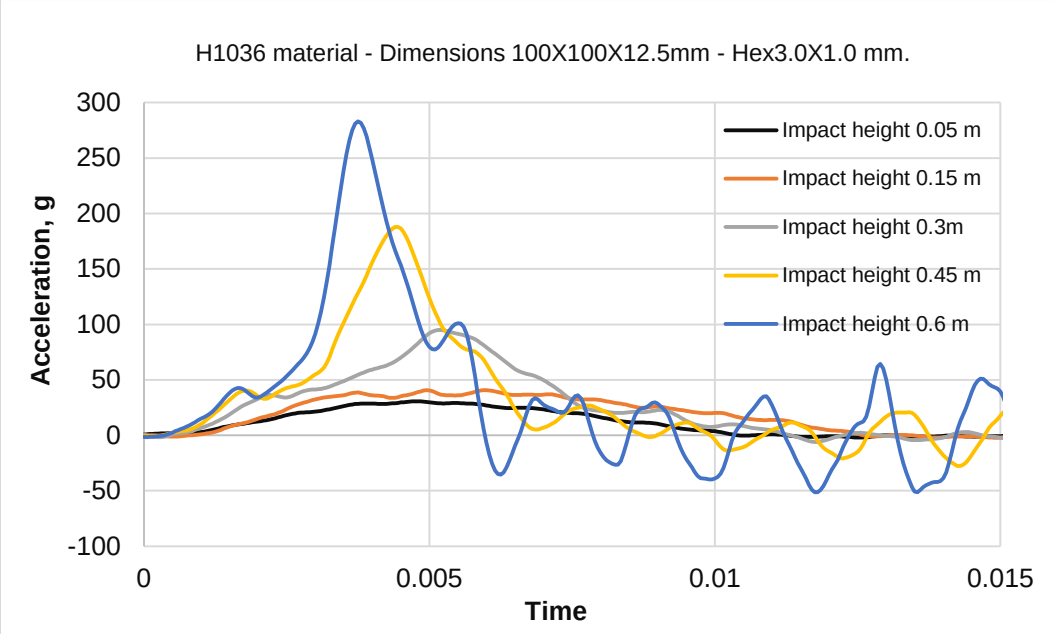

Figure 3-19 - Acceleration time history of the H1036 material at cells dimensions Hex3.0X1.0mm.

3.2.3 **H781 Material**

In this section, the response of H781 material will be shown. The H781 material is shown in the Figure 3-20. Two different wall thicknesses, t_w, of cells are used, namely, 1.0 mm and 1.5 mm. The material thickness, d, is kept constant at 12.5 mm. Also, a square shape sample is used. The cell size, c, is kept constant at 4.7 mm for both wall thickness.

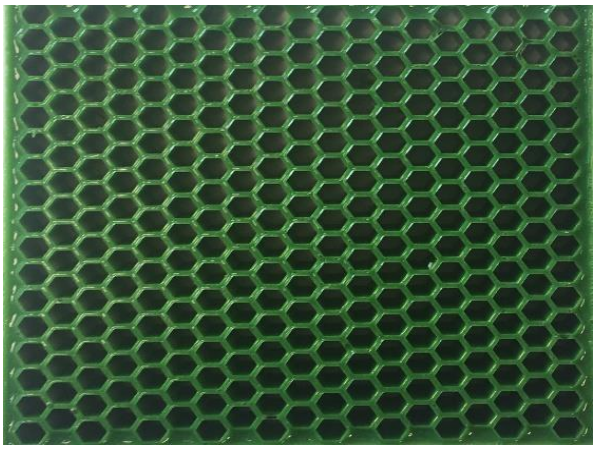

Figure 3-20 - H781 material

3.2.3.1 The Maximum Acceleration during Step Impact Height of H781 Material.

The maximum acceleration due to step impact of the 1.0 mm and 1.5 mm wall thicknesses are shown in the Figure 3-21. The H781 material at both of the wall thicknesses of 1.0 mm and 1.5 mm behaves as a relatively stiff material at every impact height. At the wall thickness of 1.0 mm, H781 material reaches the acceleration of 250.0 g at the impact height of 0.47 m. Also, the H781 material at the wall thicknesses of 1.5 mm reaches the acceleration of 250.0 g at impact height equal to 0.42 m.

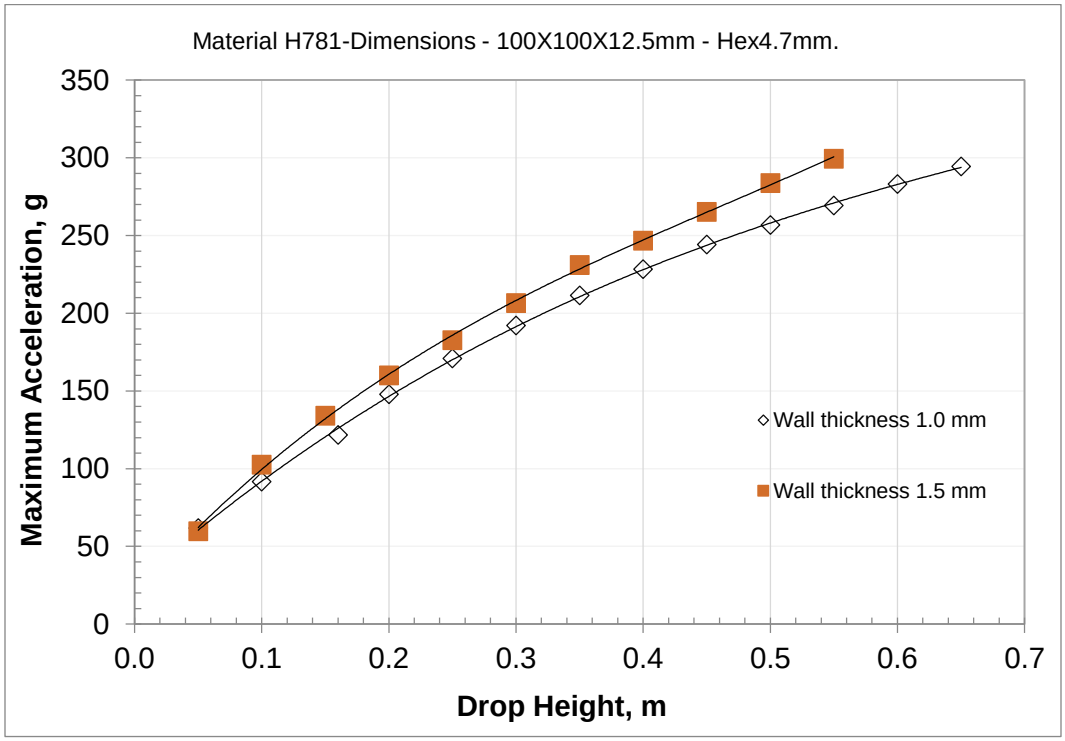

Figure 3-21 - The acceleration behaviour of H781 material for various wall thicknesses.

3.2.3.2 Force vs Displacement of H781 Material for Various Walls Thicknesses.

Load versus displacement curves during step impact height for the wall thickness 1.0 mm of H781 material is shown in Figure 3-22. A low displacement percentage is expected for the H781 material because it is a relatively stiff material. Looks like there is an initial stiffness increase in this material with drop height. The higher impact velocity causes the material to act stiffer and is rate dependent. At a force of 12kN the displacement of the sample with a wall thickness of 1.0 mm is 3.1 mm, which is a displacement percentage is 24.8 %.

The load versus displacement curves during step impact height for the wall thickness 1.5 mm can be seen in Appendix C and shows at a force of 12kN, the displacement of the 1.5 mm wall thickness sample is 2.7 mm corresponding to a displacement percentage of 21.6%.

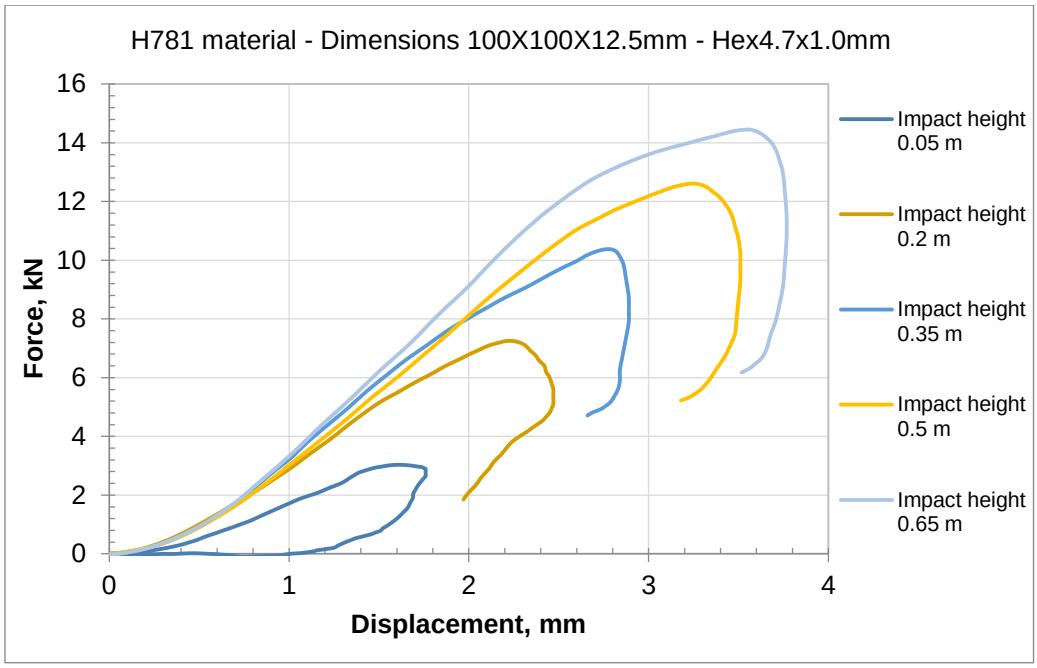

Figure 3-22 - The force versus the displacement of the H781 material at the wall thickness 1.0 mm.

3.2.3.3 **The Acceleration Time History for H781 Material.**

Figure 3-23 shows the time history at stepped impact height for the thickness 1.0 mm of the H781 material. It is clear as shown in the figure that the higher impact height gives greater acceleration and shorter period time because the H781 material consolidates increasingly more as the impact energy increases. Estimates of the impact periods are 0.0028sec and 0.0044sec for drop heights of 0.65m and 0.05m, respectively.

The time history at stepped impact height for the wall thicknesses 1.5 of the H781 material can be seen in Appendix D and shows the impact periods are 0.0025sec and 0.0038sec for drop heights of 0.55m and 0.05m, respectively.

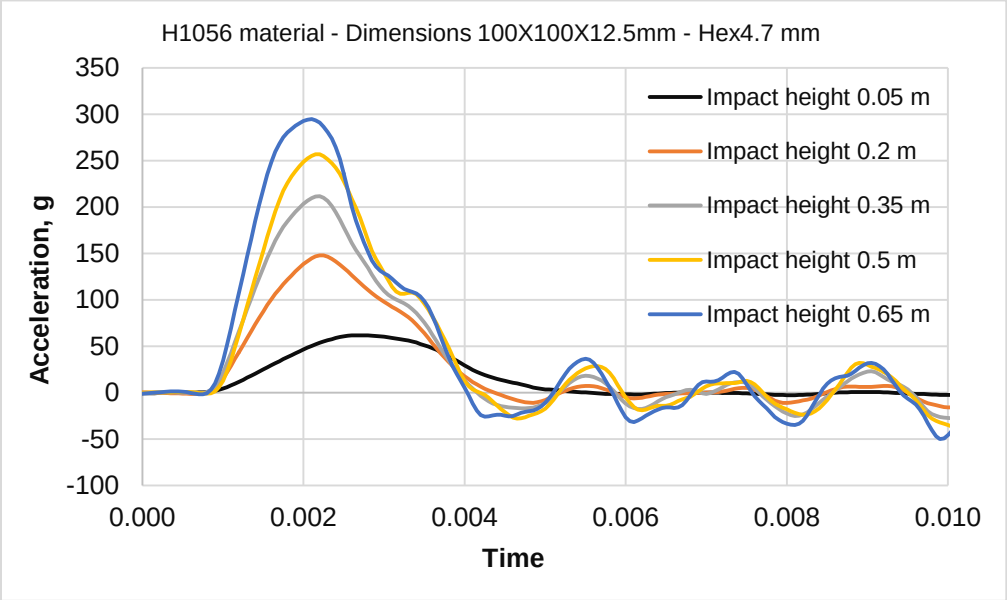

Figure 3-23 - Acceleration time history of the H781 material at the wall thickness of 1.0mm.

3.2.4 **H561 Material**

The response of H561 material will be shown in this section. Circular and square sample are used. The regular hexagonal shape only was used for the circular samples. Two different material thicknesses are used which are 6.5 mm and 12.5 mm. For both of the thicknesses of 6.5 mm and 12.5 mm, two different cell wall thickness of the cells of 1.0 mm and 1.5 mm are studied. The material cell size, c, is kept constant at 4.7 mm.

Regarding to the square samples, regular and irregular cells shapes are used. Five different cells dimensions are used for the regular shapes, namely, Hex3.0x0.8mm, Hex3.0x1.0mm, Hex4.7x1.0mm, Hex6.0x1.0mm and Hex8.0x1.0mm. Also, three different cells shapes are used for the irregular samples, namely, T1, T2 and T3. The material thickness is kept constant at 12.5 mm for the square samples. The square and circular regular samples of the H561 material are shown in the Figure 3-24. The same mass (5kg) and shape (127 mm radius spherical) of the impactor are used for both of the circular and square samples.

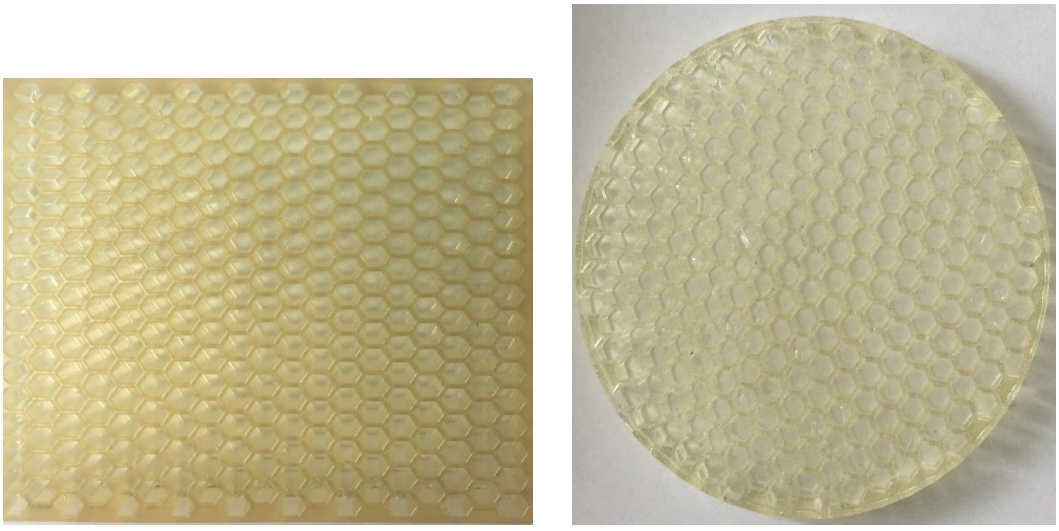

A) B)

Figure 3-24 – H561 material, (A) is honeycomb square sample shape and (B) is honeycomb circular sample shape, regular cell shapes with c=4.7mm tw = 1 mm (D) of the for both of them.

3.2.4.1 **Circular Shapes**

In this subsection, the maximum acceleration during step impact, acceleration time history and force versus displacement of the circular sample of the H561 samples will be shown.

3.2.4.1.1 **The Maximum Acceleration during Step Impact Height of the Circular Sample of H561 Material.**

At the material thickness 12.5 mm, the maximum acceleration due to step impact of the 1.0 mm and 1.5 mm wall thicknesses samples are shown in Figure 3-25. The H561 material at wall thickness of 1.0 mm behaves as a soft material at the lower impact height and its response increases gradually until impact height 0.6 m then it begins to consolidate. It reaches the acceleration of 250.0 g at the impact height of 0.98 m. The samples with a 1.5 mm wall thickness behaves stiffer at the beginning until impact height 0.4 m then it enters a force limiting phase due to buckling of the cells. It reaches the acceleration of 250.0 g at impact height equal to 1.28 m.

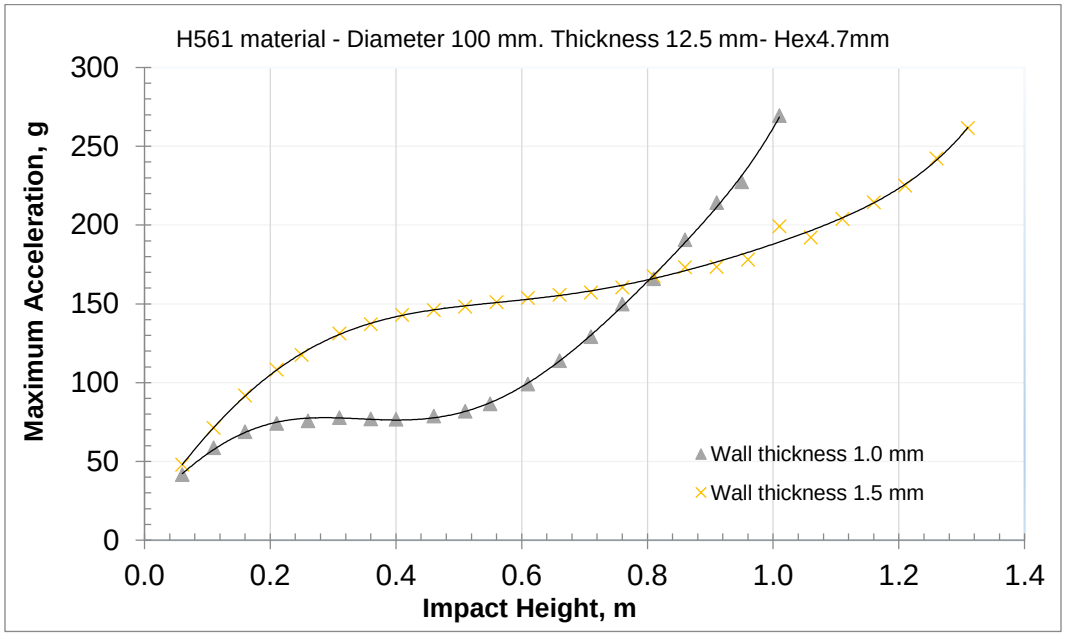

Figure 3-25 - The acceleration behavior of circular samples of H561 material for various wall thicknesses.

3.2.4.1.2 **Force vs Displacement of the Circular Sample of H561 Material for Various Walls Thicknesses.**

The load versus displacement curves during step impact for the 1.0 mm wall thickness and 12.5 mm total thickness of the H651 material is shown in Figure 3-26. At a force of 12kN the displacement is 9.1 mm corresponding to a displacement percentage of 72.8%. Also, at the same value of the force, the displacement of the 1.5 mm thick sample is 7.3 mm, which is a displacement percentage is 58.4 %. The load versus displacement curves during step impact for the 1.5 mm wall thickness and 12.5 mm total thickness of the H651 material can be seen in the appendix C.

Regarding the material thickness of 6.5 mm, the displacement of the 1.0 mm and 1.5 mm wall thicknesses are 4.5 mm and 3.5 mm, respectively, corresponding to a displacement percentage of 69.2% and 53.8%, respectively. The load versus displacement curves during step impact height for the samples can be seen in the appendix C, too.

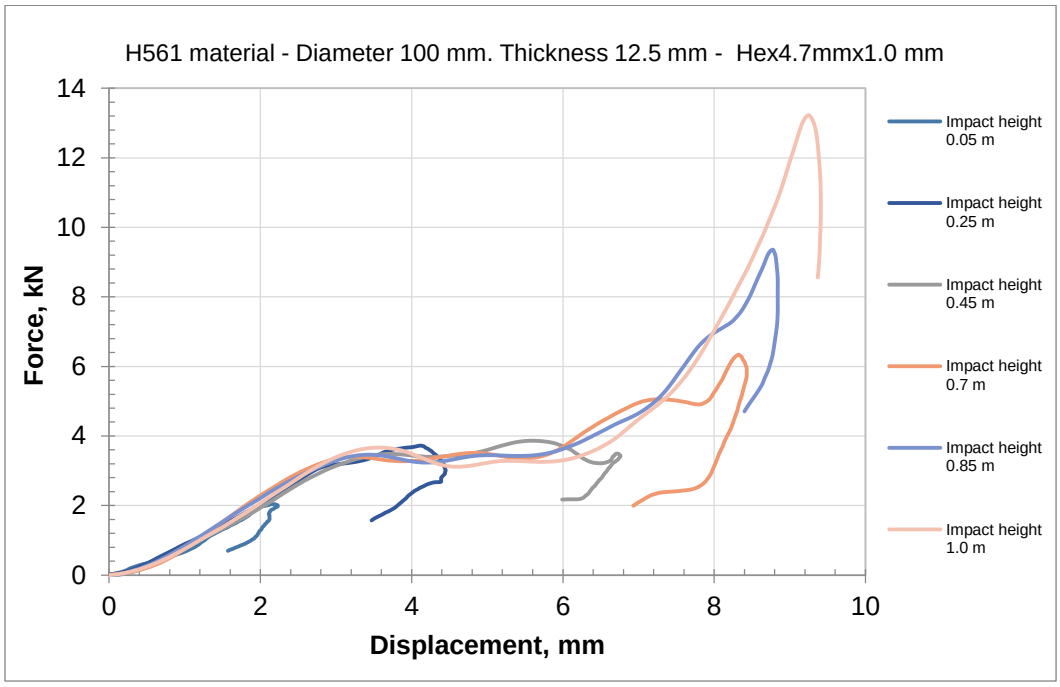

Figure 3-26 - The force versus the displacement of the H561 material at the wall thickness 1.0 mm for the material thickness 12.5 mm.

3.2.4.1.3 **Acceleration Time History for H561 Material.**

Figure 3-27 shows the time history at stepped impact height for the 1.0 mm wall thickness and 12.5 mm total thickness of the H561 material. It is clear as shown in the figure that the higher impact height gives greater acceleration and shorter period. Estimates of the impact periods are 0.0064sec and 0.0075sec for drop heights of 1.1m and 0.85m, respectively.

The time history at stepped impact height for the 1.5 mm wall thickness and 12.5 mm total thickness of the H561 material can be seen in the appendix D and shows the impact periods are 0.009sec and 0.0058sec for drop heights of 0.05m and 1.3m, respectively. Also, the time history at stepped impact height for the 1.0 mm and 1.5 mm wall thicknesses and 6.5 mm total thickness of the H561 material can be seen in the appendix D.

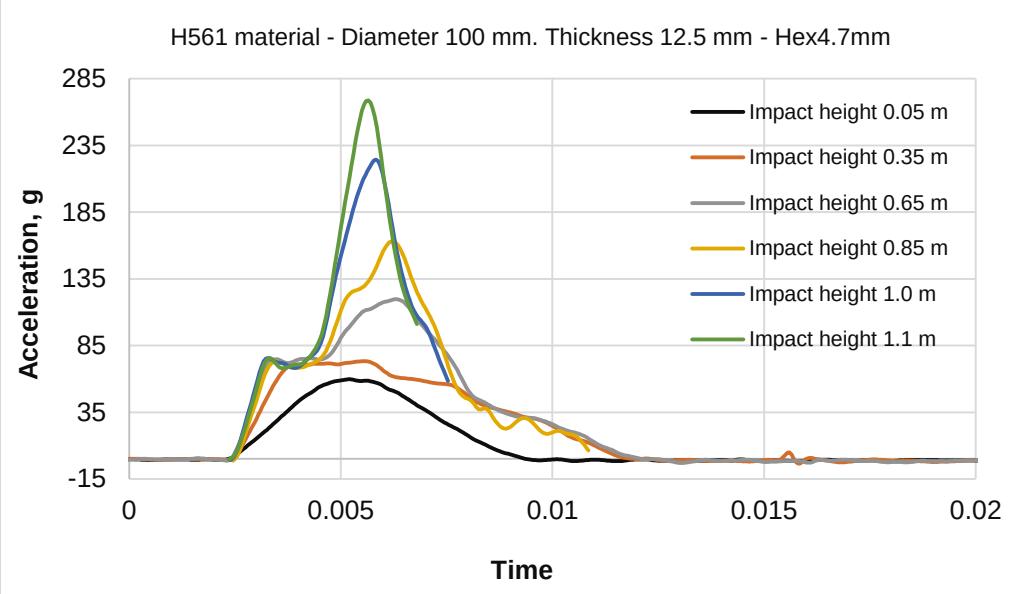

Figure 3-27 - Acceleration time history for the circular sample of H561 material at the wall thickness 1.0 mm and material thickness 12.5 mm.

3.2.4.2 **Square Shapes**

Square specimens of the H561 material were also tested. Five different cells dimensions are used for the regular shapes, namely, Hex3.0x0.8mm, Hex3.0x1.0mm, Hex4.7x1.0mm, Hex6.0x1.0mm and Hex8.0x1.0mm. Also, three different cells shapes are used for the irregular samples, namely, T1, T2 and T3. The material thickness, d, is kept constant at 12.5 mm. The regular and irregular

samples of the H561 material are shown in the Figure 3-28. The same mass (5kg) and shape (127 mm radius spherical) of the impactor are used.

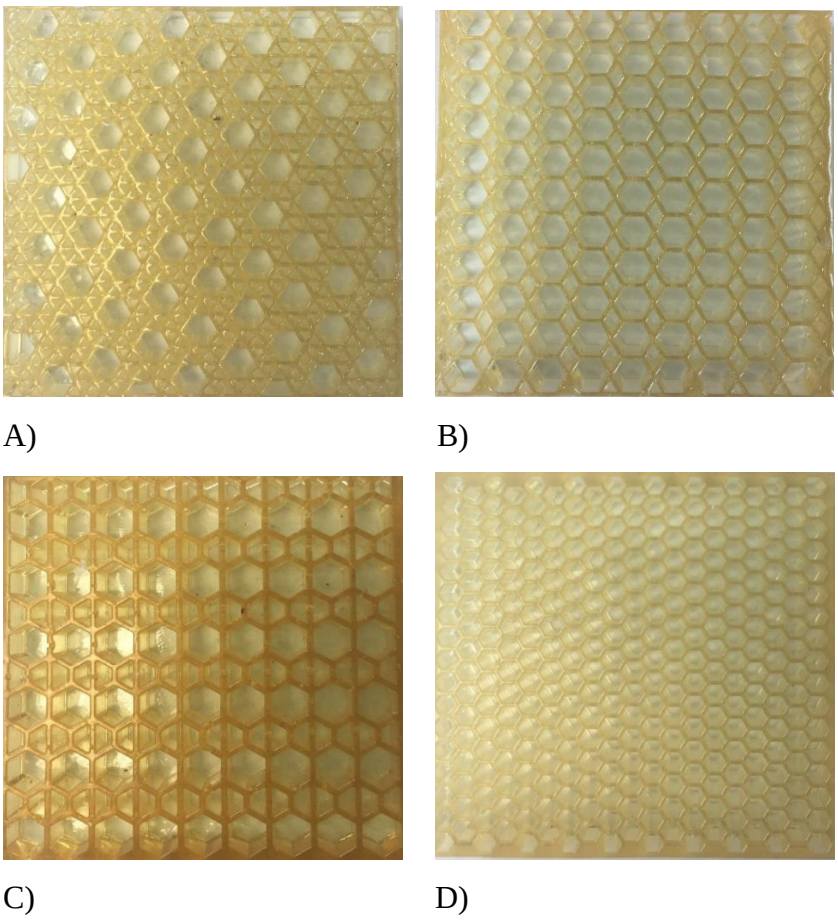

A) B)

C) D)

Figure 3-28 - Honeycomb shape named T1 (A), T2 (B) and T3(C) and the regular hexagonal with c=4.7mm tw = 1 mm (D) of the H561 material.

3.2.4.2.1 The Maximum Acceleration during Step Impact of the H561 Material.

The maximum acceleration due to step impact of the Hex3.0x1.0mm, Hex4.7x1.0mm, Hex6.0x1.0mm, Hex8.0x1.0mm and Hex3.0x0.8mm cell dimensions are shown in the Figure 3-29. The cells dimensions of Hex4.7X1.0mm behave as a relatively soft material and it reaches the acceleration of 250.0 g at

impact height equal to 0.98 m. Also, the H561 material at cell dimensions of Hex8.0X1.0mm behaves as a soft material at the lower impact height and its response increases gradually until impact height 0.4 m then it behaves as a stiffer material due to consolidation. It reaches the acceleration of 250.0 g at the impact height of 0.66 m. Finally, the Hex3.0x1.0mm, Hex6.0x1.0mm, and Hex3.0x0.8mm cell dimensions reach the acceleration of 250.0 g at the impact heights of 1.07m, 0.79m and 1.07m, respectively.

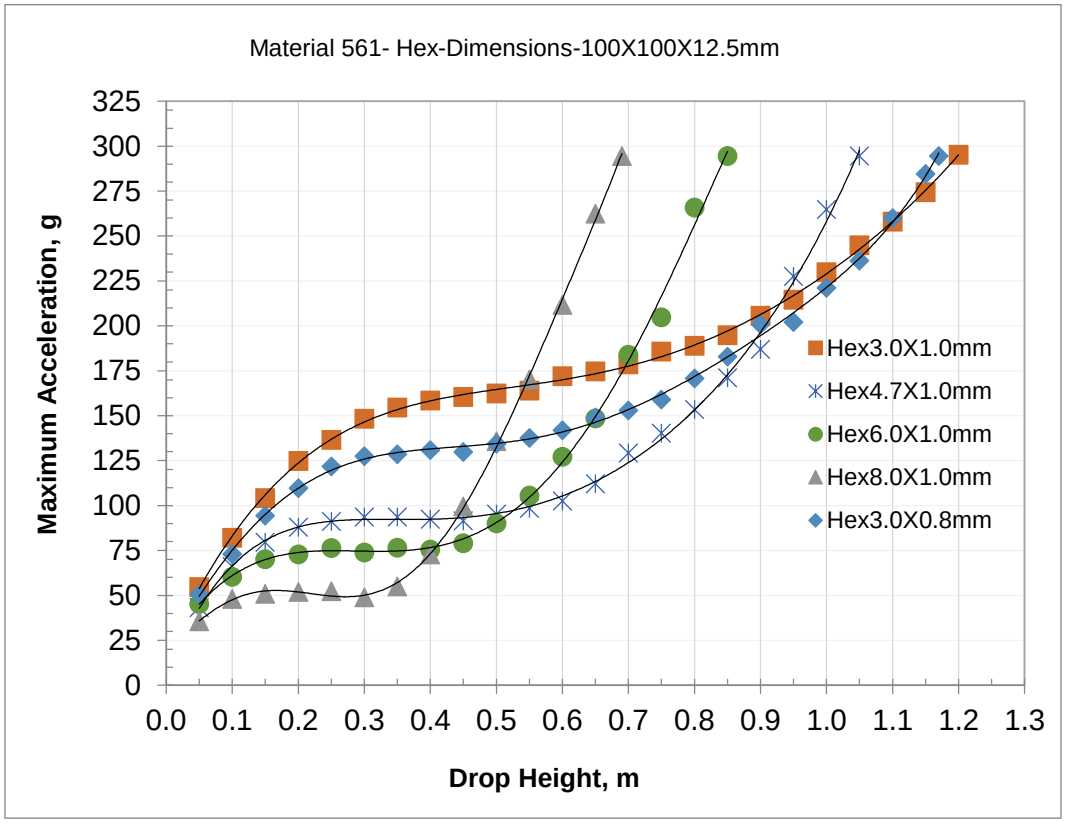

Figure 3-29 - The acceleration behavior of H561 material for the regular cells shape.

3.2.4.2.2 Force vs Displacement of H561 Material for Various Cells Dimensions.

Load versus displacement curves for the cell dimensions of Hex4.7x1.0mm for the H561 material is shown in Figure 3-30. At a force of 12kN, the displacement of the cell dimensions of Hex4.7x1.0mm is 9.15 mm which corresponds to the displacement percentage of 73.2 %. The load versus displacement curves for cells dimensions of Hex3.0x1.0mm, Hex6.0x1.0mm, Hex8.0x1.0mm and Hex3.0x0.8mm can be seen in Appendix C and shows the displacements at a force 12kN are 7.6mm, 9.5mm, 9.9mm and 8.1mm, respectively corresponding to displacement percentage 60.8%, 76.0%, 79.2% and 64.5% respectively.

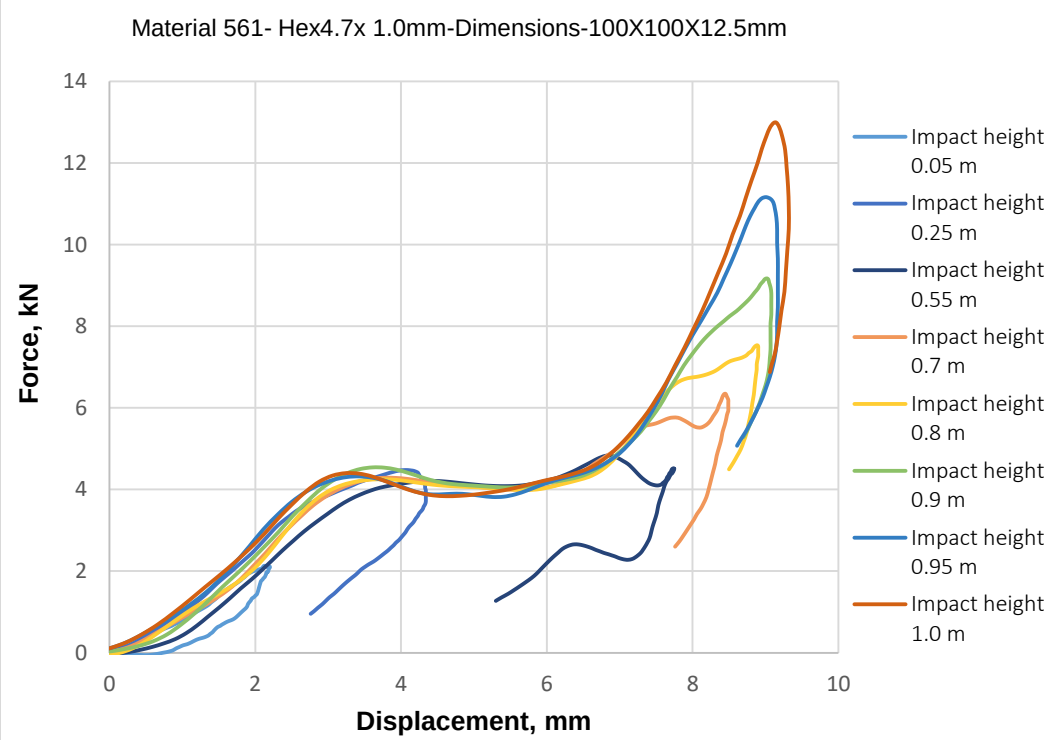

Figure 3-30 - The force versus the displacement of the H561 material at the regular cells dimensions Hex4.7x1.0mm.

3.2.4.2.3 **The Acceleration Time History for H561 Material.**

Figure 3-31 shows the time history at various step impact heights for the cell dimensions of Hex4.7x1.0mm of the H561 material. It is clear as shown in the figure that the higher impact height gives greater acceleration and shorter time period time. Estimates of the impact periods are 0.0067sec and 0.008sec for drop heights of 1.0m and 0.75m, respectively.

The time history at stepped impact height for cells dimensions of Hex3.0x1.0mm, Hex6.0x1.0mm, Hex8.0x1.0mm and Hex3.0x0.8mm of H561 material are given in Appendix D. For example, cells dimensions of Hex3.0X1.0mm shows the impact periods are 0.006sec and 0.005sec for drop heights of 0.05m and 1.2m, respectively

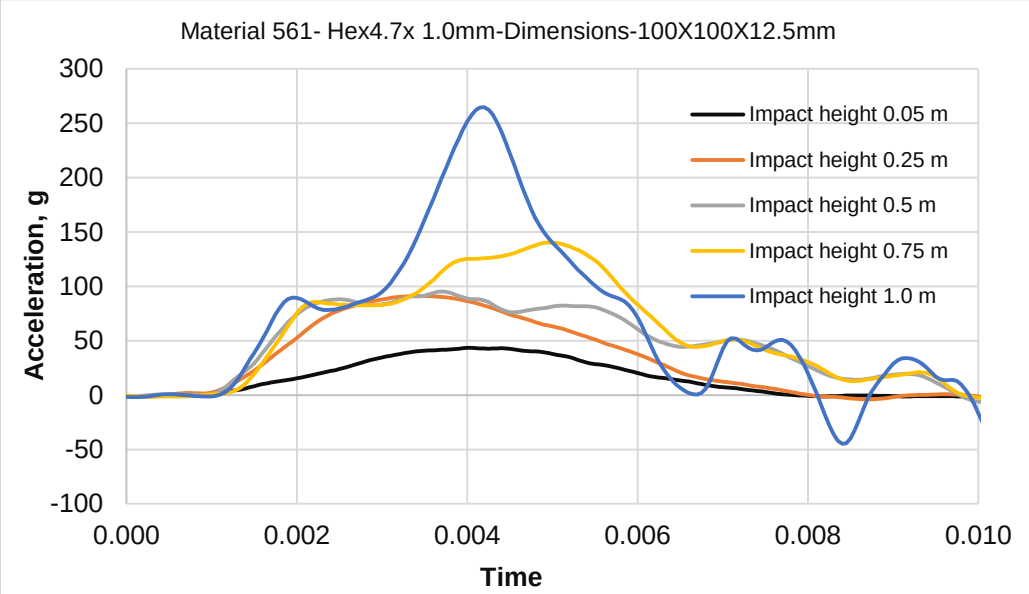

Figure 3-31 - Acceleration time history of the H561 material at cells dimensions Hex4.7X1.0mm.

3.3 Results of the Two-Layer Samples

In this part, the tests results of the two layers samples will be shown. The samples are classified according to total materials thickness as 12.5mm and 24.5mm. Five different samples for both of the 12.5mm and 24.5mm, namely, P25_H561, P15_H1056, P25_H1036, P09_H1036 and P09_H561 as shown in the Figure 3-32. The same mass (5kg) and shape (127 mm radius spherical) of the impactor are used. Furthermore, all samples have the same length and width, namely 100mm x 100mm.

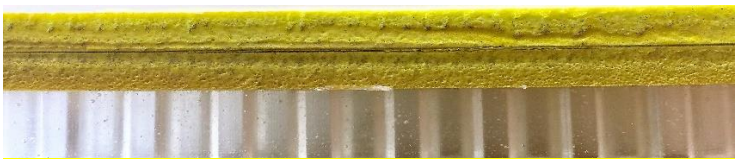

A)

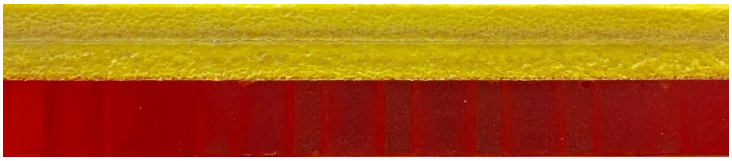

B)

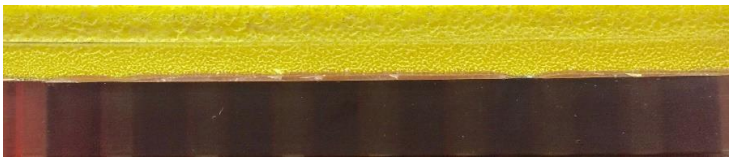

C)

Figure 3-32 - Two layers samples named P15_H1056 (A), P25_H1036 and P09_H1036 (B), P25_H561 and P09_H561 same to (C) of the two layers samples.

3.3.1 The Maximum Acceleration during Step Impact of the Two Layers Samples.

The maximum acceleration during step impact of the two layer samples at the thickness 12.5mm and 24.5mm are shown in the Figures 3-33 and 3-34, respectively. At the thickness 12.5 mm, the samples P25_H561, P15_H1056, P25_H1036, P09_H1036 and P09_H561 reach the acceleration of 250.0 g at the impact heights of 1.2m, 1.08m, 1.0m, 0.75m and 0.91 m respectively. Regarding to samples thickness of 24.5mm, the samples P25_H561, P15_H1056, P25_H1036, P09_H1036 and P09_H561 reach the acceleration of 250.0 g at the impact heights of 2.42m, 2.0m, 2.17m, 1.39m and 1.94m respectively. The P09_H1036 sample at total thicknesses of 12.5mm and 24.5mm behave as a soft material at the lower impact height and their response increases gradually until impact height 0.35m and 0.65m, respectively, then they begin to consolidate.

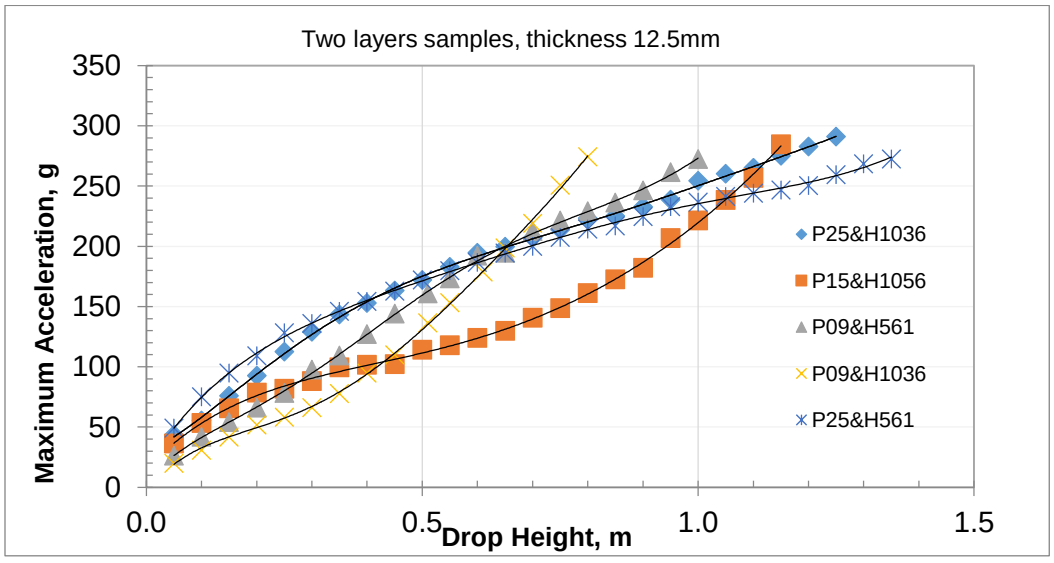

Figure 3-33 - The acceleration behavior of the two layers samples at the total thickness 12.5mm.

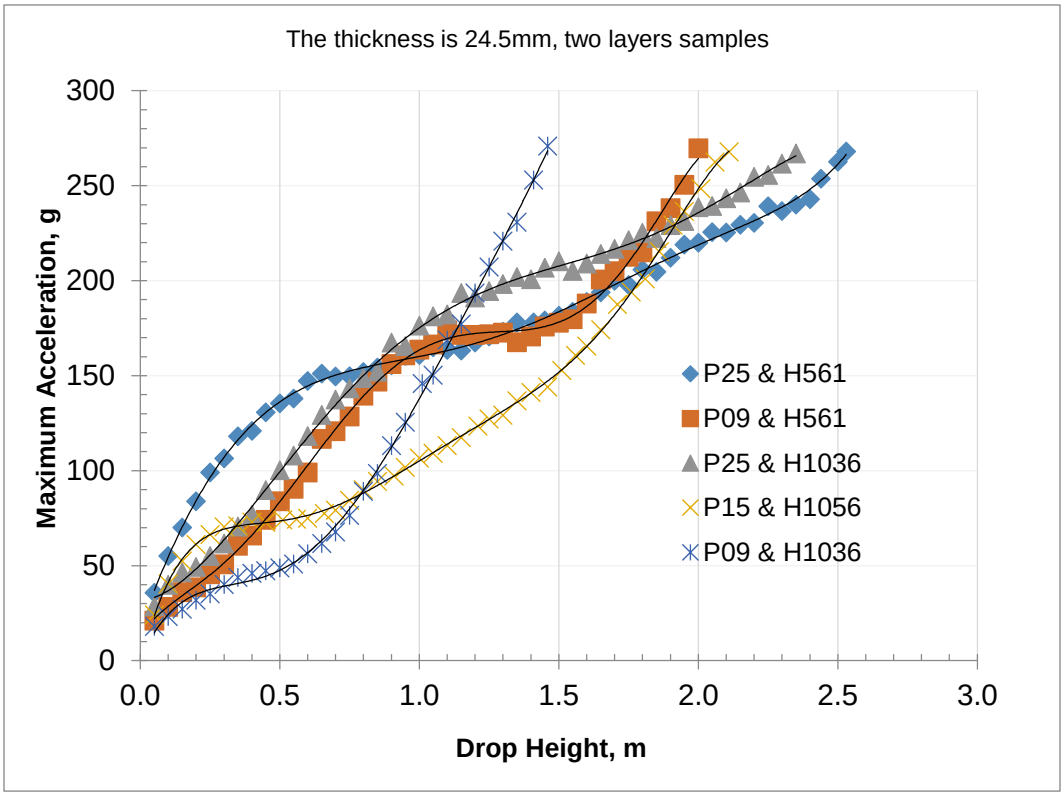

Figure 3-34 - The acceleration behavior of the two layers samples at the total thickness 24.5mm.

3.3.2 **Force vs Displacement of Dilatant-Honeycomb Two Layers Samples.**

Load versus displacement curves for the P09_H1036 samples at the total samples thickness 12.5mm and 24.5mm are shown in Figures 3-35 and 3-36, respectively. The load versus displacement curves of P25_H561, P15_H1056, P25_H1036, and P09_H561 at the total samples thickness 12.5mm and 24.5mm can be seen in Appendix C.

At a force of 12kN and total thickness 12.5mm, the displacement of P25_H561, P15_H1056, P25_H1036, P09_H1036 and P09_H561 samples are 6.85mm, 9.5mm, 8.3, 9.8 and 8.3mm which correspond to the displacement percentage of

55.2%, 76%, 66.4%, 78.4% and 66.4%, respectively. Also, at a force of 12kN and total thickness 24.5mm, the displacement of P25_H561, P15_H1056, P25_H1036, P09_H1036 and P09_H561 samples are 13.2mm, 19.2mm, 14.3, 19.5 and 18.3mm which correspond to the displacement percentage of 53.9%, 78.4%, 58.4%, 79.6% and 74.7%, respectively.

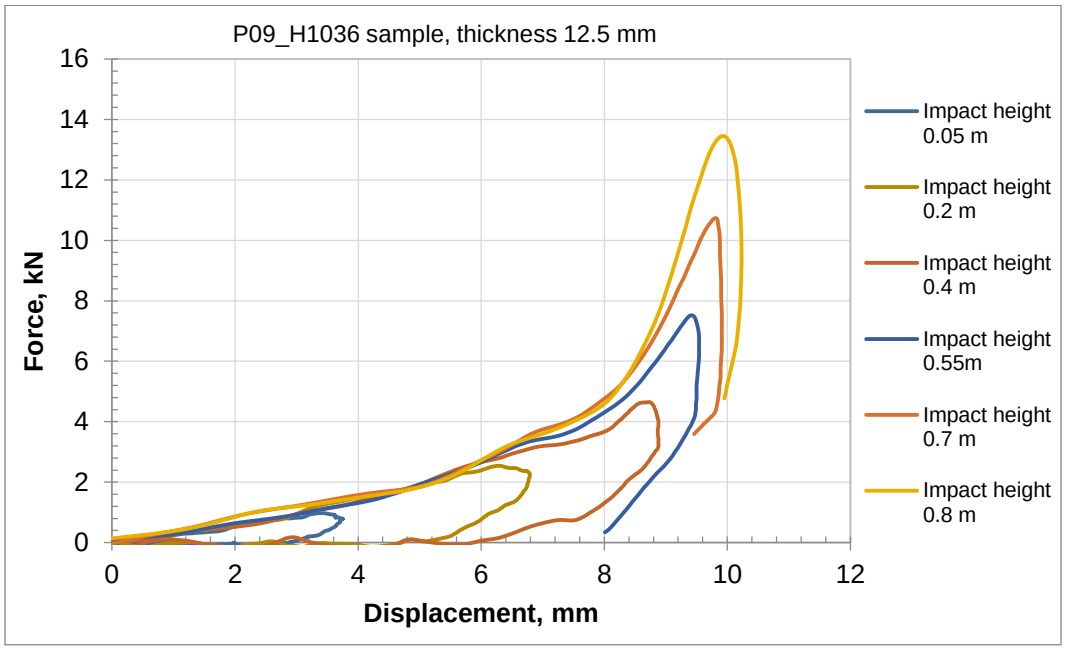

Figure 3-35 - The force versus the displacement of P09_H1036 samples at the sample thickness 12.5 mm.

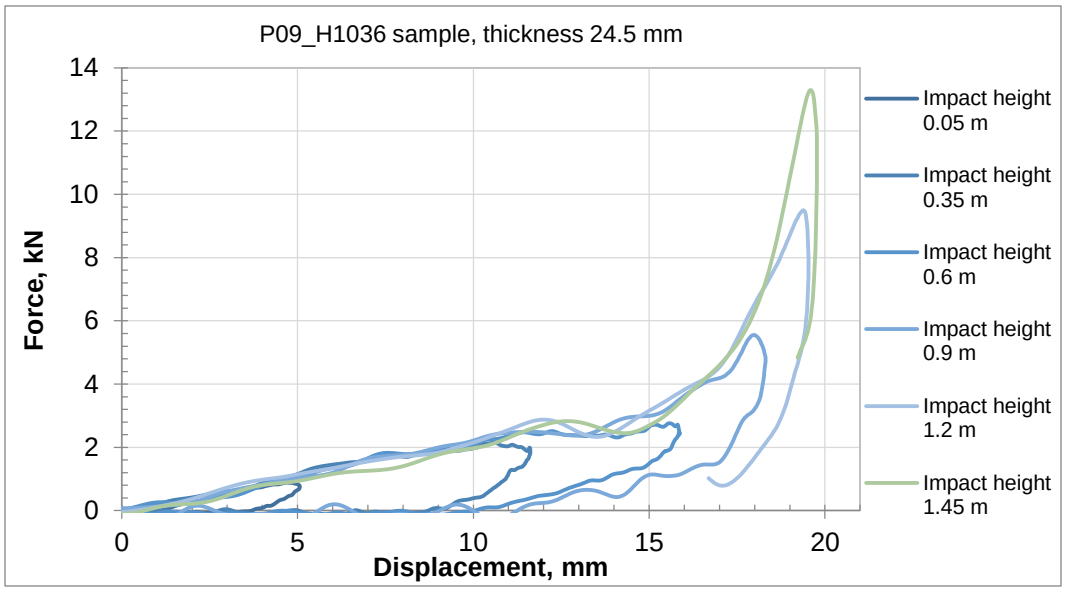

Figure 3-36 - The force versus the displacement of P09_H1036 samples at the sample thickness 24.5 mm.

3.3.3 The Acceleration Time History for Dilatant-Honeycomb Two Layers Samples.

The time history at various step impact heights for P09_H1036 samples at the total samples thickness 12.5mm and 24.5mm are shown in Figures 3-37 and 3-38. The time history at various step impact heights of P25_H561, P15_H1056, P25_H1036, and P09_H561 samples at the total samples thickness 12.5mm and 24.5mm can be seen in Appendix C. It is clear as shown in the figures that the higher impact height gives greater acceleration and shorter time period time.

For the thickness 12.5mm of the P09_H1036 sample, estimates of the impact periods are 0.008sec and 0.0092sec for drop heights of 0.8m and 0.55m, respectively. Also, at the thickness 24.5mm of the P09_H1036 sample, estimates of the impact periods are 0.0106sec and 0.0129sec for drop heights of 1.45m and 0.6m, respectively.

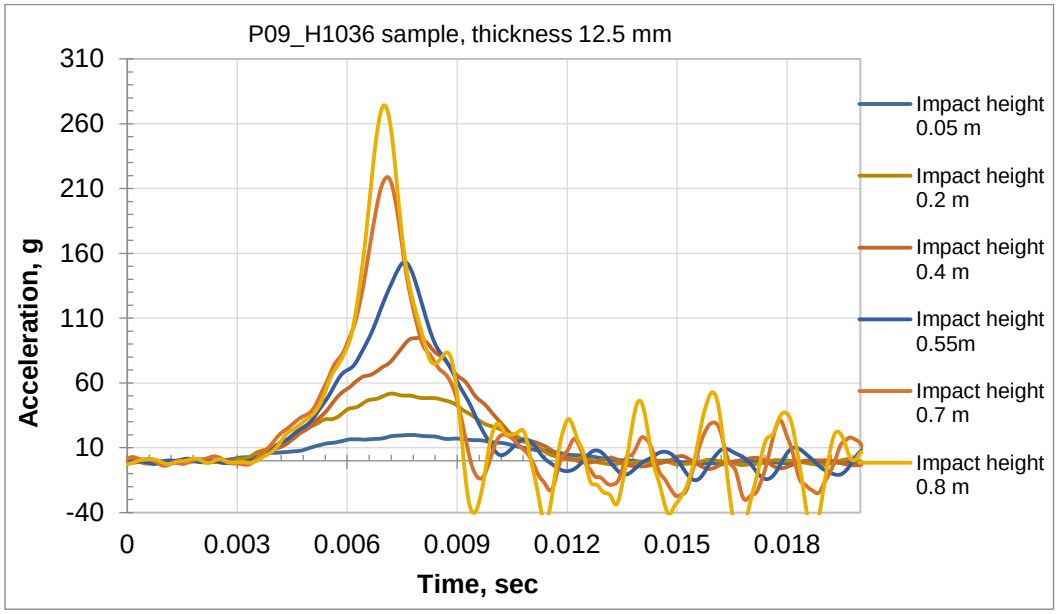

Figure 3-37 - Acceleration time history of the P09_H1036 sample at cells at the total thickness 12.5 mm.

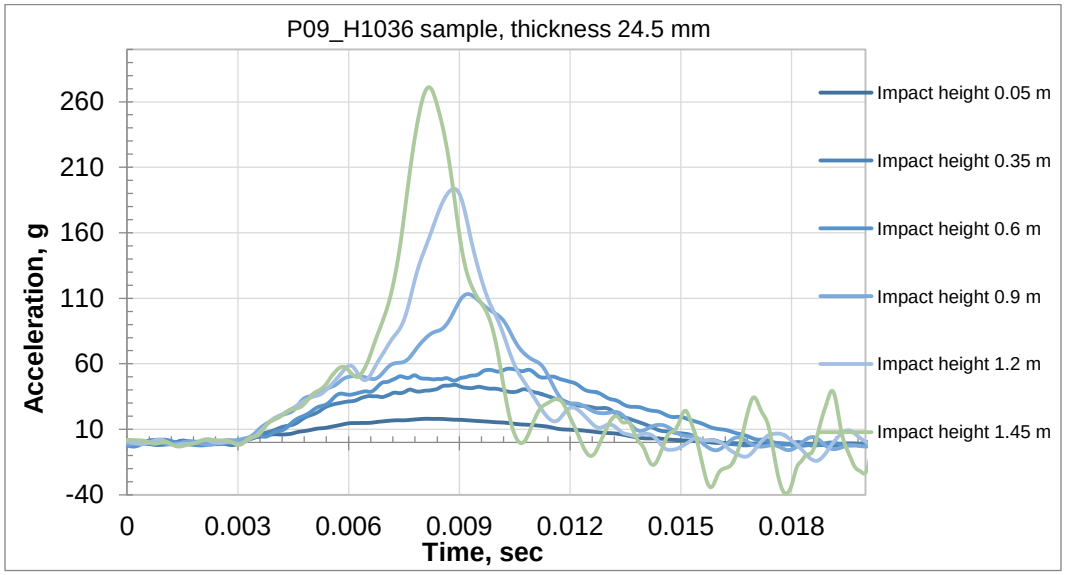

Figure 3-38 - Acceleration time history of the P09_H1036 sample at the total thickness 24.5 mm.

3.4 Results of Five Layers Samples

In this part, the tests results of the five layers samples will be shown. Namely, R1007, R2007, R3007 and R4007 as shown in the Figure 3-39. Photographs A, B, C and D represent R1007, R2007, R3007 and R4007, respectively. The same mass (5kg) and shape (127 mm radius spherical) of the impactor are used. Furthermore, all samples have the same diameter, namely 100mm.

A)

B)

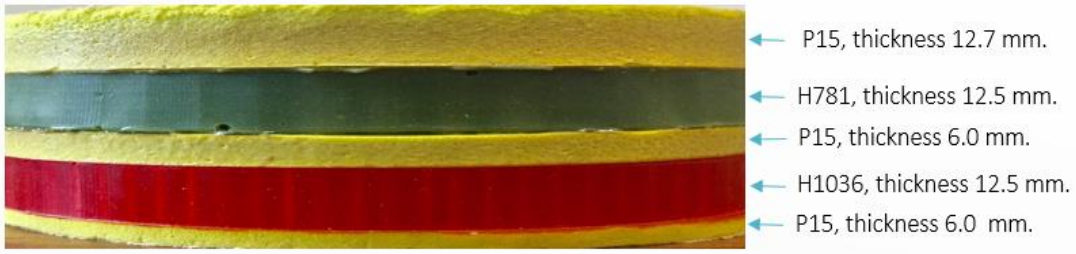

C)

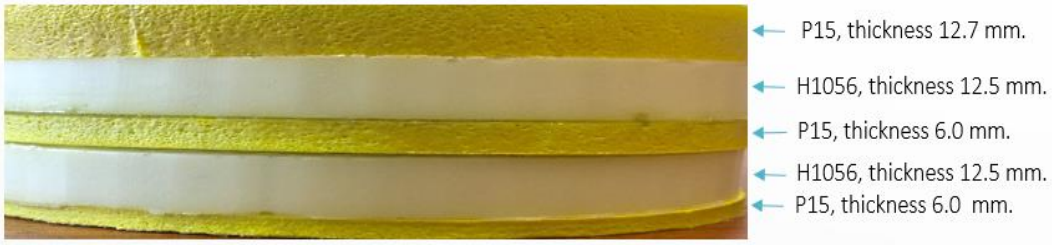

D)

Figure 3-39 - Five layers samples named R1007 (A), R2007 (B), R3007 (C) and R4007 (D).

3.4.1 The Maximum Acceleration during Step Impact Height of the Five Layers Samples

The maximum acceleration due to step impact of the R1007, R2007, R3007 and R4007 are shown in the Figure 3-40. The R1007 sample reaches the acceleration of 100.0 g at the impact height of 1.4 m. Also, R2007 sample reaches the acceleration of 100.0 g at impact height equal to 2.2 m. Furthermore, R3007 and R4007 samples reach the acceleration of 100.0 g at impact heights equal to 2.15 m and 2.35 m, respectively.

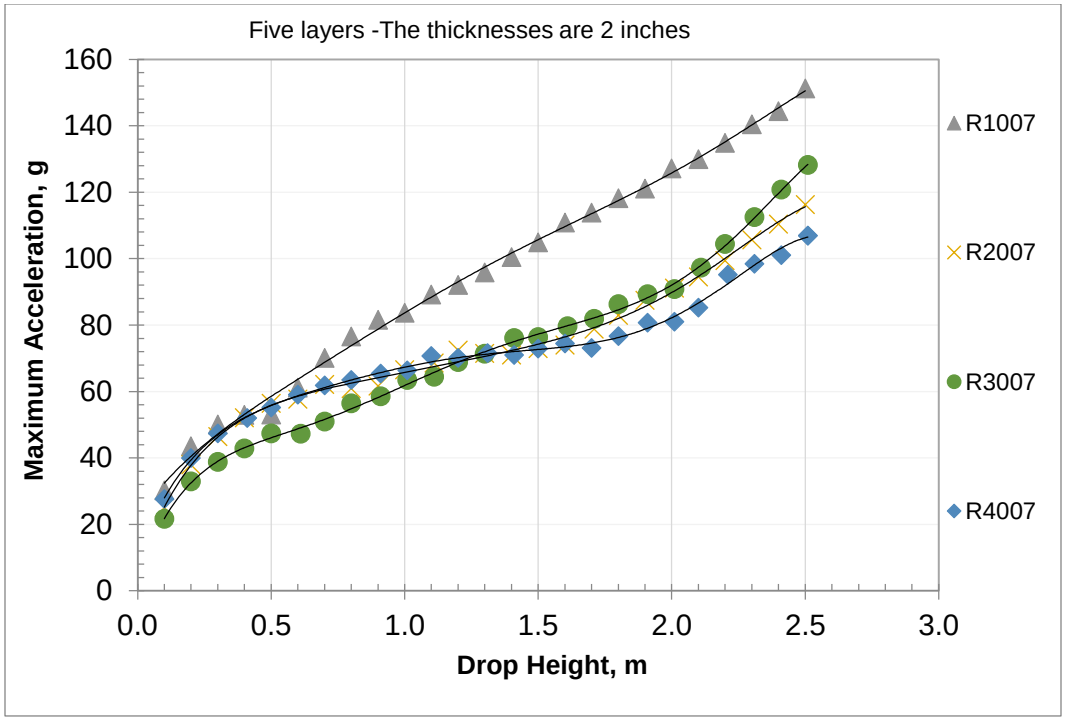

Figure 3-40 - The maximum acceleration during step impact height of the five layers samples.

3.4.2 **Force vs Displacement of Five Layers Samples.**

Load versus displacement curves for R1007 sample is shown in Figure 3-41. At a force of 5kN, the displacement of R1007 sample is 25.5 mm which corresponds to the displacement percentage of 51.3 %. The load versus displacement curves for R2007, R3007 and R4007 samples can be seen in Appendix C and shows the displacements at a force 5kN are 34.0mm, 32.6mm, and 33.1 mm, respectively corresponding to displacement percentage 68.4%, 65.6.0% and 66.6% respectively.

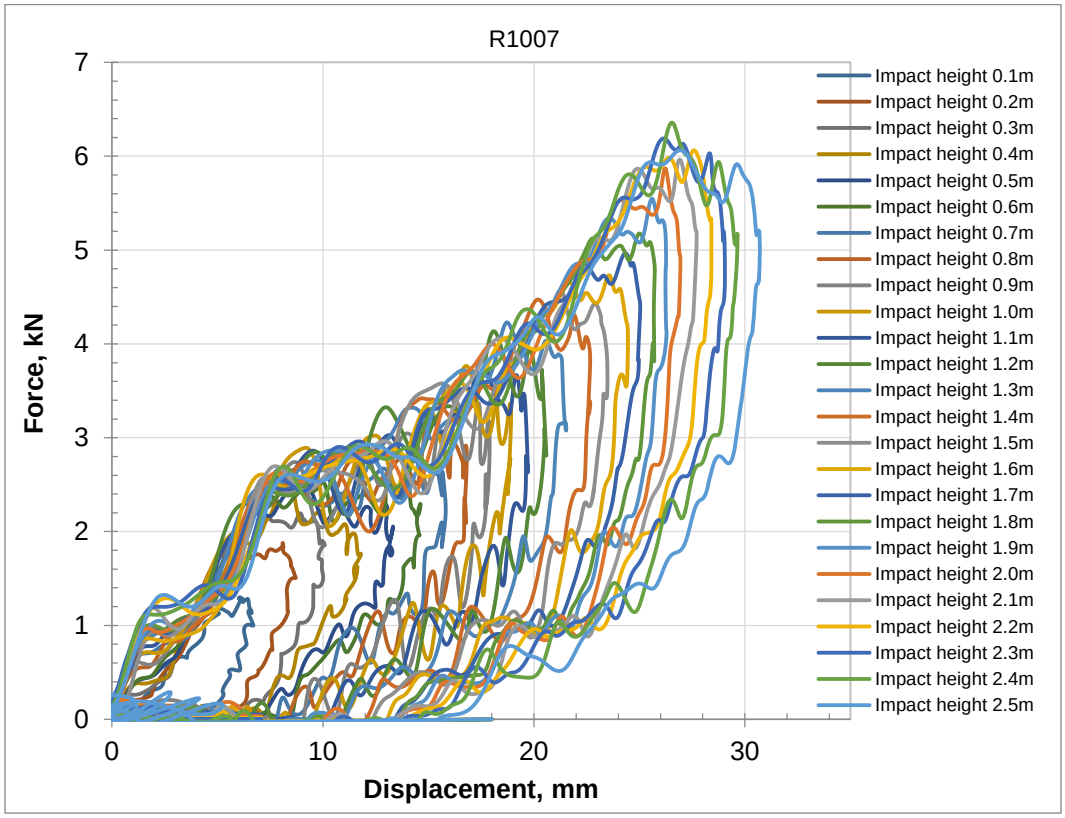

Figure 3-41 - The force versus the displacement of R1007 sample.

3.4.3 The Acceleration Time History of Five Layers Samples.

Figure 3-42 shows the time history at various step impact heights for the R1007 sample. It is clear as shown in the figure that the higher impact height gives greater acceleration and shorter time period time. Estimates of the impact periods are 0.014sec and 0.012sec for drop heights of 0.1m and 2.5m, respectively.

The time history at stepped impact height for R2007, R3007 and R4007 are given in Appendix D. For example, R3007 sample shows the impact periods are 0.0156sec and 0.0168sec for drop heights of 2.5m and 0.1m, respectively

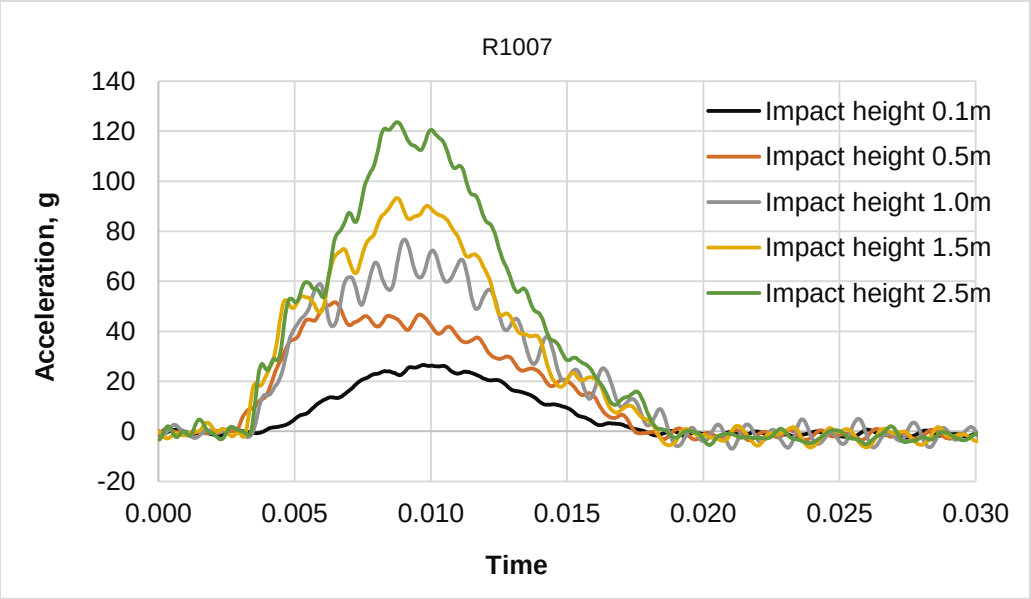

Figure 3-42 - Acceleration time history of theR1007 sample.

CHAPTER FOUR

COMPARISONS

This chapter will present comparisons between the experimental data sets presented in Chapter 3. The response of the foam and honeycomb materials will be compared among themselves and then to each other. In addition the response of the multi-layered system will be evaluated.

4.1 Single Layer Materials

4.1.1 Dilatant Material

Impact response of the dilatant foam materials is studied in this section. Response of materials with varying hardness and density will be compared at different impact heights struck with a 127mm radius impactor of 5 kg mass. There are three materials that are the focus of this effort, namely P09, P15 and P25 materials and are classified according to the material density.

Also, response of materials with varying thicknesses, five different thicknesses of the P15 material have been tested for this comparison, namely, 3 mm, 4 mm, 6 mm, 9.5 mm and 12.7 mm

A summary of the materials was provided in Table 3-1, section 1.1, chapter three.

4.1.1.1 Comparison of Dilatant Materials at Different Density

4.1.1.1.1 Response to Step Impact

Response of the three baseline foam materials at 6mm total thickness under step impact is given in Figure 4.1. According to the tests and the material response portrayed the P09 material acts as a softer material, as anticipated. The acceleration of P09 material is the lesser of the three if the impact height (energy) is below

0.11m. After that, the acceleration of this material dramatically increases due to consolidation of the foam. The imposed 250g limit is reached at a drop height of approximately 0.3 m. This increase gives us indication that P09 material is sub optimal for protection at impact height higher than 0.11 m.

The P15 material response is stiffer than the P09 material. This reality is very clear in Figure 4-1, where P09 material reaches the 250g acceleration at height 0.3 m while P15 material does not reach maximum value of the acceleration until the impact height of 0.6 m.

The last one of the three materials is P25. This material is stiffest acting material and reaches the 250g value of the acceleration at the impact height of 0.58 m. The materials P09 and P15 materials give the same results at impact height of 0.12 m. Also, P09 and P25 material give same acceleration at impact height of 0.2 m. Moreover, P15 and P25 materials give same value of acceleration at impact height of 0.6 m

As a result, if using a single 6mm thick layer the designer should choose the P09 material if the required impact height less than 0.12 m. Also the P15 is the best choice for the impact height between 0.12 m and 0.6 m. Moreover, the P25 is the best if the required impact is greater than 0.6 m.

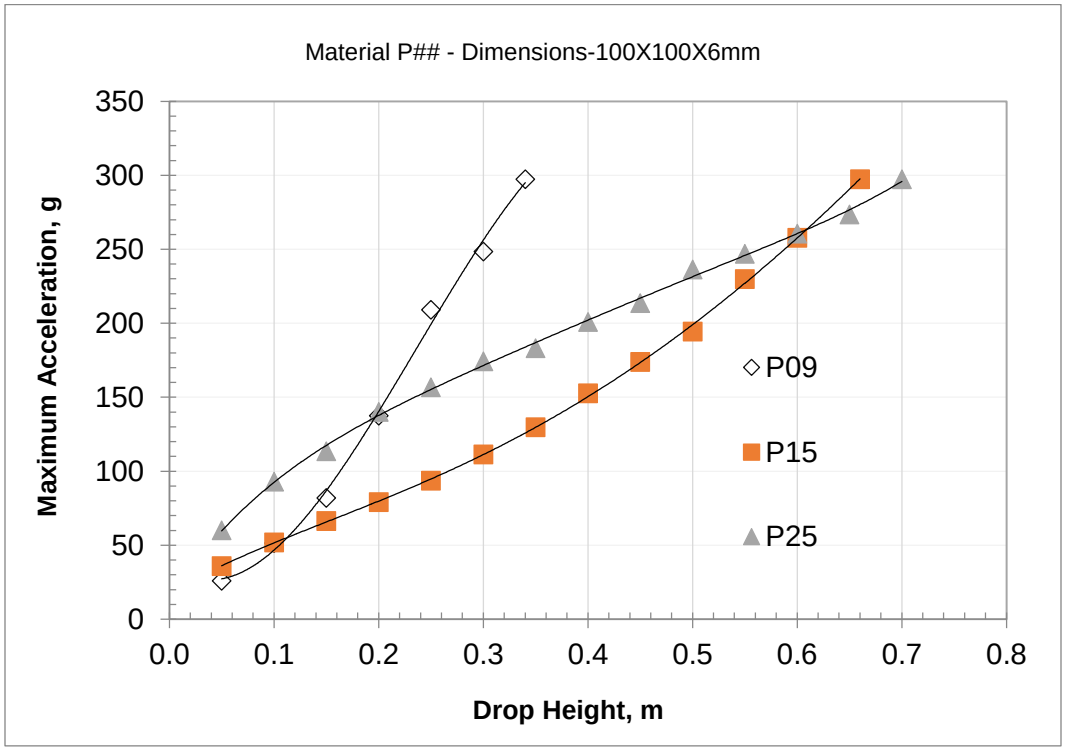

Figure 4-1 - The acceleration behavior of P09, P15 and P25 materials at different impact height.

4.1.1.1.2 **Force vs Displacement during Step Impact.**

Figure 4-2 shows force versus displacement results of the 6mm thick P09, P15 and P25 materials recorded during the last impact step. According to the data, the displacement of P09 material is significantly more than the others materials. Also, the P25 material gives the lowest value of the total displacement. The displacement at load 12kN of P09 material is 4.8mm which represent 80.0% from the total thickness indicating a significant consolidation. The displacement of P15 material is 4.1 mm at the peak load 12kN which represent 66.7% of the total thickness. Also, the P15 material gives good result at the lower impact height where

the acceleration gradually increase at the beginning. The third material is P25, as we mentioned, this material is stiffer than P09 and P15, for that it is expected to get the lowest displacement. The value of the displacement of P25 material at peak load 12 kN is 2.8 mm which represent 46.7% from the total thickness.

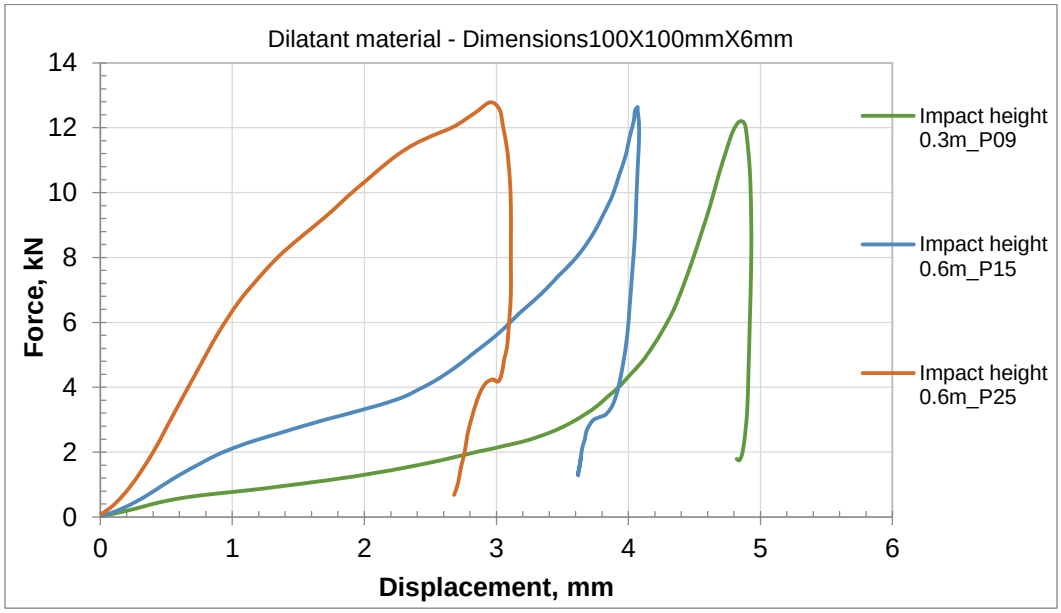

Figure 4-2 - The displacement of P09, P15 and P25 materials at the thickness 6mm and the impactor is R-127mm

4.1.1.1.3 **Acceleration Time History at the Same Impact Height.**

The acceleration time history at an impact height of 0.3m is shown in Figure 4-3. The peak acceleration and time history signatures of the 3 materials are significant different. For example, at impact height 0.3 m the maximum value of acceleration for P25 material is 174 g while at the same impact height, the maximum value of acceleration for P15 and P09 material is 111g and 250g respectively. Furthermore, according to Figure 4-3, the time period of the

increasing of the acceleration for P15 material is much longer than P09 and P25 materials which means the P15 material has the ability to absorb impulse at a lower level of force compared to the others materials. In short, before we decide which material is the best, we have to know the design requirements. In other word, it is very important to know the required impact height.

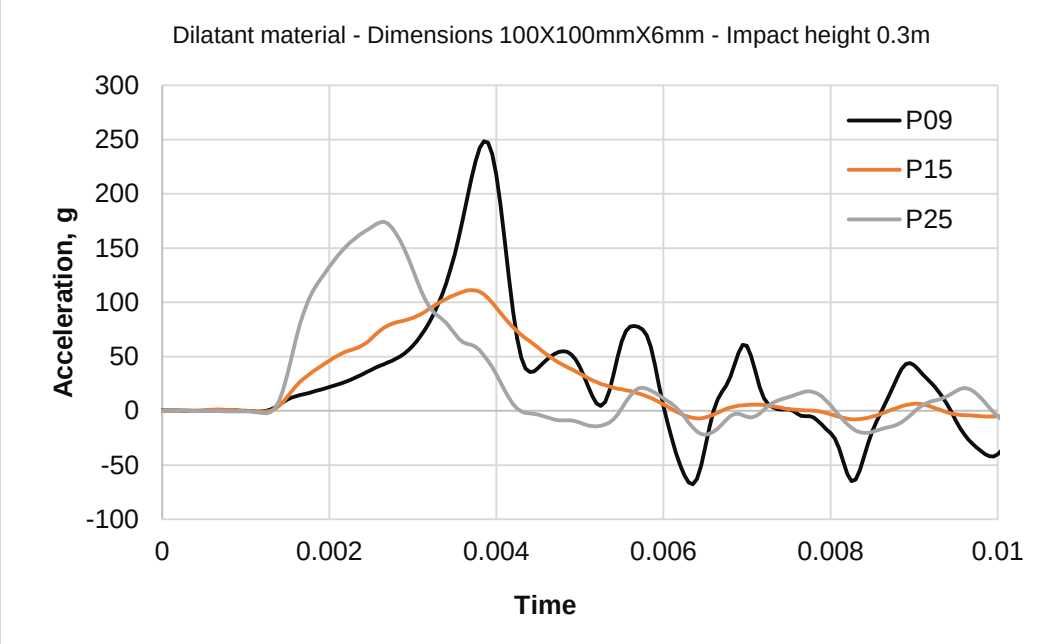

Figure 4-3 - The acceleration time history of the P09, P15 and P25 at the same impact height

Table 4-1 shows a summary of the response parameters for the three materials at 6mm thickness. It is clear the P09 is invalid to use it for protection design at the maximum value of the acceleration. On the other hand, P25 material is little bit better than P15 material at the maximum value of the acceleration.

Table 4-1 - Summary of comparison between P09, P15 and P25 material at 6mm thickness.

Material	Max Force kN	Displacement at force of 12 kN	Displacement Percentage % at 12 kN	Impactor Height At the max force	Acceleration g
P09	12.1	4.8	80.0	0.3	250
P15	12.5	4.1	68.3	0.6	260
P25	14.4	2.8	46.7	0.7	297.3

4.1.1.2 **Comparison of Dilatant Materials at Different Thicknesses**

In this section a summary of the effect of thickness on the impact height, the maximum value of the acceleration, and the displacement percentage is given. The same mass (5kg) and shape (127 mm radius spherical) of the impactor are used. Furthermore, all samples have the same length and width, namely 100mm x 100mm. The P15 material is used for this comparison due to the wide range of thicknesses available.

4.1.1.2.1 **The Maximum Acceleration during Step Impact.**

Five different thicknesses of the P15 material have been tested for this comparison, namely, 3 mm, 4 mm, 6 mm, 9.5 mm and 12.7 mm. Figure 4-4 shows the maximum acceleration behavior of P15 material at different impact heights and thicknesses. At the thickness 3 mm, the acceleration increased dramatically and it reached 250 g at impact height of 0.24 m. At the 4 mm thickness, the P15 material initially has almost has the same response as the 3 mm thickness except it reaches a maximum acceleration of 250g at impact height of 0.32 m. The response of the 6 mm thickness changes gradually as it reaches an acceleration of the 250 g at impact height of 0.59 m. The fourth test was conducted on the thickness of 9.5 mm, the maximum acceleration is 250 g at impact height of 1m. Finally, the last test was conducted on the thickness of 12.7mm. An impact height of 1.48 m is recorded when the acceleration equals to 250 g.

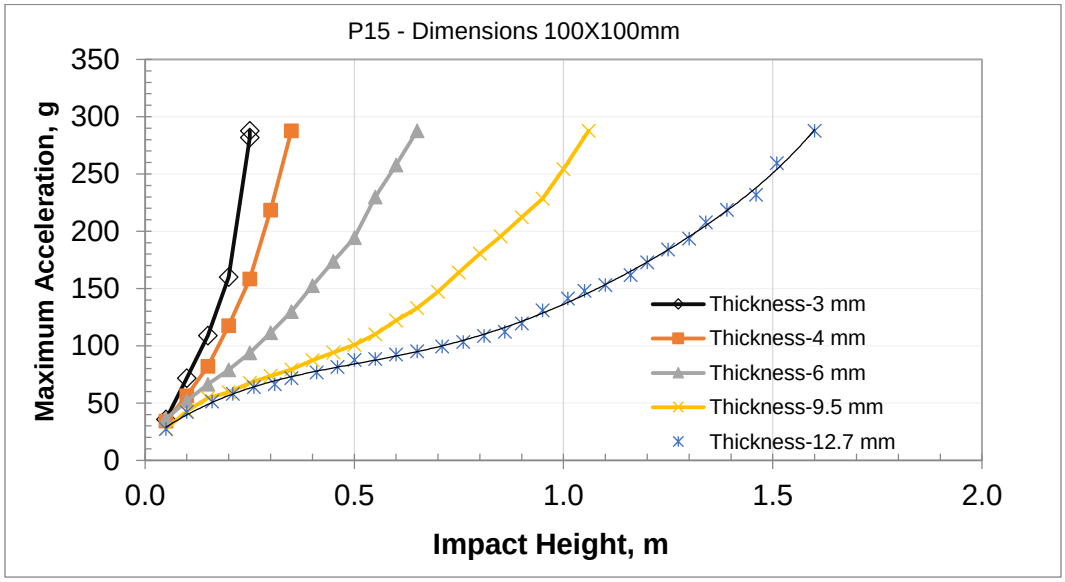

Figure 4-4 - The acceleration behavior of P15 material at different impact heights for various thicknesses

4.1.1.2.2 **Force vs Displacement of P15 at Various Thickness**

Figure 4-5 presents the force versus displacement response for different thickness of the P15 material. The curve at maximum displacement is presented as it essentially envelopes the load versus displacement curves at lower impact height that are presented in Appendix A. Relative displacement are compared at a force level of 12kN. According to the tests, the displacement of the 3mm thick P15 is 2.28 mm which means the displacement percentage is 76 % of the total thickness. Also, at the thickness of 4 mm of P15, the displacement value equals to 2.82 mm which means the displacement percentage is 70.5 %, it is little less than the thickness of 3 mm. Furthermore, the displacement of the thickness of 6 mm is 4.0 mm and displacement percentage is 66.7 %. We notice the displacement percentage decreased when the thickness was increased. Moreover, at the thickness 9.5 mm of P15, the displacement value equals to 6.77mm and the percentage of this displacement is 71.3%. In spite of the thickness of 9.5 mm has high displacement percentage, it stills valid for protection design. The last thickness of P15 material is 12.7 mm. The displacement 8.9 mm and displacement percentage is 70.1 %.

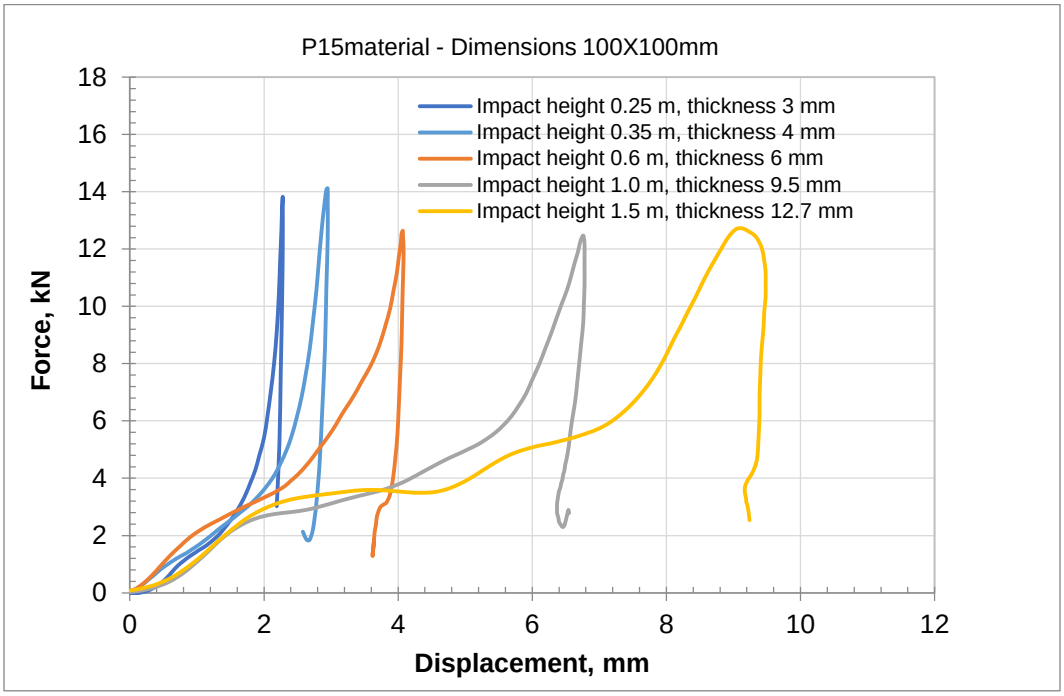

Figure 4-5 - The displacements of P15 material at the maximum value of the acceleration for various thicknesses

4.1.1.2.3 **Acceleration Time History at the Same Impact Height.**

One of the most important comparisons is between the different thicknesses at same impact height to see how the impact period is affected by the changing of the thickness. In Figure 4-6, we used five different thicknesses at impact height of 0.25 m. This impact height was selected because it was the peak observed in the 3mm thick tests. It is clear as shown in the figure below, the thinner material gives a shorter impact period (0.0039sec) and significant rebounding is observed due to the consolidation that occurs. Also, we note that the 9.5 mm and 12.7 mm thicknesses give the approximately same value of maximum acceleration and time period because the thickness 9.5 is enough to achieve the minimum value of

acceleration at the given impact height. Finally, at the same impact height, the maximum value of acceleration for thicknesses of 3 mm, 4 mm, 6 mm, 9.5mm and 12.7 mm are 260g, 159g 93.4g 66g and 66 g, respectively.

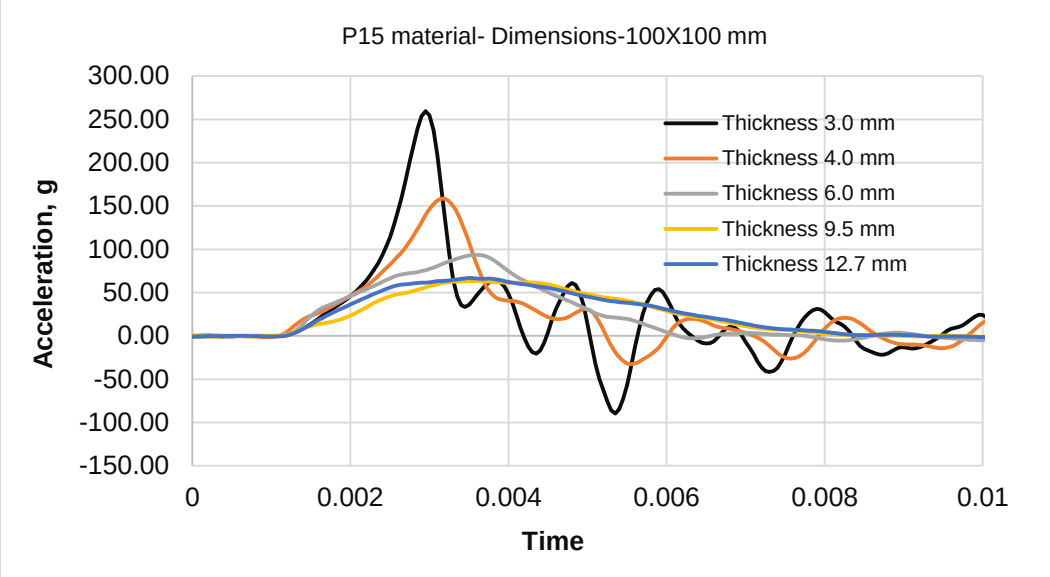

Figure 4-6 - The acceleration time history for different thicknesses of the P15 at the same impact height of 0.25 m for various thicknesses.

Table 4-2 compares the maximum force, displacement and displacement percentage. Furthermore, the table shows maximum impact height of the impactor without exceed the maximum value of the acceleration for the five different thicknesses.

Table 4-2 - Summary of the P15 material at various thickness

Thickness mm	Max Force kN	Max Displacement mm at 12kN	Displacement Percentage % at The 12kN Force	Impactor Height m	Acceleration g at The Given Impact Height
12.7	12.7	8.9	70.1	1.5	260
9.5	12.4	6.77	71.3	1	254.3
6	12.52	4.0	66.7	0.6	257
4	14.116	2.82	70.5	0.35	287.8
3	13.827	2.28	76	0.25	281

4.1.2 **Honeycomb Material**

The honeycomb material is another single layer material that was tested. It has a varying cellular structure that can be classified by cell shape, cell size, cell wall thickness, total thickness and material hardness. The baseline shape is a regular hexagonal with constant wall thickness. Other variants were investigated as described preciously in Section 3.2, chapter three.

The honeycomb structure was created with the aid of silicone molds using different variants of urethane material. A summary of the materials was provided in Tables 3-2 and 3-3, chapter three.

4.1.2.1 The Effect of the Wall Thickness of the Circular Samples.

In this comparison, circular shaped samples of 100 mm diameter were tested using the spherical impactor with diameter 127 mm. In these tests the same material thickness of 6.5mm was used with varying wall thickness and the regular H561 material. The cell size is kept constant at 4.7 mm for both samples. The cell wall thicknesses was 1.0 mm or 1.5 mm.

4.1.2.1.1 The Maximum Acceleration for Circular Shaped Regular Honeycomb

The maximum acceleration due to step impact of the 1.0 mm and 1.5 mm samples are shown in the Figure 4-7. The H561 material at wall thickness of 1.5 mm reaches the acceleration of 250 g at the impact height of 0.61 m. On the other hand, the H561 material at the wall thickness 1.0 mm reaches the acceleration of 250.0 g at impact height equal to 0.55m. At the impact height 0.51 m, both of the walls thicknesses 1.0 mm and 1.5 mm are at the same value of acceleration. Below this value the less stiff sample with the 1mm wall thickness results in lower acceleration.

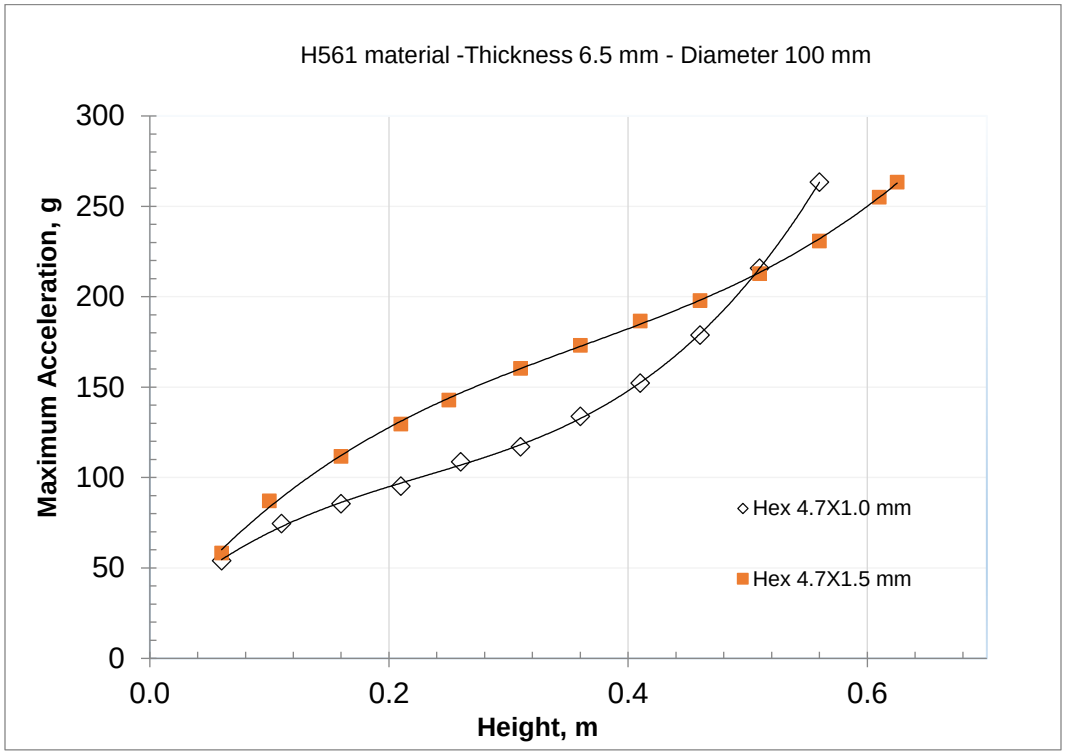

Figure 4-7 - The acceleration behavior of H561 material at different wall thickness for circular samples

4.1.2.1.2 **Force vs Displacement of H561at Various Wall Thicknesses.**

Load versus displacement curves for the circular samples are shown in Figure 4-8. At a force of 12kN the displacement of the wall thickness of 1.0 mm is 4.44 mm which means the displacement percentage is 68.3 %. On the other hand, at the wall thickness 1.5 mm, the displacement value equals 3.5 mm which means the displacement percentage is 53.8 %.

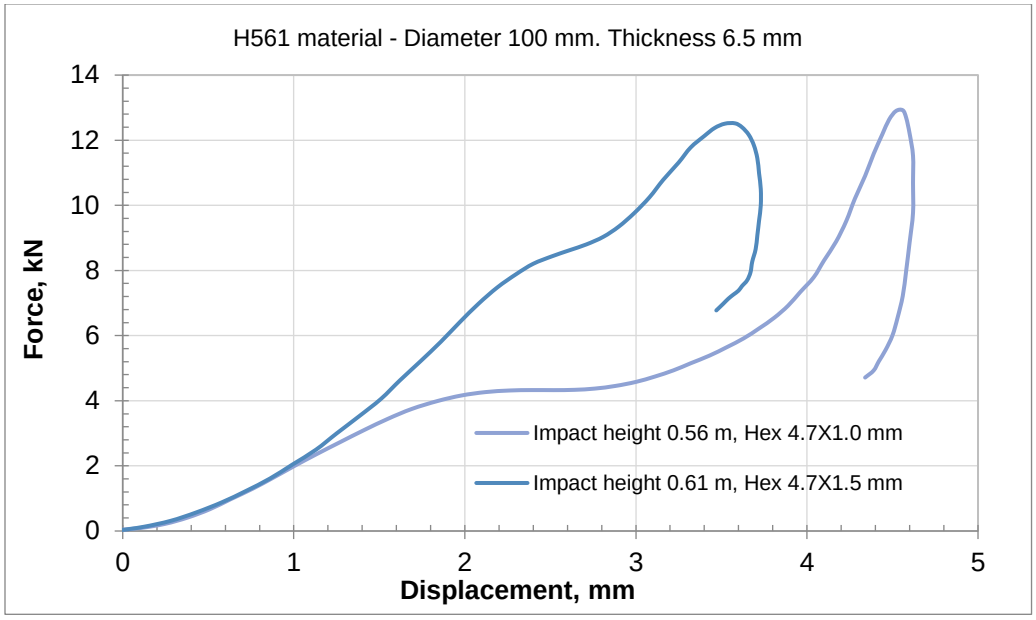

Figure 4-8 - The displacements of H561 material at different wall thicknesses for circular shapes.

4.1.2.1.3 **Acceleration Time History at the Same Impact Height.**

Figure 4-9 shows the influence of different wall thicknesses on time history at impact height of 0.35 m. It is clear as shown in the figure that the thicker wall gives greater acceleration and shorter period time at this impact height. At the wall thickness of 1.0 mm, the maximum acceleration is 132 g. On the other hand, at the wall thickness of 1.5 mm, the maximum acceleration is 186 g.

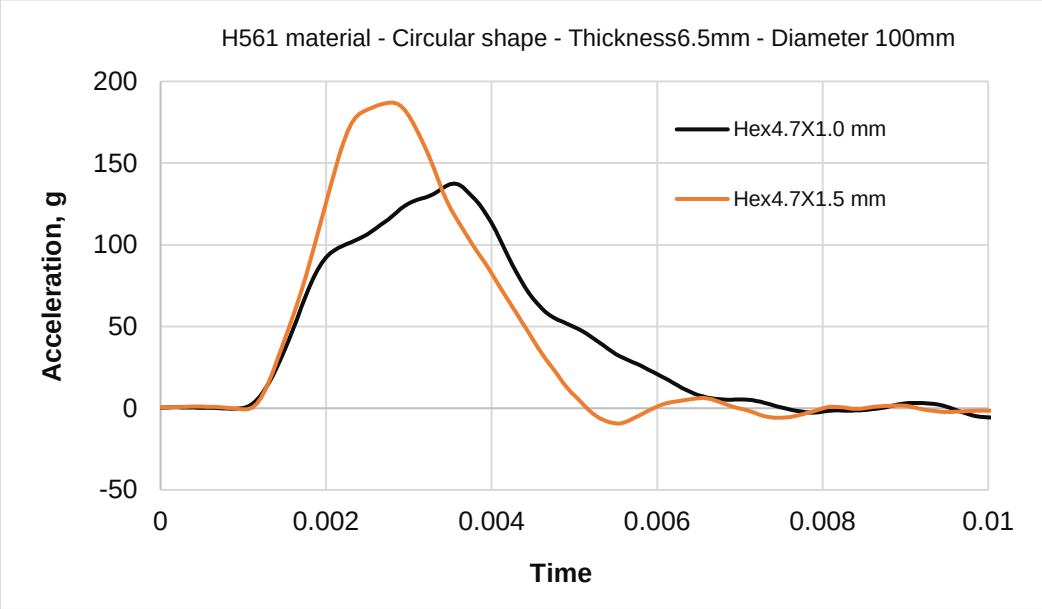

Figure 4-9 - The acceleration time history of the H561 at the same impact height and different wall thicknesses of the cells.

Also, Table 4-3 compares the maximum force, displacement and percentage of the displacement. Also, the table shows maximum impact height of the different wall thicknesses without exceed the maximum value of the acceleration.

Table 4-3 - Summary for the comparison of H561 round samples at different wall thickness of the cells

Cell Dimensions mm	Wall Thickness mm	Thick ess mm	Max Force kN	Max Displacemer mm at 12kN	Displacemen Percentage % at 12kN	Impactor height	Maximum Acceleration g
1.0xHex 4.7	1	6.5	12.9	4.44	68.3	0.56	263.4
1.5xHex 4.7	1.5	6.5	12.5	3.35	53.8	0.61	255.4

4.1.2.2 **Square Sample of Honeycomb Materials.**

In this section the response of square shape samples will be compared using the spherical impactor (type R127 mm) and same sample thickness. Different cells dimensions, cell shape and material stiffness of the honeycomb materials are used. The materials used in the tests are H561, H781, H1036 and H1056 materials. The material thickness is kept constant at 12.5 mm. Variants in cell shape are also included.

4.1.2.2.1 **Honeycomb Materials at Different Cell Shape.**

In this part, we will compare differences between four different cell shapes of the H561 material. We named them T1, T2, T3 and the regular hexagonal shape as shown in Figure 4-10. Photographs A, B, C and D represent T1, T2, T3 and the regular shape, respectively.

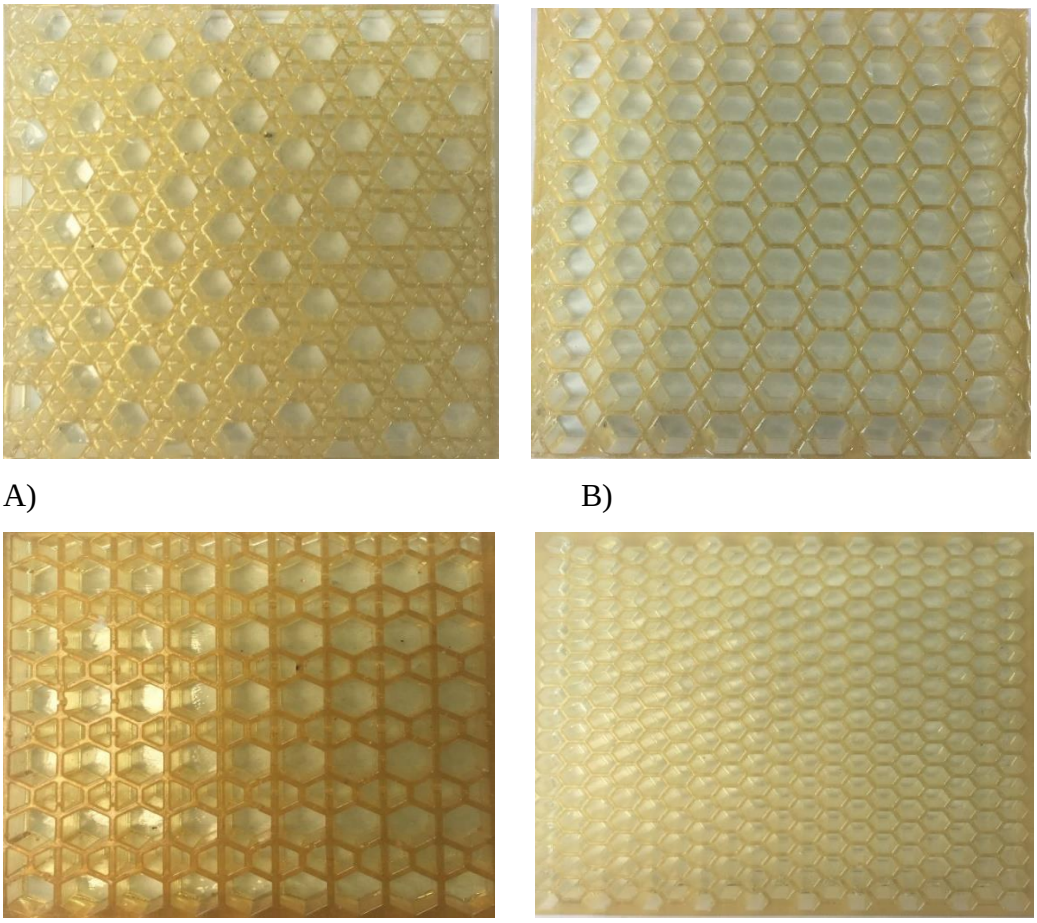

A) B)

C) D)

Figure 4-10 – Honeycomb shape named T1 (A), T2 (B) and T3(C) and the regular hexagonal with c=4.7mm tw = 1 mm (D) of the H561 material.

4.1.2.2.1.1 **The Maximum Acceleration Comparing Honeycomb Cell Structure.**

According to the tests and the materials responses, T2 material is softer than T1, T3 and the regular hexagonal shape as show in Figure 4-11. The acceleration of T2 is significantly lower than the others if the required impact height less than 0.45 m. In the figure 4-11, we notice the T2 material reaches the acceleration of

250 g at impact height of 0.62 m. The T3 material responds initially stiffer than the T2 material. If we compare it with T2 only, it responds with lower acceleration for impact height greater than 0.45. The last one of the irregular shapes is T1. This material is the stiffest responding and it does not reach the acceleration of 250g until the impact height of 1.00 m. Furthermore, the materials T1 and T2 gives the same results at impact height of 0.6 m. Also, T1 and T3 give approximately the same values of maximum acceleration at impact height of 0.74 m. Moreover, T2 and T3 give the same value of maximum acceleration at impact height of approximately 0.47 m.

The regular hexagonal shape is similar in behavior to T3 if the impact height less than 0.35 m. Beyond 0.45 m level it shows less acceleration than the others until impact height of 0.98 m where T1 becomes more optimal.

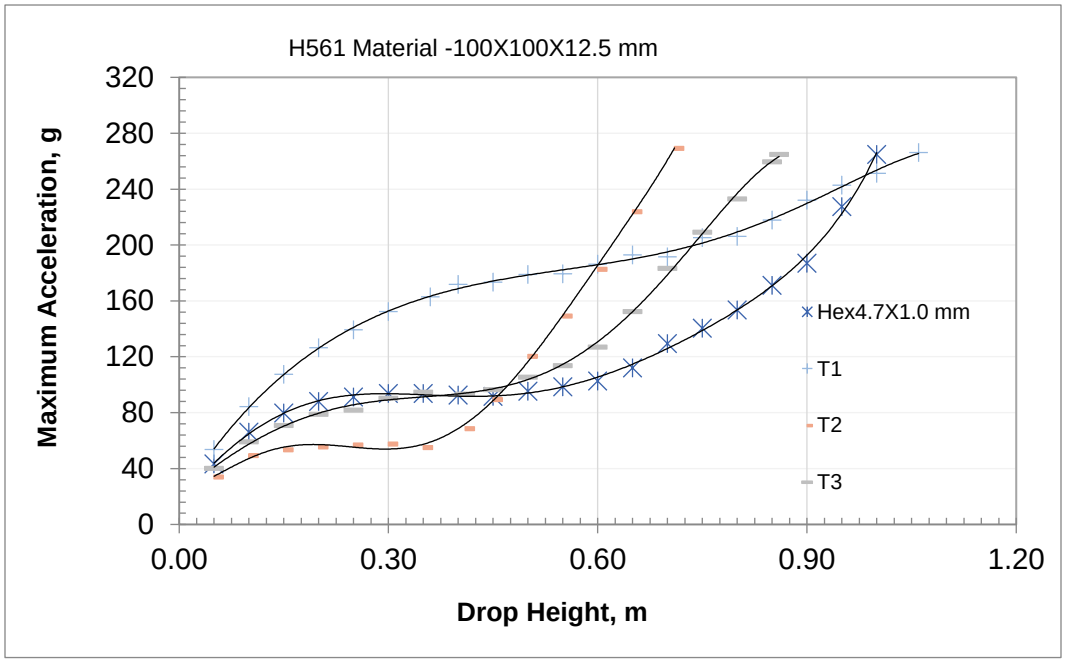

Figure 4-11 – Step impact tests of H561 material for different cells shapes

4.1.2.2.1.2 **Force vs Displacement during Step Impact.**

Figure 4-12 shows the force versus displacement for T1, T2, T3 and the regular hexagonal shape. The displacement of T2 material is greater than the others cells shapes and T1 material gives lowest value of the displacement. These results are expected because the cell wall thickness of T1 is very thick as shown Figure 4-10A. At a force of 12kN, the displacement of T1 material is 6.86, which represents 54.9 % from the total thickness which is 12.5 mm. This percentage gives as an indication that T1 is very stiff material. Regarding to the T2 material, the displacement of this material is 9.3 mm which represents 74.4 % from the total thickness. The results of this material is accepted because the maximum value of the displacement is less than 80 % percent at the maximum value of the acceleration. The third material is T3, the displacement of this material is 8.87 mm which represents 70.1% from the total thickness. The last one is the regular shape. The displacement of this one is 9.1 mm which means the percentage displacement is 72.8 %.

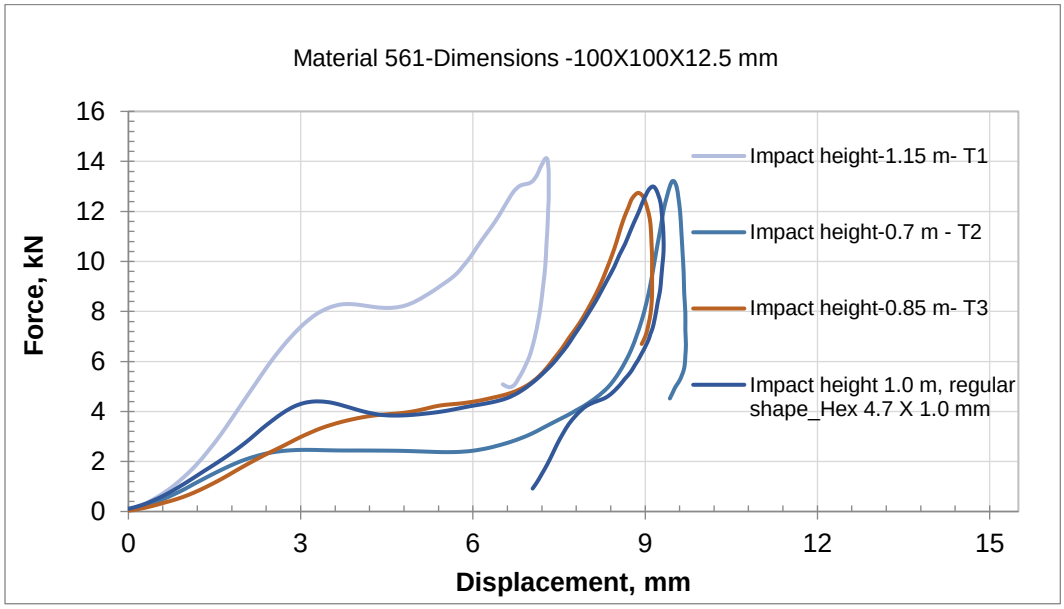

Figure 4-12 - The displacement shape of H561 material for different cell shapes

4.1.2.2.1.3 **The Acceleration Time History at the Same Impact Height.**

Acceleration time histories for T1, T2, T3 and the regular hexagonal shape are presented in Figure 4-13 at impact height 0.7 m. The maximum acceleration recorded are 191 g, 269 g, 182 g and 129 g, for T1, T2, T3 and the regular hexagonal shape respectively. Moreover, the time period of the increasing of the acceleration for regular one is much longer than T1, T2 and T3 materials which is reasonable because the acceleration of the regular one is less than the others materials at the impact height 0.7 m.

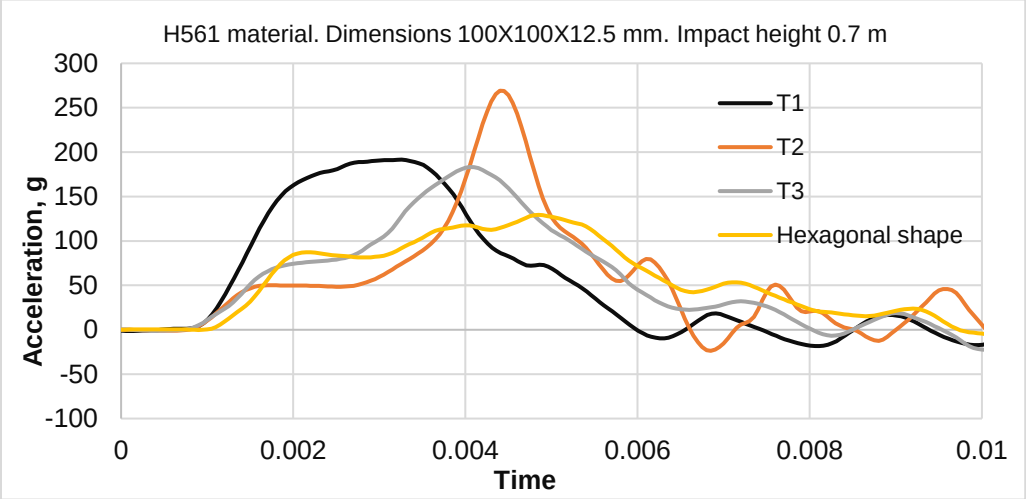

Figure 4-13 - The acceleration time history of the T1, T2, T3 and the regular hexagonal shape at the same impact height.

Table 4-4 shows the most important information for comparison between all of the four shapes at the same materials thicknesses.

Table 4-4 - Summary for the comparison of H561 square samples at different cells sizes.

Sample	Max Force kN	Max Displacement at 12kN	Displacement Percentage % at 12kN	Impactor height m	Acceleration g
T1	14.13	6.86	54.9	1.15	288.1
T2	13.204	9.3	74.4	0.7	270
T3	12.718	8.87	70.1	0.85	260
Regular shape	12.97	9.1	72.8	1.0	264.8

4.1.2.2.2 **Hexagonal Honeycomb Materials at Different Density**

In this section we will compare the influence of material durometer between different honeycomb materials. All of these materials have a regular hexagonal cell shape with dimensions of 100X100X12.5 mm. Also, the cell dimensions are t_w=1.0 mm and c=4.7 mm. The comparison will be between H561, H781, H1036 and H1056 honeycomb materials. The reasons for this kind of comparison is to see which material gives the optimal impact height, displacement and time period at the maximum value of the acceleration. The four materials are shown in A, B, C and D of Figure 4-14.

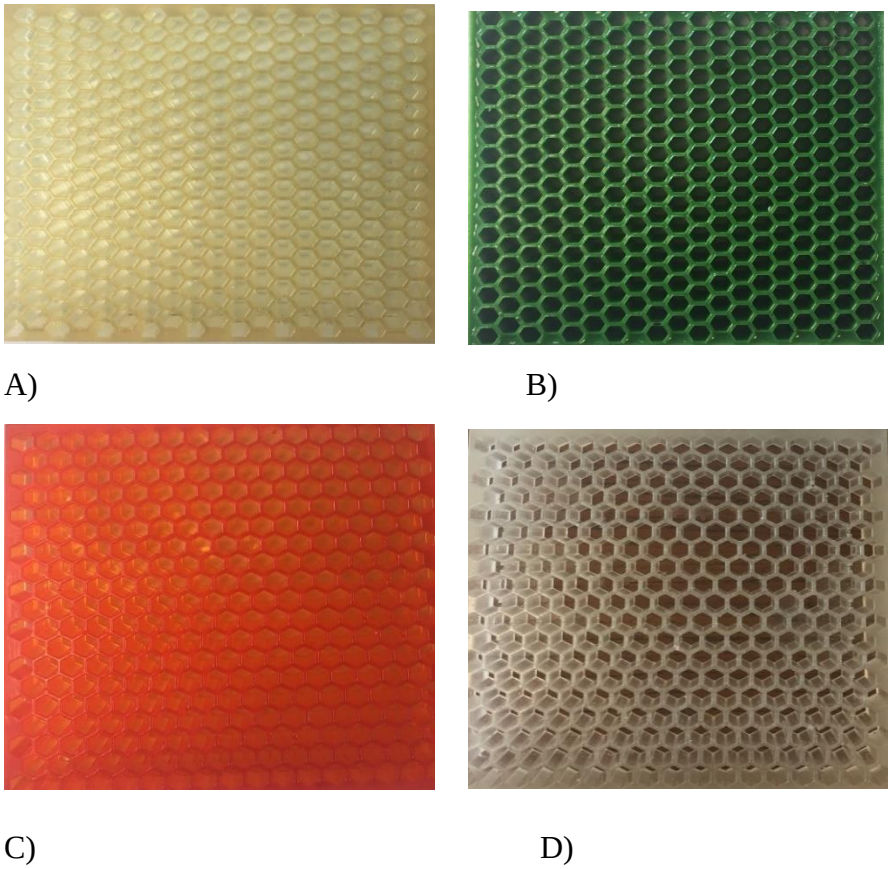

A) B)

C) D)

Figure 4-14 - A, B, C and D portray H561, H781, H1036 and H1056, respectively.

4.1.2.2.2.1 The Maximum Acceleration Comparing Honeycomb Materials

Figure 4-15 presents the results of the step impact for the H561, H781, H1036 and H1056 materials being compared. According to the tests, the H1036 and H1056 materials are considered softer than H561 and H781 materials. Also, the H1036 and H1056 materials give lesser impact acceleration at the lower impact height. These materials consolidate quickly and behave much stiffer and the acceleration dramatically increases as the impact height increases. The H1036 and H1056 materials reach the acceleration of 250 g at impact heights 0.43 m and 0.47 m, respectively as shown in Figure 4-15.

The H781 material does not reach the 250 g of the acceleration until the impact height of 0.48 m. This material behaves as very stiff material at every impact height.

The last one of the four materials is H561. This material gives the higher impact height at the 250 g of the acceleration where it reaches this value of the acceleration at the impact height 0.98 m.

As a result, before we decide which material is the best, we have to know the required impact height for the design. If the required impact height less than 0.15 m, the H1036 material gives the minimum value of the acceleration. The H1056 is the best choice if the required impact height between 0.25 m and 0.3 m. Anyway, the H561 is the best material if the required impact height between 0.3 m and 1.0 m.

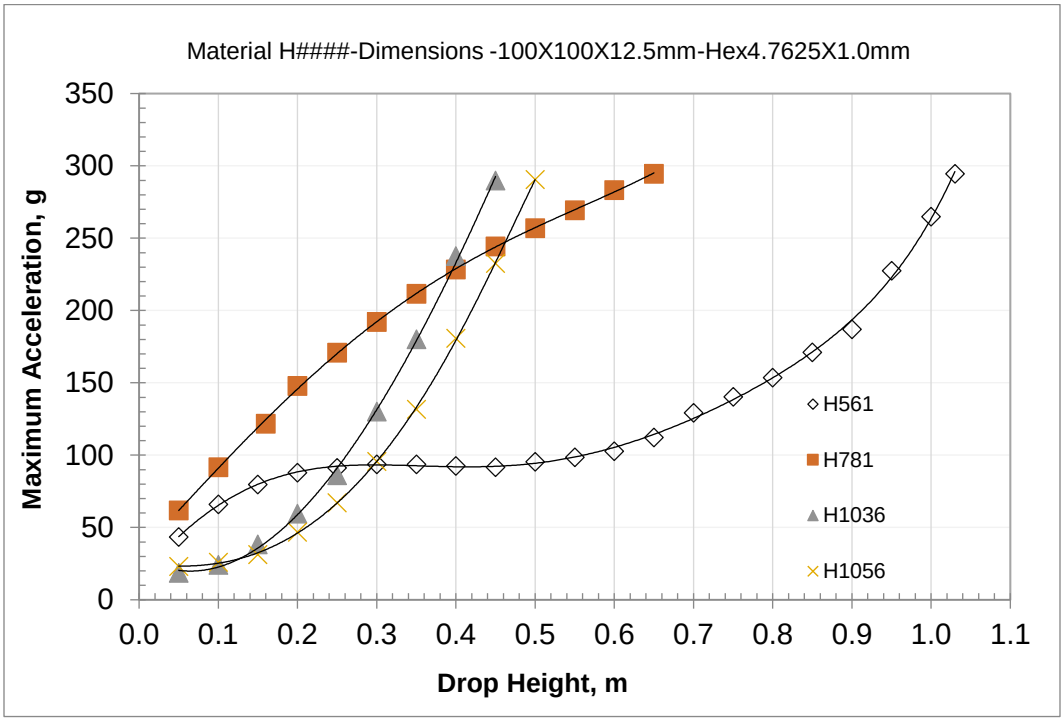

Figure 4-15 – Step impact of honeycomb materials at the same cells shapes and dimensions.

4.1.2.2.2.2 **Force vs Displacement during Step Impact.**

Figure 4-16 shows the force versus displacement for H561, H721, H1036 and H1056 materials. The H561, H1036 and H1056 go throw three phases which are initial phase (materials behaves as soft materials) then buckling phase and then consolidation phase. H781 did not reach the buckling phase during the tests. The displacement of H1036 material is greater than the others materials and H781 material gives lowest value of the displacement. These facts are expected because the H781 material very stiff. At a force of 12kN, the displacement of H1036 material is 9.3 which represents 74.4 % from the total thickness which is 12.5 mm.

This percentage gives as an indication that H1036 is very soft material. Regarding to the H1056 material, the displacement of this material is 9.2 mm which represents 73.6 % from the total thickness. The results of this material is accepted because the maximum value of the displacement is less than 80 % percent at the maximum value of the acceleration. The third material is H781 material, the displacement of this material 3.12 mm which represents 25% from the total thickness. The last one is the H561 material. The displacement of this one is 9.1 mm which means the percentage displacement is 72.8 %.

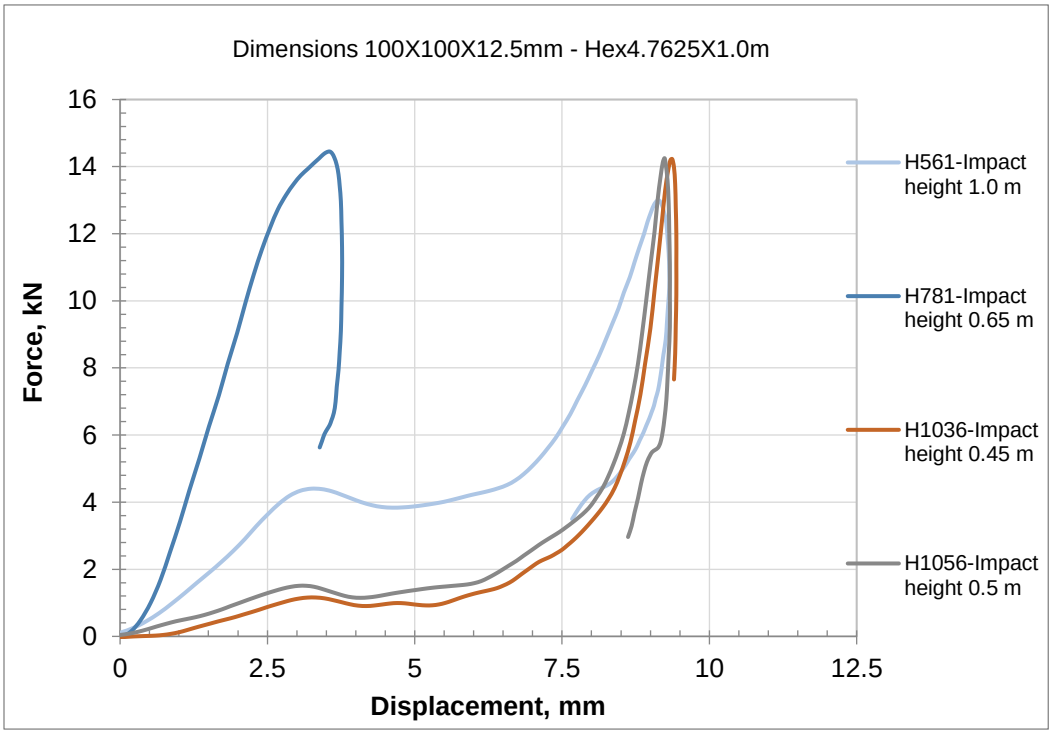

Figure 4-16 - The force versus displacement of the H561, H721, H1036 and H1056 materials at the maximum values of the acceleration

4.1.2.2.2.3 **Acceleration Time History at the Same Impact Height.**

Acceleration time histories for the H561, H721, H1036 and H1056 materials are presented in Figure 4-17 at impact height 0.45 m. The maximum acceleration recorded are 94.4 g, 241 g, 289 g and 232 g, for the H561, H721, H1036 and H1056 materials, respectively. Moreover, the time period of the increasing of the acceleration for H561 material is much longer than H781, H1036 and H1056 materials where the estimates impact period for H561, H781, H1036 and H1056 are 0.0093sec, 0.00345sec, 0.0039sec and 0.00425sec, respectively. It is reasonable because the acceleration of the H561 material is less than the others materials at the impact height 0.45 m. In short, before we decide which material is the best, we have to know the requirements for protection design.

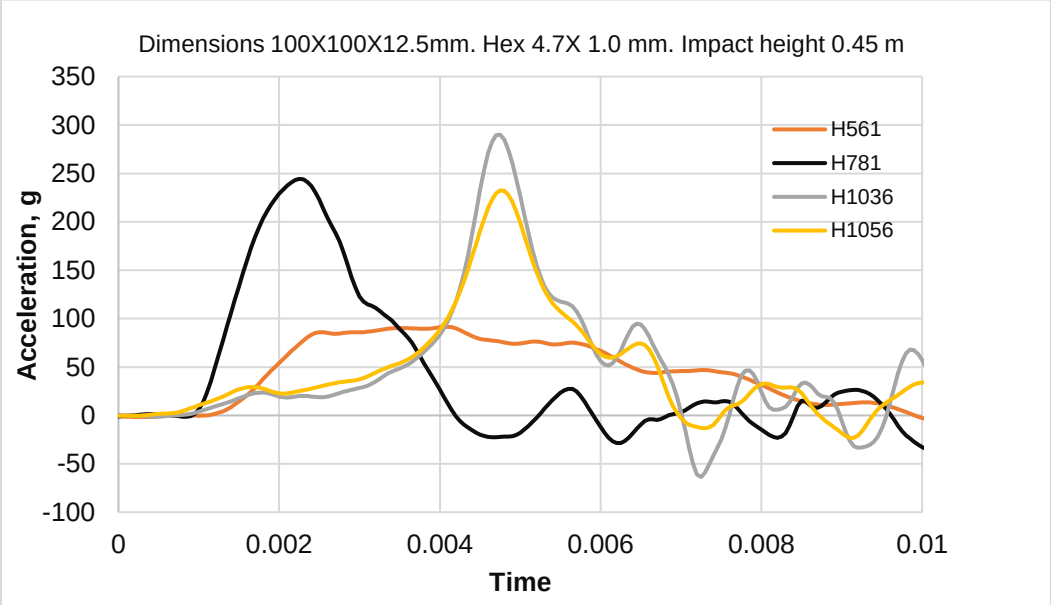

Figure 4-17 - The acceleration time history of H561, H721, H1036 and H1056 materials at the same impact height.

The table 4-5 shows the most important information for the comparison between all of the four materials at the same cells dimensions.

Table 4-5 - Summary of the comparison of the different honeycomb materials at the same hexagonal shape and dimensions.

The material	Max Force kN	Max Displacement at 12kN	Displacement Percentage % at 12kN	Impactor height m	Acceleration g
H561	12.96	9.1	72.8	1.0	264.8
H721	14.45	3.1	25	0.65	294.6
H1036	14.069	9.3	74.4	0.45	290
H1056	14.069	9.2	73.6	0.5	290.6

4.1.2.2.3 **Hexagonal Honeycomb Materials at Different Cell Size.**

In this section we will compare the influence of cell sizes of the honeycomb materials. The hexagonal shapes of H561 material is used for this comparison due to the wide range of cells sizes available. We named them 3mm, 4.7mm, 6.0 mm and 8.0mm. The same mass (5kg) and shape (127 mm radius spherical) of the impactor are used. Furthermore, all samples have the same length, width and thickness, namely 100mm x 100mm 12.5 mm. Also, all samples have the same wall thickness, namely 1.0 mm. The reasons from this comparison are to see the effect of wall cell size on the impact, the maximum value of the acceleration, and the displacement percentage.

4.1.2.2.3.1 The Maximum Acceleration Comparing Honeycomb Different Cells Sizes

According to the tests and the materials responses, the cell size of 8.0 mm is softer than cell sizes of 3.0 mm, 4.7 mm and 6.0 mm as show in Figure 4-18. The acceleration of the cell size 8.0 mm is significantly lower than the others if the required impact height less than 0.40 m. In the figure 4-18, we notice the cell size 8.0 mm reaches the acceleration of 260 g at impact height of 0.65 m. The cell size 6.0 mm responds initially stiffer than the 8.0 mm. Also, the cell size 6.0 mm with lower acceleration for impact heights between 0.4 m and 0.5m. The third cell size is 4.7 mm. The cell size of 4.7 does not reach the acceleration of 260g until the impact height of 0.99 m. Also, the cell size 4.7 mm with lower acceleration for impact heights between 0.5 m and 0.95m. The last cell size is 3.0 mm. The cell size of 3.0 mm does not reach the acceleration of 260g until the impact height of 1.1 m. Also, the cell size 3.0 mm with lower acceleration for impact height greater than 0.95m.

Furthermore, the cell sizes of 6.0 mm and 8.0 mm give the same results at impact height of 0.4 m. Also, the cell sizes of 4.7 mm and 6.0 mm give approximately the same values of maximum acceleration at impact height of 0.5 m. Moreover, cell sizes of 3.0 mm and 4.7 mm give the same value of maximum acceleration at impact height of approximately 0.95 m.

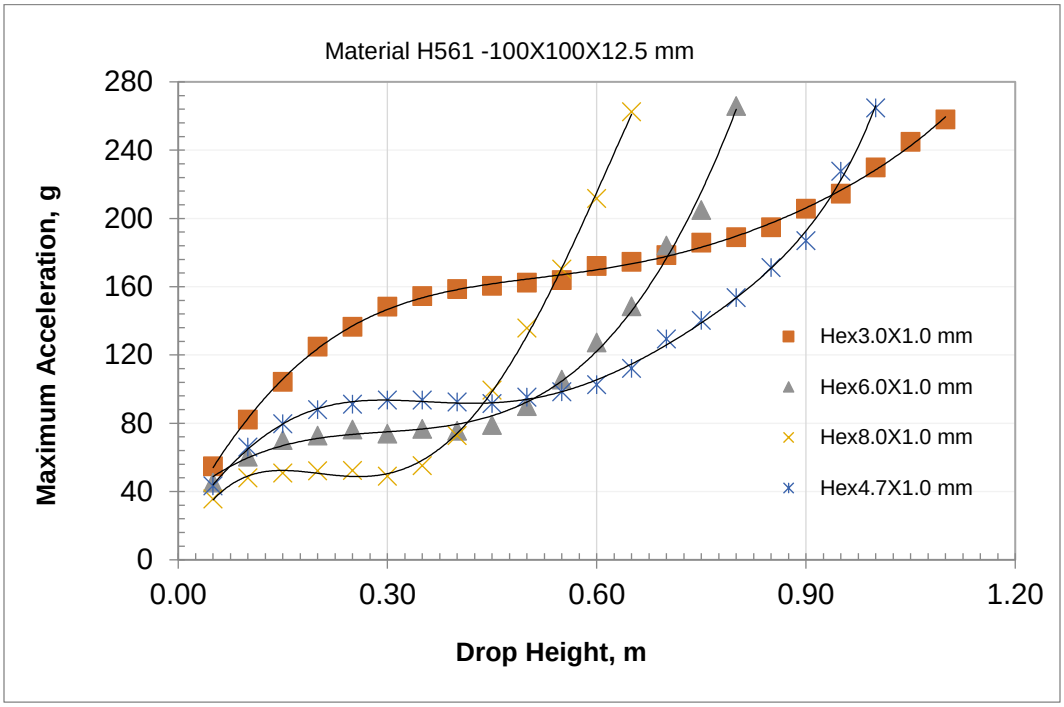

Figure 4-18 - The increasing of the acceleration of honeycomb materials at different cells sizes.

4.1.2.2.3.2 **Force vs Displacement during Step Impact.**

Figure 4-19 shows the force versus displacement for the cells sizes of 3.0 mm, 4.7 mm, 6.0 mm and 8.0 mm. The displacement of the 8.0 mm cell size is greater than the others cells dimensions. Also, the cell size 3.0 mm gives lowest value of the displacement. These facts are expected because the cell size thickness of 3.0 mm is very small. At a force of 12kN, the displacement of 3.0 mm cell size is 7.6 mm which represents 60.8 % from the total thickness which is 12.5 mm. This percentage gives as an indication that the cell size made the material very stiff. Regarding to the cell size 4.7 mm, the displacement of this cell is 9.1 mm which

represents 72.8 % from the total thickness. The results of this material is accepted because the maximum value of the displacement is less than 80 % percent at the maximum value of the acceleration. The third cell size is 6 mm, the displacement of this one is 9.5 mm which represents 76% from the total thickness. The last one is the cell size 8.0 mm. The displacement of this one is 9.9 mm which means the percentage displacement is 79.2 %.

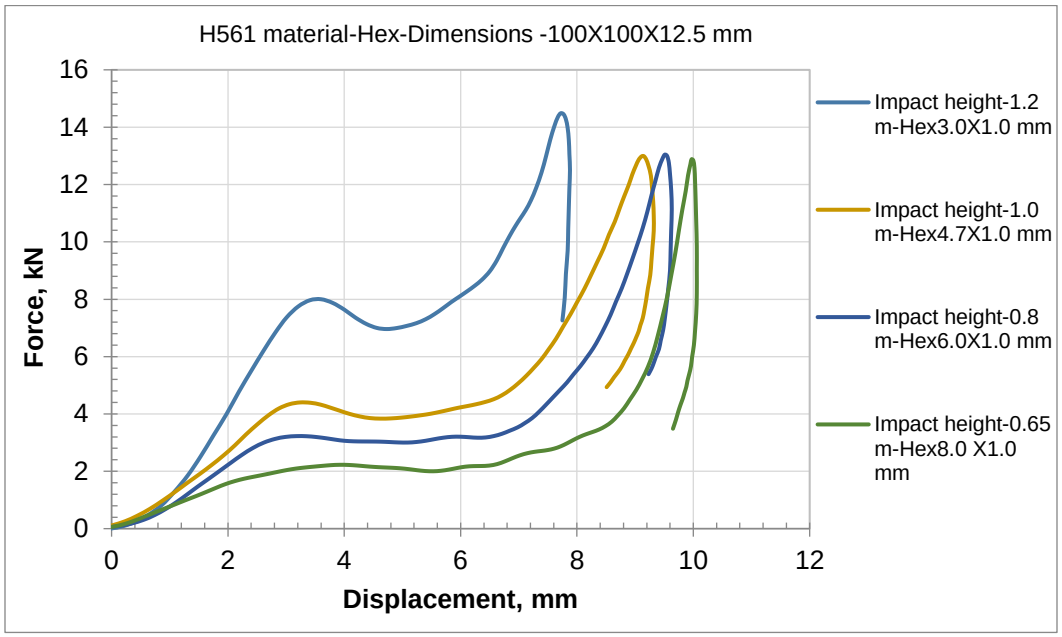

Figure 4-19 - The displacements of the four different cells sizes of the hexagonal honeycomb H561 material at the maximum value of the acceleration.

4.1.2.2.3.3 **Acceleration Time History at the Same Impact Height.**

Acceleration time histories for the cells sizes of 3.0 mm, 4.7 mm, 6.0 mm and 8.0 mm are presented in Figure 4-20 at impact height 0.65 m. The maximum acceleration recorded are 174 g, 112 g, 148 g and 262 g, for the cells sizes of 3.0 mm, 4.7 mm, 6.0 mm and 8.0 mm respectively. Moreover, the time period of the increasing of the acceleration for 4.7 cell size is longer than 3.0 mm, 6.0 mm and

8.0 mm cells sizes where the estimates impact period for 3.0 mm, 4.7mm, 6.0 mm and 8.0 mm cells sizes are 0.0056sec, 0.0086sec, 0.00855sec and 0.00605sec, respectively. It is reasonable because the acceleration for the cell size of 4.7 mm is less than the others cells size at the impact height 0.65 m. In short, before we decide which cell size is the best, we have to know the requirements for protection design.

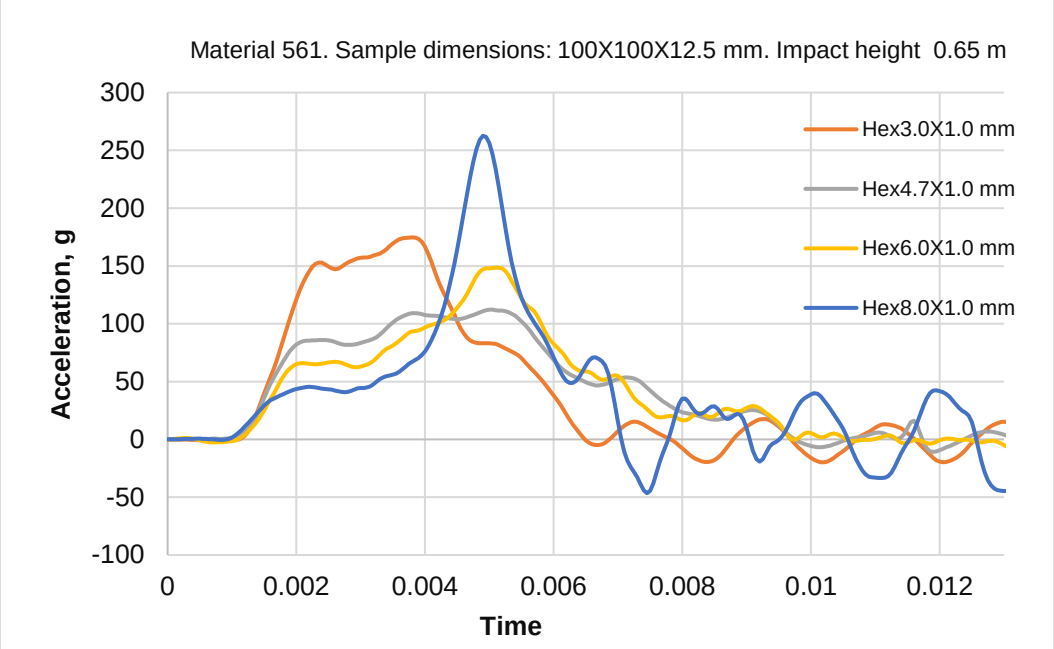

Figure 4-20 - The acceleration time history for the four different cells sizes of H561 materials at the same impact height.

The table 4-9 shows the most important information for the comparison between all of the five different cells dimensions of H561 hexagonal material.

Table 4-6 - Summary for comparison of H561 square samples at different cells sizes.

The cell dimensions	Max Force kN	Max Displacement at 12kN	Displacement Percentage % at 12kN	Impactor height m	Acceleration g
Hex3X1.0	14.27	7.6	60.8	1.2	295.3
Hex4.7X1.0	12.875	9.1	72.8	1.0	264.8
Hex6.0X1.0	13.04	9.5	76.0	0.8	265.9
Hex8.0X1.0	12.703	9.9	79.2	0.65	262.6

4.2 **Multi-Layered Materials**

Using multi-layered sample can be beneficial if the design is to be optimized for more than one level of impact energy. Also, we can increase the accepted impact height of the materials without increase the materials thickness. Furthermore, we can involve both the soft and stiff materials where the soft materials absorbs energy at low impact energy and the stiff materials performs at the greater impact height.

4.2.1 **Two Layers Samples**

In this part of comparison, two layers samples are tested. The purpose from this kind of test is to use the honeycomb and dilatant materials at the same time in one sample. The samples consists of various combination of soft and hard materials.

All of the samples consist from dilatant and honeycomb materials and the final thicknesses are 12.5 mm and 24.5 mm. For the final thickness 12.5 mm, the dimensions of the dilatant and honeycomb materials are 100X100X6 mm and 100X100X6.5 mm, respectively. Also, for the 24.5 mm thick samples, the

dimensions of the dilatant and honeycomb materials are 100X100X12 mm and 100X100X12.5 mm, respectively.

Five samples are used. The first sample consists from soft material in top with stiff material in the bottom, namely the P09 material with H561 material. The second sample consists of the stiff material on top with soft material on the bottom, namely the P25 material with H1056 material. The third sample consist of two stiff materials, namely the P25 material and H561 material. The forth material consists of two soft materials, namely the P09 material and H1036 material. The last one consists of the P15 material and H1056 material.

4.2.1.1 **Comparison at Thickness 12.5 mm**

In this part of comparison we will compare the maximum values of the acceleration during step impact between the five different samples. Namely, P25_H561, P15_H1056, P25_H1036, P09_H1036 and P09_H561. Also, we will compare the acceleration time history at the same impact height. Furthermore, we will compare the maximum value of the displacement for all of the five samples at the maximum value of the acceleration which is 250 g. The total thickness of these samples is 12.5 mm. The same mass (5kg) and shape (127 mm radius spherical) of the impactor are used

4.2.1.1.1 The Maximum Acceleration during Step Impact.

As shown in the figure 4-21 and according to the tests and the responses of the two layers materials, the P25- H561 sample reaches the 250g acceleration at impact height 1.18 m. This reality does not mean this sample gives the lower value of the acceleration at every impact height because it consists from two stiff materials. This sample gives higher maximum acceleration at the low impact height if we compare it with others samples. For example, if we want to choose a material for protection and the value of the permitted acceleration of this material is 100 g when the impactor impacts it. The sample of P25-H561 reaches this value at impact height 0.2 m. On the other hand, all of the others samples give higher impact height than the sample of P25_H561. As a result, it is important to know the behavior of the samples at every impact height to choose the best for specific design. Also, the samples of P15_H1056, P25_H1036, P09_H1036 and P09_H561 reach the 250g acceleration at impact heights 1.08 m, 1.0 m, 0.75 m and 0.91 m

The P09_H1036 sample gives the lower value of the acceleration if required impact height is 0.4 m or less than 0.4 m. Anyway, the behavior of this sample change and the acceleration dramatically increases for the impact height greater than 0.4 m. Also, P15_H1056 gives the lower value of the acceleration for impact heights between 0.4 m and 1.06 m. Furthermore, the P25-H561 gives the lower value of the acceleration for impact heights more than 1.06 m

Finally, as shown in the figure, it is clear which one behaves as soft material and which one behaves as a stiff material at step impact.

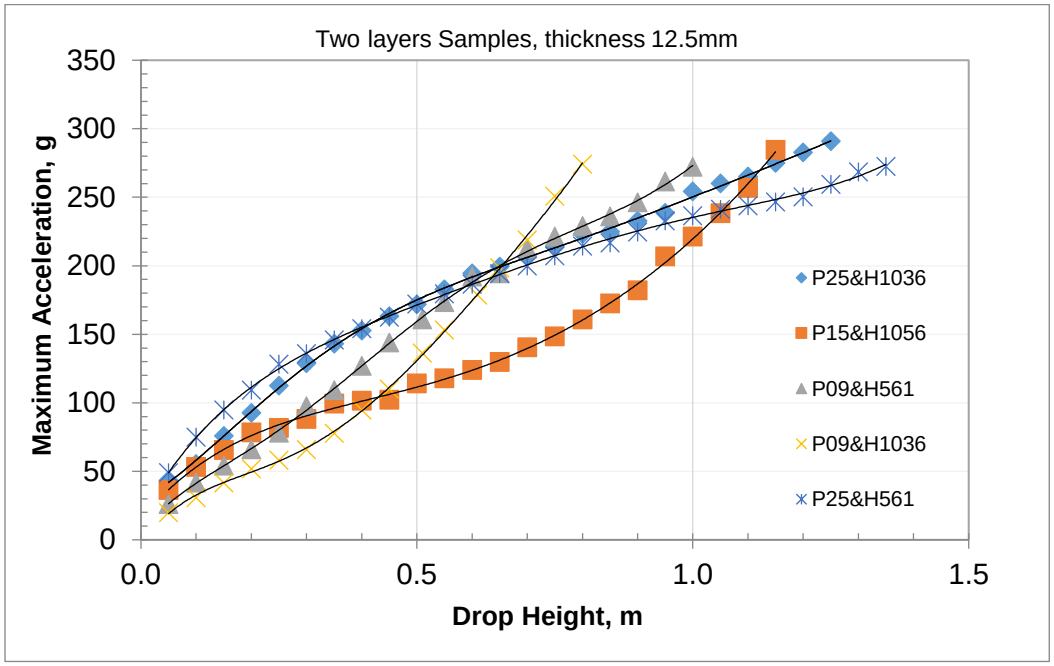

Figure 4-21 - The increasing of the acceleration of the two layers materials.

4.2.1.1.2 **The Force vs Displacement during Step Impact**

Figure 4-22 presents the force versus displacement response for different two layers samples of the P25_H561, P15_H1056, P25_H1036, P09_H1036 and P09_H561. The curve at maximum displacement is presented as it essentially envelopes the load versus displacement curves at lower impact height that are presented in Appendix A. Relative displacement are compared at a force level of 12kN. According to the tests, the displacement of the sample P25_H561 is 6.9 mm which means the displacement percentage is 55.2 % of the total thickness. Also, at the P15_H1056 sample, the displacement value equals to 9.5 mm which means the displacement percentage is 76.0 %, it is more than the sample of

P25_H561. Furthermore, the displacement of the P25_H1036 sample is 8.3 mm and displacement percentage is 66.4 %. Moreover, at the sample of P09_H1036, the displacement value equals to 9.8 mm and the percentage of this displacement is 78.4 %. The last sample is P09_H561. The displacement 8.3 mm and displacement percentage is 66.4 %.

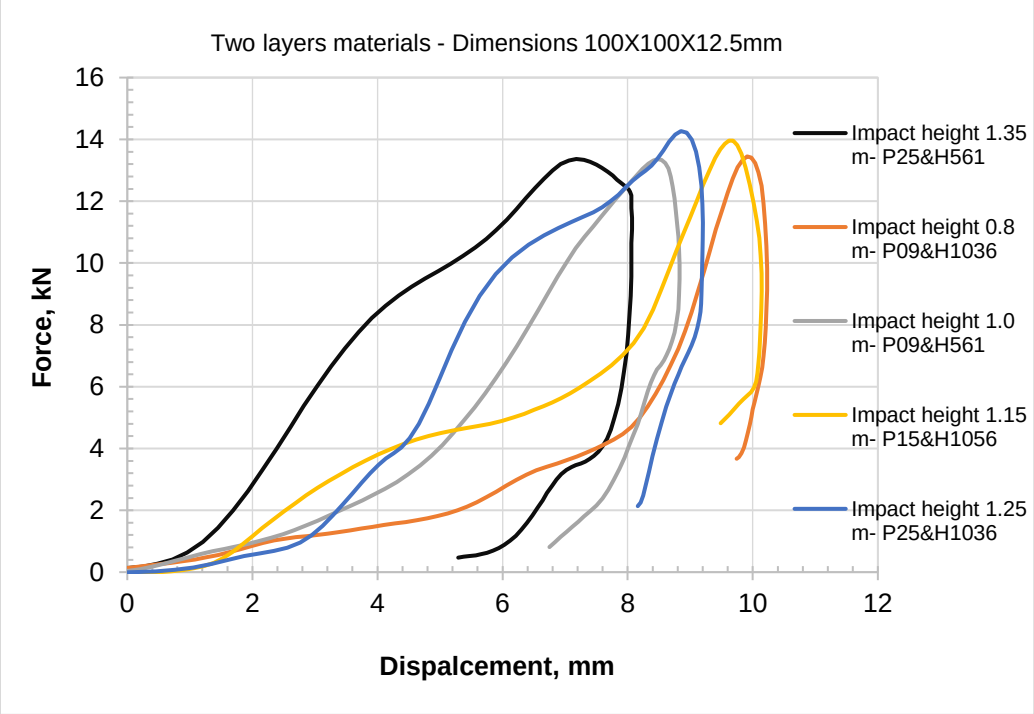

Figure 4-22 - The maximum values of the displacements of the two layers materials

4.2.1.1.3 **Acceleration Time History at the Same Impact Height.**

The acceleration time history at an impact height of 0.8 m is shown in Figure 4-23. The peak acceleration and time history signatures of the 5 samples are significant different. For example, at impact height 0.8 m the maximum value of acceleration for P25_H561 sample is 213 g while at the same impact height, the maximum value of acceleration for P15_H1056, P09_H561, P25_H1036, and

P09_H1036 samples is 159g, 229 g, 224 g and 274 g respectively. Furthermore, according to Figure 4-23, the time period of the increasing of the acceleration for P15_H1056 material is longer than P25_H561, P09_H561, P25_H1036, and P09_H1036 samples where the estimates impact periods for_P15_H1056, P25_H561, P09_H561, P25_H1036, and P09_H1036 are 0.007sec, 0.00525sec, 0.0064sec, 0.00595sec and 0.0057sec, respectively. This means the P15_H1056 sample has the ability to absorb impulse at a lower level of force compared to the others materials. In short, before we decide which sample is the best, we have to know the design requirements. In other word, it is very important to know the required impact height.

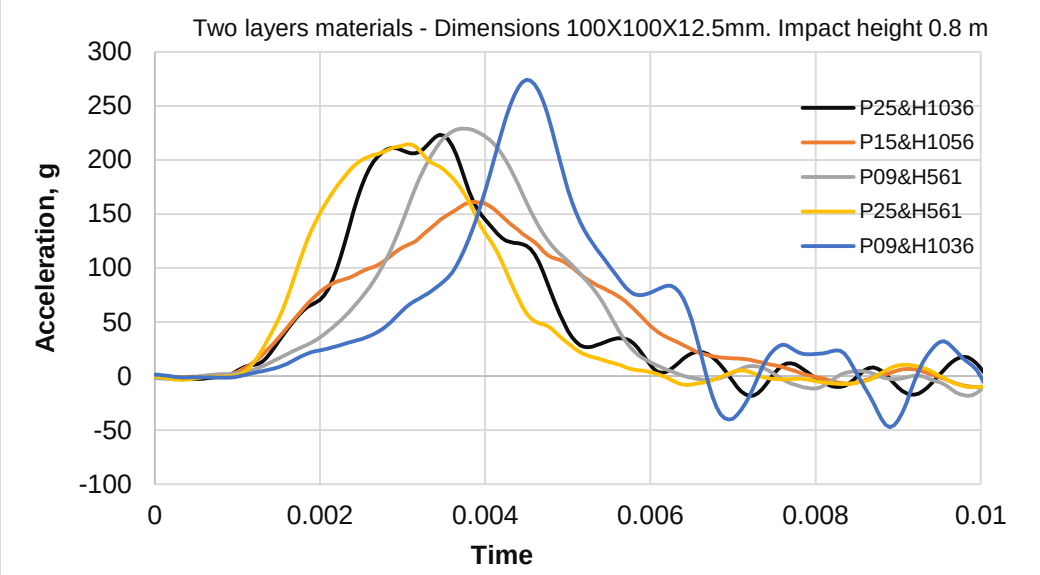

Figure 4-23 - The acceleration time history for the two layers materials at the same impact height for thickness 12.5 mm.

The table 4-7 shows summary for the comparison of the multilayers samples of P25_H561, P15_H1056, P25_H1036, P09_H1036 and P09_H561 samples at the total thickness 12.5 mm.

Table 4-7 - Summary of the two layers square samples at the total thickness 12.5 mm.

The Material name	Max Force kN	Displacement at force 12 kN	Displacement Percentage % at force 12 kN	Impactor height m	Acceleration g
P25_H561	13.3	6.85	55.2	1.35	272.5
P15_H1056	14	9.5	76	1.15	284.6
P25_H1036	14.2	8.3	66.4	1.25	290.9
P09_H1036	13.08	9.8	78.4	0.8	274.2
P09_H561	13.37	8.3	66.4	1.0	272.4

4.2.1.2 **Comparison at Thickness 24.5 mm**

In this part of comparison we will compare the maximum values of the acceleration during step impact between five different samples. We named them P25_H561, P15_H1056, P25_H1036, P09_H1036 and P09_H561. Also, we will compare the acceleration time history at the same impact height. Furthermore, we will compare the maximum value of the displacement for all of the five samples at the maximum value of the acceleration which is 250 g. The total thickness of these

samples is 24.5 mm. The same mass (5kg) and shape (127 mm radius spherical) of the impactor are used.

4.2.1.2.1 The Maximum Acceleration during Step Impact.

As shown in the figure 4-24 and according to the tests and the responses of the two layers materials, the P25- H561 sample reaches the 250g acceleration at impact height 2.4 m. This reality does not mean this sample gives the lower value of the acceleration at every impact height because it consists from two stiff materials. This sample gives higher maximum acceleration at the low impact height if we compare it with others samples. For example, if we want to choose a material for protection and the value of the permitted acceleration of this material is 100 g when the impactor impacts it. The sample of P25-H561 reaches this value at impact height 0.25 m. On the other hand, all of the others samples give higher impact height than the sample of P25_H561 at 250g acceleration. As a result, it is important to know the behavior of the samples at every impact height to choose the best for specific design. Also, the samples of P15_H1056, P25_H1036, P09_H1036 and P09_H561 reach the 250g acceleration at impact heights 2.0 m, 2.2 m, 1.4 m and 1.95 m

The P09_H1036 sample gives the lower value of the acceleration if required impact height is 0.8 m or less than 0.8 m. Anyway, the behavior of this sample change and the acceleration dramatically increases for the impact height greater than 0.8 m. Also, P15_H1056 gives the lower value of the acceleration for impact heights between 0.8 m and 1.8 m. Furthermore, the P25-H561 gives the lower value of the acceleration for impact heights more than 1.8 m

Finally, as shown in the Figure below, it is clear which one behaves as soft material and which one behaves as a stiff material at step impact.

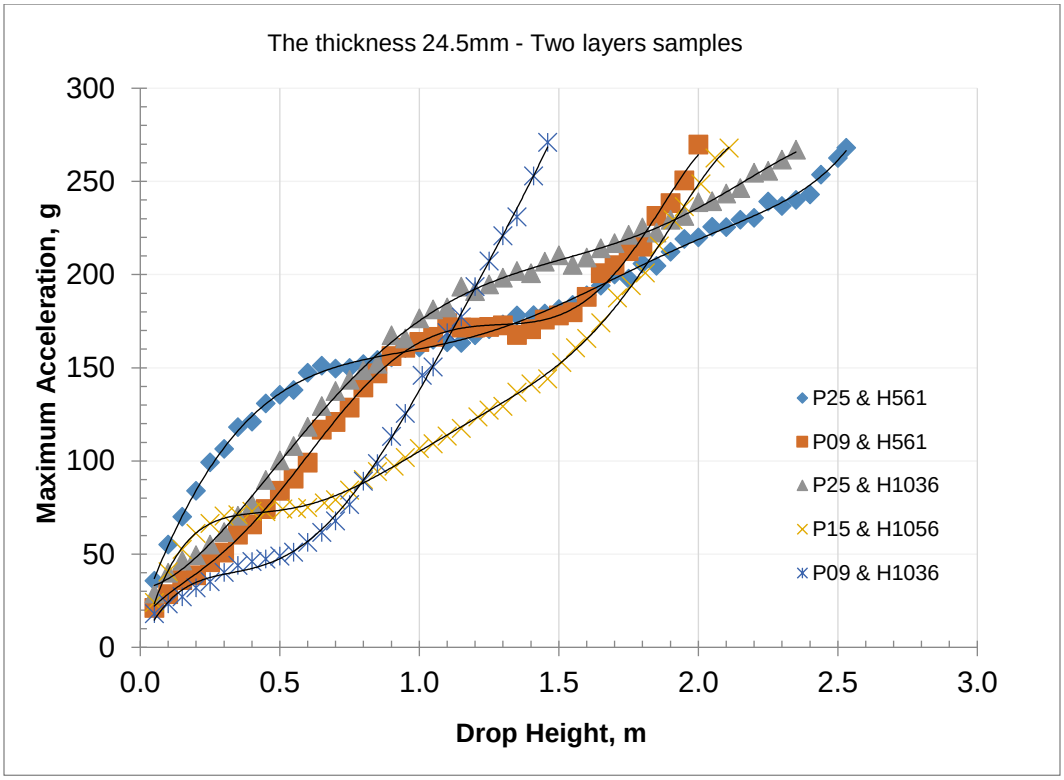

Figure 4-24 - The increasing of the acceleration of the two layers materials at thickness 24.5 mm

4.2.1.2.2 **Force vs Displacement during Step Impact**

Figure 4-25 presents the force versus displacement response for different two layers samples of the P25_H561, P15_H1056, P25_H1036, P09_H1036 and P09_H561. The curve at maximum displacement is presented as it essentially envelopes the load versus displacement curves at lower impact height that are

presented in Appendix A. Relative displacement are compared at a force level of 12kN. According to the tests, the displacement of the sample P25_H561 is 13.2 mm which means the displacement percentage is 53.9 % of the total thickness. Also, at the P15_H1056 sample, the displacement value equals to 19.2 mm which means the displacement percentage is 78.4 %, it is more than the sample of P25_H561. Furthermore, the displacement of the P25_H1036 sample is 14.5 mm and displacement percentage is 58.4 %. Moreover, at the sample of P09_H1036, the displacement value equals to 19.5 mm and the percentage of this displacement is 79.6 %. The last sample is P09_H561. The displacement 18.3 mm and displacement percentage is 74.7 %.

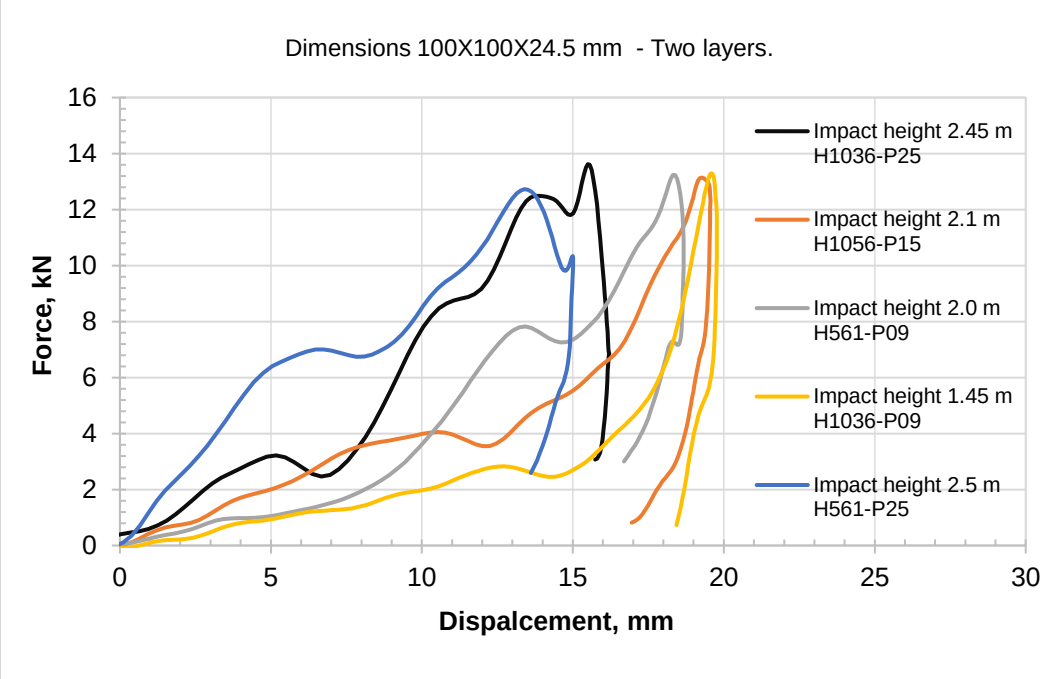

Figure 4-25 - The maximum values of the displacements of the two layers materials at the total thickness 24.5 mm.

4.2.1.2.3 **Acceleration Time History at the Same Impact Height.**

The acceleration time history at an impact height of 1.45 m is shown in Figure 4-26. The peak acceleration and time history signatures of the 5 samples are significant different. For example, at impact height 1.45 m the maximum value of acceleration for P25_H561 sample is 183 g while at the same impact height, the maximum value of acceleration for P15_H1056, P09_H561, P25_H1036, and P09_H1036 samples is 144 g, 176 g, 207 g and 271 g respectively. Furthermore, according to Figure 4-26, the time period of the increasing of the acceleration for P15_H1056 material is much longer than P25_H561, P09_H561, P25_H1036, and P09_H1036 samples where the estimates impact periods for P15_H1056, P25_H561, P09_H561, P25_H1036, and P09_H1036 are 0.0106sec, 0.0071sec, 0.00865sec, 0.00875sec and 0.00745sec, respectively. This means the P15_H1056 sample has the ability to absorb impulse at a lower level of force compared to the others materials. In short, before we decide which sample is the best, we have to know the design requirements. In other word, it is very important to know the required impact height.

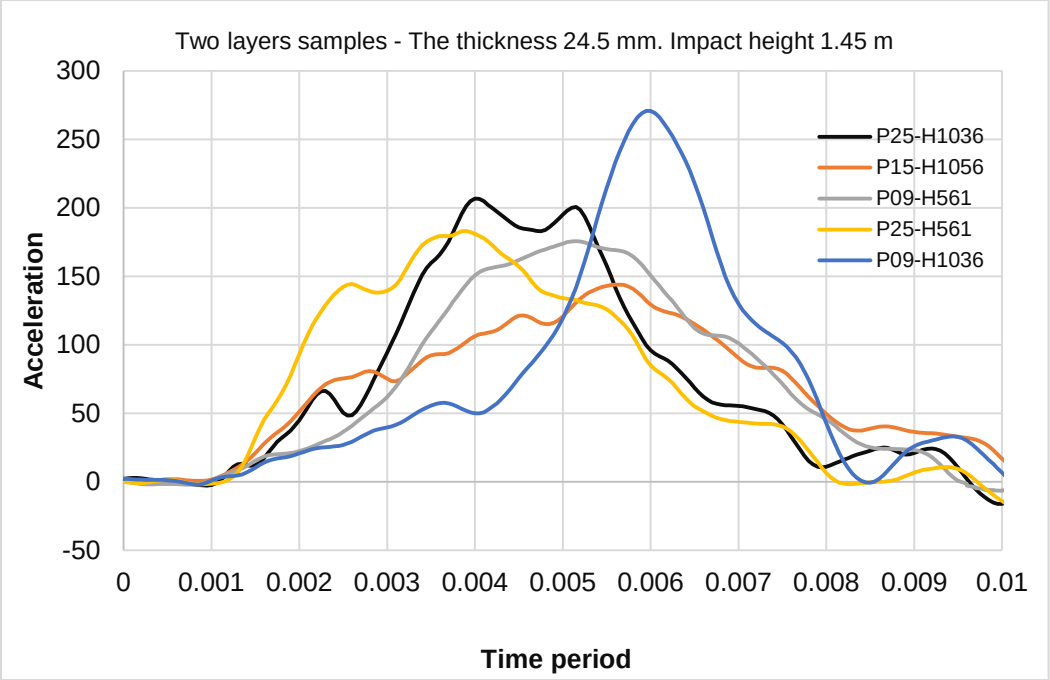

Figure 4-26 - The acceleration time history for the two layers materials at the same impact height.

The table 4-8 show most important information for the comparison between the two layers samples of P25_H561, P15_H1056, P25_H1036, P09_H1036 and P09_H561.

Table 4-8- Summary of the two layers square samples at the total thickness 24.5 mm.

The material name	Max Force kN	Max Displacement at force 12kN	Displacement Percentage % at force 12kN	Impactor height m at max force	Acceleration g
P25_H561	12.64	13.2	53.9	2.5	262.6
P15_H1056	13.057	19.2	78.4	2.11	267.9
P25_H1036	13.498	14.3	58.4	2.45	277.7
P09_H1036	13.287	19.5	79.6	1.46	270.9
P09_H561	13.2287	18.3	74.7	2.0	269.8

CHAPTER FIVE

DISCUSSION AND RECOMMENDATION FOR FUTURE WORK

Prevention of impact related injury is important to the population in general and especially to athletes and the elderly. According to the Centers for Disease Control and Prevention (CDC), most of the traumatic brain injuries (TBI) happen because of falls. Regarding the elderly population, in 2009 about 20,000 people died due to falls and the percentage rate is increasing, [3]. Accordingly, use of impact resistant materials to prevent head injury and concussion is the subject of much study in protective equipment for sports and other activities. Understanding the mechanical response of impact resistant materials and how this response changes with geometric and material parameters is important when designing and optimizing new materials. At a given impact energy, the most optimal material response should have a stiffness allowing for maximum energy absorption through deformation processes which will decrease the forces due to the impact. In actual situations impact energy levels are unknown and an optimal solution at one input may not be optimal at another. Accordingly, researchers and specification writers are now looking at multiple input criteria for impact resisting products.

In this study, the variation in impact performance with material properties and geometry of urethane honeycomb and polymeric foam materials were quantified so that they can eventually be used to create a design criterion that can achieve an optimal performance requirement for multi-level input criteria. Results of the single-layer foam material showed that a stiffer material is generally more optimal as the impact height increases. Stiffness in the foam materials tested is directly related to the density. Regarding the results of the single-layer urethane honeycomb, increasing of the material thickness has the same net effect as in the foam. Overall stiffness of the honeycomb material is controlled by the material

durometer and the cell structure, predominately the solids ratio. Modification of the cell wall thickness or the cell size leads to changes in response that can be used to optimize the structure under impact. In addition, several combinations of multilayered structures were tested. Layered structures can be used to mitigate impact over a wider range of input energy than could a single layer material.

Figure 5-1 shows the difference between a more traditional expanded polypropylene (EPP) foam impact protection material and the protection materials tested in this study (urethane honeycomb and polymeric foam materials). The protection materials cover a wide range of impact response and have potential for use in many applications.

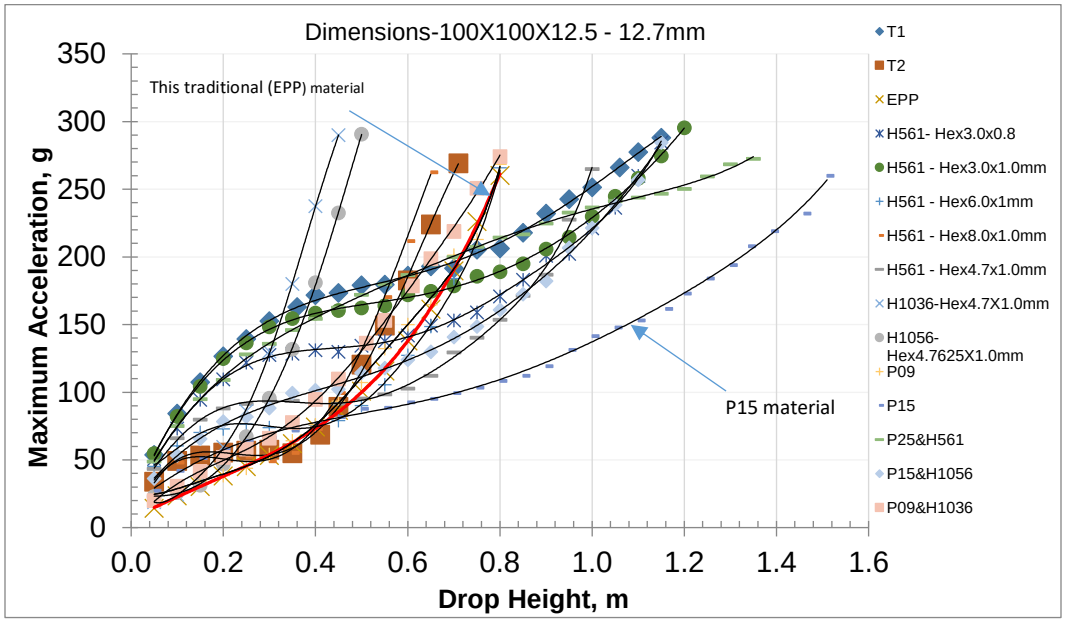

Figure 5-1 -the difference between the used protection materials in the football helmets and the protection materials we used

5.1 Effect of Thickness for Foam Materials.

This section presents a case study for selecting the optimal material for a single impact level criteria when the thickness is not constrained. The fundamental selection is the requirement for the material thickness at a given impact height. This case study is intended to demonstrate the influence of material thickness when all else is equal. For the same density foam, the dilatant materials response depends on one parameter which is the material thickness. As a result, a chart can be developed relating the material thickness to the impact height and the maximum acceleration. Figure 5-2 shows such a chart for the P15 material as an example for foam materials. At a given impact height and allowed acceleration, the suitable thickness can be selected. For example, if the required acceleration and impact height are to be no more than 100g and 0.5 m respectively, a thickness of 9.5 mm is selected from the chart. A similar process can be used for the P09 and P25 materials but will require impact testing at additional thicknesses for completeness. A general observation made from Figure 5-2 is that with all else equal increasing material thickness results in lower maximum acceleration.

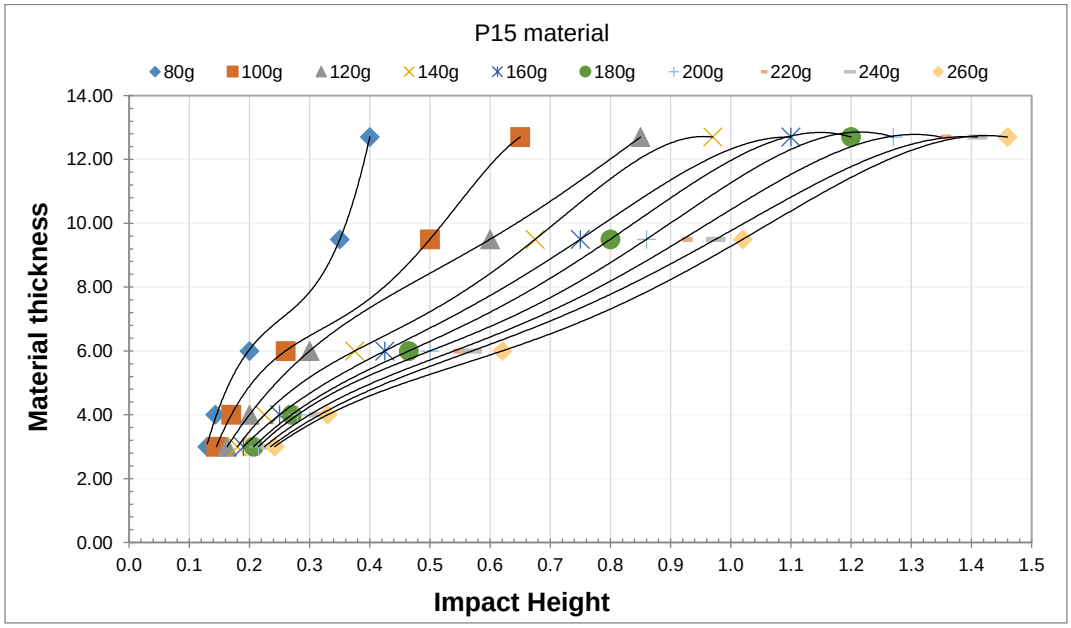

Figure 5-2 - P15 material chart is used for choosing the best thickness according to the required acceleration and impact height.

5.2 Soft Headgear Case Study.

Headgear used for soccer is of the soft type and a preliminary selection using our data set will be presented as a second case study for soft headgear. Sports such as football, lacrosse and ice-hockey use a hard shell helmet whose response will depend on the interaction of the shell and impact resisting materials. Although the materials tested in this study can be readily inserted as the impact protection in hard shell helmets the results shown would be influenced by the shell and therefore not directly related unless studied in the combined model. Soccer helmets on the other hand are soft shell and the presented results can be directly related. To prevent or reduce the risk of the concussion due to head contact of soccer players, ASTM F2439 presents criteria for soccer helmets. This specification requires that the

maximum acceleration be less than 80g at impact velocity of $2.50\ \mathrm{m/s} \pm 5\ \%$ (impact height: ~0.32m) [24] and [25]. This specification uses a Hybrid III head neck assembly with a total mass of 8.8 kg. This results in an impact energy of 27.5 J.

Due to difference in the test apparatus the soccer headgear criteria can not be directly implemented. Instead the drop criteria will be modified slightly for this example. For this case study a drop height of 0.4 m with a projectile impact of 5kg mass (same as in the experimental database) will be used along with a maximum acceleration limit of 80g. There are several potential alternatives as a preliminary design selection that keep with this criteria. To limit to 80g the results of the single-layer foam material, P15 gives a 0.45m impact height at a 12.7mm thickness while it gives 0.37m impact height at 9.5mm thick. By using interpolation, the estimated thickness of P15 to achieve the 80g limit is 10.7mm. For the P09 material a similar analysis is done where it gives the 80g limit at 0.4m impact height at 12.2mm thickness. This was calculated using interpolation between the thicknesses 6.0mm and 12.7mm. The results of a single-layer H561 honeycomb material, with a total thickness of 12.5mm at the cells dimensions 4.7x1.0mm, 6.0 x1.0mm, and 8.0x1.0mm give the 80g limit at impact heights 0.5m, 0.47m and 0.42m, respectively. As a result, we can achieve our case study criteria by using estimated cells size ~9.0 x1.0mm. Also, another approach would be to decrease the material thickness to approximately 11.5mm using the regular dimensions of the cells (4.7x1.0mm). Furthermore, the T2 material (irregular cell shape of H561 material) at the total thickness 12.5mm gives impact height 0.43, as a result, we can achieve our case study if we decrease the thickness to approximately 11.5mm. Regarding to the results of multilayered structures (two layers), at the total thickness12.5mm, there is only one sample out of the current database that is valid for this case study which is P09_H1036. This 12.5mm thick sample was at the 80g limit with an

impact height of 0.38m. It is estimated that the proposed criteria can be achieved if the total thickness is increased to approximately 13.5mm. Additional combinations need to be investigated to assess the selection of an optimal multi-layered structure.

5.3 Discussion and Conclusion of Single-Layer and Multi-Layered Materials at Thickness between 12.5 mm-12.7 mm.

Thus far, we have shown the results for the dilatant materials, honeycomb materials and multi-layered materials (foam-honeycomb). These results are for thicknesses ranging between 3 mm-50 mm. Regarding the foam materials, softer materials such as the P09 material gives lower maximum acceleration at the lower impact energy levels because it behaves as a soft flexible material. As the input energy increases the more stiff material are more optimal.

For the honeycomb materials numerous variants were tested. For example, different material stiffness, cells shapes and cell dimensions. These results are discussed individually. Furthermore, two layers samples were tested consisting of the foam and honeycomb materials.

The Figure 5-3 shows the comparison between the samples that gives the highest performance at nearly the same thicknesses. Some materials give minimum values at the lower impact height and some others samples give minimum values of the acceleration at the higher impact height. Also, we note that out of the currently teste materials of 12.5mm thickness the P15 material is optimal for a wide range of impact height >0.5m as shown in the figure.

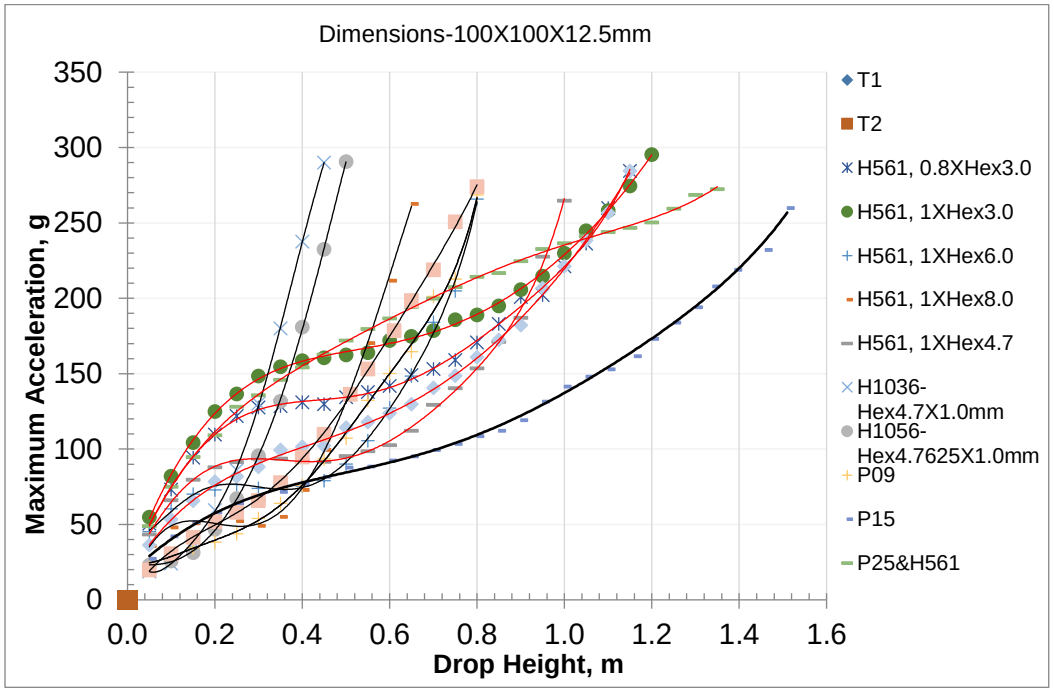

Figure 5-3 - The samples that has highest performance at thicknesses between 12.5mm-12.7 mm

As a result, Figure 5-4 shows the samples that have the highest performance over any range of the samples currently tested. By using this graph, the designer can choose a material for the impact height less than 1.5 m and with a thickness of 12.5 mm +/-. For example, the regular dimensions of the H1036 material is the best choice if the required impact height less than 0.1 m. Also, P15 material is the best choice if the required impact height between 0.46 m and 1.5 m. The design selection becomes more difficult if the material thickness is a variant and if layering is considered.

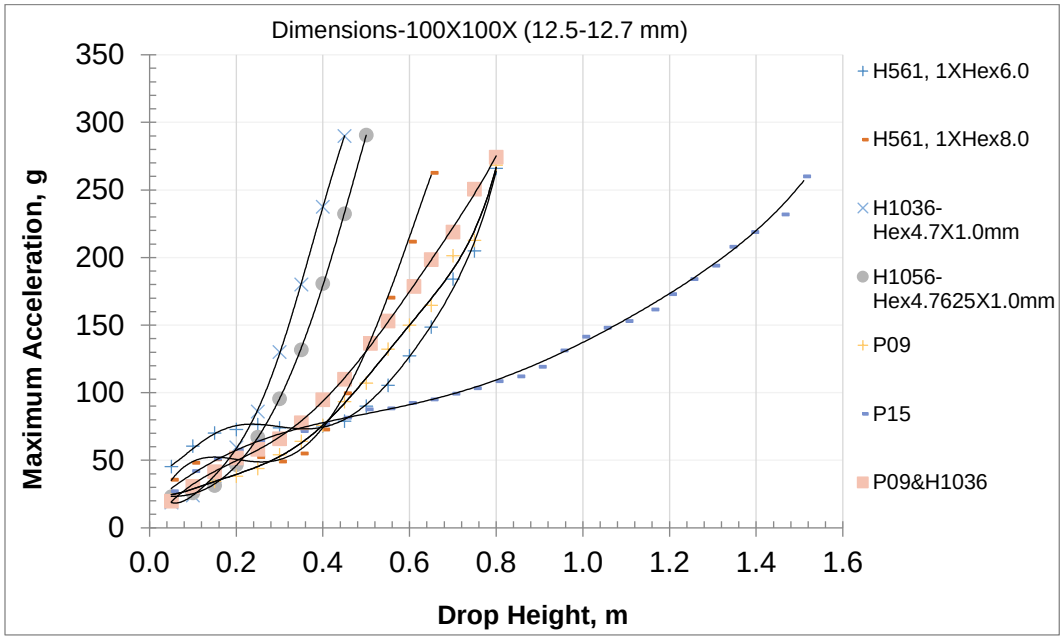

Figure 5-4 - The best samples among the samples that has highest performance at thicknesses between 12.5mm-12.7 mm.

5.4 Future Work

Understanding the mechanical response of impact resistance and how this response changes with geometric and material parameters is important and needs hundreds of tests to cover this subject experimentally due to the many different variants of the dilatant and honeycomb materials and geometry. Implementing a predictive mathematical model would be a logical next step in this endeavor. This would allow for prediction of the response as subjected to the many parameters and input conditions. The work presented is a database that can be used as verification in a modeling effort.

5.4.1 Additional Variants for Single-Layer Samples

For future work several variants of single-layer materials are recommended for study as follows:

1- Completing the testing at other thicknesses for both the foam and honeycomb materials.
2- Using new cell shapes, dimensions and material hardness of the honeycomb materials.
3- Implement techniques to reduce density without influencing performance.
4- Improve response through dilatancy.

5.4.2 Run Experiments for Multi-Layered Samples

There are a multitude of combination possible when a multi layered system is considered. Models for predicting the multi-layer response is highly desirable. In addition, testing of multi-layered system will be required for verification of predictive models.

1- Using samples consisting of three or more layers which include the foam and honeycomb materials at the same total thicknesses as shown in the Figure 5-5.

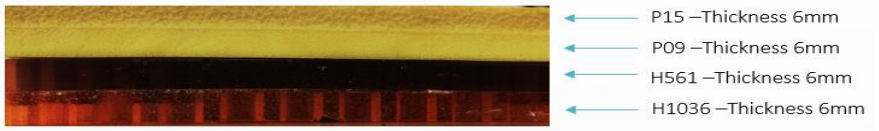

A)

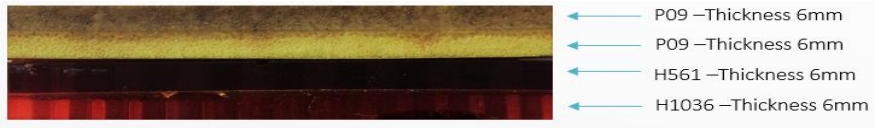

B)

Figure 5-5 - Photographs A and B show two examples for the multi-layered samples at the same total thickness.

2- Using different total thickness.

3- Using different cellular structure of the dilatant materials with the regular and irregular honeycomb materials.

5.4.3 Case study of optimal designs for different application.

The current work directly pertains to soft helmets but many protective devices use a hard outer shell. There are numerous potential applications for this material system that includes the following:

Potential applications with soft shell materials include:

1) Elderly headgear
2) Soccer headgear
3) Basketball headgear

Potential applications with hard shells and impact resisting inner liner materials include:

1) Football
2) Ice-Hockey
3) Lacrosse
4) Bicycling
5) Horseback Riding Helmets

REFERENCES

[1] The National Electronic Injury Surveillance System (NEISS). https://www.cpsc.gov/Research--Statistics/NEISS-Injury-Data, https://www.cpsc.gov/s3fs-public/2015%20Neiss%20data%20highlights.pdf

[2] The Centers for Disease Control and Prevention (CDC).

https://www.cdc.gov/homeandrecreationalsafety/falls/adultfalls. html

[3] Edgecomb, M.A. Finite Element and Experimental Analyses of Head Protective Gear to Mitigate Head Injuries Due to Falls. Thesis. The University of Maine, 2012

[4] Tyrell, D., Severson, K., and Marguis, B. (1995) "Analysis of Occupant Protection Strategies in Train Collisions", Crashworthiness and Occupant Protection in Transportation Systems, ASME, AMD, Vol. 210, BED, Vol. 30.

[5] Torkestani, Ahad, Mojtaba Sadighi, and Reza Hedayati. Effect of material type, stacking sequence and impact location on the pedestrian head injury in collisions (12/2015): 130-39. Http://ac.els-cdn.com.prxy4.ursus.maine.edu/S0263823115300963/1-s2.0-S0263823115300963-main.pdf?_tid=a3ec17a2-4ef6-11e7-b1c2-00000aab0f01&acdnat=1497220867_7749d06a1d8ef64d4cddba66a1f64df5. N.p., Dec. 2015. Web.

[6] Boden, Barry P., Robin L. Tacchetti, Robert C. Cantu, Sarah B. Knowles, and Frederick O. Mueller. "Catastrophic Head Injuries in High School and College Football Players." 1 July 2007. Web.

[7] McCrory, Paul R. "Brain injury and heading in soccer Head to ball contact is unlikely to cause injury but head to head contact might." US National Library of Medicine National Institutes of Health (16 Aug 2003).

[8] Scott MDCM, Delaney, J. "Head Injuries Presenting to Emergency Departments in the United States From 1990 to 1999 for Ice Hockey, Soccer, and Football." Clinical Journal of Sport Medicine (03/2004): 80 --87. Web.

[9] http://assets.nydailynews.com/polopoly_fs/1.1159315.1347589531!/img/ httpImage/image.jpg_gen/derivatives/landscape_1200/cutler.jpg

[10] http://www.hollywoodreporter.com/sites/default/files/imagecache/ thumbnail_570x321/2012/06/tackle_a.jpg

[11] Cusimano, Michael D., Bhanu Sharma, David W. Lawrence, Gabriela Ilie, Sarah Silverberg, and Rochelle Jones. "Trends in North American Newspaper Reporting of Brain Injury in Ice Hockey." (April 17, 2013): n. pag. Web.

[12] Medicaldaily.com http://images.medicaldaily.com/sites/medicaldaily.com/ files/styles/large/ public/2014/01/19/hockey-injuries.jpg

[13] www.bruinsdaily.com. https://www.bruinsdaily.com/wpcontent/uploads/ 2013/05/Round2Game5-Bos-NY-32.jpg

[14] hexcel.com. http://www.hexcel.com/Products/Honeycomb/ HexWeb-Honeycomb?ljs=en

[15] gupta-verlag.com. https://www.gupta-verlag.com/news/technology/13223/ d3o-launches-new-range-of-footwear-cushioning-pu-materials

[16] Foo, Choon Chiang , Gin Chai Boay, and Leong Seah Keey. "Mechanical properties of Nomex material and Nomex honeycomb structure." (October 2007): 588-594. Web.

[17] Wang, Jie, Anthony M. Waas, and Hai Wang. "Experimental and numerical study on the low-velocity impact behavior of foam-core sandwich panels." (February 2013): 298-311. Web.

[18] www.xrd.tech http://www.xrd.tech/documents/2830/XRD-Extreme-Impact-Protection---General-Overview.aspx

[19] CTE Center, http://www.bu.edu/cte/about/what-is-cte/

[20] McCrea, Michael A. Mild Traumatic Brain Injury and post-concussion Syndrome. 198 Madison Avenue, New York 10016: Oxford U, 2008. Print.

[21] Sawal, Nurashikin, Abdul Basit Mohd Nazri, and Hazizan Md Akil. "Effect of Cell Size Material on the Mechanical Properties of Honeycomb Core Structure." International Journal of Science and Research (IJSR) (2013): 80-84. Web.

[22] K.R. R, Amakrishnan, Viot P., Shankar K., and Guerard S. "A comparative study of the impact properties of sandwich materials with different cores." EDP Sciences (2012): n. pag. Web.

[23] Lin, C.Y, L.T. Chang, T.J Huang, K.H Tsai, C.S Li, and G.L Chang. "Finite Element Analysis of Honeycomb-Core Foam on Shock-Absorbing Capability against Childhood Head Injury." (n.d.): 135-38. Web.

[24] ASTM Standard F2439 ASTM Standard C33, 2016 "Standard Specification for Headgear Used in Soccer," ASTM International, West Conshohocken, PA, www.astm.org

[25] ASTM Standard F1446 “Standard Test Methods for Equipment and Procedures Used in Evaluating the Performance Characteristics of Protective Headgear”, ASTM International, West Conshohocken, PA, www.astm.org

APPENDIX A

CAD DRAWINGS

A.1 **R74 mm**

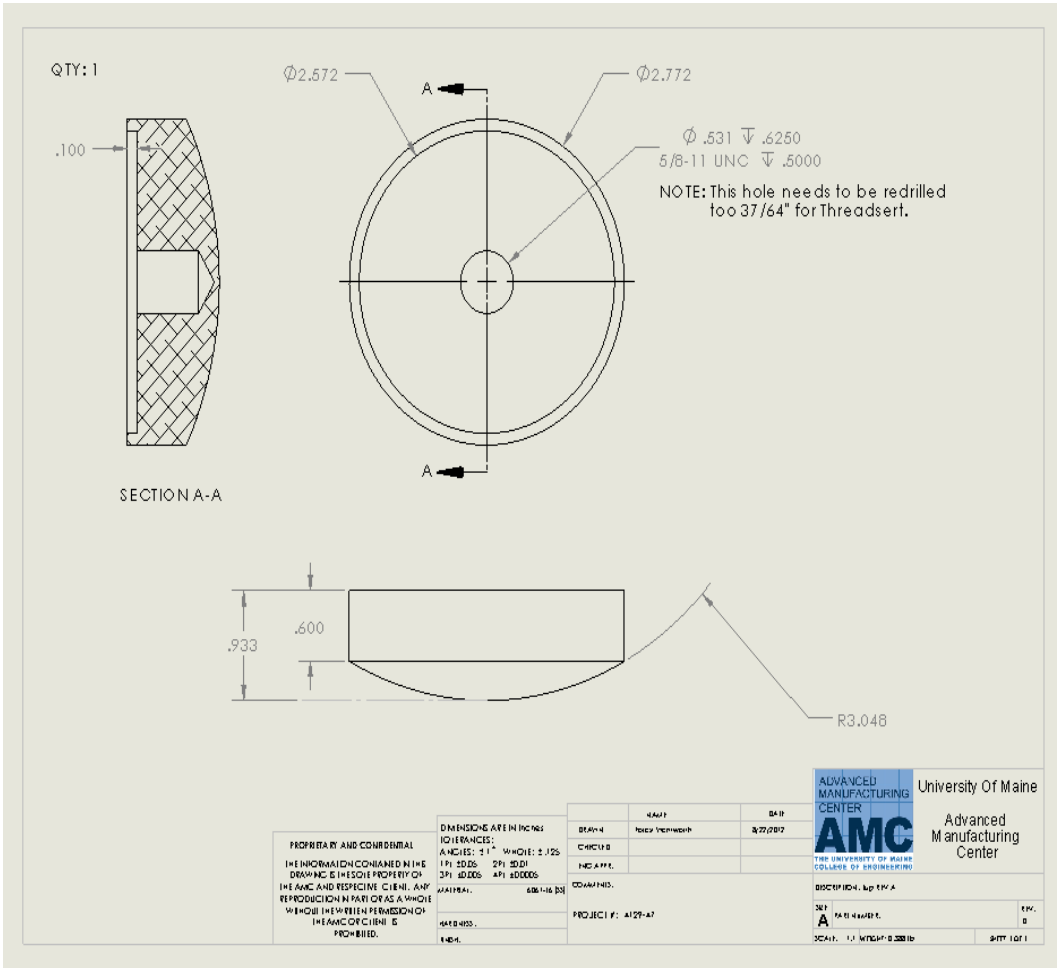

Figure A-1- Spherical impactor-Radius 74 mm.

A.2 **R127 mm**

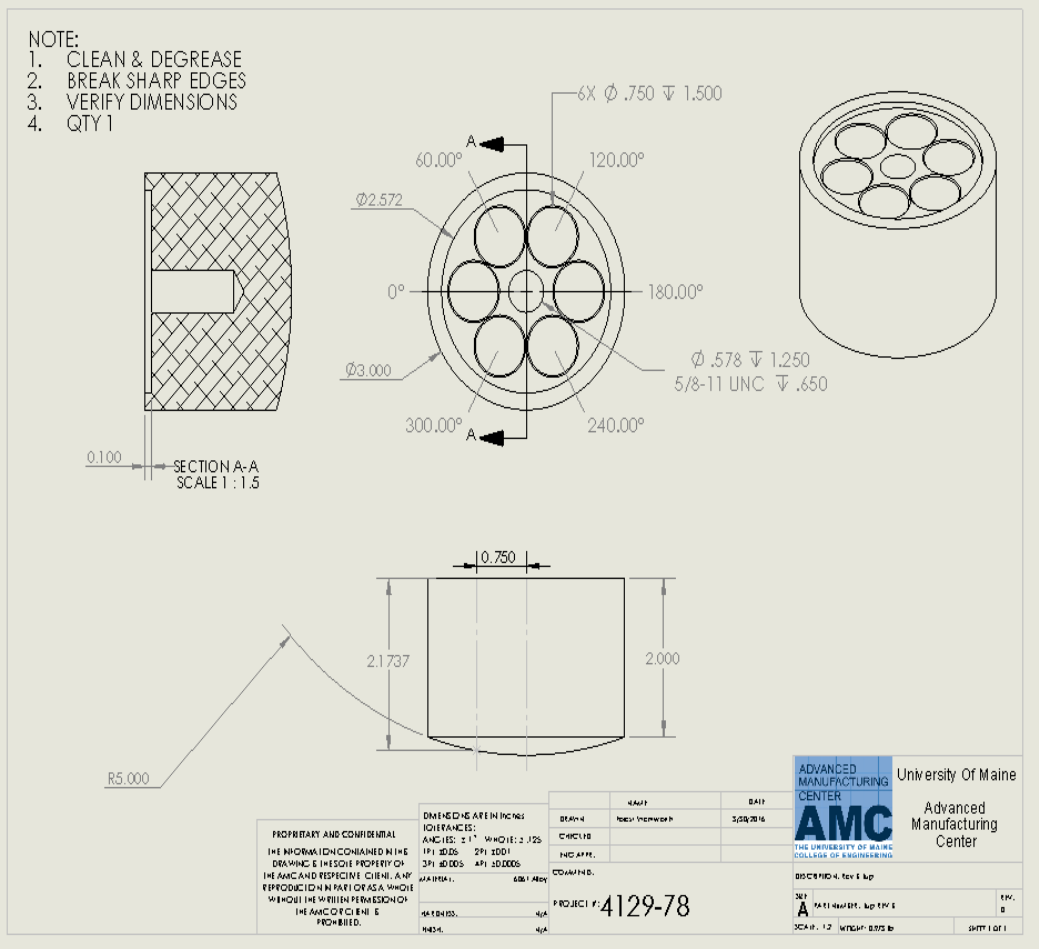

Figure A-2 - Spherical impactor-Radius 74 mm.

APPENDIX B

STEP IMPACT

B.1 Football Protection Material

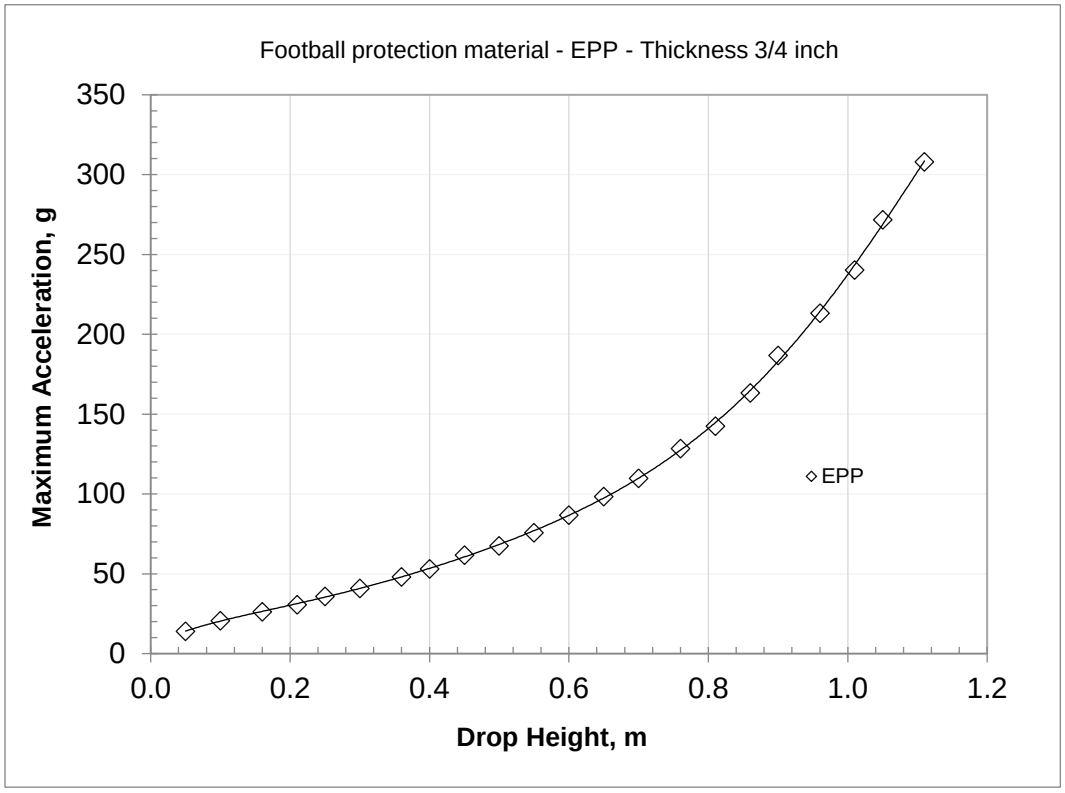

Figure B-1 - The acceleration behavior of the football protection material at the thickness of ¾ inch.

APPENDIX C

FORCE VS DISPLACEMENT CURVES

C.1 Dilatant Materials

C.1.1 P09

C.1.1.1 Thickness 6 mm

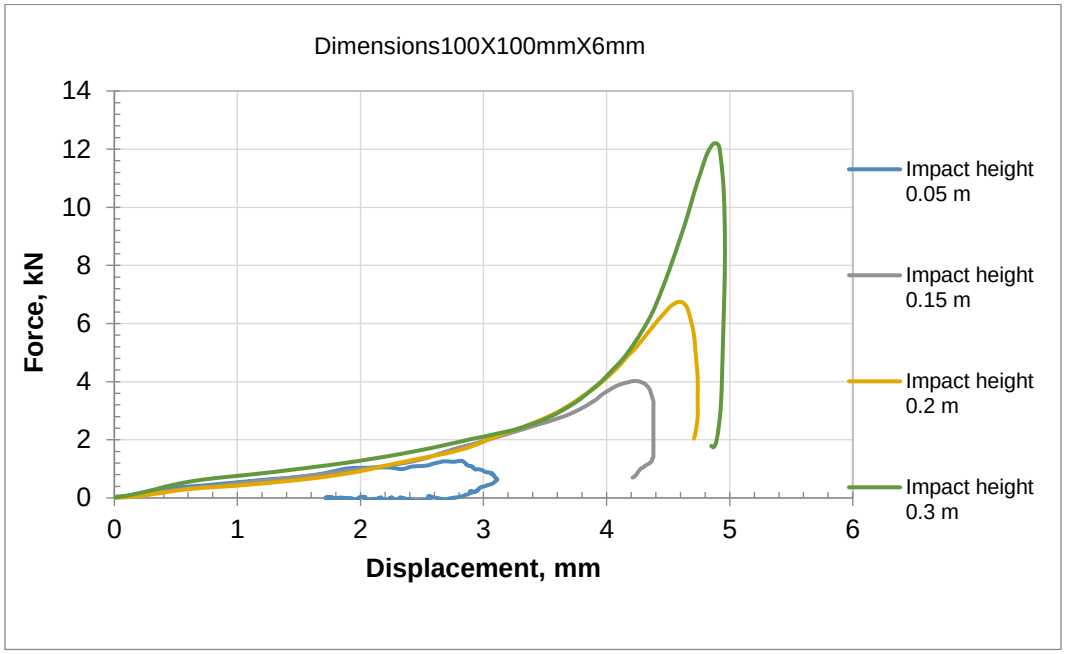

Figure C-1 - The force versus the displacement of the P09 material at the thickness 6.0 mm.

C.1.2 **P15 Material**

C.1.2.1 **Thickness 3 mm**

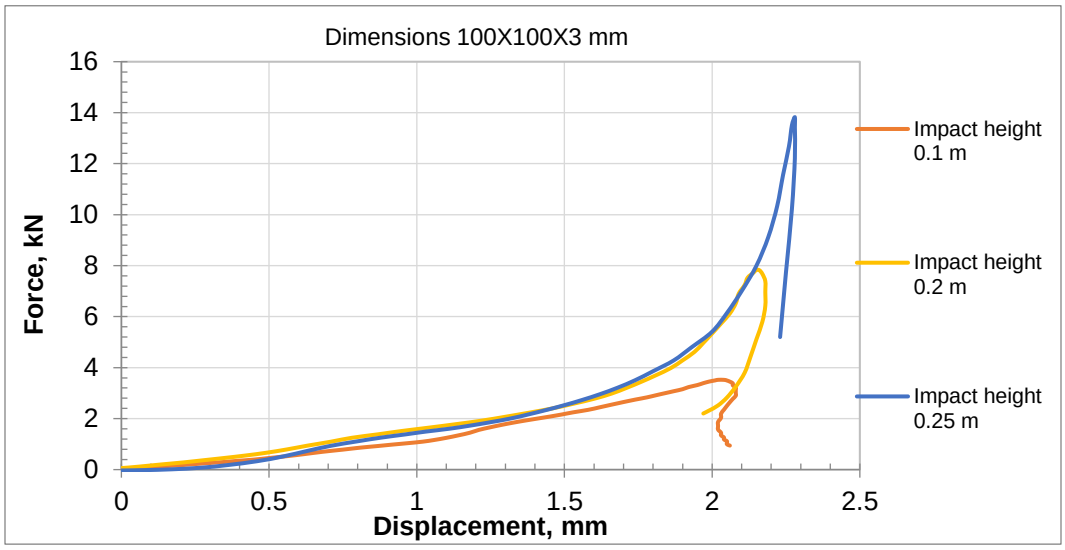

Figure C-2 - The force versus the displacement of the P15 material at the thickness 3.0 mm.

C.1.2.2 **Thickness 4 mm**

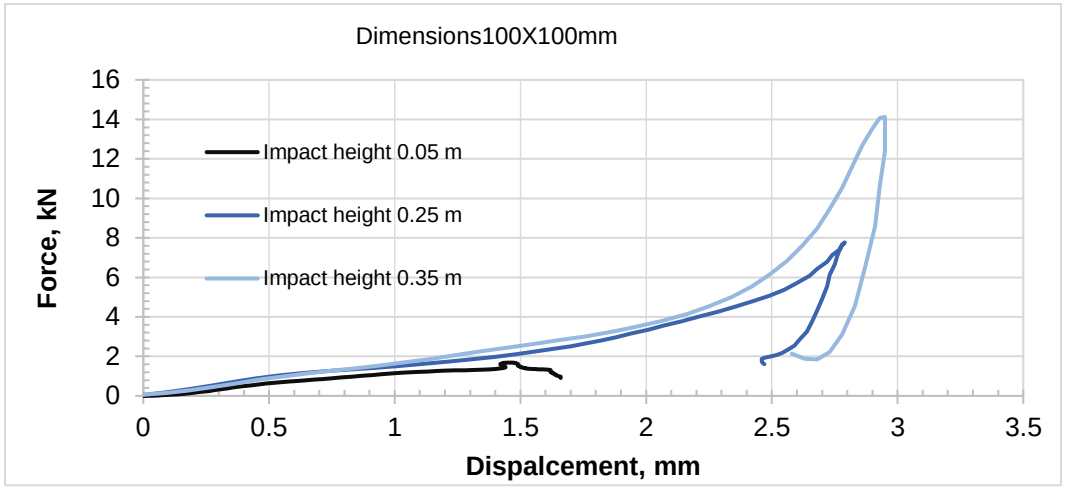

Figure C-3 – The force versus the displacement of the P15 material at the thickness 4.0 mm.

C.1.2.3 **Thickness 6 mm**

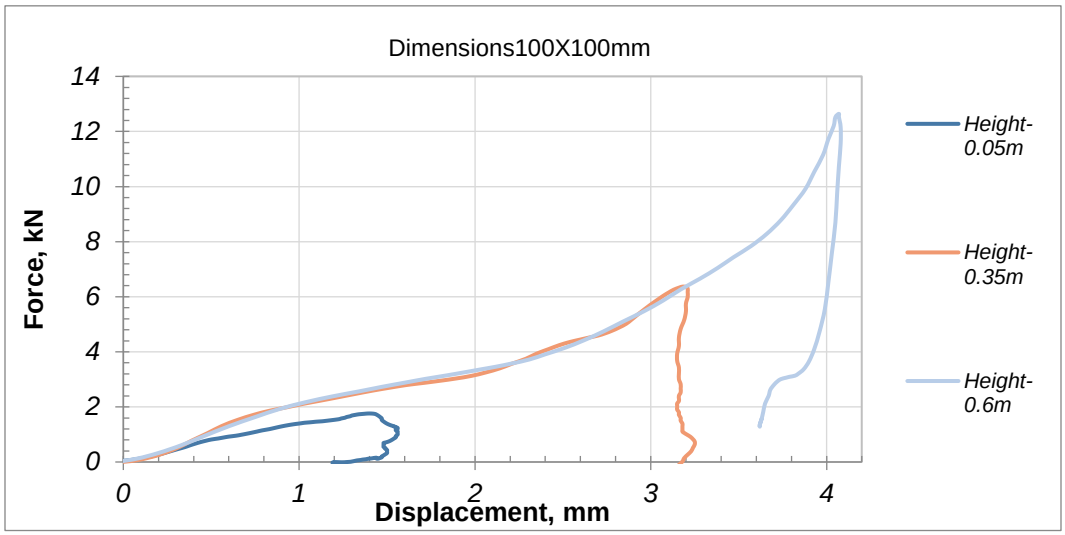

Figure C-4 - The force versus the displacement of the P15 material at the thickness 6.0 mm.

C.1.2.4 **Thickness 9.5 mm**

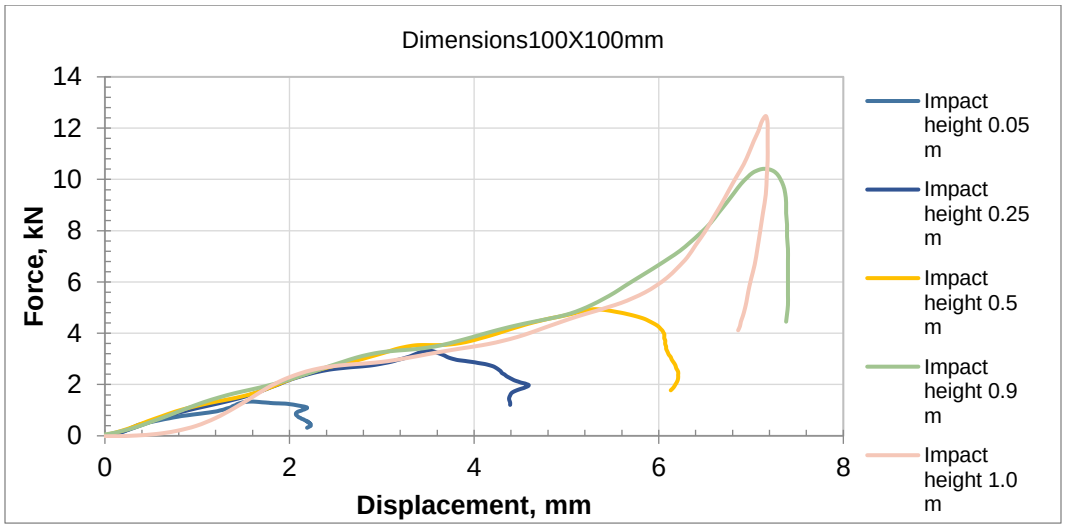

Figure C-5 - The force versus the displacement of the P15 material at the thickness 9.5 mm.

C.1.3 **P25 Material**

C.1.3.1 **Thickness 2 mm**

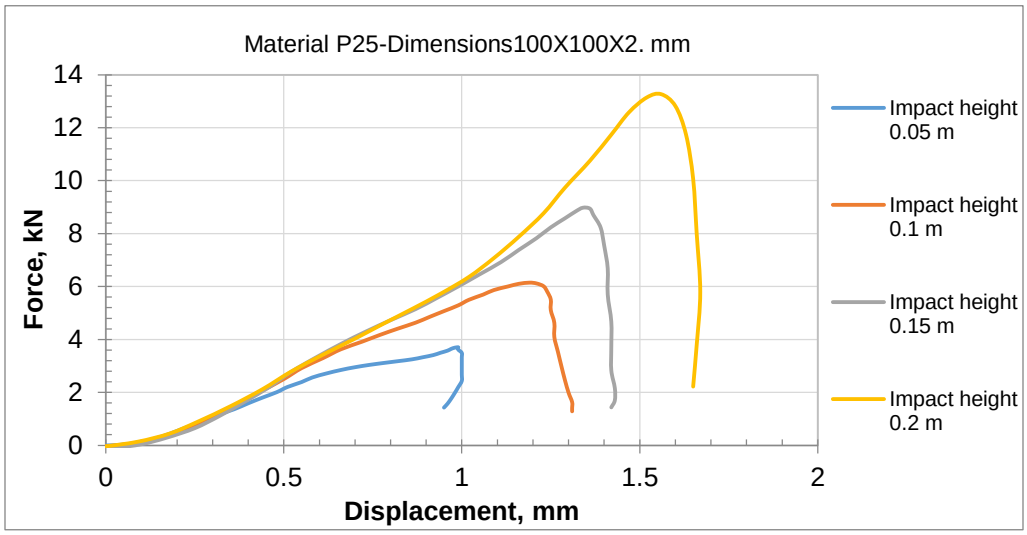

Figure C-6 - The force versus the displacement of the P25 material at the thickness 2.0 mm.

C.1.3.2 **Thickness 3 mm**

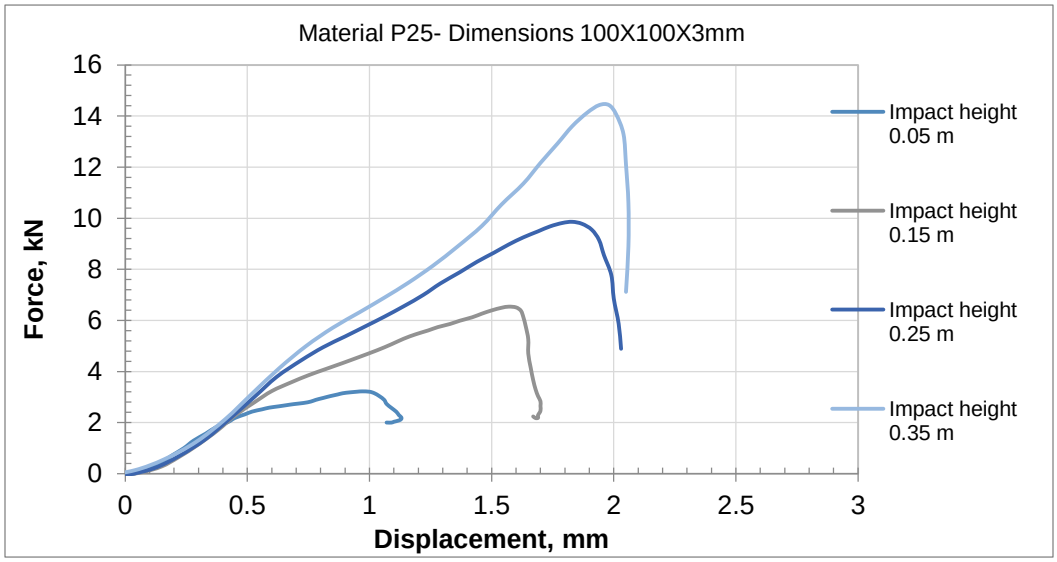

Figure C-7 - The force versus the displacement of the P25 material at the thickness 3.0 mm.

C.2 **Honeycomb Materials**

C.2.1 **H1056 Material**

C.2.1.1 **Wall Thickness 1.5 mm**

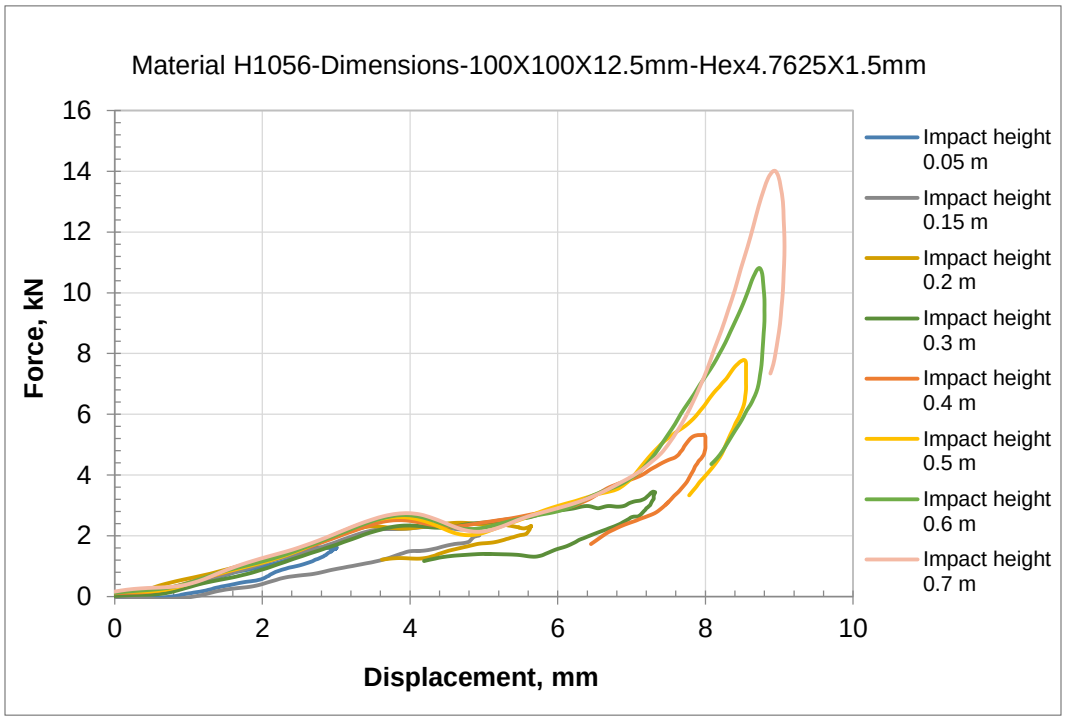

Figure C-8 - The force versus the displacement of the H1056 material at the cells dimensions Hex4.7625X1.5mm.

C.2.2 **H1036 Material**

C.2.2.1 **Cells Dimensions Hex 4.7X1.0 mm**

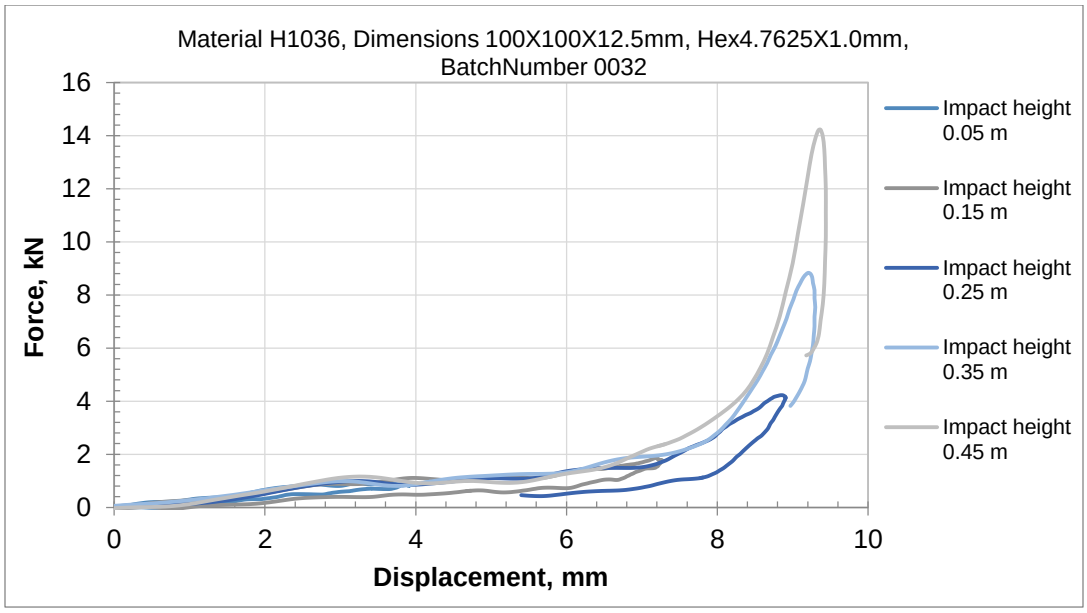

Figure C-9- The force versus the displacement of the H1036 material at the cells dimensions Hex4.7625X1.0mm.

C.2.2.2 **Cells Dimensions Hex 4.7X1.5 mm**

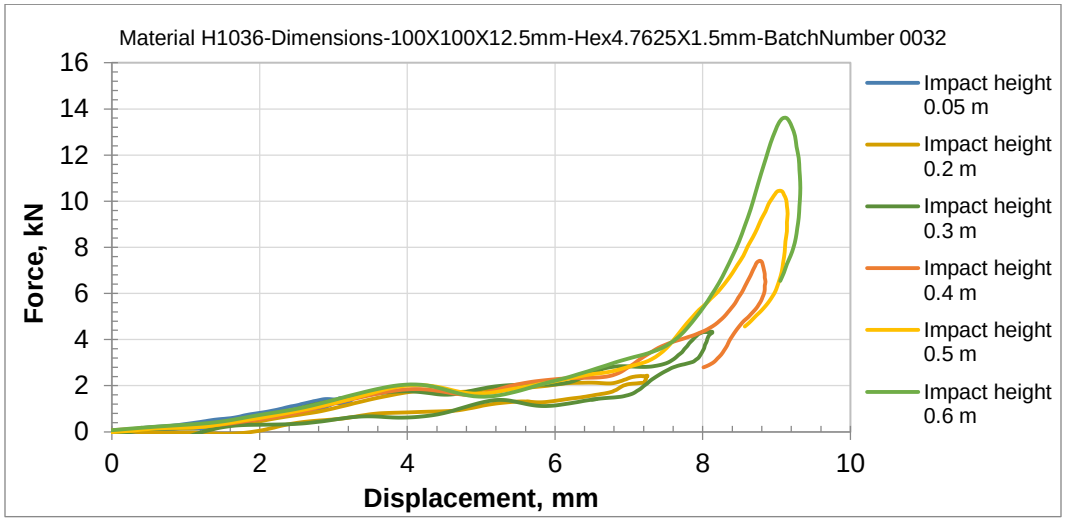

Figure C-10- The force versus the displacement of the H1036 material at the cells dimensions Hex4.7625X1.5mm.

C.2.3 **H781 material**

C.2.3.1 **Cells Dimensions Hex 4.7X1.5 mm**

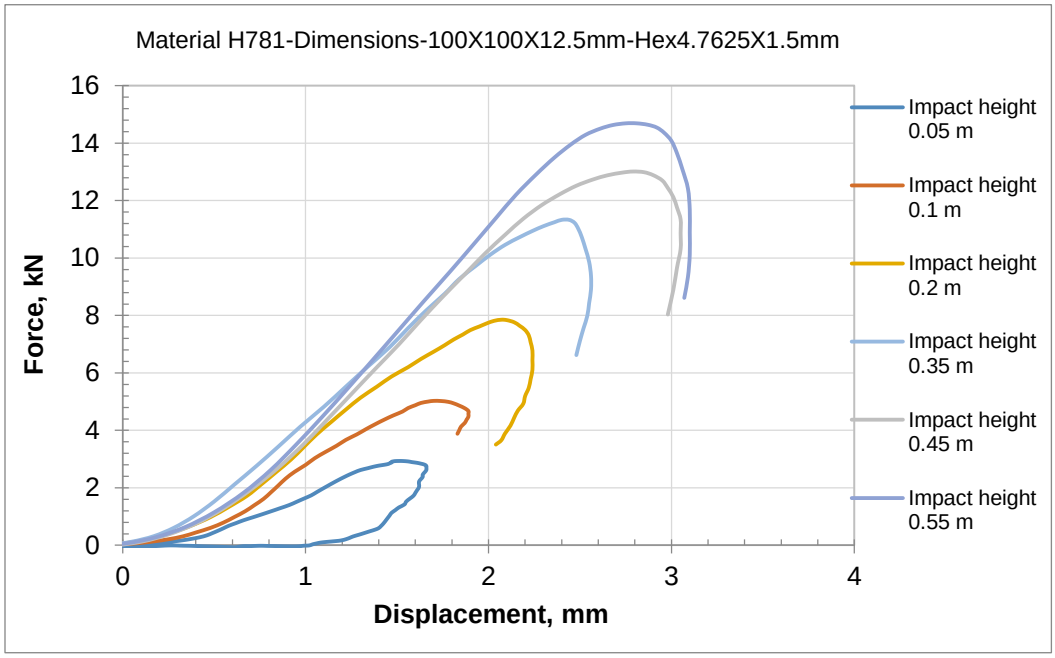

Figure C-11 - The force versus the displacement of the H781 material at the cells dimensions Hex4.7625X1.5mm.

C.2.4 **H561 material**

C.2.4.1 **Circular Samples**

C.2.4.1.1 **Material Thickness 6.5 mm**

C.2.4.1.1.1 **Wall Thickness 1.0 mm**

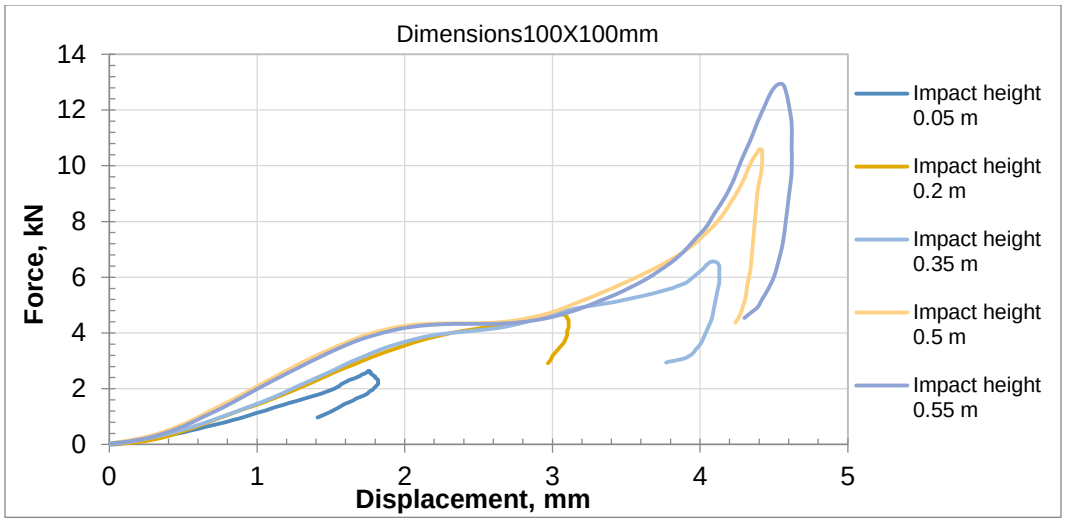

Figure C-12 - The force versus the displacement of the circular sample of H561 material at the cells dimensions Hex4.7625X1.0mm and sample thickness 6.5 mm.

C.2.4.1.1.2 **Wall Thickness 1.5 mm**

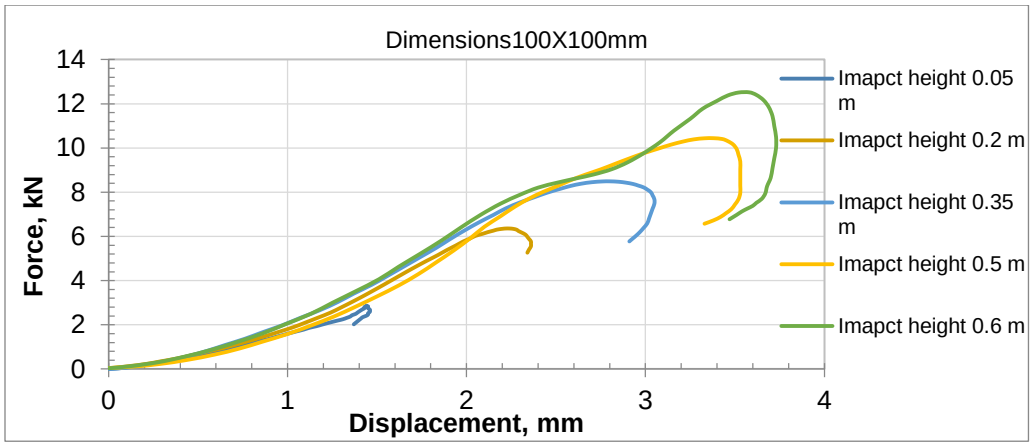

Figure C-13 - The force versus the displacement of the circular sample of H561 material at the cells dimensions Hex4.7625X1.0mm and sample thickness 6.5 mm.

C.2.4.1.2 **Material Thickness 12.5 mm**

C.2.4.1.2.1 **Wall Thickness 1.5 mm**

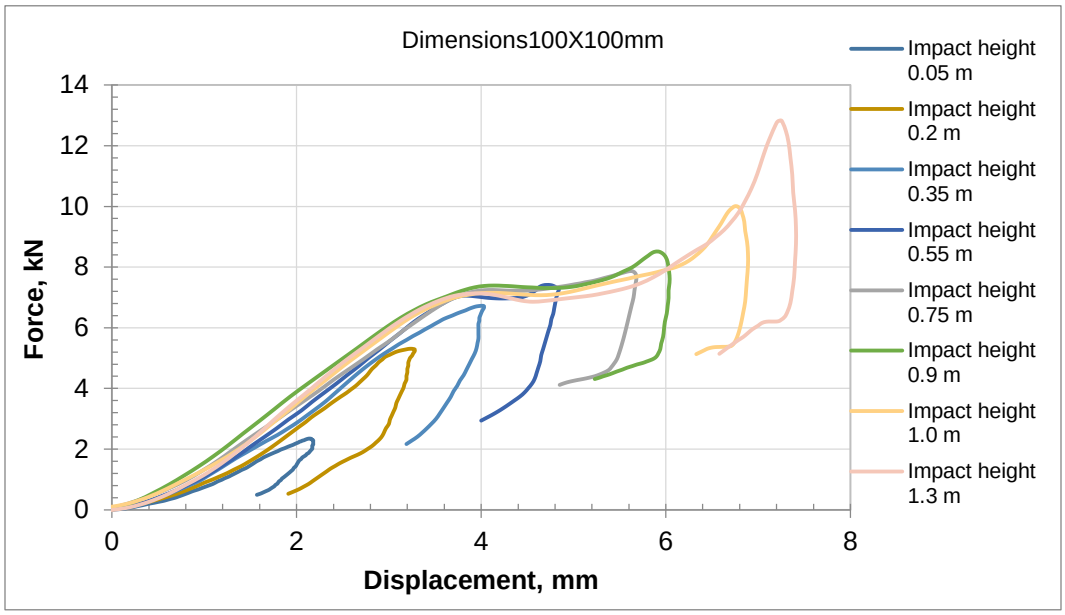

Figure C-14 - The force versus the displacement of the circular sample of H561 material at the cells dimensions Hex4.7625X1.5mm and sample thickness 12.5 mm.

C.2.4.2 **Square Samples**

C.2.4.2.1 **Regular Shape**

C.2.4.2.1.1 **Hex3.0X1.0mm**

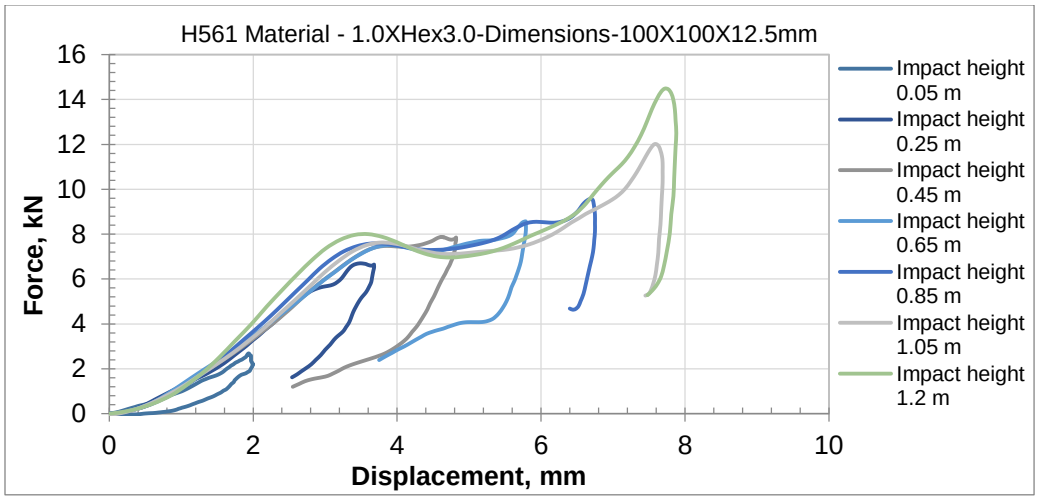

Figure C-15 - The force versus the displacement of the square sample of H561 material at the cells dimensions Hex3.0x1.0mm and sample thickness 12.5 mm.

C.2.4.2.1.2 **Hex4.7X1.0mm**

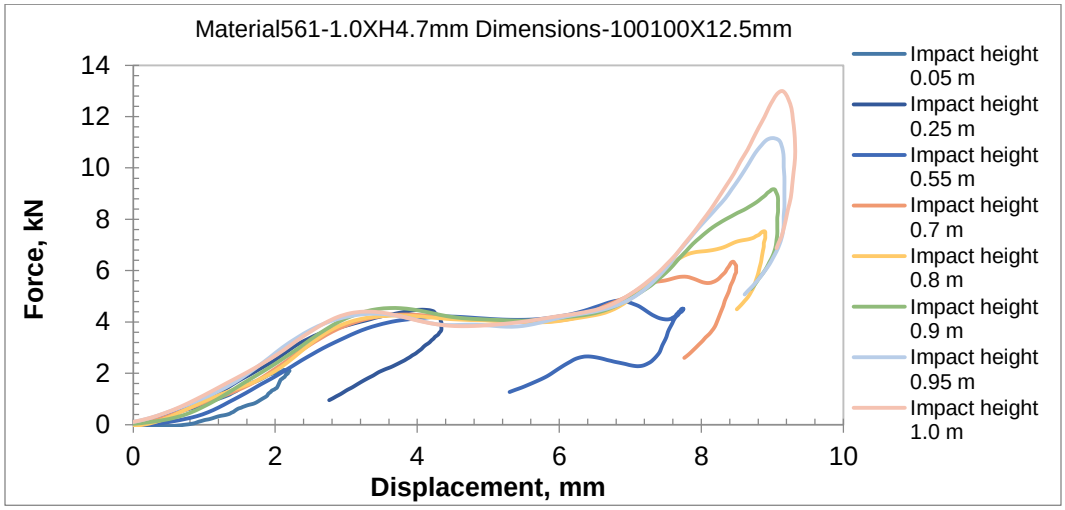

Figure C-16 - The force versus the displacement of the square sample of H561 material at the cells dimensions Hex4.7x1.0mm and sample thickness 12.5 mm.

C.2.4.2.1.3 **Hex6.0X1.0mm**

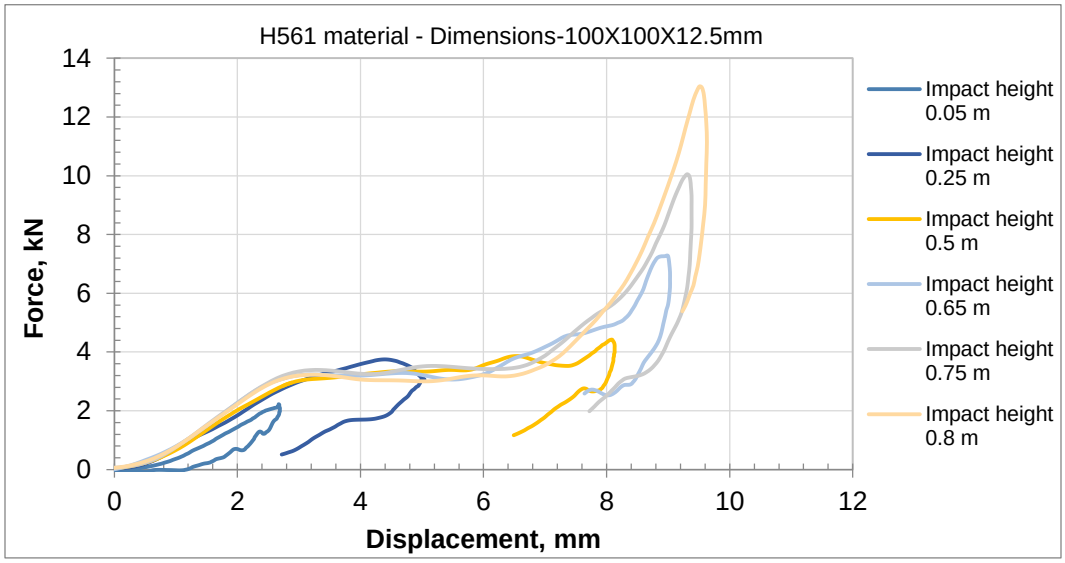

Figure C-17 - The force versus the displacement of the square sample of H561 material at the cells dimensions Hex6.0x1.0mm and sample thickness 12.5 mm.

C.2.4.2.1.4 **Hex8.0X1.0mm**

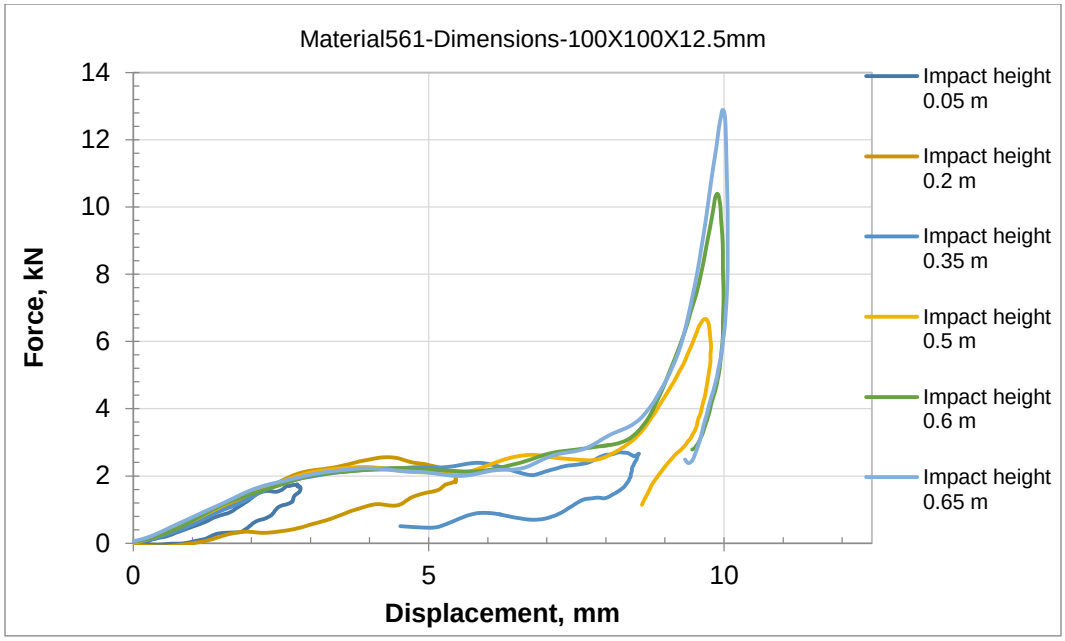

Figure C-18 - The force versus the displacement of the square sample of H561 material at the cells dimensions Hex8.0x1.0mm and sample thickness 12.5 mm.

C.2.4.2.1.5 **Hex3.0X0.8mm**

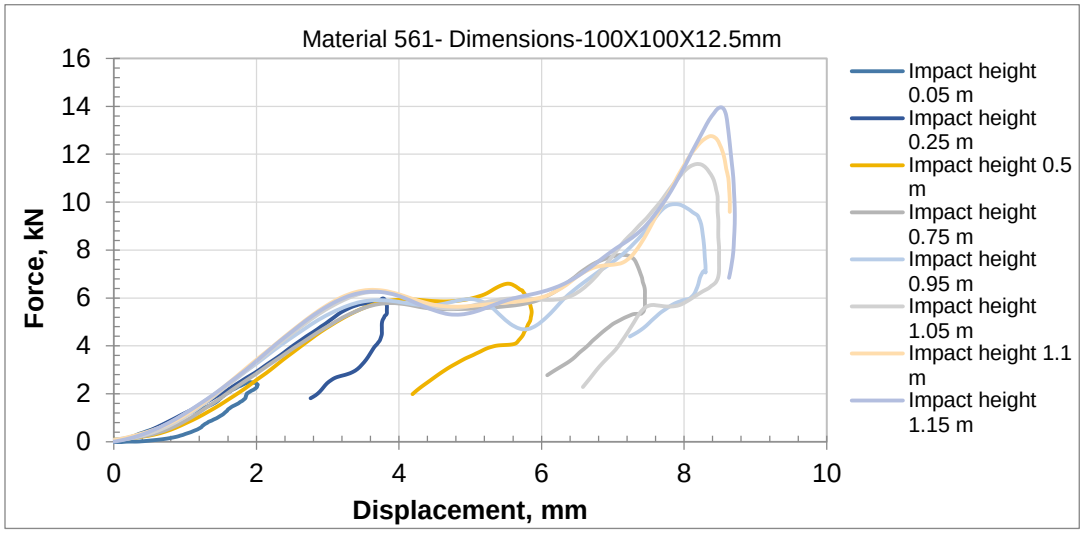

Figure C-19 - The force versus the displacement of the square sample of H561 material at the cells dimensions Hex3.0x0.8mm and sample thickness 12.5 mm.

C.2.4.2.2 **Irregular Cell Shapes**

C.2.4.2.2.1 **T1 Sample**

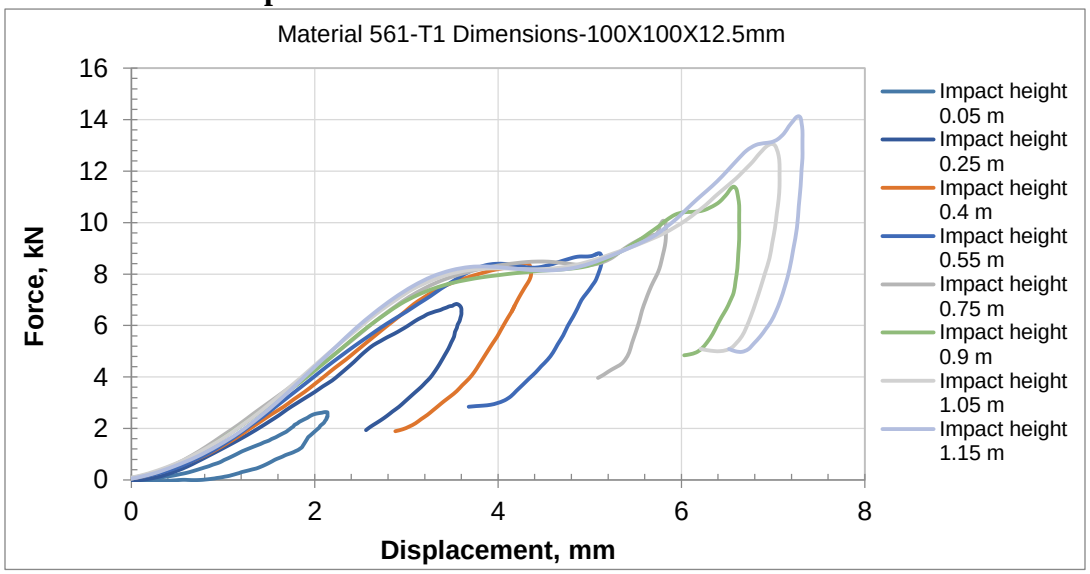

Figure C-20 - The force versus the displacement of the T1 sample of H561

C.2.4.2.2.2 **T2 Sample**

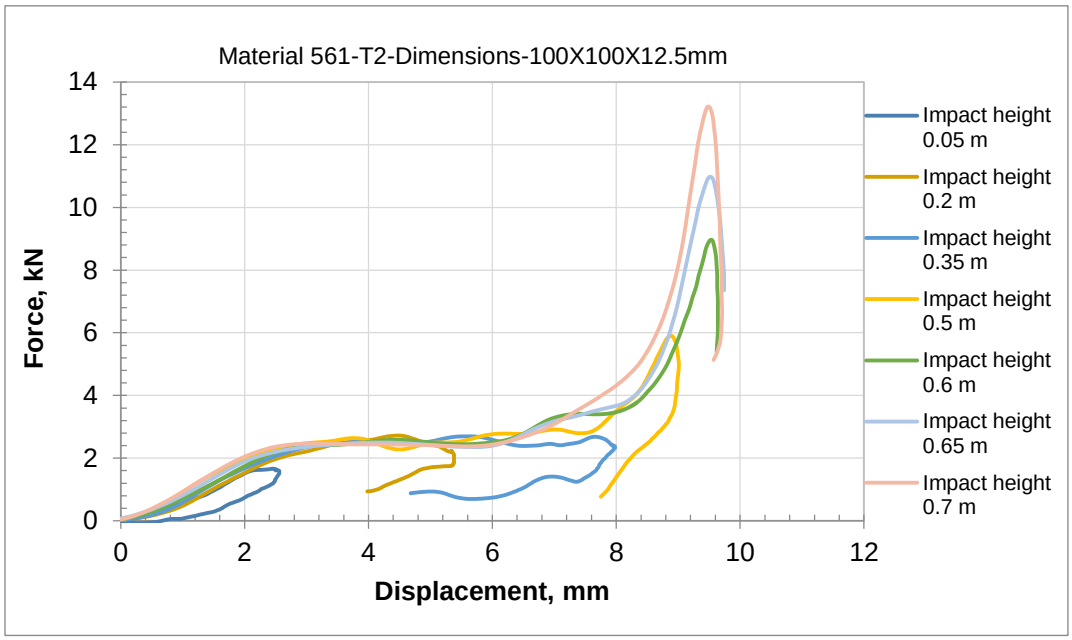

Figure C-21 - The force versus the displacement of the T2 sample of H561

C.2.4.2.2.3 **T3 Sample**

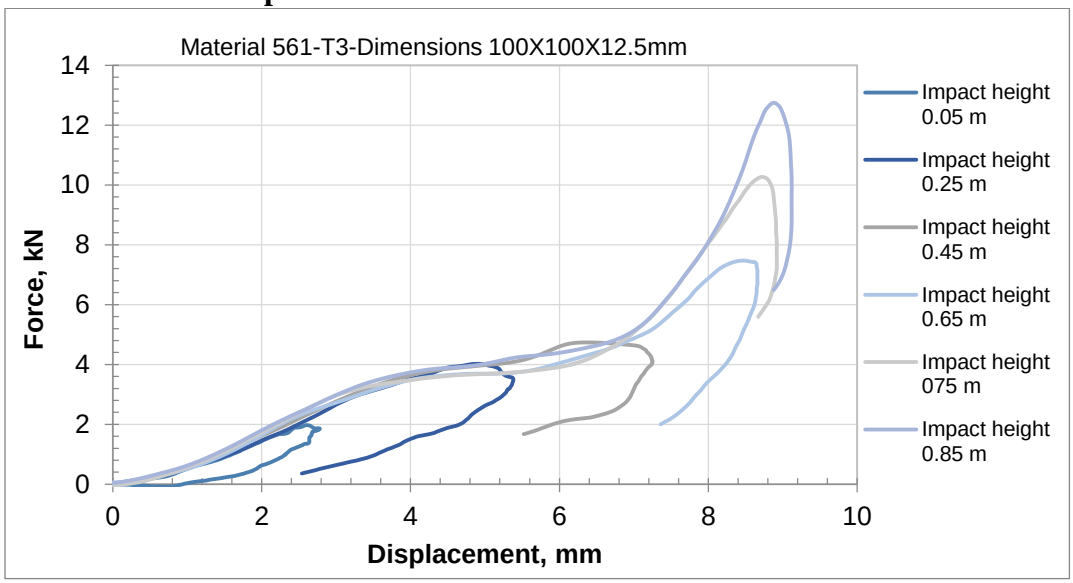

Figure C-22 - The force versus the displacement of the T3 sample of H561

C.3 **Results of Dilatant-Honeycomb Samples (Two Layers)**

C.3.1 **Samples Thickness 12.5 mm**

C.3.1.1 **P25_H561**

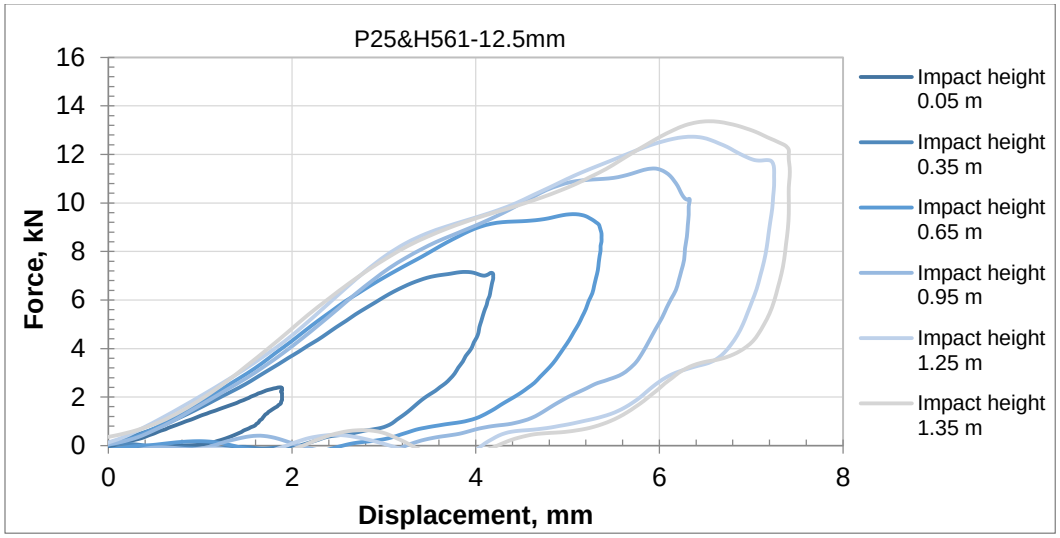

Figure C-23 - The force versus the displacement of the P25_H561 sample.

C.3.1.2 **P15_H1056**

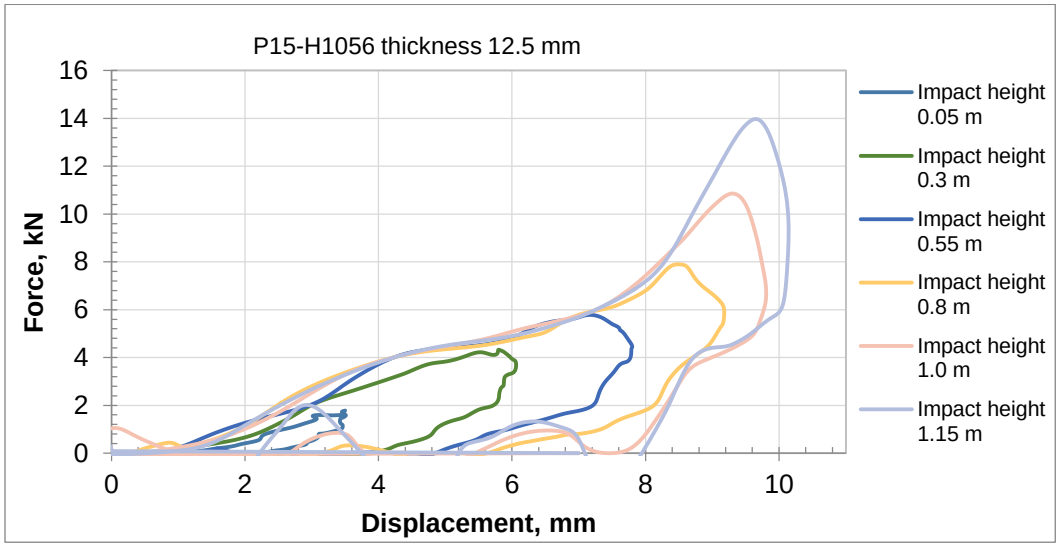

Figure C-24 - The force versus the displacement of the P15_H1056 sample.

C.3.1.3 **P25_H1036**

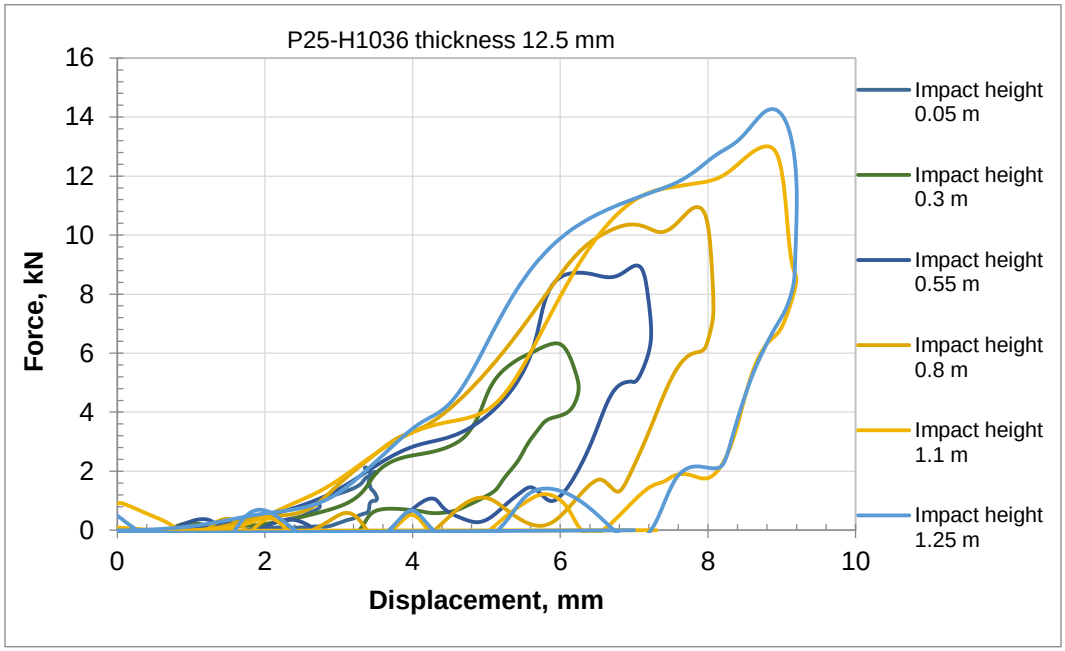

Figure C-25 - The force versus the displacement of the P25_H1036 sample.

C.3.1.4 **P09_H561**

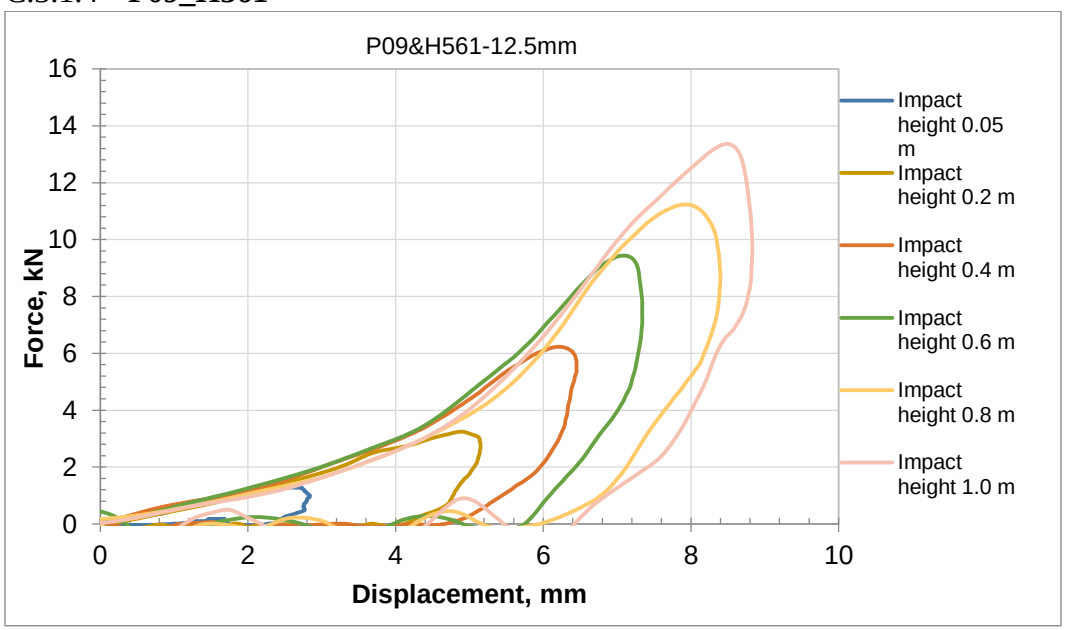

Figure C-26 - The force versus the displacement of the P09_H561 sample.

C.3.2 **Samples Thickness 24.5 mm**

C.3.2.1 **P25_H561**

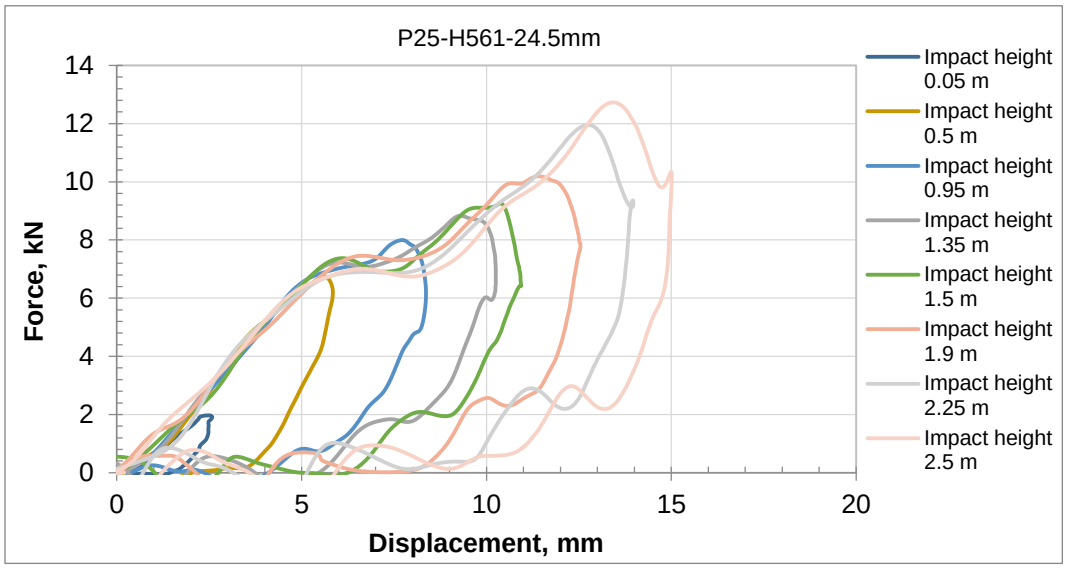

Figure C-27 - The force versus the displacement of the P25_H561 sample.

C.3.2.2 **P15_H1056**

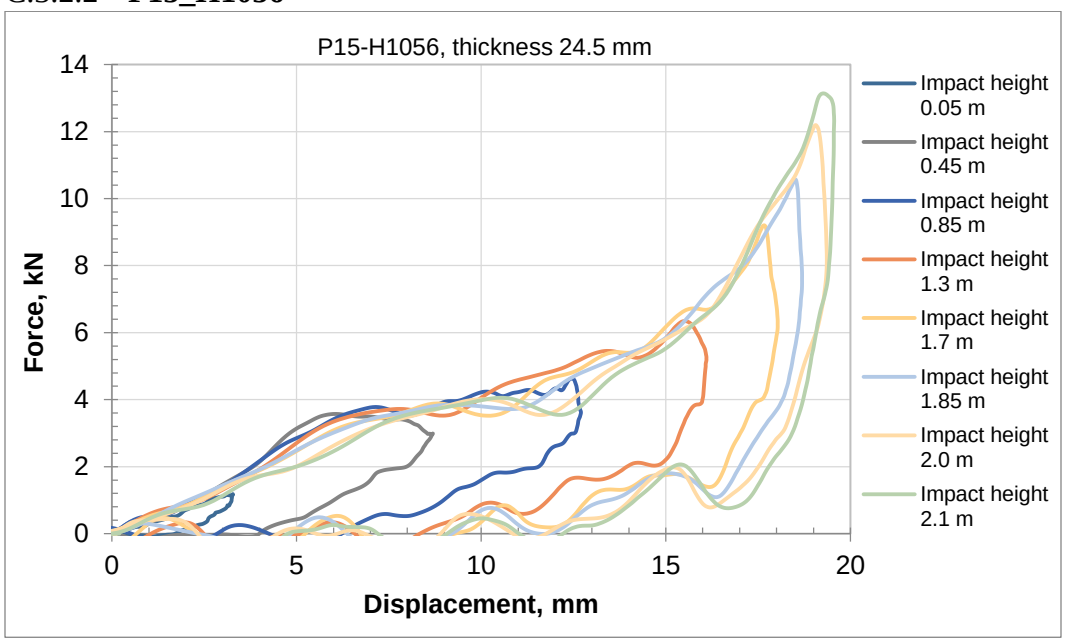

Figure C-28 - The force versus the displacement of the P15_H1056 sample.

C.3.2.3 **P25_H1036**

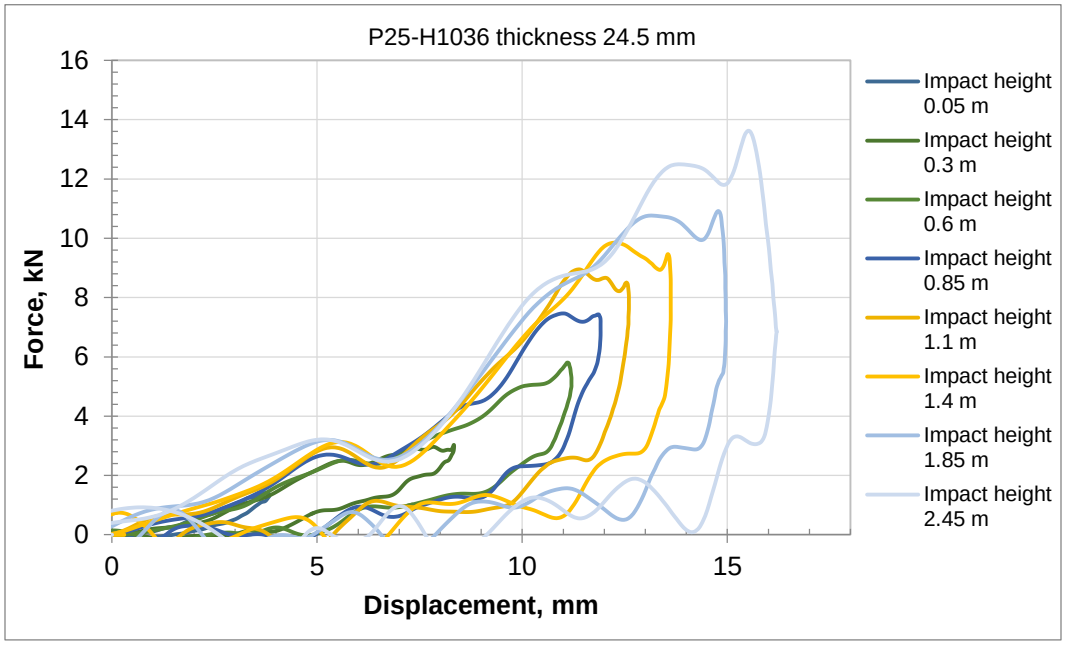

Figure C-29 - The force versus the displacement of the P25_H1036 sample.

C.3.2.4 **P09_H561**

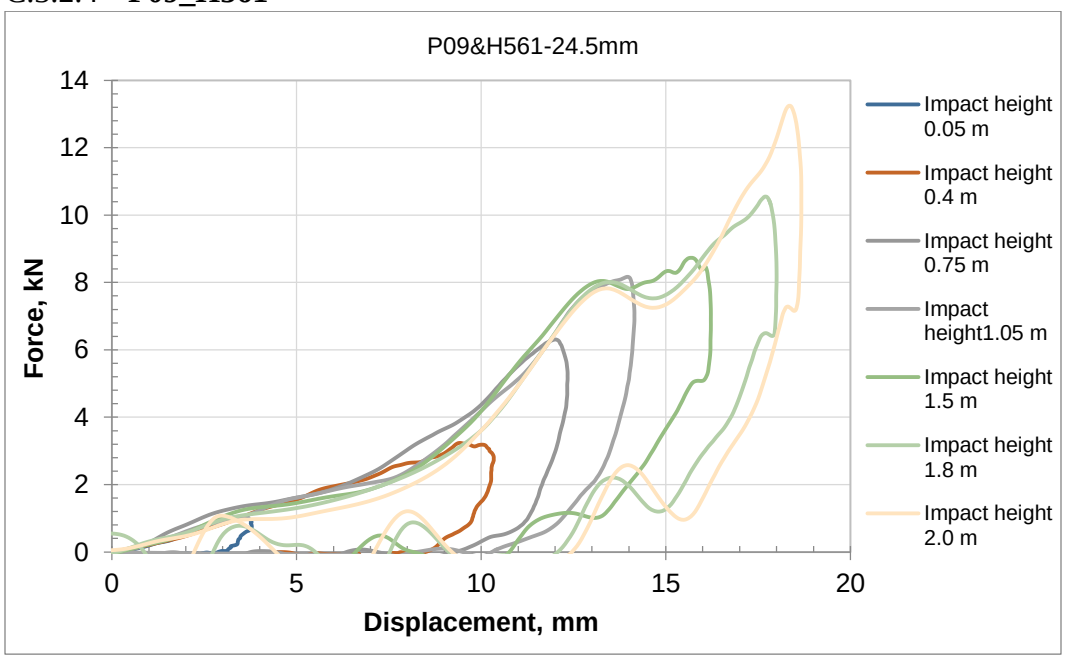

Figure C-30 - The force versus the displacement of the P09_H561 sample.

C.4 **Five Layers Samples**

C.4.1 **R1007**

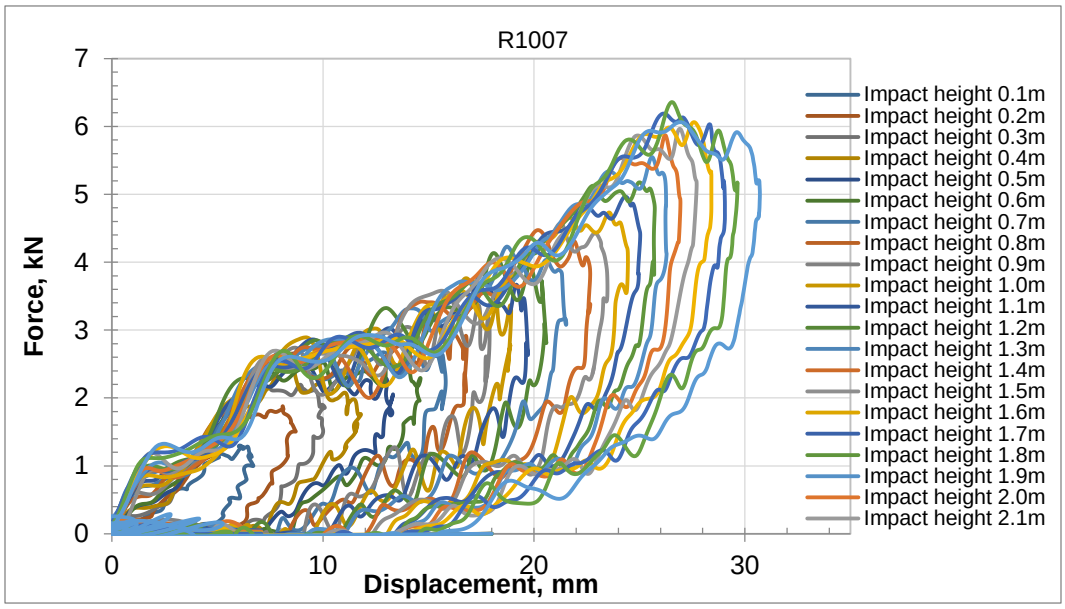

Figure C-31 - The force versus the displacement of the R1007 sample.

C.4.2 **R2007**

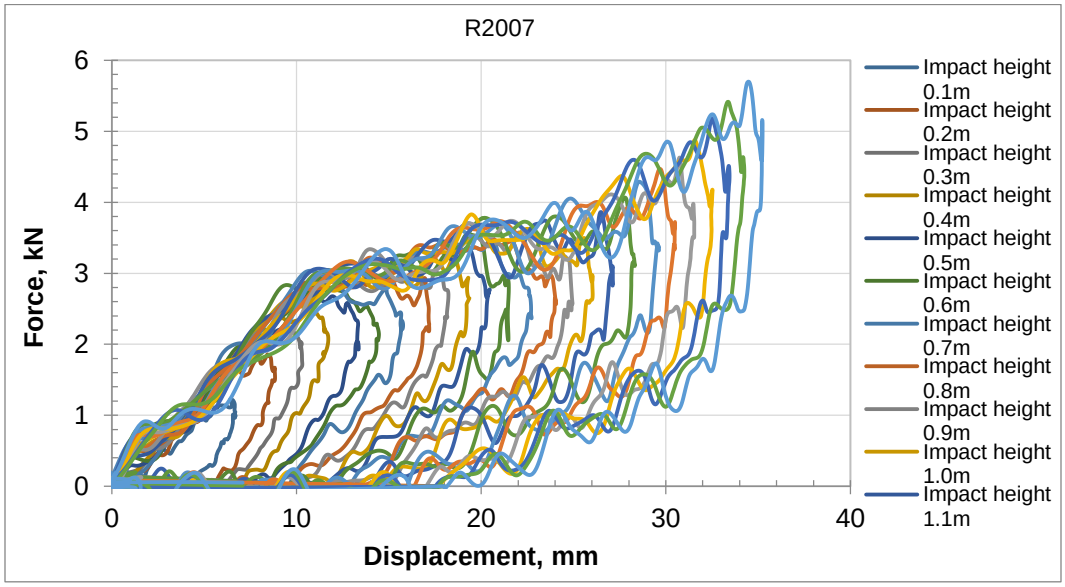

Figure C-32 - The force versus the displacement of the R2007 sample.

C.4.3 **R3007**

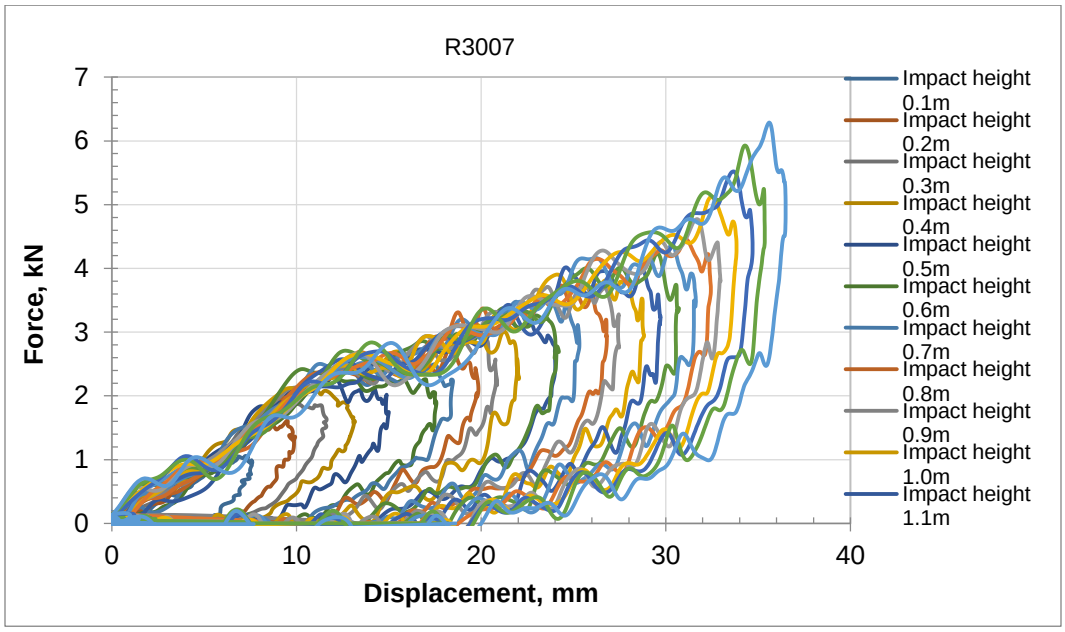

Figure C-33 - The force versus the displacement of the R1007 sample.

C.4.4 **R4007**

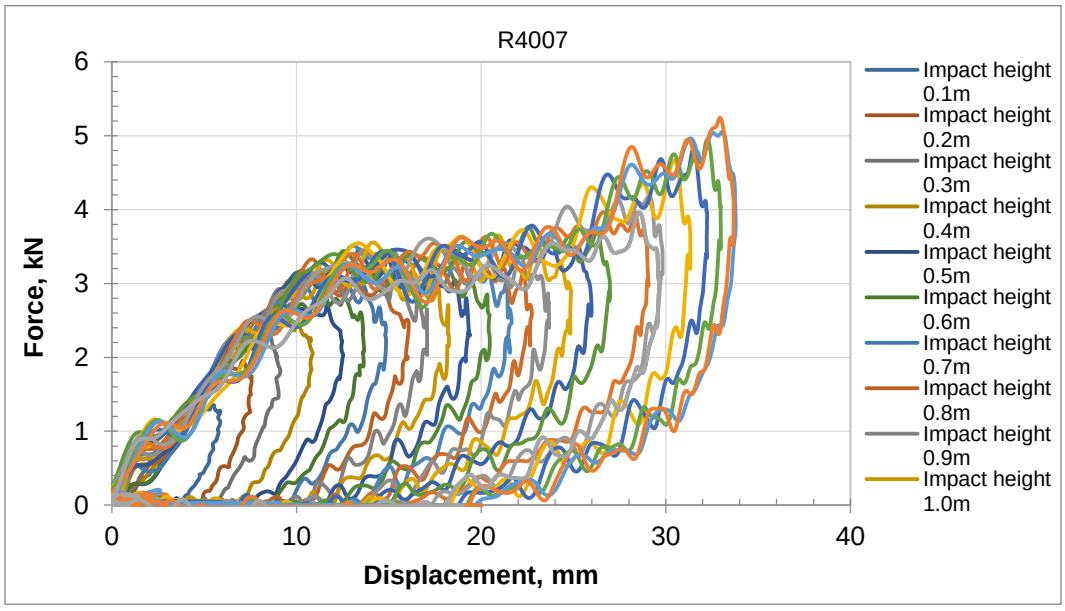

Figure C-34 - The force versus the displacement of the R1007 sample

APPENDIX D

TIME HISTORY

D.1 Dilatant Materials

D.1.1 P09-

D.1.1.1 Thickness 6 mm

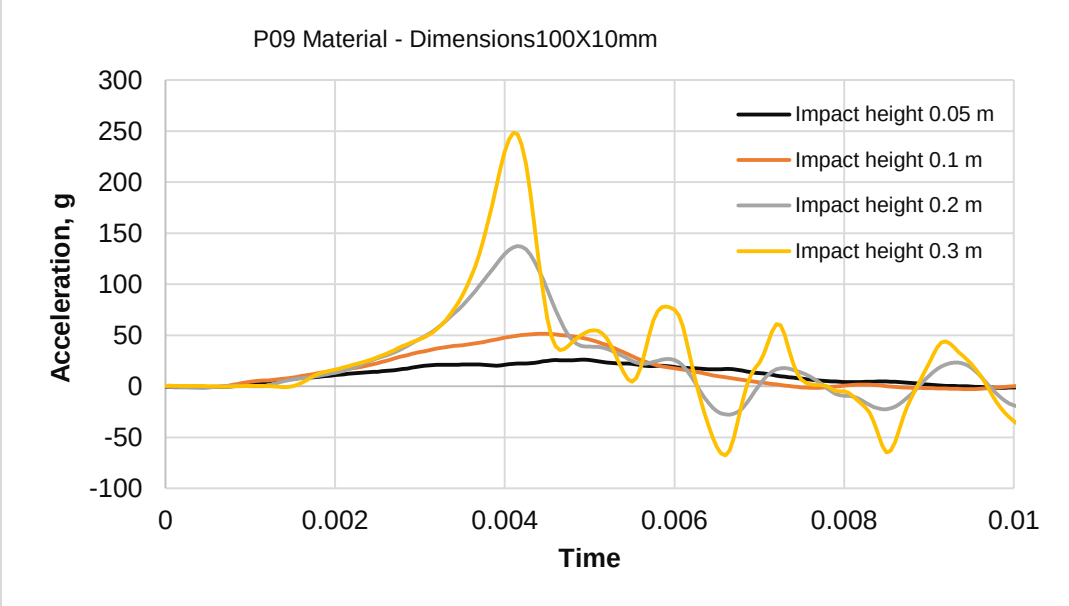

Figure D-1 -The acceleration time history of the 6.0 mm thick P09 material.

D.1.2 **P15 Material**

D.1.2.1 **Thickness 3 mm**

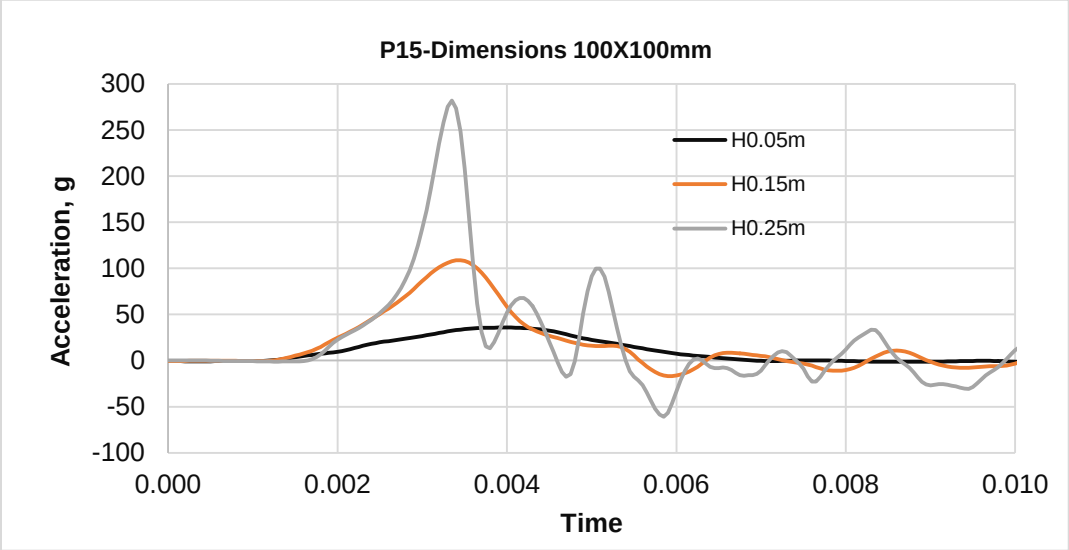

Figure D-2 - The acceleration time history of the 3.0 mm thick P15 material.

D.1.2.2 **Thickness 4 mm**

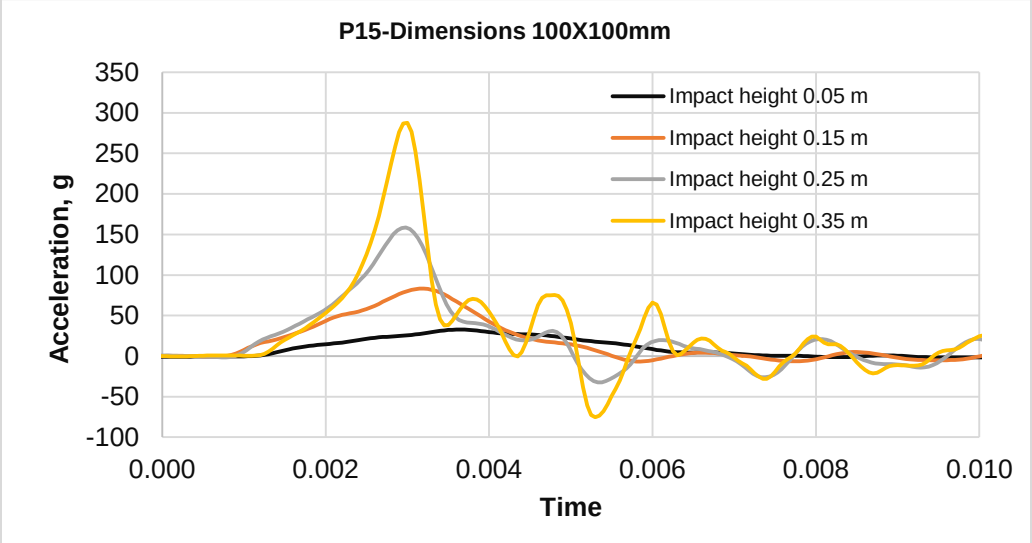

Figure D-3 - The acceleration time history of the 4.0 mm thick P15 material.

D.1.2.3 **Thickness 6 mm**

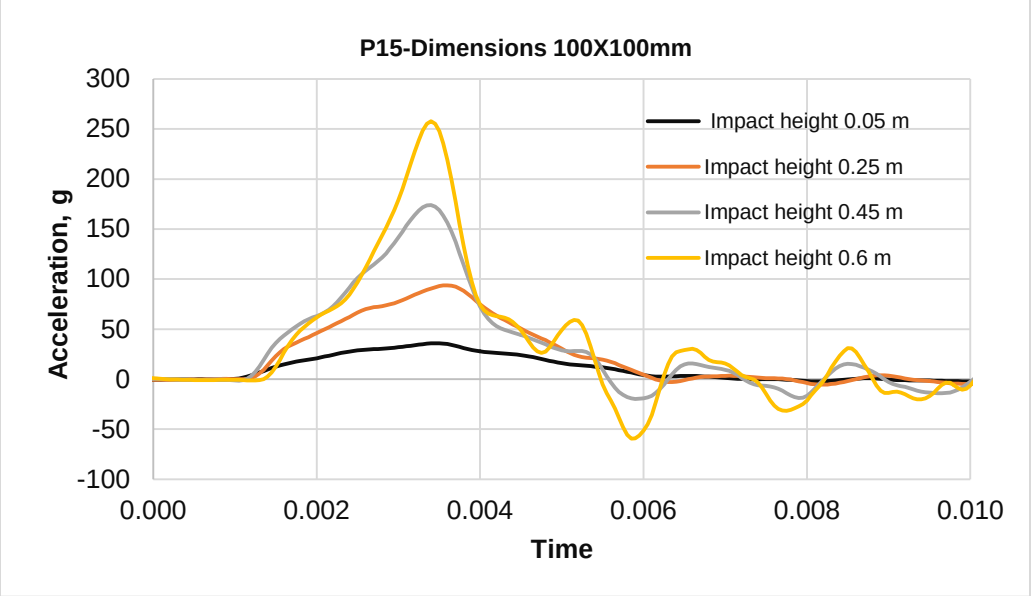

Figure D-4 - The acceleration time history of the 6.0 mm thick P15 material.

D.1.2.4 **Thickness 9.5 mm**

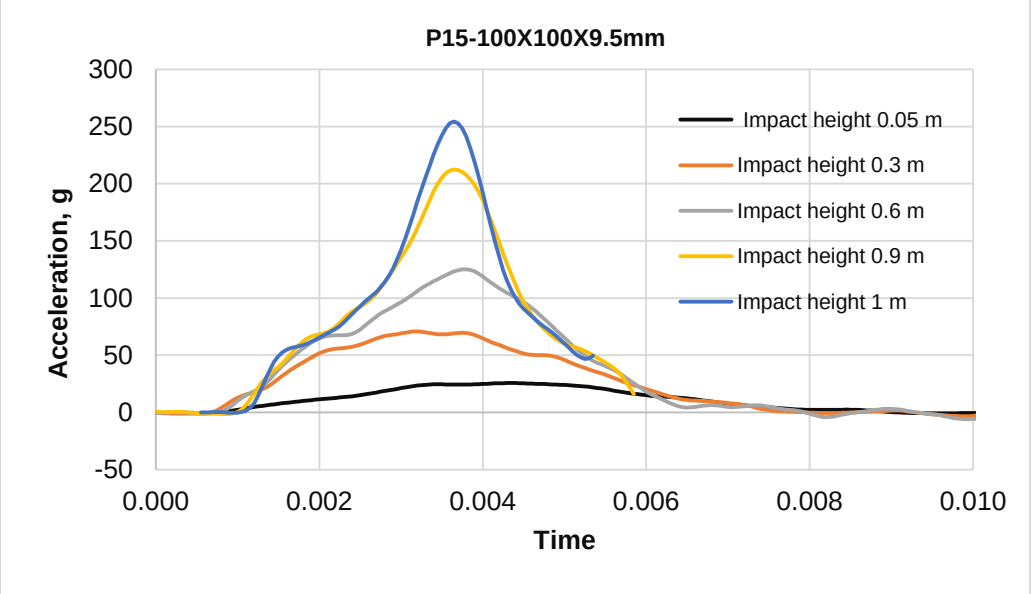

Figure D-5 - The acceleration time history of the 9.5 mm thick P15 material.

D.1.3 **P25 Material**

D.1.3.1 **Thickness 2 mm**

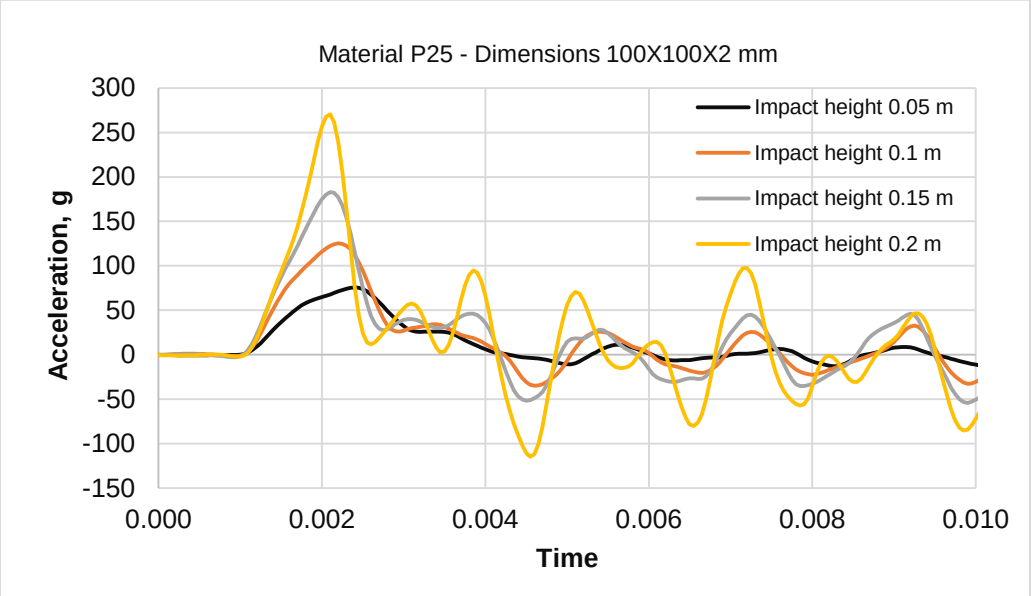

Figure D-6 - The acceleration time history of the 2.0 mm thick P25 material.

D.1.3.2 **Thickness 3 mm**

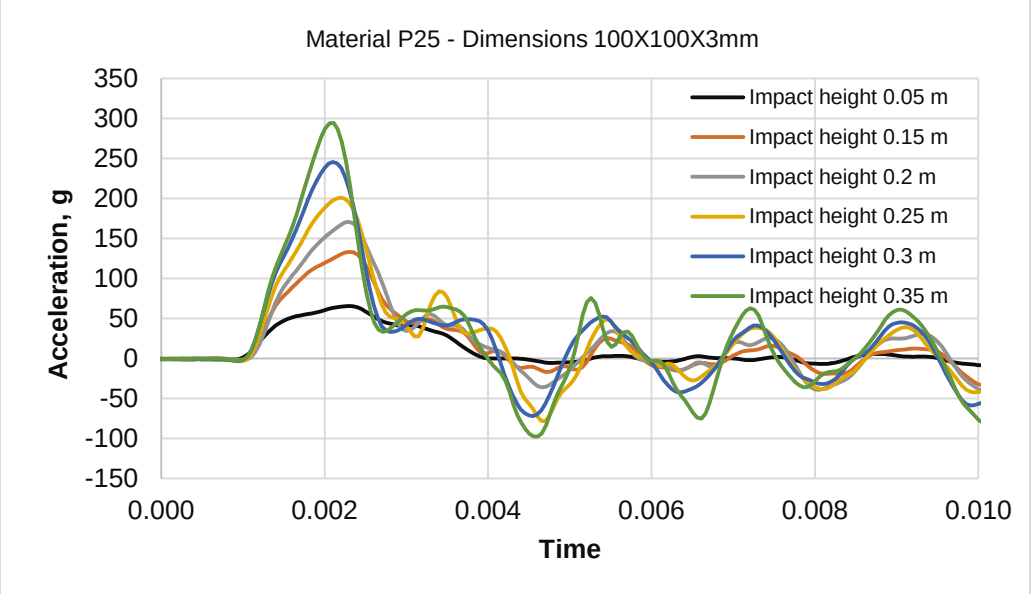

Figure D-7 - The acceleration time history of the 3.0 mm thick P25 material.

D.2 **Honeycomb Materials**

D.2.1 **H1056 Material**

D.2.1.1 **Wall Thickness 1.5 mm**

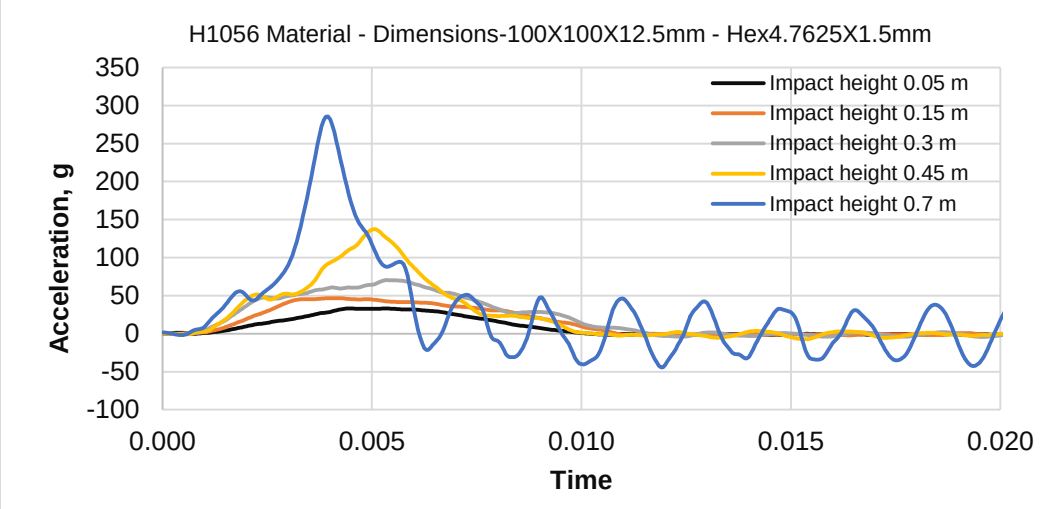

Figure D-8 - Acceleration time history of the H1056 material at cells dimensions Hex4.7X1.5mm.

D.2.2 **H1036 Material**

D.2.2.1 **Cells Dimensions Hex 4.7X1.0 mm**

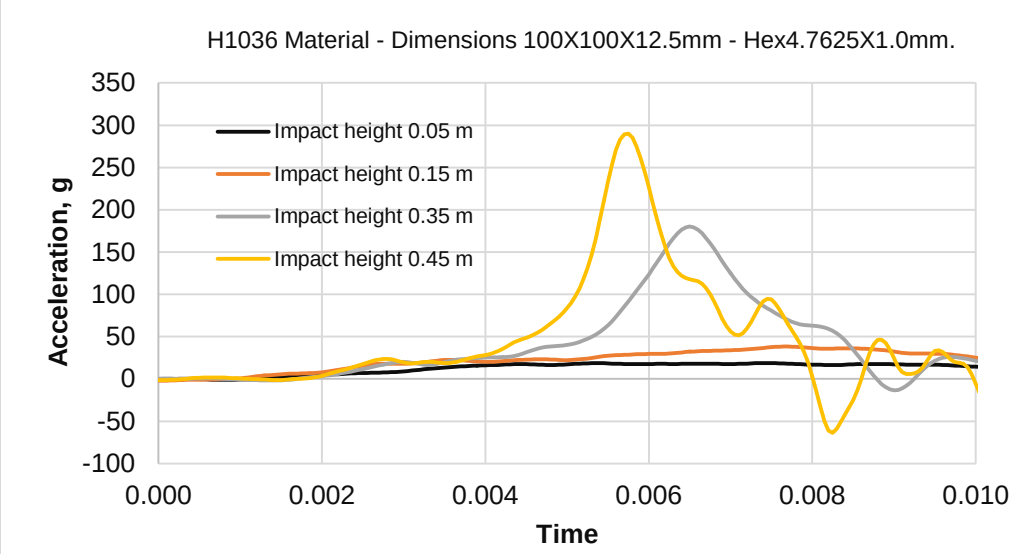

Figure D-9 - Acceleration time history of the H1036 material at cells dimensions Hex4.7X1.0mm.

D.2.2.2 **Cells Dimensions Hex 4.7X1.5 mm**

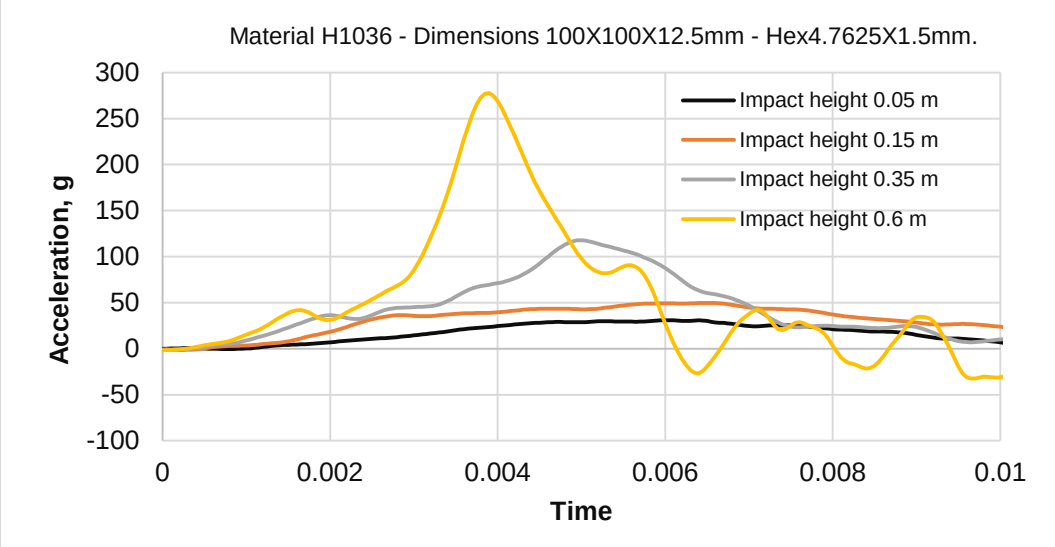

Figure D-10 - Acceleration time history of the H1036 material at cells dimensions Hex4.7X1.5mm.

D.2.3 **H781 Material**

D.2.3.1 **Cells Dimensions Hex 4.7X1.5 mm**

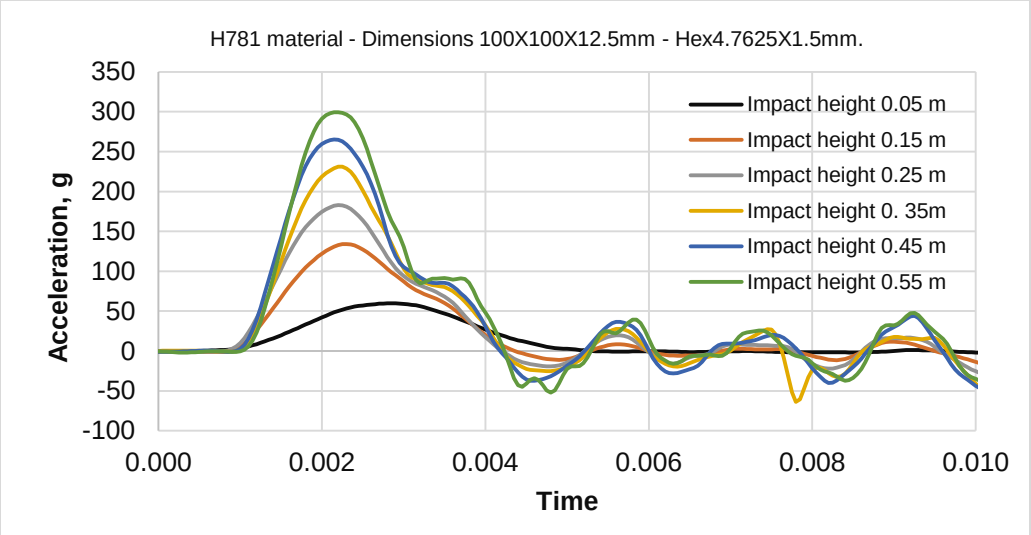

Figure D-11 - Acceleration time history of the H781 material at cells dimensions Hex4.7X1.5mm.

D.2.4 **H561 Material**

D.2.4.1 **Circular Samples**

D.2.4.1.1 **Material Thickness 6.5 mm**

D.2.4.1.1.1 **Wall Thickness 1.0 mm**

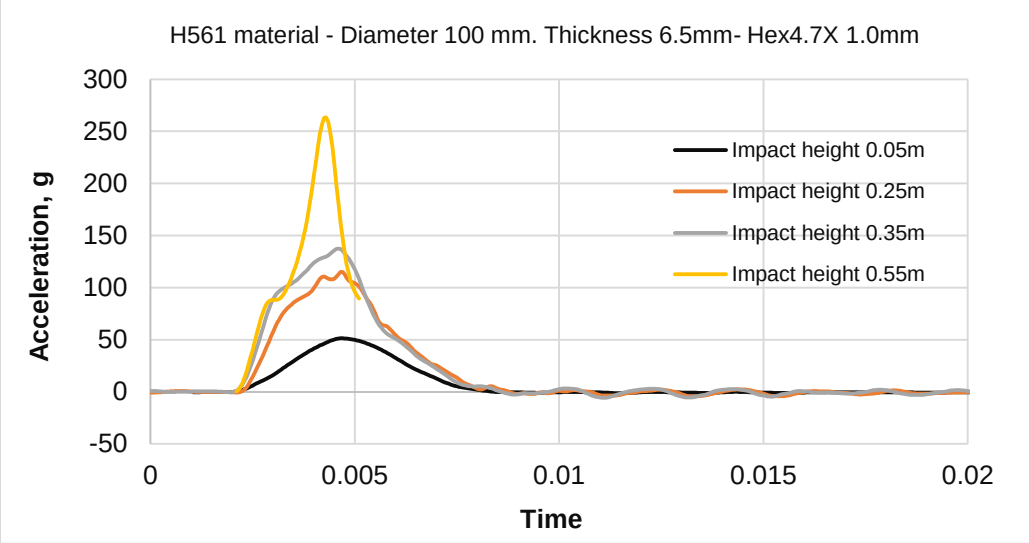

Figure D-12 - Acceleration time history of the circular sample of H561 material at cells dimensions Hex4.7X1.0mm and material thickness 6.5mm.

D.2.4.1.1.2 **Wall Thickness 1.5 mm**

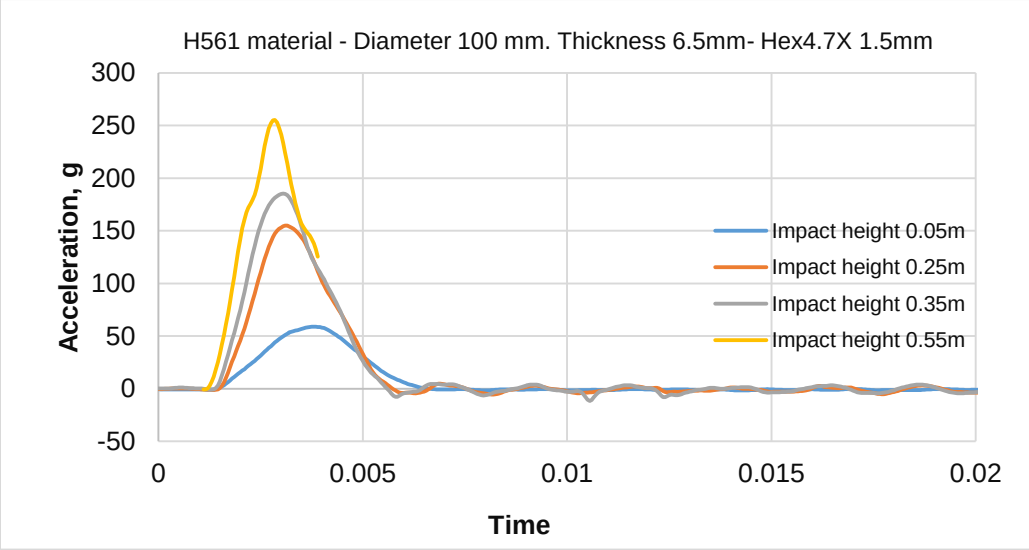

Figure D-13 - Acceleration time history of the circular sample of H561 material at cells dimensions Hex4.7X1.5mm and material thickness 6.5mm.

D.2.4.1.2 **Material Thickness 12.5 mm**

D.2.4.1.2.1 **Wall Thickness 1.5 mm**

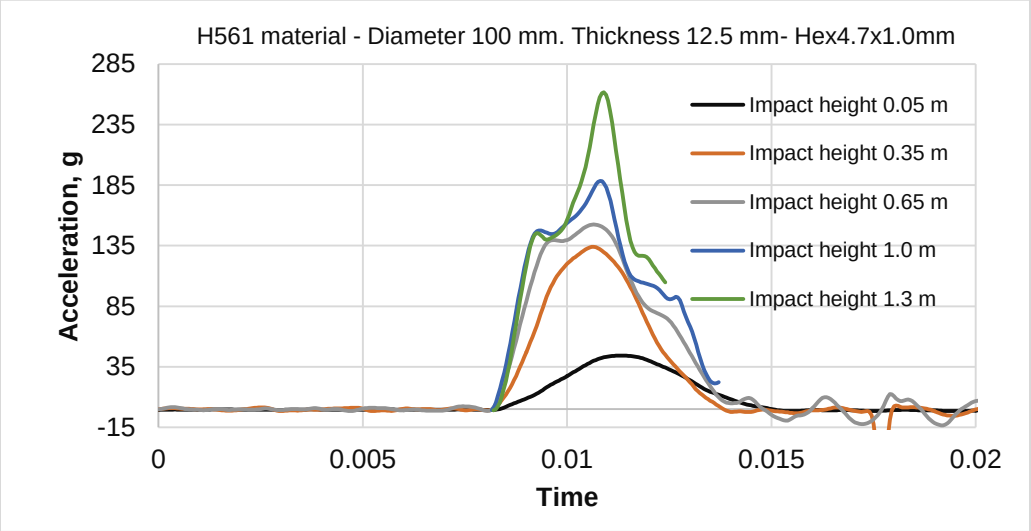

Figure D-14 - Acceleration time history of the circular sample of H561 material at cells dimensions Hex4.7X1.5mm and material thickness 12.5mm.

D.2.4.2 **Square Samples**

D.2.4.2.1 **Regular Cell Shapes**

D.2.4.2.1.1 **Hex3.0X1.0mm**

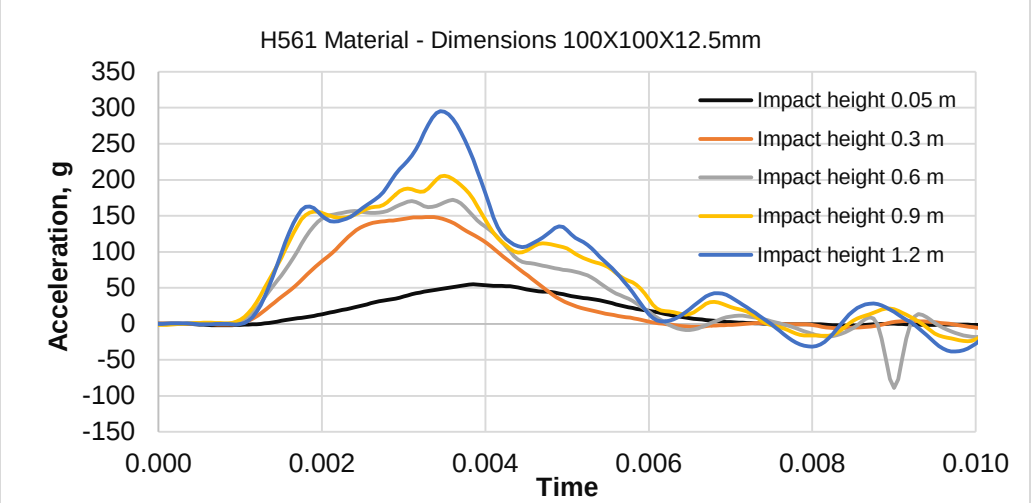

Figure D-15 - Acceleration time history of the circular sample of H561 material at cells dimensions Hex3.0X1.0mm.

D.2.4.2.1.2 **Hex4.7X1.0mm**

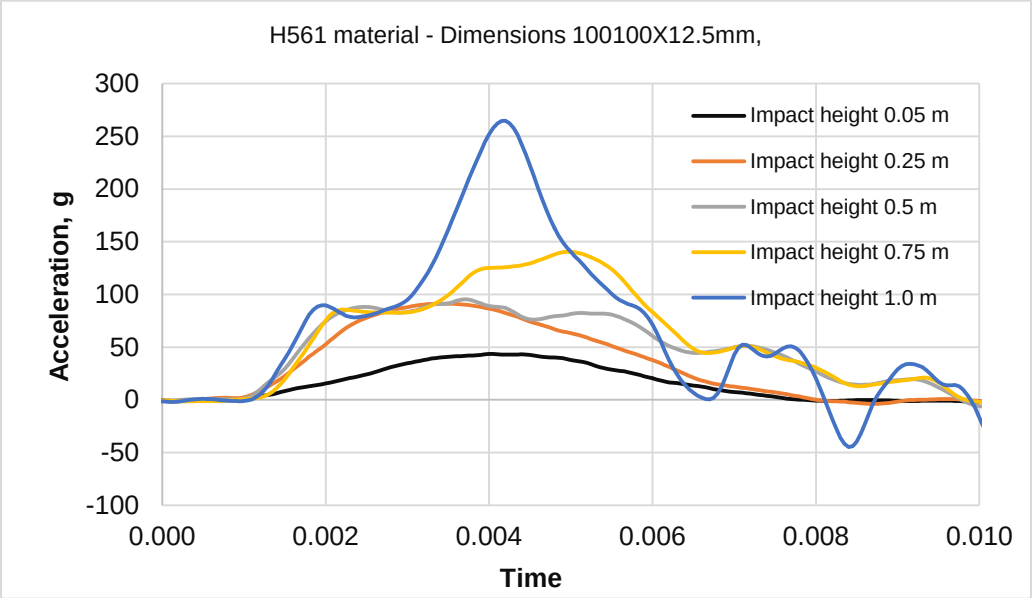

Figure D-16 - Acceleration time history of the circular sample of H561 material at cells dimensions Hex4.7X1.0mm.

D.2.4.2.1.3 **Hex6.0X1.0mm**

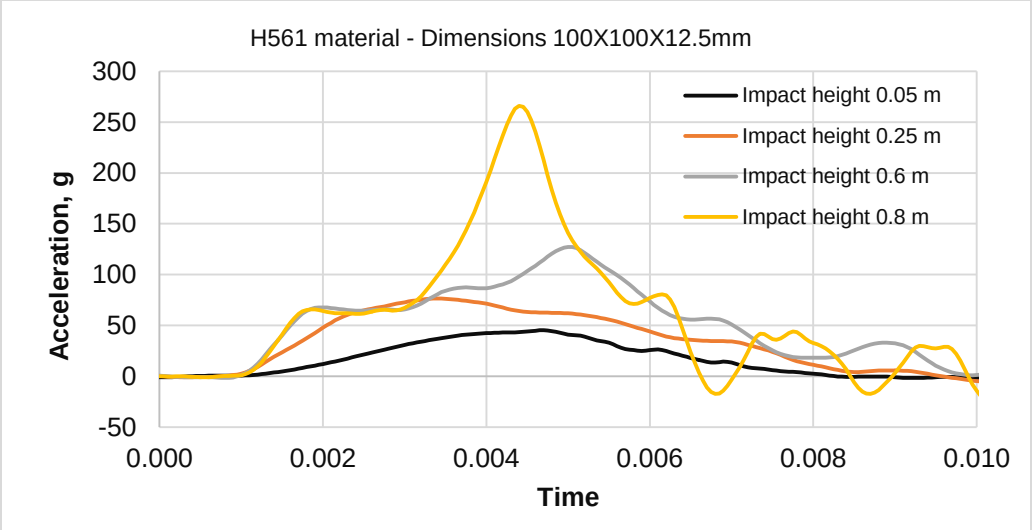

Figure D-17 - Acceleration time history of the circular sample of H561 material at cells dimensions Hex6.0X1.0mm.

D.2.4.2.1.4 **Hex8.0X1.0mm**

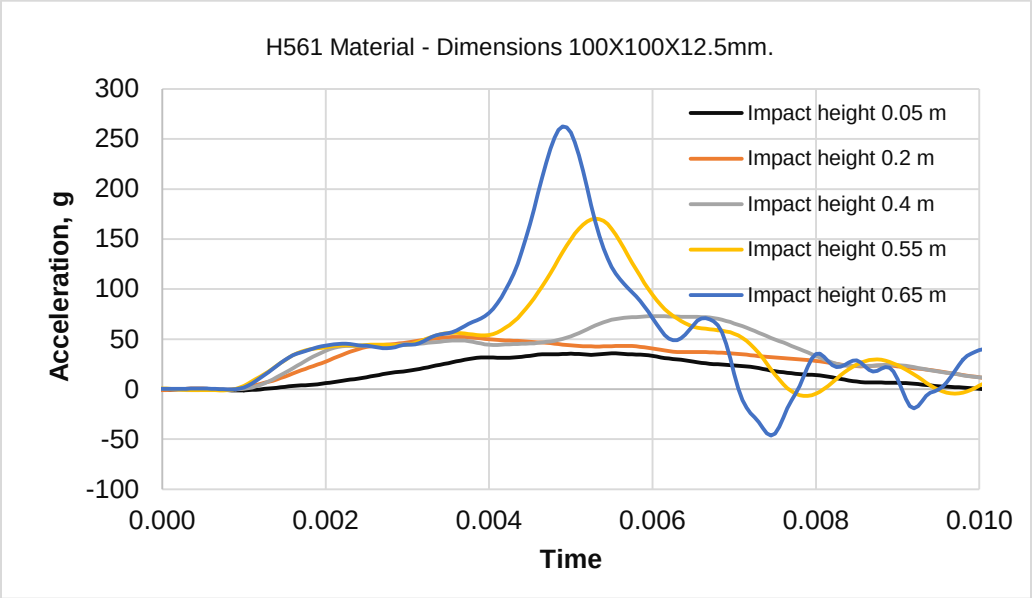

Figure D-18 - Acceleration time history of the circular sample of H561 material at cells dimensions Hex8.0X1.0mm.

D.2.4.2.1.5 **Hex3.0X0.8mm**

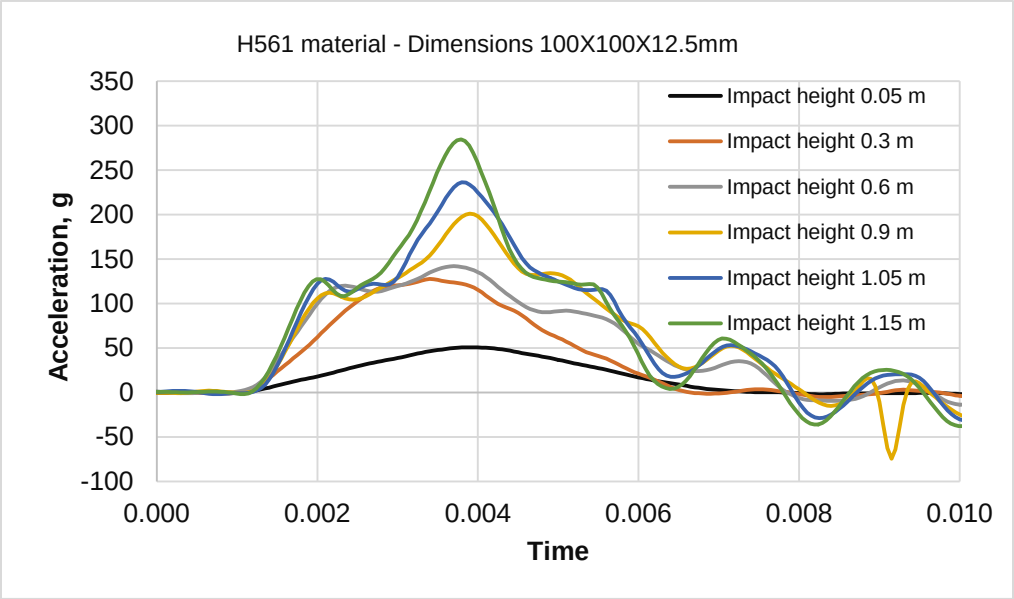

Figure D-19 - Acceleration time history of the circular sample of H561 material at cells dimensions Hex3.0X0.8mm.

D.2.4.2.2 **Irregular Cell Shapes**

D.2.4.2.2.1 **T1 Sample**

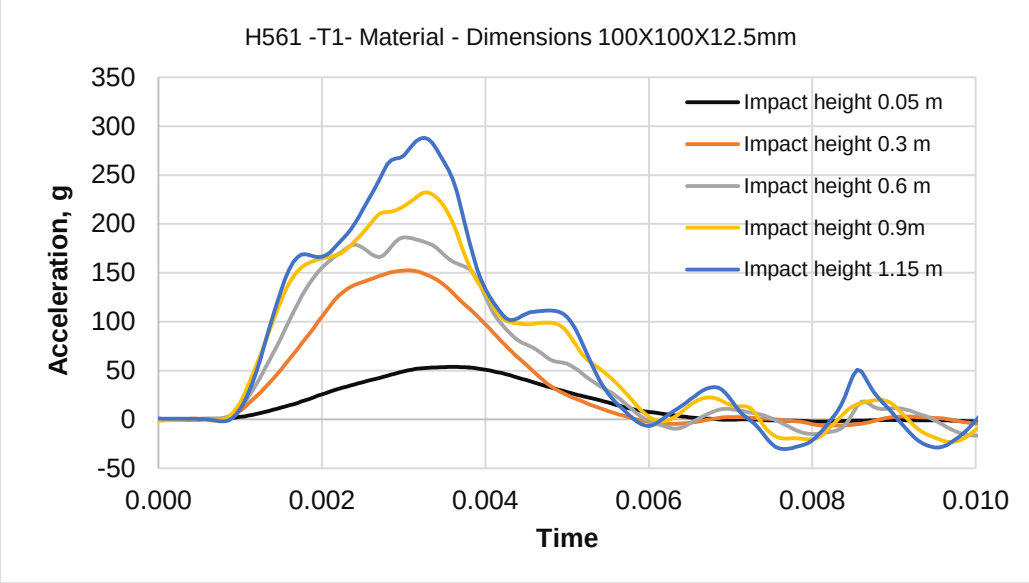

Figure D-20 - Acceleration time history of the T1 sample of H561 material.

D.2.4.2.2.2 **T2 Sample**

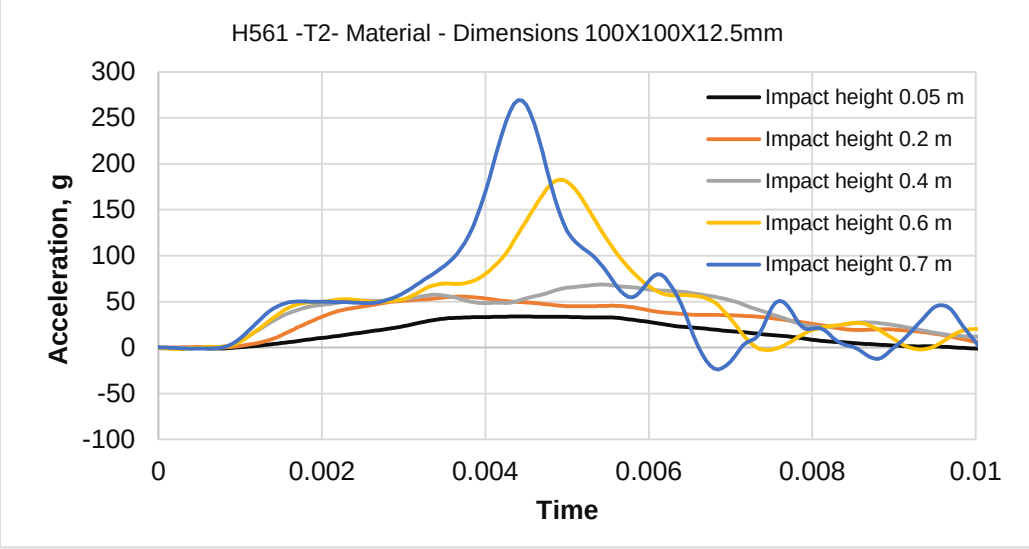

Figure D-21 - Acceleration time history of the T2 sample of H561 material.

D.2.4.2.2.3 **T3 Sample**

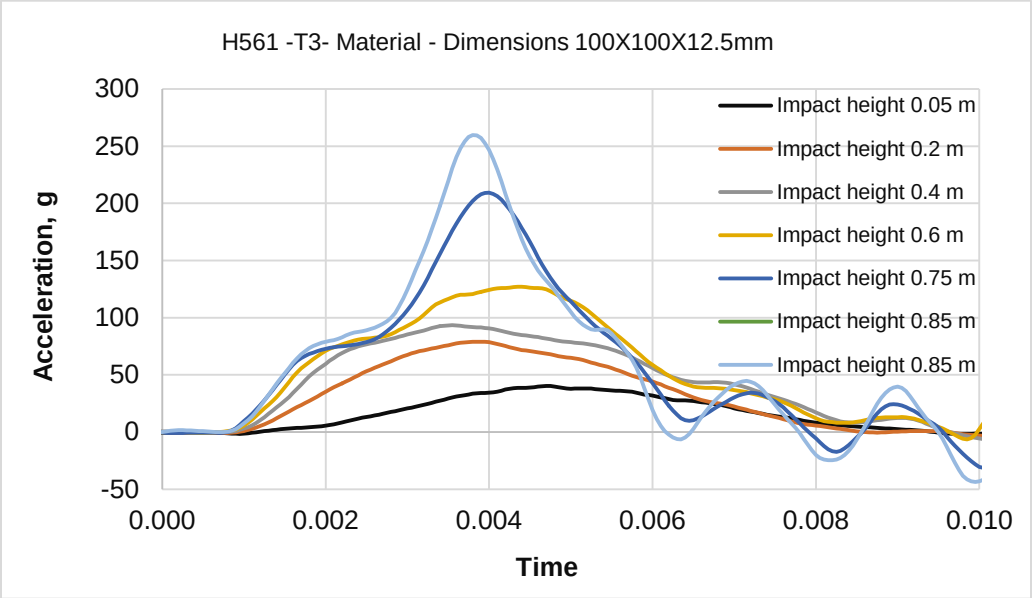

Figure D-22 - Acceleration time history of the T3 sample of H561 material.

D.3 **Results of Dilatant-Honeycomb Samples (Two layers)**

D.3.1 **Samples Thickness 12.5 mm**

D.3.1.1 **P25_H561**

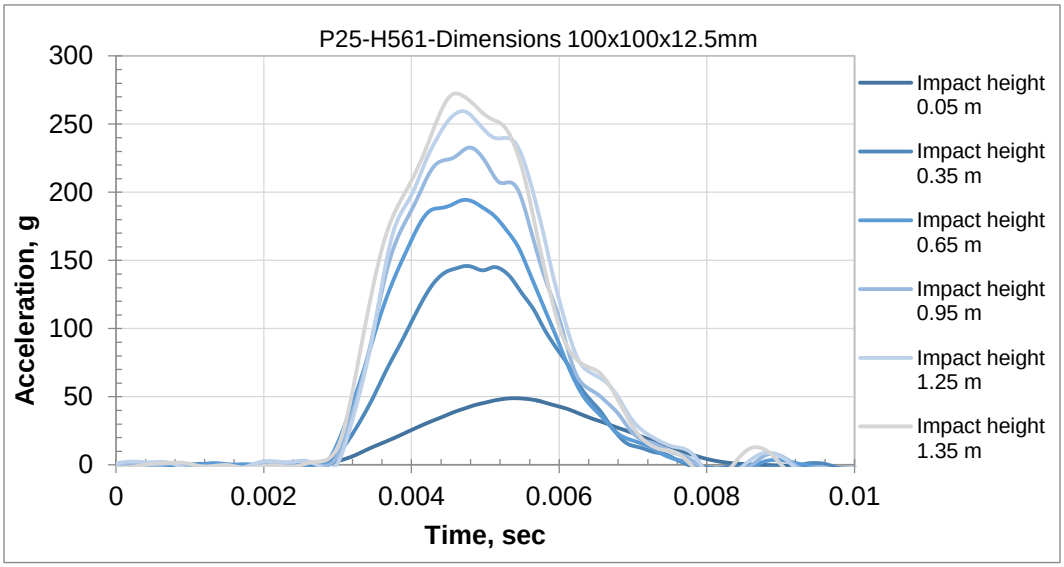

Figure D-23 - Acceleration time history of the P25_H561 sample at the total thickness 12.5 mm.

D.3.1.2 **P15_H1056**

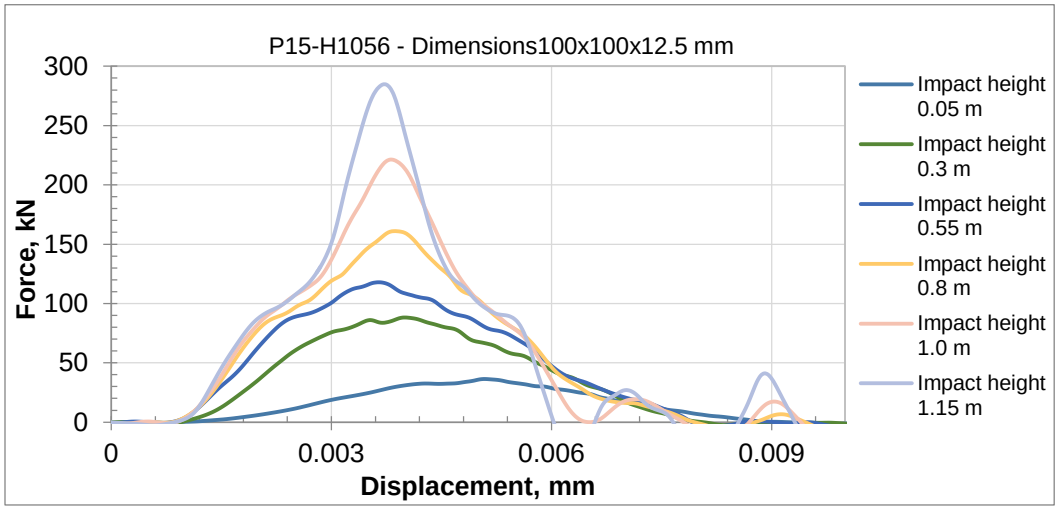

Figure D-24 - Acceleration time history of the P15_H1056 sample at the total thickness 12.5 mm.

D.3.1.3 **P25_H1036**

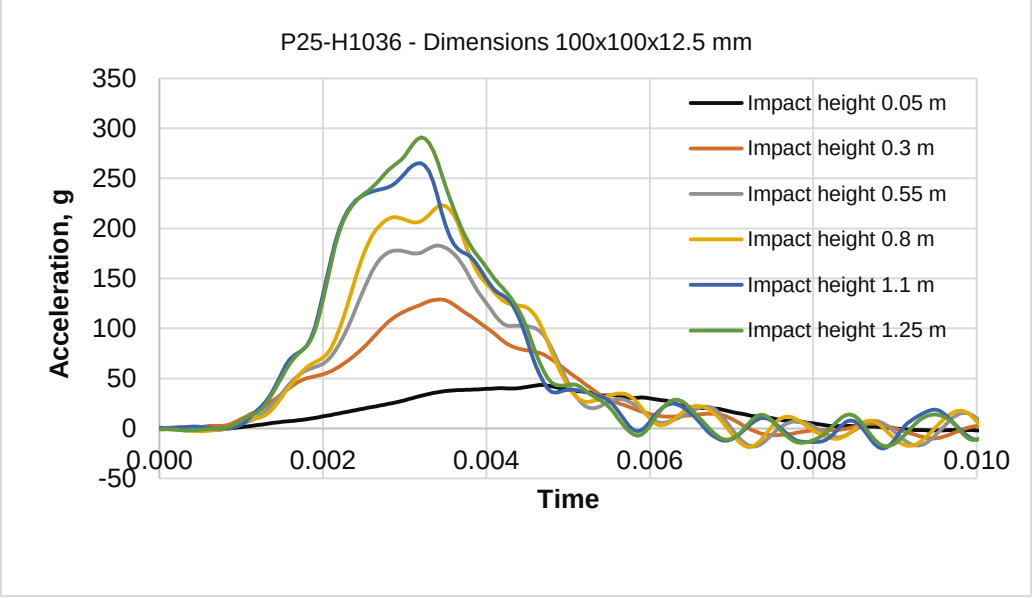

Figure D-25 - Acceleration time history of the P25_H1036 sample at the total thickness 12.5 mm.

D.3.1.4 **P09_H561**

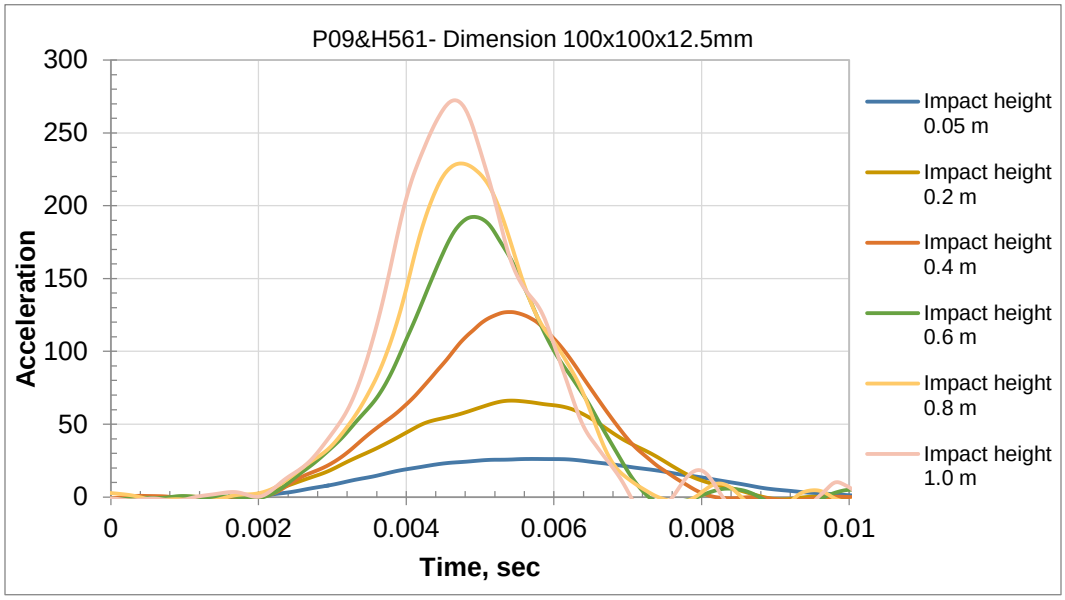

Figure D-26 - Acceleration time history of the P09_H561 sample at the total thickness 12.5 mm.

D.3.2 **Samples Thickness 24.5 mm**

D.3.2.1 **P25_H561**

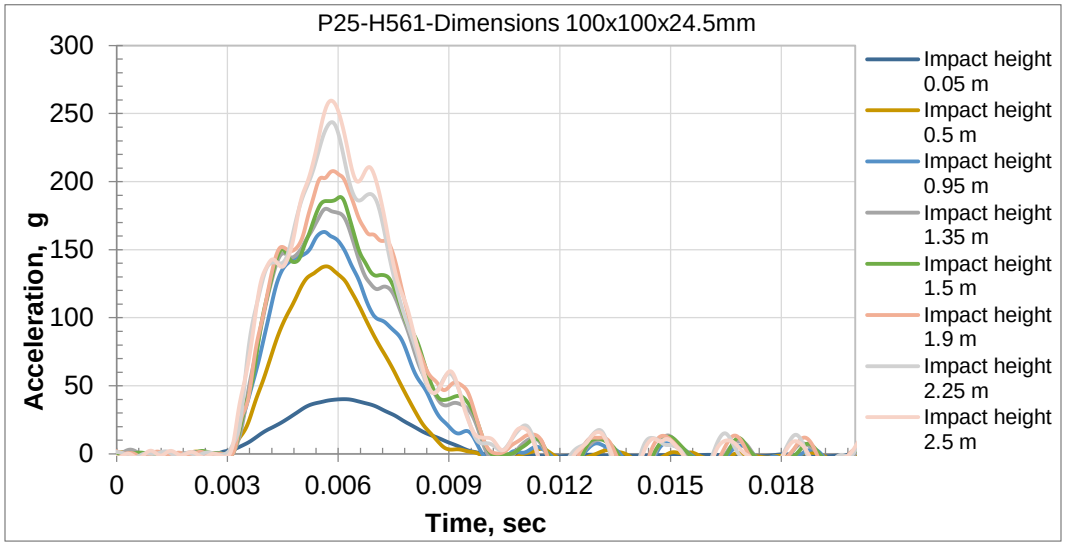

Figure D-27 - Acceleration time history of the P25_H561 sample at the total thickness 24.5 mm.

D.3.2.2 **P15_H1056**

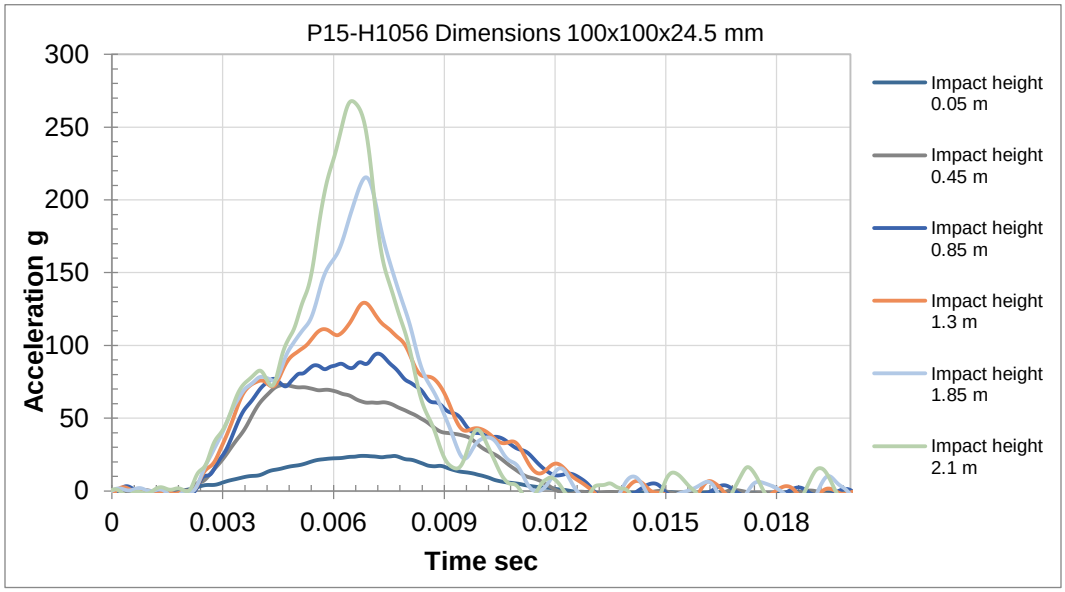

Figure D-28 - Acceleration time history of the P15_H1056 sample at the total thickness 24.5 mm.

D.3.2.3 **P25_H1036**

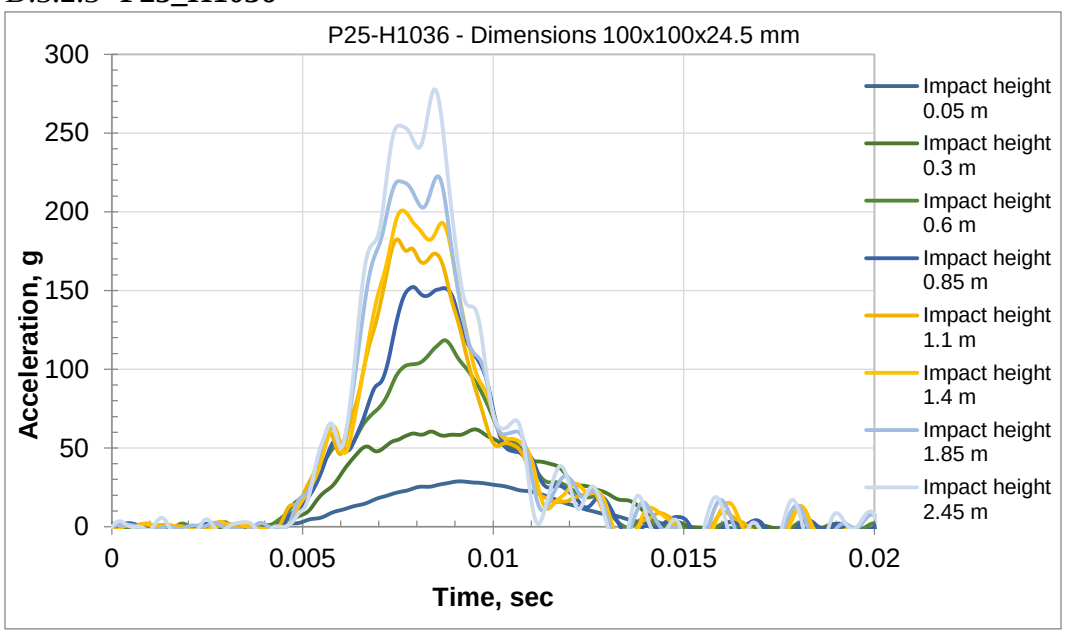

Figure D-29 - Acceleration time history of the P25_H1036 sample at the total thickness 24.5 mm

D.3.2.4 **P09_H561**

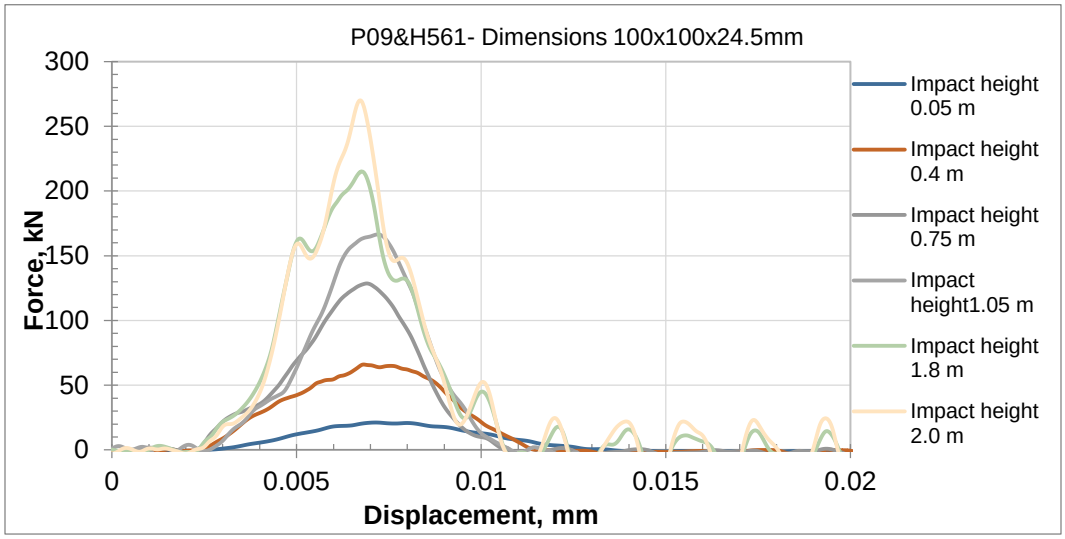

Figure D-30 - Acceleration time history of the P09_H561 sample at the total thickness 24.5 mm.

D.4 **Five Layers**

D.4.1 **R1007**

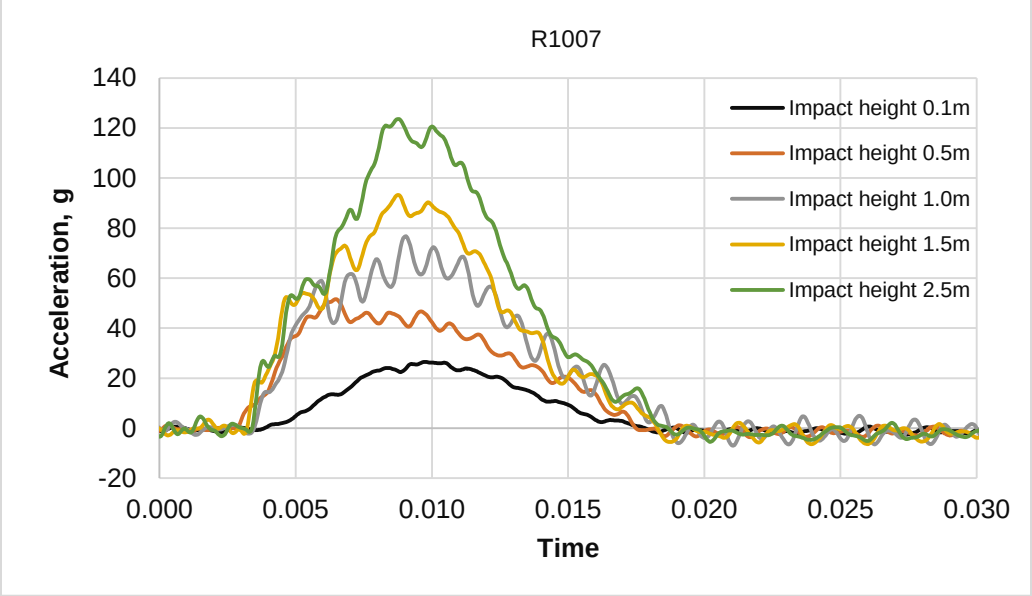

Figure D-31 - Acceleration time history of the R1007 sample.

D.4.2 **R2007**

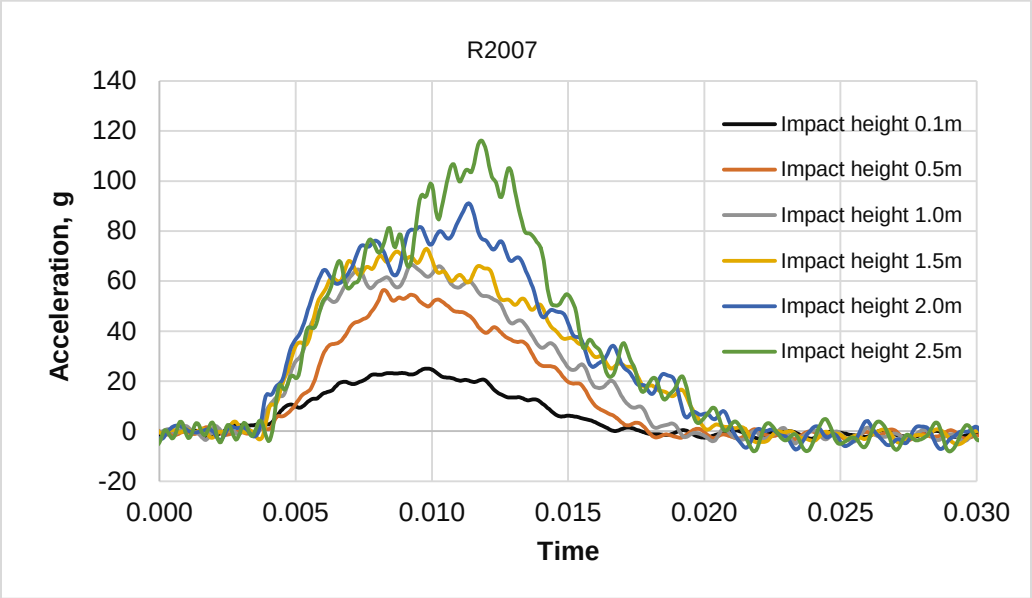

Figure D-32- Acceleration time history of the R2007 sample.

D.4.3 **R3007**

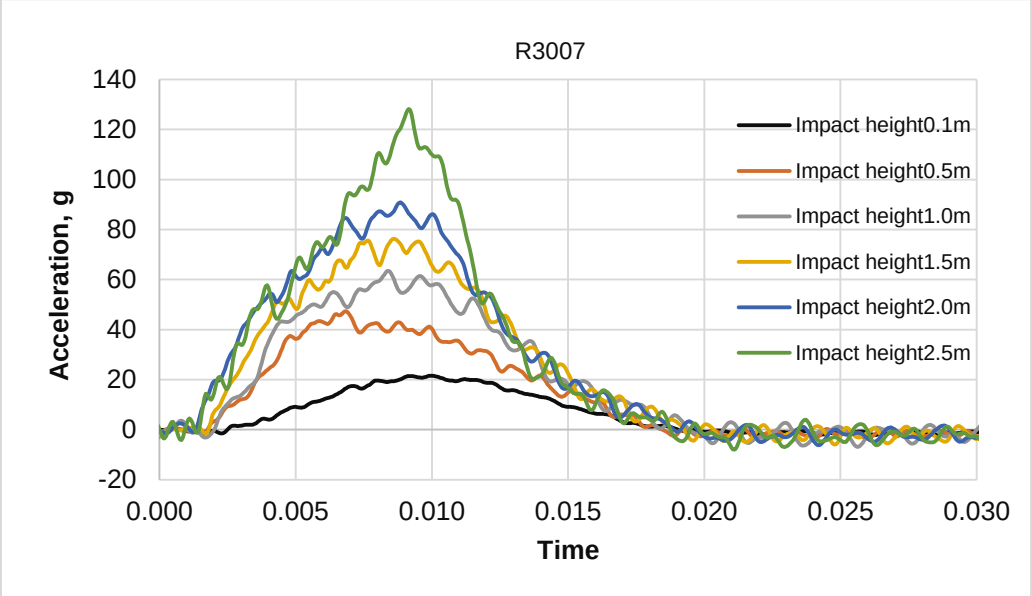

Figure D-33- Acceleration time history of the R3007 sample.

D.4.4 **R4007**

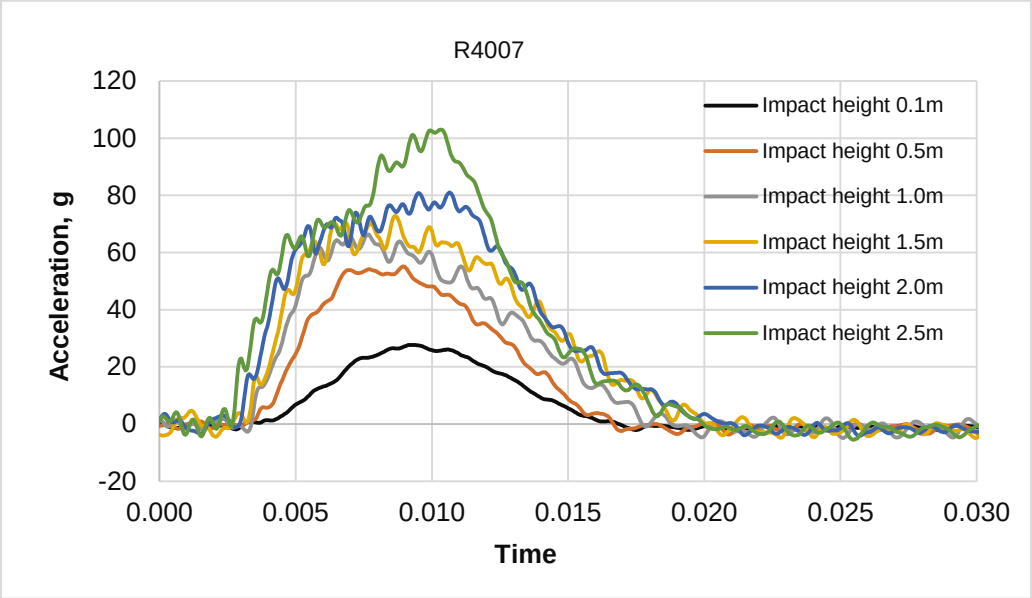

Figure D-34- Acceleration time history of the R4007 sample.

BIOGRAPHY OF THE AUTHOR

Karrar Al-Quraishi was born in Wasit, Iraq on July 21, 1988. He graduated from the University of Technology in Iraq with a Bachelor of Science in Mechanical Engineering in Jun of 2012. He is a candidate for the Master of Science degree in Mechanical Engineering from the University of Maine in August, 2017.